GEORGIA DOT RESEARCH PROJECT 21-04

Final Report

PRAGMATIC PRECAST/PRESTRESSED GIRDER ACCEPTANCE CRITERIA

Office of Performance-based Management and Research
600 West Peachtree Street NW | Atlanta, GA 30308

July 2025

TECHNICAL REPORT DOCUMENTATION PAGE

1. Report No.: FHWA-GA-25-2104	2. Government Accession No.: N/A	3. Recipient's Catalog No.: N/A
4. Title and Subtitle: Pragmatic Precast/Prestressed Girder Acceptance Criteria		5. Report Date: July 2025
		6. Performing Organization Code: N/A
7. Author(s): Lauren Stewart (PI), Ph.D., P.E.; Lawrence Kahn (coPI), Ph.D.; Karl F. Meyer, Ph.D., P.E.; Giovanni Loreto, Ph.D.; and Ana K. Contreras, EIT		8. Performing Organization Report No.: 21-04
9. Performing Organization Name and Address: Georgia Institute of Technology Office of Sponsored Programs 505 Tenth Street, NW Atlanta, Georgia 30332-0420 (404) 894-4819		10. Work Unit No.: N/A
		11. Contract or Grant No.: PI# 00181720
12. Sponsoring Agency Name and Address: Georgia Department of Transportation (SPR) Office of Performance-based Management and Research 600 West Peachtree St. NW Atlanta, GA 30308		13. Type of Report and Period Covered: Final; March 2022 – July 2025
		14. Sponsoring Agency Code: N/A
15. Supplementary Notes: Prepared in cooperation with the U.S. Department of Transportation, Federal Highway Administration.		

16. Abstract:

This research addresses the lack of specific, quantitative guidelines within the Georgia Department of Transportation's (GDOT) Standard Operating Procedure 3 (SOP-3) for evaluating nonconforming precast/prestressed concrete girders. SOP-3 currently provides general recommendations but does not offer objective criteria for acceptance, repair, or rejection decisions, leading to inconsistent practices and project delays. To improve decision-making and repair strategies, this study developed and validated a tiered acceptance system tailored to GDOT's materials and construction practices. The research involved a synthesis of national guidelines, interviews with GDOT personnel and industry stakeholders, and full-scale experimental testing of BT-54 girders with simulated nonconformance issues. Results showed that top flange repairs consistently exceeded original girder strength, and bottom flange repairs were generally effective except in bearing zones, where retensioning methods failed due to poor strand-concrete bonding. Reinforced repair surfaces demonstrated strong adhesion and structural performance, reaching at least 95 percent of nominal moment capacity and 90 percent of nominal shear capacity. Recommendations include simplifying top flange repair procedures, reconsidering the use of epoxy bonding agents, and adopting stainless steel anchorage materials for bottom flange repairs. The study also suggests revisions to SOP-3 to include standardized repair procedures and calls for future research on the long-term durability of repairs under service-like loading conditions.

17. Keywords: Precast, Prestressed, Nonconformance, Repair	18. Distribution Statement: No Restriction		
19. Security Classification (of this report): Unclassified	20. Security Classification (of this page): Unclassified	21. No. of Pages: 352	22. Price: Free

Form DOT 1700.7 (8-72) Reproduction of completed page authorized

GDOT Research Project 21-04

Final Report

PRAGMATIC PRECAST/PRESTRESSED GIRDER ACCEPTANCE CRITERIA

By
Lauren K. Stewart, Ph.D., P.E.
Professor, Georgia Institute of Technology

Lawrence Kahn, Ph.D., P.E.
Professor Emeritus, Georgia Institute of Technology

Karl F. Meyer, Ph.D., P.E.
Professor of the Practice, Georgia Institute of Technology

Giovanni Loreto, Ph.D.
Associate Professor, Kennesaw State University

Ana Karina Contreras
Graduate Research Assistant, Georgia Institute of Technology

Georgia Tech Research Corporation

Contract with
Georgia Department of Transportation

In cooperation with
U.S. Department of Transportation, Federal Highway Administration

July 2025

SI* (MODERN METRIC) CONVERSION FACTORS

APPROXIMATE CONVERSIONS TO SI UNITS

Symbol	When You Know	Multiply By	To Find	Symbol
		LENGTH		
in	inches	25.4	millimeters	mm
ft	feet	0.305	meters	m
yd	yards	0.914	meters	m
mi	miles	1.61	kilometers	km
		AREA		
in^2	square inches	645.2	square millimeters	mm^2
ft^2	square feet	0.093	square meters	m^2
yd^2	square yard	0.836	square meters	m^2
ac	acres	0.405	hectares	ha
mi^2	square miles	2.59	square kilometers	km^2
		VOLUME		
fl oz	fluid ounces	29.57	milliliters	mL
gal	gallons	3.785	liters	L
ft^3	cubic feet	0.028	cubic meters	m^3
yd^3	cubic yards	0.765	cubic meters	m^3
		NOTE: volumes greater than 1000 L shall be shown in m^3		
		MASS		
oz	ounces	28.35	grams	g
lb	pounds	0.454	kilograms	kg
T	short tons (2000 lb)	0.907	megagrams (or "metric ton")	Mg (or "t")
		TEMPERATURE (exact degrees)		
°F	Fahrenheit	5 (F-32)/9 or (F-32)/1.8	Celsius	°C
		ILLUMINATION		
fc	foot-candles	10.76	lux	lx
fl	foot-Lamberts	3.426	$candela/m^2$	cd/m^2
		FORCE and PRESSURE or STRESS		
lbf	poundforce	4.45	newtons	N
lbf/in^2	poundforce per square inch	6.89	kilopascals	kPa

APPROXIMATE CONVERSIONS FROM SI UNITS

Symbol	When You Know	Multiply By	To Find	Symbol
		LENGTH		
mm	millimeters	0.039	inches	in
m	meters	3.28	feet	ft
m	meters	1.09	yards	yd
km	kilometers	0.621	miles	mi
		AREA		
mm^2	square millimeters	0.0016	square inches	in^2
m^2	square meters	10.764	square feet	ft^2
m^2	square meters	1.195	square yards	yd^2
ha	hectares	2.47	acres	ac
km^2	square kilometers	0.386	square miles	mi^2
		VOLUME		
mL	milliliters	0.034	fluid ounces	fl oz
L	liters	0.264	gallons	gal
m^3	cubic meters	35.314	cubic feet	ft^3
m^3	cubic meters	1.307	cubic yards	yd^3
		MASS		
g	grams	0.035	ounces	oz
kg	kilograms	2.202	pounds	lb
Mg (or "t")	megagrams (or "metric ton")	1.103	short tons (2000 lb)	T
		TEMPERATURE (exact degrees)		
°C	Celsius	1.8C+32	Fahrenheit	°F
		ILLUMINATION		
lx	lux	0.0929	foot-candles	fc
cd/m^2	$candela/m^2$	0.2919	foot-Lamberts	fl
		FORCE and PRESSURE or STRESS		
N	newtons	0.225	poundforce	lbf
kPa	kilopascals	0.145	poundforce per square inch	lbf/in^2

* SI is the symbol for the International System of Units. Appropriate rounding should be made to comply with Section 4 of ASTM E380. (Revised March 2003)

TABLE OF CONTENTS

LIST OF FIGURES

LIST OF TABLES

EXECUTIVE SUMMARY

The Georgia Department of Transportation (GDOT) currently relies on Standard Operating Procedure 3 (SOP-3) for the quality control and assurance of precast/prestressed concrete girders. Although SOP-3 addresses general issues such as longitudinal cracking, shrinkage, and alkali–silica reaction, it lacks specific, quantitative criteria for determining whether a girder should be accepted, accepted with repairs, or rejected. This absence of clear guidelines often leads to inconsistent decision-making, disputes between owners and fabricators, and delays in project delivery.

To address these challenges, the research team developed and validated a tiered acceptance system tailored to GDOT's practices and materials. The study involved a comprehensive review of national guidelines and unpublished research, interviews with GDOT personnel and industry stakeholders, and full-scale experimental testing of BT-54 girders with simulated nonconformance issues. The primary goal was to classify girders into three categories—accept without repair, accept with repair, or reject—based on structural performance and service life implications.

Experimental results demonstrated that top flange repairs performed exceptionally well, often exceeding the strength of the original flanges. Bottom flange repairs were generally effective, except in bearing zones where retensioning methods failed due to inadequate bonding between strands and concrete. All reinforced repair surfaces, regardless of epoxy coating, sustained loads equal to or greater than 95 percent of nominal moment capacity or 90 percent of nominal shear capacity.

Based on these findings, several recommendations are made. For top flange repairs, it is advised to post-install straight reinforcing bars and bend them after epoxy anchoring, simplifying the process. However, the use of epoxy bonding agents should be reconsidered, as they were difficult to apply and did not improve bond strength in testing. For bottom flange repairs, open-top access for concrete placement is preferred, and stainless-steel anchors and wire are recommended for better performance. Self-consolidating concrete (SCC) proved effective and is recommended for future use, whereas repair mortar was found unsuitable for large or bottom-facing repairs.

The study also provided a draft preliminary guide to use in place of, or as a revision to, SOP-3 that included standardized repair procedures for common nonconformance issues based on the strength tests that were conducted in this research. Future research should investigate the long-term durability of these repairs under cyclic and fatigue loading to better simulate service conditions and ensure lasting performance.

CHAPTER 1. INTRODUCTION

MOTIVATION

Publications by the Precast/Prestressed Concrete Institute (PCI),[1] as well as several departments of transportations (DOTs) across the country, provide guidelines with the primary objective of establishing a user's manual for the acceptance, repair, or rejection of precast/prestressed concrete girders with many types of cracking. (See references 2, 3, 4, and 5.) However, these guidelines are not specific to the practices and materials used in Georgia. Currently, the Georgia Department of Transportation (GDOT) uses *Standard Operating Procedure 3 (SOP-3): Quality Control and Quality Assurance of Precast/Prestressed Concrete Members and Structural Precast Concrete Members*, developed in 2014.[6] In general, most of the SOP-3 document focuses on problems associated with longitudinal cracking, shrinkage, temperature, and alkali–silica reaction. SOP-3 is general and does not provide predetermined limits or an objective decision-making tool to determine if a girder can be accepted, accepted with repairs, or rejected.

Because GDOT lacks pragmatic decision-making guidelines for precast/prestressed concrete girders, decisions often lead to owner–fabricator disputes, increased time delays, and acceptance of structural elements that are less than ideal. As a response, the main objective of this research is to recommend a tiered acceptance system with specific limits that can be used by GDOT and industry to determine the appropriate path for girders with the most relevant nonconformance issues. To do this, the project focuses on the investigation and quantification of common nonconformance issues in girders typically

encountered in GDOT projects and their effect on service life and ultimate strength of members.

RELEVANT LITERATURE

Several documents address quality and nonconformance for both cosmetic and noncosmetic girder issues. (See references 1, 2, 3, 4, 5, 6, and 7, and footnote 1). In 2006, the PCI published the *Manual for the Evaluation and Repair of Precast, Prestressed Concrete Bridge Products*[1] (MNL-137), which aimed to achieve a greater degree of uniformity among owners, engineers, and precast producers. The first edition of the PCI MNL-137 in 2006 has been the standard. The manual has troubleshooting and repair procedures depending on the location, orientation, and size of the nonconformance issue. Specifically, the nonconformance issues addressed in the PCI MNL-137 regarding beams include transverse cracks originating at the top of beams, vertical and diagonal cracks at the bottom of beams, vertical through cracks in beams, horizontal end cracks in webs and flanges, bottom flange cracks at beam ends, corner spalls or corner crack, partially cracked top flanges, random honeycombing and voids, random top flange cracks, short projected strand or rebar, and missing projected strand or rebar. The damaged prestressed members fall into three categories: (1) products that can be accepted without repair, (2) products that can be accepted with repair, and (3) products that must be rejected. In a later publication, guidelines for the resolution of nonconformance were also addressed.[7]

Several DOTs across the country have published similar guidelines with the primary objective of establishing a user's manual for the acceptance, repair, or rejection of

[1] Smith, J. (2020, September). Personal interview.

precast/prestressed concrete girders with many types of cracking. (See References 2, 3, 4, and 5) These manuals are, primarily, the result of experience gained in the inspection of precast/prestressed concrete products and include practices and procedures found to produce satisfactory results. Currently, Georgia uses SOP-3 developed in 2014.[6] In general, most of the SOP-3 document focuses on problems associated with longitudinal cracking, shrinkage, temperature, and alkali–silica reaction. Further, SOP-3 provides a general statement requiring submittal for approval of the damage and recommended repair to the inspector. However, it does not provide guidelines or predetermined quantitative limits for the inspector to determine objectively the acceptance, repair, or rejection of damaged girders.

GDOT has funded previous related research by the principal investigators (PIs) of this study. A multi-phase prior effort focused on developing finite element and cohesive zone models that were able to predict the response of precast/prestressed girders that were repaired by epoxy deposition. The researchers in that study designed and implemented experiments to test epoxy-repaired concrete beams.[8] Additionally, the PIs published a GDOT research report for a project that produced a draft SOP for introducing penalty and other contracting mechanisms for inadequate concrete cover that reduced service life.[9]

Various research programs, including those of the co-PIs, have used full-scale testing to investigate the behavior of precast beams. Full-scale testing of concrete girders has also been performed in other laboratories to measure flexural and shear capacity of concrete beams.[10,11,12] Multiple researchers performed large-scale testing to assess shear behavior of prestressed concrete girders, loading with a single concentrated load to failure,[10,11,12]

and performed large-scale flexural testing of double-tee bridge beams conducting four-point bending tests on the girders until failure.[13]

RESEARCH OBJECTIVES

This research combined academic literature as well as unpublished research, computational and design models, GDOT personnel and repair contractor interviews, and experimental investigations. From those sources, the research team recommends a tiered acceptance system with specific limits for use by GDOT and industry to determine the appropriate path for girders with the most relevant nonconformance issues. Specifically, the goal of this research was to provide a guideline to classify commonly nonconforming girders into three categories: accept without repairs, accept with repairs, and reject.

The objectives of this multi-university collaborative research were as follows:

- **Objective 1.** To collect and quantify the types and occurrences of girder nonconformance in GDOT precast/prestressed bridge projects via interviews with GDOT, contractors, and fabricators.
- **Objective 2.** To thoroughly review and synthesize quality requirements from other state agencies as well as a wealth of unpublished research, utilizing the PIs' networks within organizations.
- **Objective 3.** To utilize computational and design models, combined with full-scale experimental investigations to determine tiered acceptance thresholds for the most common nonconformance issues. This objective was facilitated through industry cooperation, with fabricators providing nonconforming specimens for testing.

- **Objective 4.** To assess which nonconformance issues are associated with possible service life reduction, making contracting recommendations for appropriate contracting structures (e.g., penalties) for nonconforming elements.
- **Objective 5.** To summarize research findings in a pragmatic form by providing recommendations and a clear roadmap for a tiered acceptance system via a draft GDOT quality manual for precast/prestressed girders.

ORGANIZATION OF REPORT

Including this introductory chapter, this report is organized into 10 chapters, which describe the work as follows:

- Chapter 2 describes the design and construction of four full-scale BT-54 girder specimens that were cast to include simulated typical nonconformance issues.
- Chapter 3 details the repair techniques that were used to repair the simulated nonconformance issues. Specifically, the chapter includes general repair procedures, top flange repair procedures with serviceability validation experiments, and five bottom flange repair procedures (including retensioning) with small-scale validation tests.
- Chapter 4 describes the full-scale experimental setups for tests that were developed to isolate flexure, shear, and bond behaviors.
- Chapter 5, chapter 6, chapter 7, and chapter 8 present the test results for each of the four girders individually.

- Chapter 9 synthesizes the individual test data to provide a general discussion on the findings.
- Finally, chapter 10 summarizes the research project by including conclusions, recommendations, and draft guidelines.

A draft preliminary guide to use in place of, or as a revision to, SOP-3 that includes standardized repair procedures for common nonconformance issues based on the strength tests that were conducted in this research is provided in appendix K.

TEST NOMENCLATURE AND MATRIX

This research consists of four girder specimens (numbered 1 through 4) that are tested multiple times in either shear or flexure to characterize various repairs that were placed within the girder. The test number is formed by #.#.A, where the first number is the girder number, the second number is the test number that was performed on that girder, and the letter A is either "S" for a shear experiment or "F" for a flexure experiment. Within each test, specific repair(s) are considered. Those are numbered as #.#BCC, where the first number is the girder number; the second number is the repair number within the girder (see chapter 2); and the first letter, B, indicates whether the repair is on the "L" for left or "R" for right side of the girder. The final two or three letters, CC, indicate the portion of the structure being repaired: "BZ" for bearing zone, "TF" for top flange, "BF" for bottom flange, and "TFE" for top flange end.

For example, *1.4F repair 1.3RTF* would indicate that the fourth test of Girder 1 was a flexure test and repair 3 on the right-hand top flange is being considered.

Due to the complexity of this nomenclature, the test matrix is provided in table 1 for reference throughout the report.

Table 1. Test matrix.

Test Number	Girder Number	Behavior	Repair(s) Considered	Repair Notation
1.1.S	1	Shear	Left Bearing Zone	1.1LBZ
1.2.F	1	Flexure	Left Top Flange	1.2LTF
1.3.F	1	Flexure	Left Top Flange	1.2LTF
1.4.F	1	Flexure	Left Top Flange Right Top Flange	1.3LTF 1.3RTF
2.1.S	2	Shear	Right Top Flange Left Top Flange	2.1RTF 2.1LTF
2.2.S	2	Shear	Left Top Flange	2.2LTF
2.3.F	2	Flexure	Left Top Flange	2.3LTF
3.1.S	3	Shear	Right Bottom Flange Left Bottom Flange	3.1RBF 3.1LBF
3.2.S	3	Shear	Right Bottom Flange	3.2RBF
3.3.F	3	Flexure	Right Bottom Flange Left Bottom Flange	3.3RBF 3.3LBF
4.1.S	4	Shear	Left Bearing Zone Right Top Flange Left Top Flange Left Top Flange	4.1LBZ 4.1RTF 4.1LTF 4.4LTF
4.2.S	4	Shear	Right Bearing Zone Right Top Flange Right Top Flange End Left Top Flange	4.2RBZ 4.2RTF 4.2RTFE 4.2LTF
4.3.F	4	Flexure	Left Top Flange	4.3LTF

CHAPTER 2. FULL-SCALE SPECIMEN DESIGN

This chapter describes the design and construction of the four BT-54 girders that were used to simulate typical nonconformities.

NONCONFORMING GIRDER DESIGN

Based on a review of PCI MNL-137 and interviews with concrete industry professionals, the girders' nonconformity locations were determined to replicate the most common types of damage or construction errors encountered. Table 2 provides an overview of the nonconformance issues designed into the four BT-54 girders and how many times they occurred during the project. In total, 23 nonconformities were constructed into the girders.

Table 2. Overview of nonconformance issues designed into the four girders.

Nonconformance Issue	Number of Occurrences
Top flange damage at girder ends (<2 ft)	1
Top flange damage at girder ends (>2 ft)	1
Top flange damage NOT at girder ends (<2 ft)	3
Top flange damage NOT at girder ends (>2 ft)	9
Bulb damage in bearing zone (strands exposed)	3
Bulb damage NOT in bearing zone (strands exposed)	5
Bulb damage NOT in bearing zone (strands NOT exposed)	1

Determining the location of the nonconformities required estimating the potential extent of the damage resulting from the load applied during the experiment. In general, the experiments were designed to have three individual load tests per girder: one at each of the two beam ends (shear) and one at the midspan (flexure). Table 3 provides the nomenclature used to communicate the location of the repair within the girder designs. Figure 1 though

figure 4 depict the nonconformity locations of each girder, with a summary for each of the four beams in table 4 through table 7.

Table 3. Nomenclature for location within beam.

Location in Beam	Abbreviation
Right bearing zone	RBZ
Left bearing zone	LBZ
Right bottom flange	RBF
Left bottom flange	LBF
Right top flange	RTF
Left top flange	LTF
Right top flange end	RTFE

At the girder ends, nonconformities were planned in or near the bearing area or on the top flange, but generally not in both regions concurrently. In two bearing areas, strand retensioning was required before the repair could be made. In addition, top flange nonconformities were planned at varying distances from the point of bearing to examine the impact of shear. A similar protocol was followed such that nonconformities were placed at the midspan in either the bulb or the top flange but generally not in both. In some cases, nonconformities were placed on both sides of the girder to examine potential stability issues. Pictures of each nonconformity are found in appendix A.

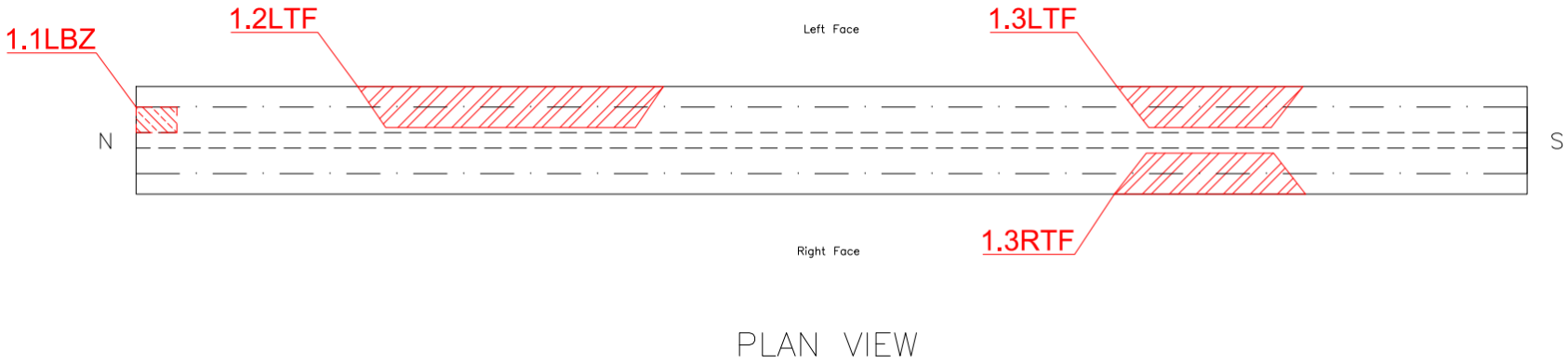

Figure 1. Schematic. Girder 1 nonconformity locations.

Table 4. Summary of Girder 1 nonconformities.

Repair Label	Location and Size	Research Intent
1.1LBZ	Left bearing zone (north end); 16 in. long, 10 in. deep, 5 in. tall	Investigate influence of repair in transfer and bearing regions. Typically, heavy reinforcement/congested area prone to honeycombing. In addition, investigate ability to retension end exposed prestressing strands after transfer. Repair depth exceeds MNL-137 limit.
1.2LTF	Left top flange (north end); 121.5 in. long, 16 in. deep, 5.75 in. tall	Investigate damage due to transportation and handling, tie downs on truck, or removal of formwork. Ability to compare flange repair strength to original flange capacity. Length exceeds current maximum repair length in MNL-137.
1.3RTF	Right top flange (south end); 75 in. long, 16 in. deep, 6 in. tall	Investigate damage due to transportation and handling, tie downs on truck, or removal of formwork. Ability to compare two flange repair strengths. Length exceeds current maximum repair length in MNL-137.
1.3LTF	Left top flange (south end); 74 in. long, 16 in. deep, 5.75 in. tall	

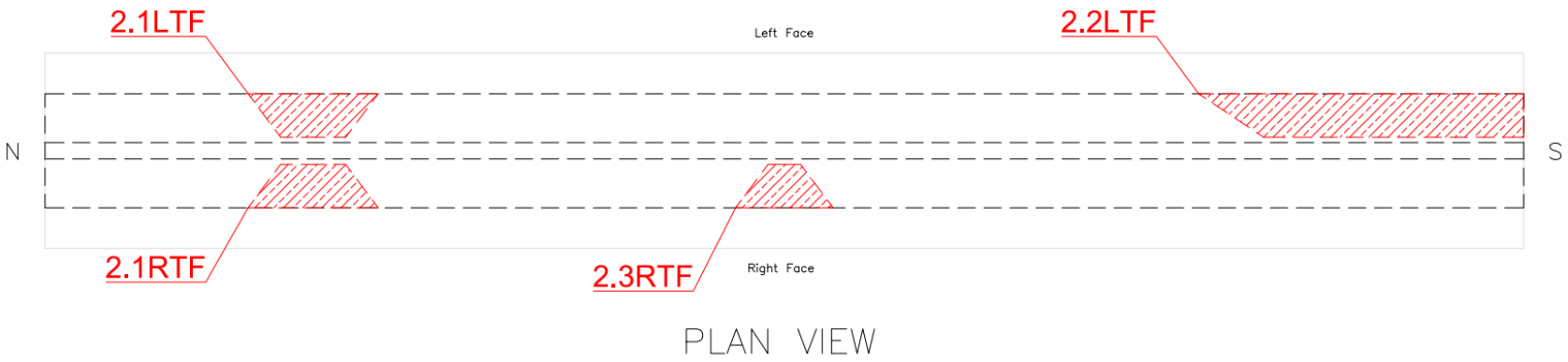

Figure 2. Schematic. Girder 2 nonconformity locations.

Table 5. Summary of Girder 2 nonconformities.

Repair Label	Location and Size	Research Intent
2.1RTF	Right top flange (north end); 53 in. long, 16 in. deep, 5.75 in. tall	Investigate damage due to transportation and handling, tie downs on truck, or removal of formwork. Ability to compare two flange repair strengths. Length exceeds current maximum repair length in MNL-137.
2.1LTF	Left top flange (north end); 51 in. long, 16 in. deep, 5.75 in. tall	
2.2LTF	Left top flange edge (south end); 126 in. long, 16 in. deep, 5.5 in. tall	Investigate damage on end of top flange due to transportation and handling, tie downs on truck, or removal of formwork. Length exceeds any current maximum repair length specified.
2.3RTF	Right top flange (midspan); 41 in. long, 16 in. deep, 5.625 in. tall	Investigate repair at location of maximum tensile stress on top flange. Length is within repair length limits of MNL-137.

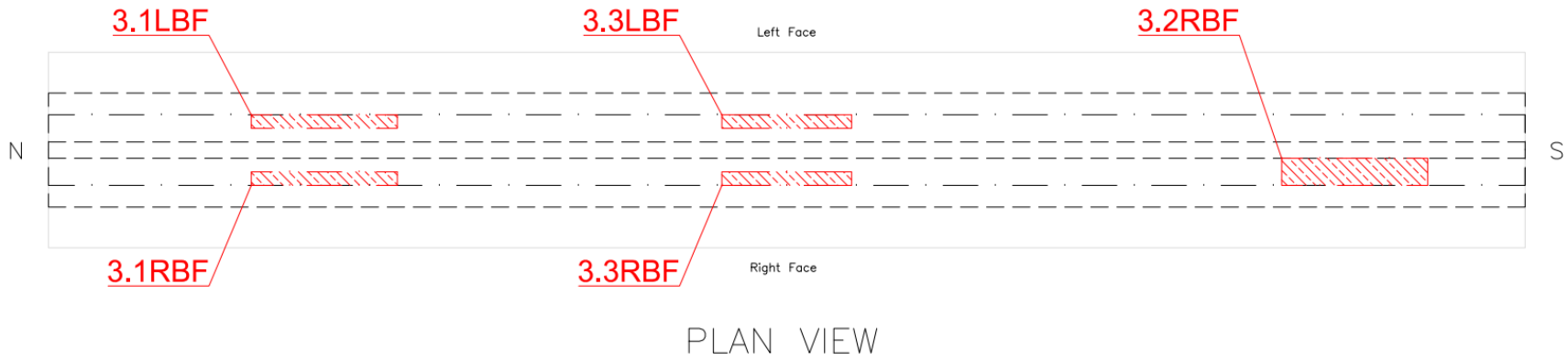

Figure 3. Schematic. Girder 3 nonconformity locations.

Table 6. Summary of Girder 3 nonconformities.

Repair Label	Location and Size	Research Intent
3.1RBF	Right bottom flange (north end) two bottom row strands exposed; 56 in. long, 5 in. deep, 9 in. tall	Investigate influence of commonly observed bottom flange area due to transportation and handling. Ability to compare different anchor methods in identical repairs. Length and depth match current MNL-137 repair length limit.
3.1LBF	Left bottom flange (north end) two bottom row strands exposed; 56 in. long, 5 in. deep, 9 in. tall	
3.2RBF	Right bottom flange (north end) two top row strands exposed; 54 in. long, 11 in. deep, 6.5 in. tall	Investigate performance of repair in development region after transfer of prestress. Length matches current MNL-137 repair length limit, but depth exceeds limit.
3.3RBF	Right bottom flange (midspan) two bottom row strands exposed; 50 in. long, 5 in. deep, 5 in. tall	Investigate influence of repair at location of maximum tensile stress on bottom flange. Ability to compare different anchor methods in identical repairs. Length and depth match current MNL-137 repair length limit.
3.3LBF	Right bottom flange (midspan) two bottom row strands exposed; 50 in. long, 5 in. deep, 7 in. tall	

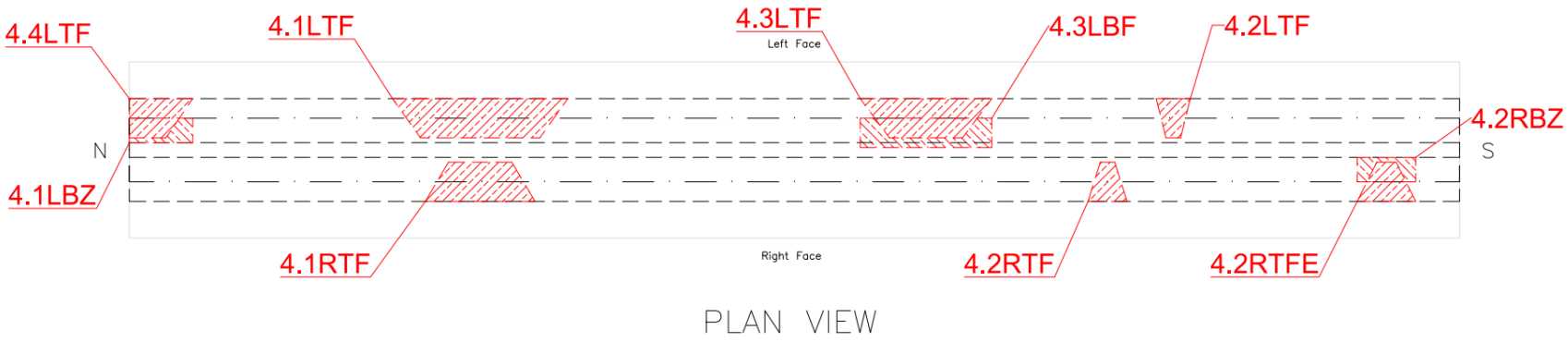

Figure 4. Schematic. Girder 4 nonconformity locations.

Table 7. Summary of Girder 4 nonconformities.

Repair Label	Location and Size	Research Intent
4.1LBZ	Left bearing zone (north end); 25 in. long, 10.5 in. deep, 6.5 in. tall	Investigate ability to retension end exposed prestressing strands after transfer and the repair's influence on transfer length. Repair depth exceeds MNL-137 limit.
4.1RTF	Right top flange (north end); 45 in. long, 16 in. deep, 5.25 in. tall	Investigate asymmetrical length damage on top flange due to transportation and handling, tie downs on truck, or removal of formwork. Both repair lengths exceed current MNL-137.
4.1LTF	Left top flange (north end); 72 in. long, 16 in. deep, 5.5 in. tall	
4.2RBZ	Right bearing zone (south end); 26 in. long, 7 in. deep, 4.5 in. tall	Investigate performance of bottom flange repairs made after transfer of prestress. Repair depth exceeds MNL-137 limit.
4.2RTF	Right top flange (south end); 14.5 in. long, 16 in. deep, 5.5 in. tall	Investigate top flange ability to support deck load during placement. Length is within MNL-137 limit.
4.2RTFE	Right top flange end (south end); 26 in. long, 16 in. deep, 5.5 in. tall	Investigate influence of top flange repair located directly above bottom flange repair. Length is within MNL-137 limit.
4.2LTF	Left top flange (south end); 15.5 in. long, 16 in. deep, 5.375 in. tall	Investigate top flange ability to support deck load during placement. Length is within MNL-137 limit.

Table 7. Summary of Girder 4 nonconformities (continued).

Repair Label	Location and Size	Research Intent
4.3LBF	Left bottom flange (midspan); 54-in. long, 16-in. deep, 2-in. tall	Investigate bottom flange repair with no exposed reinforcement to anchor to due to poor consolidation of concrete on the bottom of the girder.
4.3LTF	Left top flange (midspan); 55-in. long, 16-in. deep, 5.5-in. tall	Investigate influence of top flange repair located directly above bottom flange repair. Length exceeds MNL-137 limit.
4.4LTF	Left top flange edge (north end); 26-in. long, 16-in. deep, 5.5-in. tall	Investigate damage on end of top flange due to transportation and handling, tie downs on truck, or removal of formwork. In addition, investigate influence of top flange repair located directly above bottom flange repair. Length within MNL-137 limit.

An 8-in.-thick and 6-ft-wide concrete deck was used on Girders 2, 3, and 4, using the standard GDOT 3,500 psi deck mix.[14] A deck was not placed on Girder 1 to allow comparison of a repaired flange to one that was undamaged. The deck dimensions were selected to replicate a standard GDOT concrete deck placed on girders spaced at 6 ft apart. A deck allowed for testing of the currently accepted top flange repair method, which requires installation of a "c-bar" fastened into the damaged flange area and extending up into the deck. Inclusion of a deck yields more typical flexural strain distribution as well as the opportunity to examine interface shear between the top flange repair and the deck.

NONCONFORMING GIRDER SPECIMEN CONSTRUCTION

The construction of the girder specimens was accomplished at Standard Concrete Products (SCP) in Atlanta, Georgia, per the schedule shown in table 8. All four BT-54 girders were constructed concurrently in accordance with current GDOT specifications per the designs included in appendix B. The girders were each 45.5 ft long and constructed with the GDOT 8,000-psi mix design having designation 8000GA.[15] Weather conditions were overcast and dry with daily temperatures ranging from 80 to 90°F. Concrete cylinders were cast for each batch of concrete prior to detensioning. Appendix C provides the concrete mixture proportions and cylinder strength test data.

Table 8. Girder construction schedule.

Date	Event
May 10, 2024	Prestressing strand tensions and ductile reinforcement installed
May 13, 2024	Block outs installed in girders to create nonconformities
May 14, 2024	Formwork installed and concrete placed
May 15, 2024	Formwork removed and strands detensioned

Following strand tensioning and ductile reinforcement installation, block outs to simulate nonconformities were installed using sections of rigid insulation, spray foam insulation, and thin sheets of Masonite hardboard. Nonconformities on the top flanges were created following formwork installation. Figure 5 through figure 10 depict examples of block outs at various locations on the girders prior to placing concrete and following formwork removal. The process used to create block outs proved very effective and is recommended for any similar future research efforts.

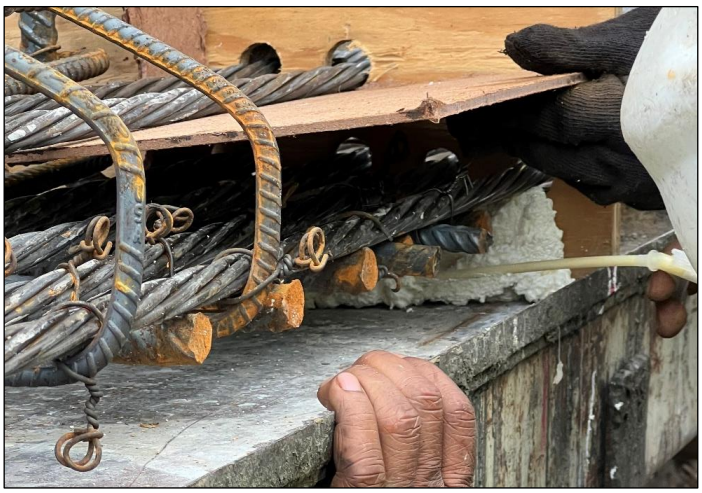

Figure 5. Photo. Typical bearing area block out.

Figure 6. Photo. Typical bottom flange block out.

Figure 7. Photo. Typical top flange block out.

Figure 8. Photo. Typical bottom flange block out after formwork removal (end view).

Figure 9. Photo. Typical bottom flange block out after formwork removal (top view).

Figure 10. Photo. Typical top flange block out after formwork removal.

Following strand detensioning, the girders were transported to the Georgia Tech Structural Engineering and Materials Laboratory (SEML) on May 17, 2024, as shown in figure 11.

Figure 11. Photo. BT-54 girders in the Georgia Tech SEML.

CHAPTER 3. FULL-SCALE SPECIMEN REPAIR

This chapter presents the methods that were used to repair the nonconformances that were constructed into the girders. First, the general girder preparation is discussed, followed by the top flange repair techniques. As part of the top flange discussion, a serviceability (deflection) validation test is included. Next, the bottom flange repair is discussed, including a set of "mini girder" experiments that were used to validate the procedure. After the top and bottom flange repairs, a section on the epoxy testing is included.

PREPARATION FOR REPAIR

The preparation for girder repair consisted of removal of spray foam insulation from bottom flange repairs, as well as Masonite and plywood block outs (see figure 12).

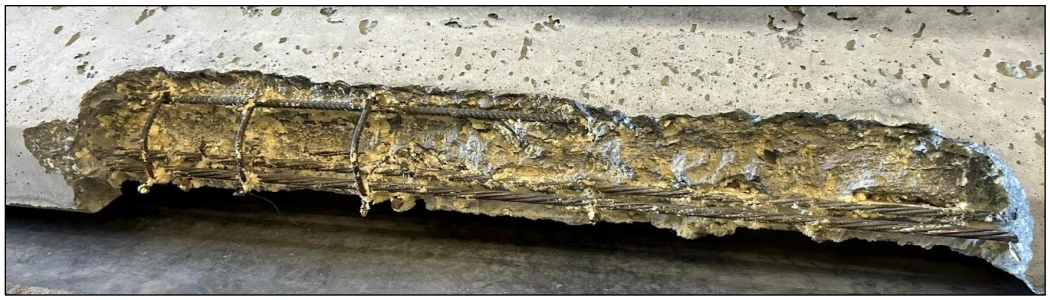

Figure 12. Photo. Spray foam block out in girder repair section before cleaning.

The removal of spray foam was facilitated using steel wire brushes attached to a cordless hammer driver-drill. Spray foam was removed until the concrete surface was visible. Then, the bottom flange repair surface was chipped with a rotary hammer tool to obtain a 0.25-in. amplitude surface (see figure 13).

Figure 13. Photo. Spray foam block out in girder repair section after preparation.

For the top flanges, the block outs were removed at SCP, and the surface of the repair areas was roughened at 0.25-in. amplitude as well (see figure 14).

Figure 14. Photo. Top flange repair surface preparation.

For surface preparation of the flange repairs, MNL-137 Chapter 4, "Methods of Patching," was used.[(1)] The concrete replacement method was chosen as the best, most common, and practical option. The surface of the bottom flange repair areas was cleaned as thoroughly as possible with the use of steel wire brushes. MNL-137 suggested using a stiff wire brush to remove debris and then water blasting and/or sandblasting the repair area; however, water blasting nor sandblasting were viable inside the laboratory space. The repair area

surface was roughened to a 0.25-in. amplitude to improve the shear friction between the existing concrete surface and the new concrete surface that was placed as the repair (see figure 15).

Figure 15. Photo. Roughened 0.25-in. amplitude surface.

TOP FLANGE REPAIR METHODS

The main repairs were top flange concrete replacement with epoxy-anchored steel reinforcement and bottom flange concrete replacement with a combination of post-installed anchors, epoxy, and/or retensioning of strands. Concrete replacement was chosen as the method of patching based on it being a standard method of repair in the industry that is the fastest, easiest, and least complex to carry out successfully. This section will focus on the top flange repair method.

Several initial steps were necessary to replace the top flange with concrete. As mentioned, the process required the surface of each repair section to be cleaned and chipped to 0.25-in. amplitude. Then, post-installed concrete anchors needed to be placed. Formwork that matched the existing flange shape had to be created as well. Lastly, on the day of casting, a two-part epoxy bonding agent had to be layered on the repair section. Before casting,

several concrete trial batches were performed to ensure the concrete replacement would match the existing girder concrete in strength.

The use of post-installed steel anchors was chosen for the top flange repair because it was an existing method of repair at SCP. The post-installed steel anchors were #3 reinforcing c-bars (see figure 16).

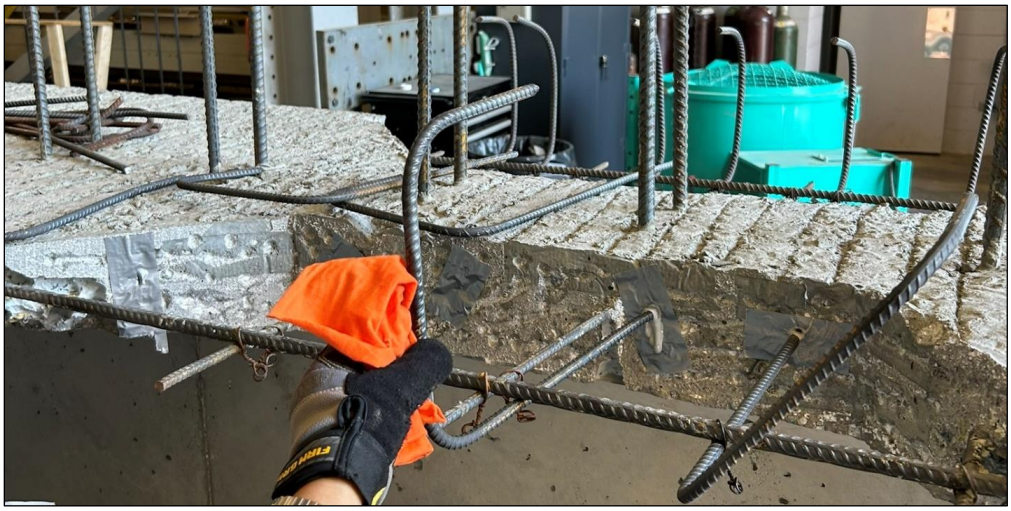

Figure 16. Photo. C-bar post-installed steel anchor.

The c-bars were bent using a rebar bender. To install the bars into the girder, 0.5-in.-diameter holes ranging from 3- to 4-in. deep were drilled into the top flange web section (see figure 17). Where possible, the holes were spaced at approximately 6 in.

Figure 17. Photo. Drilled holes for c-bars.

To anchor the c-bars into the drilled holes, a two-part epoxy anchor, Unitex Pro-Poxy 300 was used. This two-part epoxy complies with the GDOT-approved epoxy list. The drilled holes were cleaned using pressurized air with a long tube attachment that was able to reach the depth of each drilled hole. After it was cleaned once with air, a long, thin nylon brush was used to loosen any concrete residue in the hole. Once it was brushed, the drilled hole was cleaned again with the pressurized air attachment.

To install the c-bars, the two-part epoxy was inserted into the hole and filled about halfway. Then the c-bars were pushed in and held in place by one person, while another person secured it in its final position with rebar ties (see figure 18 and figure 19). The next step was to create formwork that matched the existing flange shape (see figure 20). A gap found between the angled portion of the formwork and where the top flange bevels into the web was filled using 0.25-in. foam weather stripping. The bottom of the formwork was secured in place with the use of sandbags to avoid any accidental movement of the formwork.

Figure 18. Photo. Insertion of two-part Unitex Pro-Poxy 300 into cleaned drilled holes.

Figure 19. Photo. C-bar installation.

Figure 20. Photo. Top flange repair formwork.

For the top flange repairs, the concrete mix used as the concrete replacement (for patching) was the same design mix used to cast the BT-54 prestressed concrete girders at SCP. This was done to match the repair strength to the concrete compressive strength of the girder. Standard Repair Procedure 6 in the MNL-137 encourages the concrete compressive strength of the repair to meet or exceed the existing concrete girder design strength.[1] The concrete batches were mixed at the SEML using 0.75-in. normal weight crushed stone aggregate, normal weight natural sand, and the following Sika admixtures: ViscoCrete-2100, Plastiment XR, AEA-14, and ViscoFlow-2020.

Each batch was 2 ft^3 and mixed using an Eirich R08W concrete mixer (see figure 21). The mix design for the three girders with top flange repairs is provided in appendix D. The mix design procedure consisted of mixing the coarse and fine aggregate together for 2 min, adding the cement and mixing for another 1–2 min, and adding the water with admixtures and mixing for approximately 3–4 min. The mix time after adding the water varied depending on the desired slump for the mix.

Four concrete trial batches were conducted before casting the top flange repairs to ensure that the repair concrete mix strength matches the design mix strength of the girder. Concrete cylinders measuring 4 in. × 8 in. were cast for each trial batch. For the second trial batch, cylinders were tested at 1, 3, 7, 14, 21, and 28 days to observe the strength increase behavior of the concrete. For testing all concrete cylinders, ASTM C39 guidelines were followed.[16] The strength data for all concrete cylinder tests can be found in appendix D. Once the strengths from the trial batches were consistent (around 12,000 psi) and the top flange sections were ready to be repaired, concrete replacement in the top flanges was performed.

Figure 21. Photo. Concrete mixing 2-ft^3 batches with Eirich mixer.

A bonding agent is recommended in MNL-137 Standard Operating Procedure 6. Therefore, on casting day before the concrete was poured, a two-part epoxy bonding agent, Sikadur-32, was coated on the repair surface to help the fresh concrete bond to the existing concrete. Each repair surface was cleaned with pressurized air before placing the epoxy coat, ensuring the surface was free of any dust or loose particles. Following the manufacturer's instructions for the epoxy was crucial to obtaining the correct bond strength from the product. Once the layer of epoxy bonding agent was placed on the repair surface, the concrete needed to be placed almost immediately to ensure the epoxy remained tacky during casting (see figure 22).

For repairs that were completed with more than one batch, the epoxy was constantly checked for tackiness before placement. If it was no longer tacky, a new layer of epoxy was added, as suggested by the manufacturer's instructions.

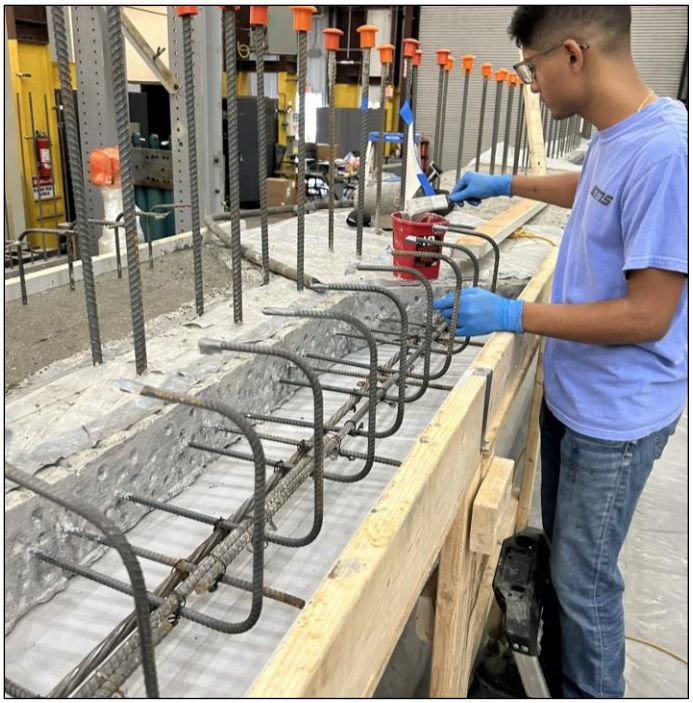

Figure 22. Photo. Placement of Sikadur-32 bonding agent layer.

Girder 2 was repaired first because it only had top flange sections to repair, followed by Girder 1 and then Girder 4. Girder 4 had the greatest number of top flange repairs. The sequence of casting top flange repairs was tightly followed because there were two time-dependent factors: the concrete batch and the epoxy bonding agent. The epoxy bonding agent was layered immediately before the water was added to the concrete batch; thus, as the epoxy bonding agent layer coating was completed, the concrete was on its way to the patch. This was possible for most smaller patches, but it became more difficult for larger patches because they required more concrete batches and therefore more time. In these instances, epoxy needed to be reapplied.

While the repairs were being cast, concrete cylinders were being made simultaneously. A slump test was performed prior to placing each repair, as well. ASTM C143 was also

followed to test the slump.[17] The measured slump for each concrete batch is provided in appendix D.

As the concrete was being placed in the repair area, it was vibrated using a 1-in.-diameter concrete vibrator. After placement, the top of the concrete repair was screeded with a 2-in. × 4-in. wooden plank to smooth the surface. After 30 min to 1 h, the surface of each concrete repair was roughened to match the 0.25-in. deep lines seen on the top existing girder surface (see figure 23).

Figure 23. Photo. Concrete repair surface grooves matching girder top flange.

After the grooves were created on the repair surface, damp burlap was placed to cover the fresh concrete. A layer of polyurethane plastic was placed to cover the burlap. These two steps ensured the fresh concrete repair cured in moist curing conditions (see figure 24). The top flange repairs were demolded 48 h after the cast (see figure 25).

Figure 24. Photo. Concrete curing conditions for top flange repair.

Figure 25. Photo. Demolding of top flange repair.

Summary of Top Flange Repair Process

The process of each top flange repair is summarized as follows:

1. Clean and chip the concrete surface to 0.25-in. amplitude.

2. Drill ¼-in.-diameter (⅛-in. larger diameter than the bar size), 4-in.-deep holes (at least 10 times the bar diameter), spaced at 6 in. apart.
3. Clean the drilled holes with pressurized air and a nylon brush.
4. Install #3 c-bars with two-part Unitex Pro-Poxy 300 as the bonding agent.

   Note: Bend the c-bars to ensure a reinforced connection between the deck and the repair.
5. Construct formwork to match the existing top flange shape.
6. Run concrete trial batches until the concrete compressive strength meets the existing girder strength.
7. When casting, layer a coat of Sikadur-32 two-part epoxy bonding agent on the repair surface.
8. Cast the concrete replacement while the bonding agent is still tacky.
9. Create grooves on the top surface to match the existing girder top surface and cure the concrete repair in moist curing conditions.

SERVICEABILITY VALIDATION OF TOP FLANGE REPAIRS (TOP FLANGE DEFLECTION TESTS)

The serviceability of the repair was verified to confirm whether the deflection was consistent across the repairs under the expected construction loads. A 250-lb point load and a 50-psf distributed load were used for this testing based on general guidelines from a GDOT bridge engineer. The point load was recreated with a person's weight plus a sandbag (see figure 26). The distributed load was recreated using 40-lb and 60-lb sandbags (see

figure 27). Deflections were measured using dial gauges attached to 2-in. × 4-in. posts. These posts were spaced uniformly across the length of each repair, and the number of posts varied based on the length of the repair. The posts were secured in place using sandbags (see figure 28).

Each repair section was tested with the point load and distributed load located directly on top of the repair and then on the other side of the top flange to check the negative and positive deflection values of the repair, respectively. Measurements were taken on both sides of the top flanges (i.e., readings on the flange side that was loaded, and readings on the flange side that was not loaded). Initial measurements of the dial gauges were taken pre-load. The 250-lb point load was placed at the center span of the top flange repair area, at the very edge of the section.

Figure 26. Photo. Point load of 250 lb on the top flange.

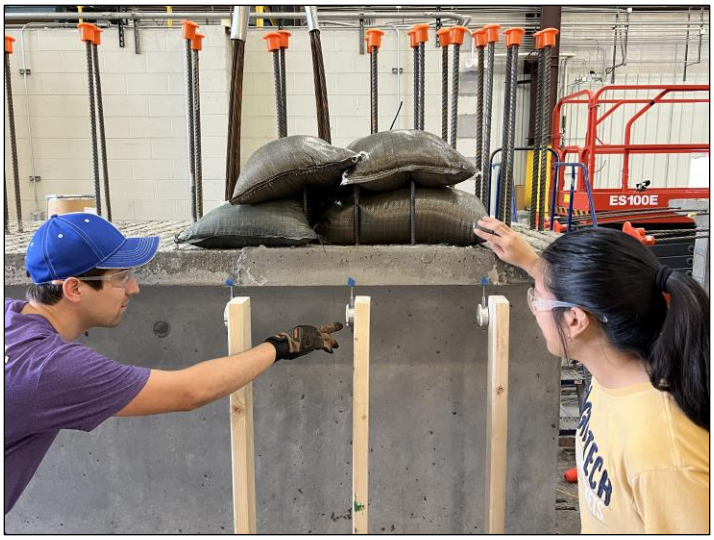

Figure 27. Photo. Distributed load of 50 psf on the top flange.

Figure 28. Photo. Dial gauge post secured with sandbags.

The deflection data for the top flange repair serviceability test can be found in appendix E. There were no signs of failure, and the girder patches remained unchanged after these validity load tests. Based on the results from the serviceability tests, it was concluded that the repairs act compositely with the existing sections.

SMALL-SCALE VALIDATION OF BOTTOM FLANGE REPAIRS (MINI GIRDERS)

Prior to conducting repairs on the full-scale girder specimens, repair methods were tested on small-scale girder specimens. These small-scale girder specimens reflected the geometry proportions of the bottom flange of a BT-54 prestressed girder. The small-scale girder specimens are referred to as "mini girders" throughout this report.

The mini girders were constructed to ensure correct bottom flange repair methods were implemented on the full-scale girder specimens to practice concrete removal, chip-hammering, placement repair with self-consolidating concrete (SCC) in areas with congested reinforcement, and attachment or repair reinforcement into congested areas. From prior investigation, bottom flange repairs are more difficult due to close spacing of prestressing strand, dog house bars, and non-prestressed reinforcement along with low cover. Two mini girders were built with bottom flange voids that mimic the nonconformances seen in the full-scale girder specimens. Voids were created using rigid foam block outs (see figure 29).

The dimensions of the mini girders were 4 ft long, 18 in. tall, and 12 in. wide on the bottom. The web portion was 6 in. thick, like that of a BT-54 girder. Number 4 reinforcing bars represented the 0.6-in.-diameter prestressing strands. Figure 30 through figure 39 illustrate the mini-girder construction and repairs.

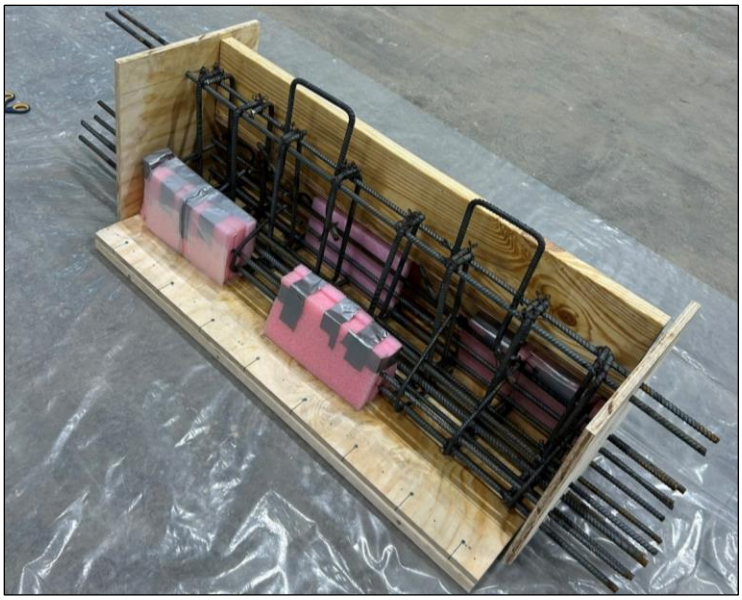

Figure 29. Photo. Foam block outs to create bottom flange voids in the mini girders.

Figure 30. Photo. Mini girder construction using the same concrete mix as used in the full-size BT-54 girders.

Figure 31. Photo. Mini girder nonconformance representing conditions comparable to repair 3.1RTF.

Figure 32. Photo. Chip hammer practice.

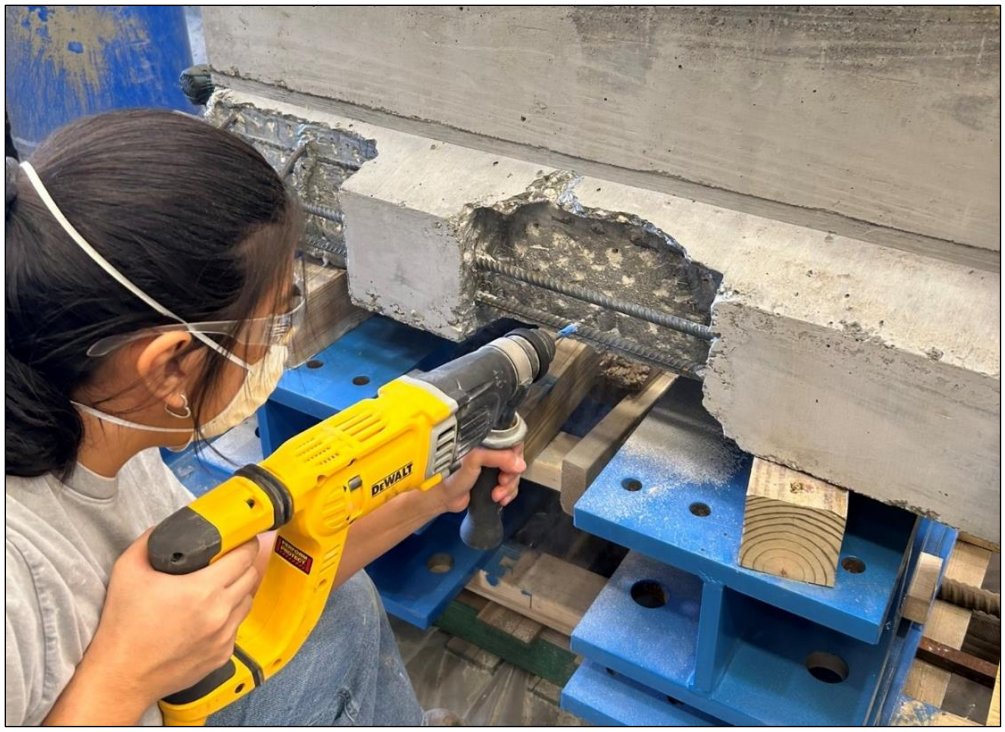

Figure 33. Photo. Practice hammer-drilling pilot holes for concrete anchors between closely spaced reinforcement.

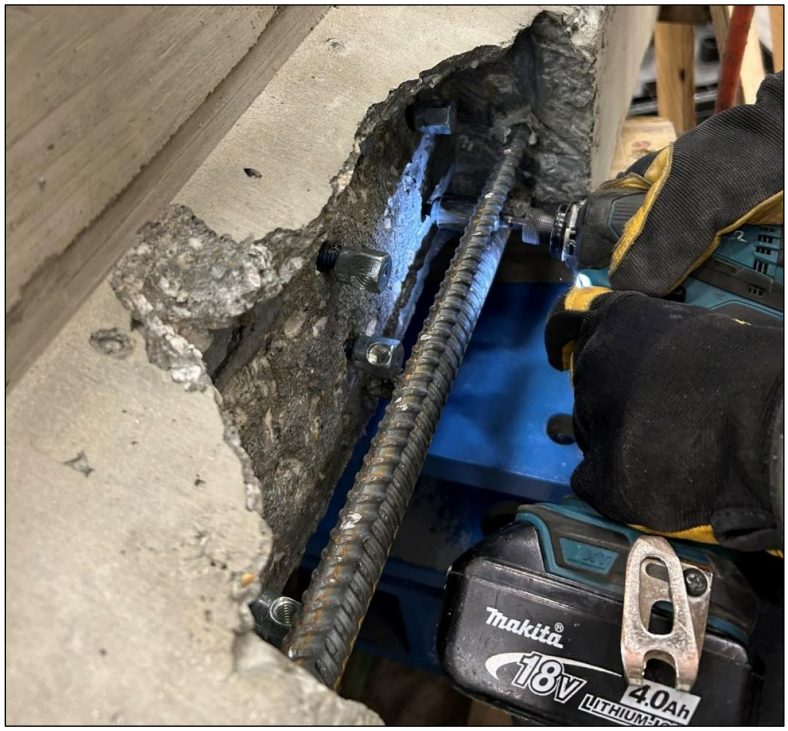

Figure 34. Photo. Practice installation of concrete anchors with holes in heads.

Figure 35. Photo. Practice installation of 12-gauge wire fed through the concrete anchor holes on longitudinal reinforcement.

Figure 36. Photo. A 12-gauge wire installation studied as an alternate to reinforcing bars originally recommended by MNL-137.

Figure 37. Photo. Installation of the epoxy bonding agent.

Figure 38. Photo. Finishing the SCC repair surface with a trowel for Mini Girder 1.

Figure 39. Photo. Bottom flange repair on Mini Girder 1 using the SCC mix.

Nineteen days after the repair, the mini girder bottom flange repairs were tested by impact with a 16-lb sledgehammer. Each patch was struck three times, with the sledgehammer being dropped from different heights. A measuring tape was used to help locate the height of each sledgehammer drop. Figure 40 shows a sledgehammer drop test on a mini girder patch with anchors. For all mini girder repairs, minimal surface chipping (see figure 41) was noted after the height-controlled sledgehammer drops.

After the height-controlled sledgehammer drops were completed, more intense sledgehammer impacts were conducted on the mini girder patches. During these impacts, corners of the edge repairs broke off (see figure 42), indicating that the patch did not dislodge from the mini girder. The corner spalling allowed viewing of the SCC cross-section and confirmed proper consolidation of the repair concrete.

Figure 40. Photo. Strength and efficacy test of 12-gauge wire reinforcement and concrete anchors by striking with a 16-lb sledgehammer.

Figure 41. Photo. Minimal surface chipping after sledgehammer impact. The sledgehammer did not crack or dislodge the patch.

Figure 42. Photo. Intense sledgehammering removed corner concrete and demonstrated good consolidation of concrete around the reinforcement and 12-gauge wires.

In summary, the two mini girder experiments demonstrated that the forming system, concrete placement, Tapcon screw anchors, and 12-gauge wire reinforcement performed well. This repair construction technique was used for the full-scale bottom flange repairs.

BOTTOM FLANGE REPAIR METHODS

The project included five types of bottom flange repairs. Method 1 for bottom flange repair was where post-installed steel anchors and wire were installed along with epoxy bonding agent. In Method 2, only epoxy bonding agent was applied, and in Method 3, only post-installed steel anchors and wire were installed. Method 4 was repairs where neither post-installed steel anchors nor epoxy were used. Method 5 was repairs in the bearing region of the girder that required retensioning of strands.

MNL-137 Standard Repair Procedure 4 states that patches located over traffic must have reinforcement or additional anchoring devices.[1] Therefore, additional concrete anchoring was used for patches that had minimal or no reinforcement. These concrete anchors were Tapcon screw anchors with 12-gauge galvanized wire.

SCC was used for all the bottom flange repairs. It had a design strength of 8,000 psi, which matched the specified girder design strength. SCC was chosen as the concrete suited for the concrete replacement due to the need for a highly flowable, small-aggregate concrete mix. Batches of 2 ft^3 were mixed using the Eirich mixer in the SEML. The concrete mix design varied from the top flange repair mix design because aggregate sizes were required to be smaller to permit flow between the prestressing strands. Normal-weight natural sand, #89 crushed stone, and #7 crushed stone were used in the SCC mix. In addition to the cement, fly ash type C was used as a secondary cementitious material to prevent concrete bleeding and segregation.

Three trial batches were conducted to test the flowability and compressive strength of the mix. The mini girders were then repaired with SCC. For every batch of SCC, an inverted slump cone test was performed to check the spread of the mix (see figure 43). The procedure in ASTM C1611 was followed for these tests.[18] Concrete cylinders (4 in. × 8 in.) were cast for each batch of SCC used in the bottom flange repairs. Cylinders (3 in. × 6 in.) were also cast for one batch to compare the concrete compressive strength difference given by the two cylinder sizes. Concrete compressive strength data are provided in appendix F for all SCC batches. GDOT Research Project 2042 on SCC and the associated thesis were key references for SCC design mixes, sampling procedures, and other items related to SCC.[19]

Figure 43. Photo. Inverse slump cone test for the SCC mix.

Bottom Flange Repair Method 1: Post-installed Anchors with Epoxy Bonding Agent

After the surfaces of the repair areas were cleaned and chipped, pilot holes were drilled for the stainless steel Tapcon concrete screw anchors. The Tapcon dimensions were 0.25 in. diameter × 1.75 in. long. Per the manufacturer installation instructions, 0.1875-in.-diameter pilot holes were drilled. The holes were drilled with the use of a rotary hammer drill (see figure 44).

Figure 44. Photo. Drilling pilot holes for stainless steel Tapcon concrete anchors.

Pilot holes were drilled in a single row, avoiding reinforcing steel and prestressing strand. Some holes needed to be drilled about 0.5-in. from the anticipated location, due to the surface roughness of the repair and the inability for the hammer drill to be exact. After the pilot holes were drilled, they were cleaned with pressurized air to help the Tapcon not get stuck. The Tapcon were installed using an impact driver.

At times, it was difficult to install the Tapcon past a 1-in. depth. Some Tapcon would strip and not anchor correctly; those that did not anchor correctly were removed and replaced with a new Tapcon. After the Tapcon were installed, the 12-gauge galvanized wire was installed (see figure 45). This galvanized wire provided anchorage for the new bottom flange concrete. One end of the wire was coiled three times around the Tapcon, and the other end of the wire was coiled twice around an interior prestressed strand. This was done using a pair of pliers and wire cutters. Some areas of the bottom flange repairs had doghouse bars, and others did not. The use of Tapcon and wire anchors was focused in areas where there was little to no existing reinforcement. Figure 46 shows a repair case where the Tapcon and wire anchors were only installed on about half of the repair length.

Figure 45. Photo. Installing 12-gauge galvanized wire.

Figure 46. Photo. Post-installed steel anchors and wire in a bottom flange repair.

Bottom Flange Repair Method 2: Epoxy Binding Agent Only

For the second bottom flange repair method, repairs with only epoxy bonding agent (i.e., no post-installed anchors) were constructed. The repairs with and without anchors were almost identical. Two 52-in.-long repairs were made using only the epoxy bonding agent with the concrete replacement (see figure 47 and figure 48).

Figure 47. Photo. Bottom flange repair 3.1RBF with no post-installed anchors.

Figure 48. Photo. Bottom flange repair 3.2RBF with no post-installed anchors.

For the bottom flange repairs, especially repair 3.1RBF, implementing the concrete replacement was difficult because there was no access point from above to pour the concrete. A takeaway from practicing on the mini-girder repairs was the need for the formwork to be removed and installed again in a quick turnaround time, particularly in cases where epoxy bonding agent was applied. Therefore, formwork for each of the bottom

flange repairs was custom-made for each repair. For Girder 3, epoxy bonding agent was used on all the repairs. The bonding agent was mixed as the water was added to the concrete mix. Then, it was layered on the target repair area simultaneous to the performance of the flow test for each SCC concrete batch. The epoxy bonding agent was applied with a 2-in. nylon brush, avoiding the reinforcement as much as possible during the application. Figure 49 shows the two-part epoxy bonding agent application.

Figure 49. Photo. Coating a bottom flange repair with Sikadur-32 epoxy.

Upon completion of the two-part epoxy bonding agent application, the formwork was reassembled. Two kinds of concrete pouring holes were included in the formwork: top pour and chimney. The top pouring hole was where the top of the repair was exposed and concrete was able to flow into the repair (see figure 50). Another lesson learned from repair of the mini girders was that confirmation was needed on whether the concrete was filling the repair void adequately. To permit viewing of the concrete installation, clear polycarbonate sheets were used for formwork (see figure 50).

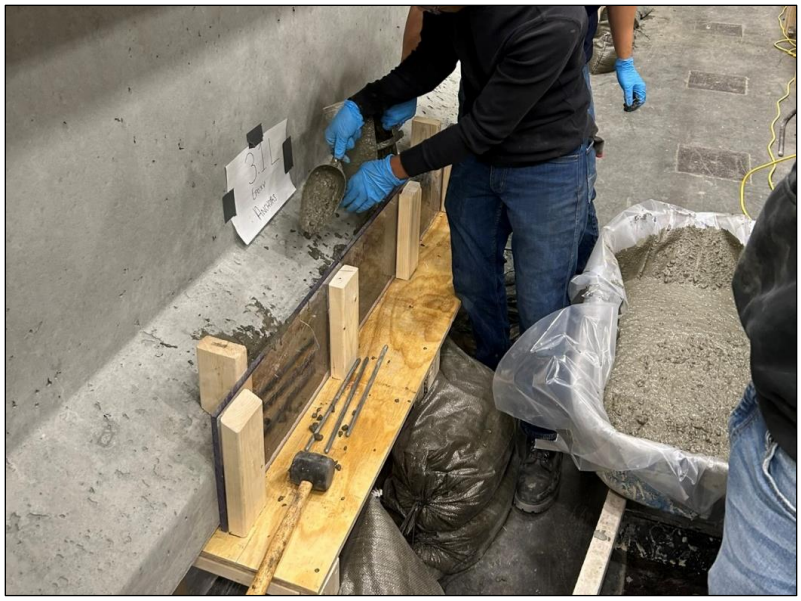

Figure 50. Photo. Placing concrete through the exposed top of a repair with polycarbonate formwork for viewing.

The second type of pouring hole practiced was the chimney, as suggested by MNL-137 Chapter 4, Section C.[1] In this process, SCC was poured into a "chimney." As the repair void was filled, an exit/vent hole would allow air to escape, ensuring the concrete filled the void completely and no air was entrapped. However, this method required more patience than the top pouring hole because the flow of SCC varied by batch. Thus, steel rods were used to help the concrete flow through the chimney. Rubber mallets were also used to vibrate the forms and help the concrete flow easier (see figure 51). The air vent consisted of $^{3}/_{16}$-in. holes drilled through the top surface of the bottom flange (see figure 52).

Figure 51. Photo. Vibrating the formwork with a rubber mallet.

Figure 52. Photo. SCC flowing out of the air vent and through the drilled hole, indicating complete concrete replacement in the repair.

When the concrete was visible through the drilled hole and flowed out of the air vent, it was confirmed that the repair void was filled. The clear polycarbonate formwork sections allowed for easy inspection of the fresh concrete repair. Some repairs were able to be

finished on the top surface after 30 min, but others were not accessible. Because only a small part of the top surface was exposed, damp burlap was not used to cover these repairs. Typically, after a day of curing, the formwork was removed from these repairs. Figure 53 shows the process of removing formwork from repair 3.3RBF.

Figure 53. Photo. Demolding of repair 3.3RBF.

It was more difficult to remove the formwork on the repairs with a chimney due to the leftover concrete that was in the chimney and air vents. Therefore, more force (e.g., use of hammers) was employed to remove this formwork. Figure 54 shows repair 3.1RBF, a repair with a chimney pouring hole, after the formwork was removed. The center concrete bulge was later reduced with a chisel.

Figure 54. Photo. Repair 3.1RBF with a chimney pouring hole after demolding.

Bottom Flange Repair Method 3: Post-installed Anchor and Wire Only

The third repair method consisted of only post-installed steel anchors and no epoxy bonding agent. This type of repair was used only in Girder 4 repair 4.3L. Epoxy bonding agent did not seem practical to use in this repair due to its large surface area, shallow depth, and inconvenient location. Placing a layer of epoxy coating and then speedily installing and securing the formwork would have been difficult because this repair is directly on the bottom of the girder. No exposed reinforcement was available to anchor the repair concrete, so post-installed anchors were necessary. MNL-137 suggests anchoring concrete repairs that are located above traffic to reinforcement.[(1)] However, the location of this repair region was heavily congested with a full row of prestressed strands on the bottom of the flange. This left little to no access for large reinforcement bars to be drilled and anchored into the girder safely without hitting any of the prestressing strands. Instead of the larger bars, stainless steel Tapcon and 12-gauge galvanized wire were placed in an approximate 6-in. × 4-in. grid. Three rows of eight Tapcon were installed, with at least 1 inch of depth. The girder was required to be lifted off the ground to install these anchors. Figure 55 shows the process of installing the Tapcon with an impact driver.

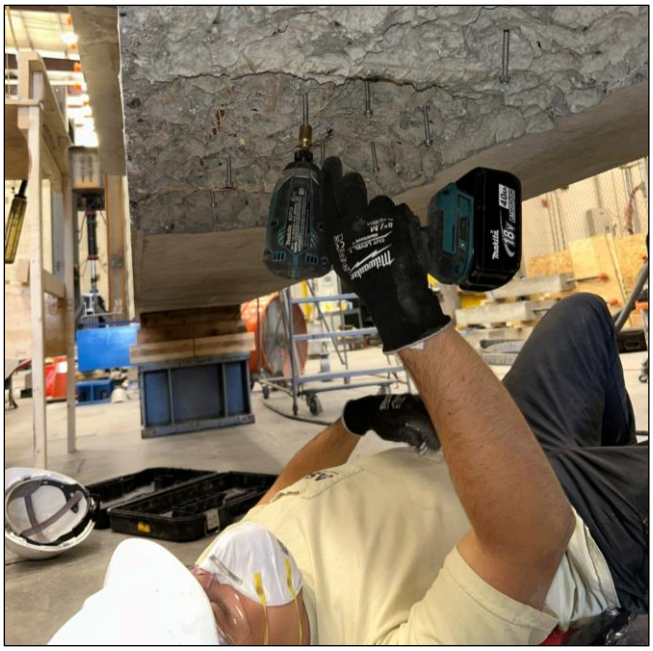

Figure 55. Photo. Installing stainless steel Tapcon into the congested repair.

Similar to the Method 1 bottom flange repairs, some anchors that did not anchor in tightly enough were removed and replaced with a new anchor. After all the anchors were secured, 12-gauge galvanized wire was coiled around each Tapcon, forming a grid (see figure 56). A pair of pliers was helpful in this process.

Figure 56. Photo. Stainless steel Tapcon and galvanized wire grid.

The concrete replacement for all bottom flange repairs consisted of SCC with a design strength of 8,000 psi, matching the design strength of the girder. However, for most SCC batches, like the girder concrete, the concrete compressive strength was tested to be higher than the design strength. Using SCC for the bottom flange repairs was helpful because most bottom flange repairs required easy-flowing, small-aggregate concrete. This was due to the high rebar congestion present in some of the repair areas, as well as the shallow depth of some of these repairs.

Aside from SCC, a small trial of SikaEmaco 425 Gel Patch mortar was performed on repair 4.3LBF. This quick-setting non-sag concrete repair mortar was mixed according to the manufacturer's instructions and placed in small (maximum 2-in.) lifts onto the overhead repair. The surface of the concrete repair was dampened with a spray bottle to help the mortar adhere. However, upon placing the mortar, it would slowly detach from the overhead surface. To mitigate this, thinner 1-in. patty-like lifts were placed. These smaller lifts needed to be thoroughly molded into the crevices of the overhead surface to prevent them from detaching and falling. With a workability of only 20–30 min, it was difficult to fill a decent portion of the repair. Therefore, only a small section of repair 4.3LBF contained this type of concrete repair mortar (see figure 57).

The remaining void on repair 4.3LBF was filled with SCC. The formwork consisted of two chimneys to pour concrete into due to the large size of the repair. The one air vent for this repair was located on the midspan of the repair. The casting procedure was the same as the previous bottom flange repairs, except no epoxy bonding agent was applied. A rubber mallet was used to help spread the concrete throughout the void. Figure 58 shows repair 4.3LBF during the concrete casting.

Figure 57. Photo. SikaEmaco 425 Gel Patch non-sag concrete repair mortar on repair 4.3LBF.

Figure 58. Photo. Repair 4.3LBF during concrete casting.

Concrete was cast until it was seen exiting the air vent slot. Because only the two chimneys were exposed, burlap and plastic were not used to cover this repair while curing. Formwork

was removed the next day. Once again, hammers and extra force were needed to remove these forms due to the extra concrete held in the chimneys. Figure 59 shows repair 4.3LBF after demolding.

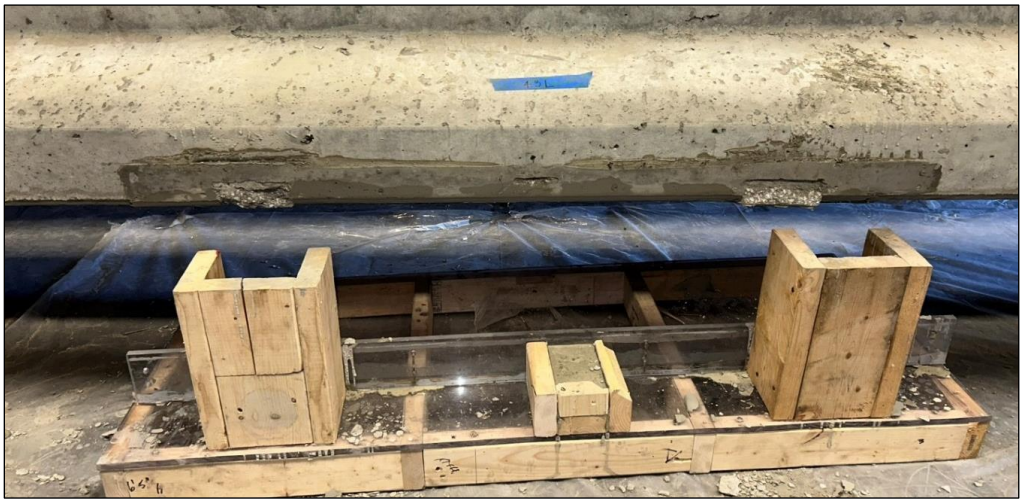

Figure 59. Photo. Repair 4.3LBF after demolding.

Bottom Flange Repair Method 4: No Post-installed Anchors or Epoxy

The fourth type of bottom flange repair used no post-installed anchors and no epoxy bonding agent. This type of repair was implemented in repair areas where heavy congestion did not allow any installation of anchors or bonding agents, notably the end zones of the girders and also on strand retensioning repair areas and bearing zone areas, which are discussed in later sections. Repair 4.2RBZ on Girder 4 is shown in figure 60.

Because repair 4.2RBZ had no access point from above, the chimney method was used to fill this repair. The formwork was the same as in the previous repairs, but it only had one chimney and one air vent due to the smaller size of the repair (see figure 61).

Figure 60. Photo. Repair 4.2RBZ with rebar congestion.

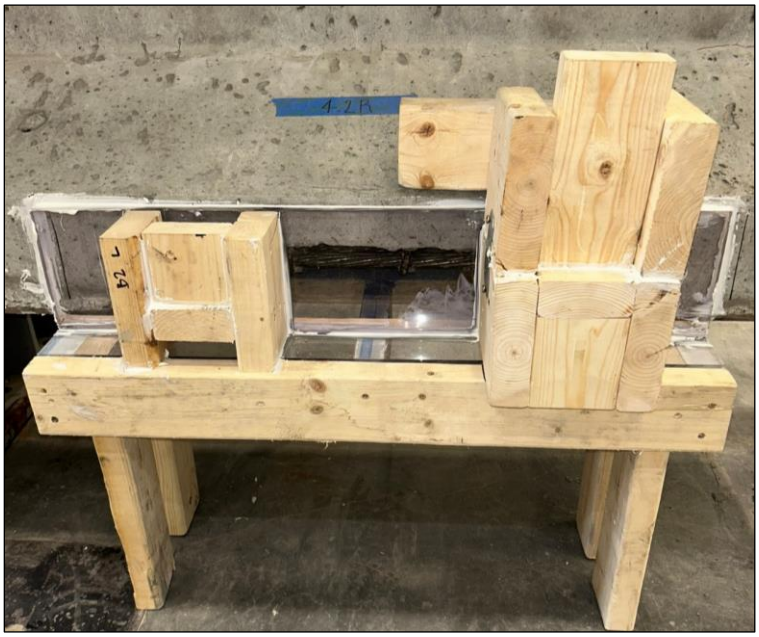

Figure 61. Photo. Formwork with one chimney for repair 4.2RBZ.

After the formwork was placed and the edges were caulked, the SCC was poured. This repair again demonstrated the usefulness of having the clear polycarbonate formwork to visually confirm the success of the SCC placement (see figure 62). Pouring continued until concrete flowed out of the air vent slot. Sandbags were placed to keep the formwork stable (see figure 63).

Figure 62. Photo. SCC flowing through the chimney formwork in repair 4.2RBZ.

Figure 63. Photo. Sandbags keeping the formwork stable after SCC replacement of the repair void.

No burlap or plastic sheeting was used to cover the chimney hole. The formwork was removed the next day with the help of hammers. Figure 64 shows the result of this repair after demolding.

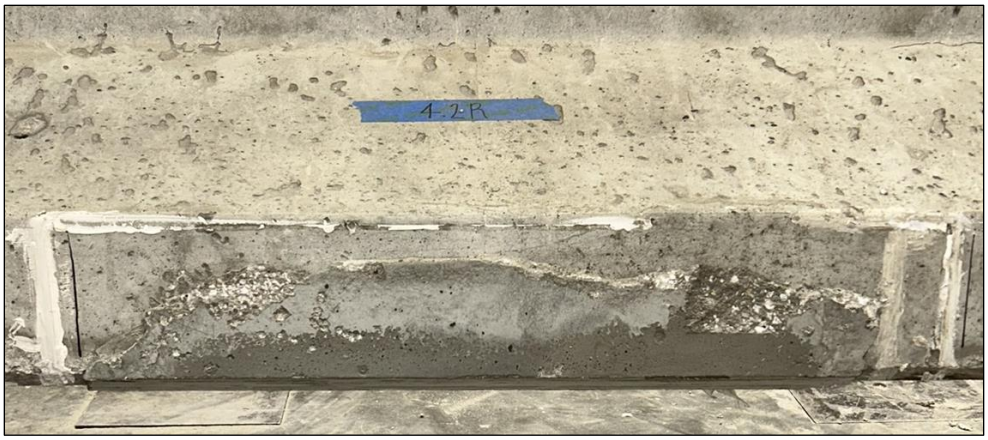

Figure 64. Photo. Repair 4.2RBZ after demolding.

Bottom Flange Repair Method 5: Prestressing Strand Retensioning

Nonconformities in the transfer region were simulated in two girders. Figure 65 and figure 66 show a nonconformity impacting four bottom strands in Girder 1 before and after repair, respectively.

Figure 65**. Photo. A nonconformity in the transfer region of Girder 1 before repair.**

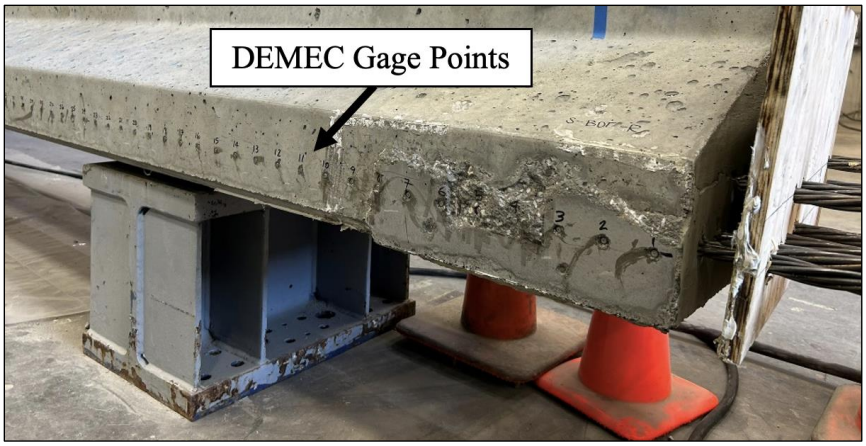

Figure 66. Photo. A nonconformity in the transfer region of Girder 1 after repair.

Figure 67 and figure 68 show a nonconformity impacting two strands on the top of the bulb in Girder 4 before and after repair, respectively. DEMEC gage points were installed on both sides of the girder (see figure 66 and figure 68) to measure concrete surface strains (CSS) at the time of detensioning and at later times. Readings between the two sides were averaged and smoothed over three readings to produce the plots shown later in this chapter.

Figure 67. Photo. A nonconformity in the transfer region of Girder 4 before repair.

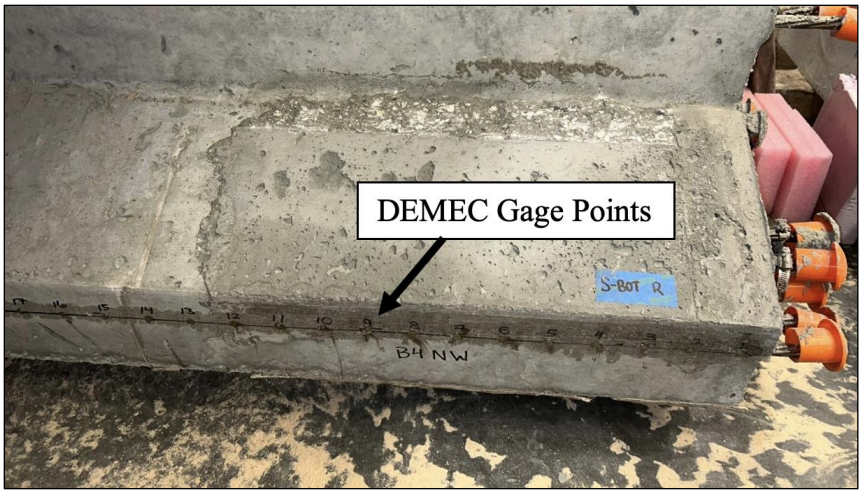

Figure 68. Photo. A nonconformity in the transfer region of Girder 4 after repair.

If nonconformity damage in the transfer region were to occur in a precast plant environment, the repairs would be accomplished prior to detensioning to ensure the strands remained at their fully tensioned force. Following repair and adequate curing time, the girders would be detensioned with the hope that the repair would transfer the prestressing force into the girder.

If damage in the transfer region were to occur after detensioning, the only option for repair would be to retension the strands using an external method, repair the damage, and then detension the strands following adequate curing time. The two girders in this study with transfer region damage were repaired using the latter method.

The dead end of the girder was anchored in place with an abutment bolted to the strong floor (see figure 69). The girder end was placed as close as possible to the abutment to reduce the length of strand between the end of the girder and the abutment. This would help limit stretch in the strands and girder movement on its supports toward the live end. Strand stretching on the dead end proved to be a challenge when retensioning the strands.

Strands on the dead end passed through the abutment and were locked in place using strand chucks. At the time of initial detensioning in the precast plant, some of the strands "birdcaged" and could not be used further without trimming off the expanded section and using a splice chuck to connect another section of undamaged strand (see figure 70). The splice chucks were provided by General Technologies, Incorporated.

Figure 69. Photo. Dead end abutment anchored to the strong floor.

Figure 70. Photo. Splice chucks used to extend strands through the abutment.

The live end was prepared in a similar manner; splice chucks were used to attach an additional length of strand such that the strand could be passed through the abutment, a load cell, strand chuck, center hole jack, and final strand chuck. The load cells were manufactured to record tension in the strands (see figure 71). The load cells were aluminum cylinders of 1.75 in. diameter and 3.50 in. length, with a center hole of 0.75 in. diameter. The Micro-Measurements CEA-13-250UWA-350 strain gauges were applied to the surface of the cylinders in a full bridge configuration. The load cells were calibrated on a Satec Systems 67-kip capacity compression testing machine by recording strains at given loads, plotting a graph, and then determining an equation for the resulting line.

Figure 71. Photo. Load cells.

The individual load cells were connected to a Vishay Measurements SB-10 switch and balance unit (SBU) such that multiple load cells could be monitored concurrently. The SBU was then connected to a Vishay Measurements P-3500 strain indicator from which strains were read and compared to the known calibration curve for each load cell. Figure 72 shows the setup on the live end of the girder with load cells connected to P-3500 strain indicators.

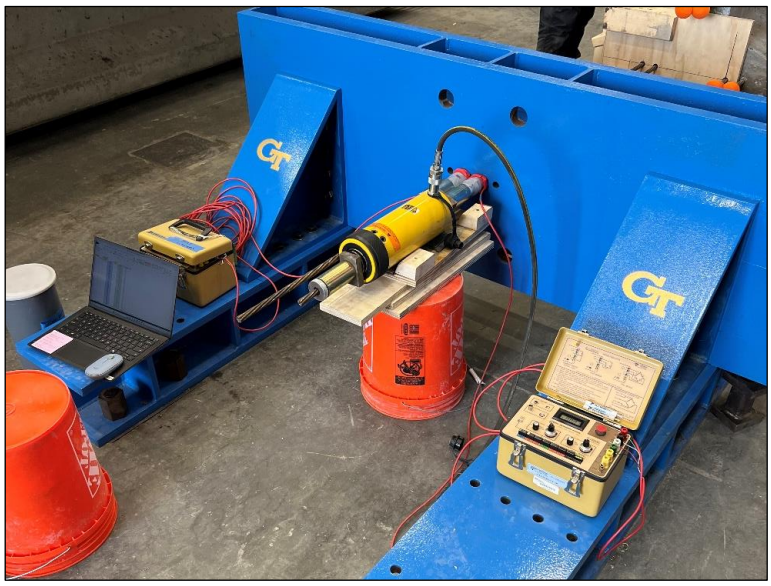

Figure 72. Photo. Live end configuration with load cells and a center hole jack.

Strand retensioning using the center hole jack proved to be a challenge. Girder 4 required retensioning of only two strands. Because it was possible to retension only one strand at a time, successive strand tensioning resulted in the reduction of tension force in the strand previously tensioned. As the process continued, moving from one strand to the next, the girder also seemed to be moving slightly toward the live end as strands on the dead end tightened before developing adequate tension to stop the girder movement. After several trial iterations of tensioning individual strands, the researchers also observed that the chucks closest to the girder were not allowing the strand to move and had become locked in place. Similar results occurred while retensioning four strands in Girder 1, despite efforts to better secure the girder in place at the dead end and to prevent the chucks closest to the live end of the girder from becoming locked.

The results of retensioning the two strands in Girder 4 (see table 9) show a large variation in the resulting strand tension forces that, on average, were less than the desired strand tension force of 44 kip initially achieved in the precast plant. Each trial focused on the first

tensioning strand 1 up to approximately 44 kip using the center hole jack, releasing pressure in the jack, moving the jack to strand 2, and repeating the process. Trial 1 resulted in an 8.45-kip tension force remaining in strand 1 and a 26.97-kip force remaining in strand 2. At the conclusion of trial 4, strands 1 and 2 remained tensioned to 17.18 and 41.84 kip, respectively, resulting in a total retensioning force of 59.02 kip, which was approximately 67.1 percent of the initial tensioning force of 88 kip achieved in the plant.

Table 9. Strand retensioning results for Girder 4.

		Strand 1 (kip)	**Strand 2 (kip)**
Trial 1	Strand 1 Re-tensioning	43.17	-
	Strand 1 Pressure Released	15.52	0.00
	Strand 2 Re-tensioning	-	44.63
	Strand 2 Pressure Released	8.45	26.97
Trial 2	Strand 1 Re-tensioning	45.46	-
	Strand 1 Pressure Released	27.79	16.55
	Strand 2 Re-tensioning	-	44.97
	Strand 2 Pressure Released	25.95	13.10
Trial 3	Strand 1 Re-tensioning	44.98	-
	Strand 1 Pressure Released	24.50	14.18
	Strand 2 Re-tensioning	-	46.15
	Strand 2 Pressure Released	23.66	19.54
Trial 4	Strand 1 Re-tensioning	-	-
	Strand 1 Pressure Released	-	-
	Strand 2 Re-tensioning	-	-
	Strand 2 Pressure Released	17.18	41.84
Final Strand Tension		17.18	41.84
Average Strand Tension		29.51	
Total Retensioning Force		59.02	
Initial Tensioning Force		88.0	
Percent of Initial Tensioning Force		67.1%	

– indicates no data available

A similar process was followed when retensioning the four strands in Girder 1 (see table 10). Retensioning Girder 1 resulted in 40 percent of the initial tension force achieved

in the plant environment. Retensioning four strands concurrently compounded the challenges observed in Girder 4 in which only two strands were retensioned.

Table 10. Strand retensioning results for Girder 1.

	Strand 1 (kip)	Strand 2 (kip)	Strand 3 (kip)	Strand 4 (kip)
Final Strand	19.76	22.62	14.77	13.30
Average Strand	17.61			
Total Retensioning	70.45			
Initial Tensioning	176.0			
Percent of Initial	40.0%			

Comparison of the resulting retensioning forces in Girders 4 and 1 with measured CSS results showed the impact of lower forces on transfer length. For Girder 4, where the retensioning force was 67.1 percent of the initial specified tension force achieved in the plant, the strands gained tension force up to a point approximately 18 in. from the end of girder, where the force level becomes more consistent (see figure 73). Using the equation $50 \cdot d_b$, the predicted transfer length is 30 in., and the observed strand force transfer over 18 in. based on CSS data is approximately 60 percent of that value.[2] This result compares favorably with the strand retensioning force of approximately 67.1 percent. Variations in CSS data from the time of release through 14 days can be explained in part by temperature variations at the time readings were taken.

The Girder 1 strands gained tension force up to a point approximately 15 in. from the end of girder, where the force level dropped off at the edge of the repair (see figure 74). With the predicted transfer length being 30 in. (again, using $50 \cdot d_b$), the observed strand force

[2] In the equation, d_b is the bar diameter.

transfer over 15 in. based on CSS data is approximately 50 percent of that value. This result also compares favorably with the strand retensioning force of approximately 40.0 percent. Variations in CSS data from the time of release through 7 days can be explained in part by temperature variations at the time readings were taken.

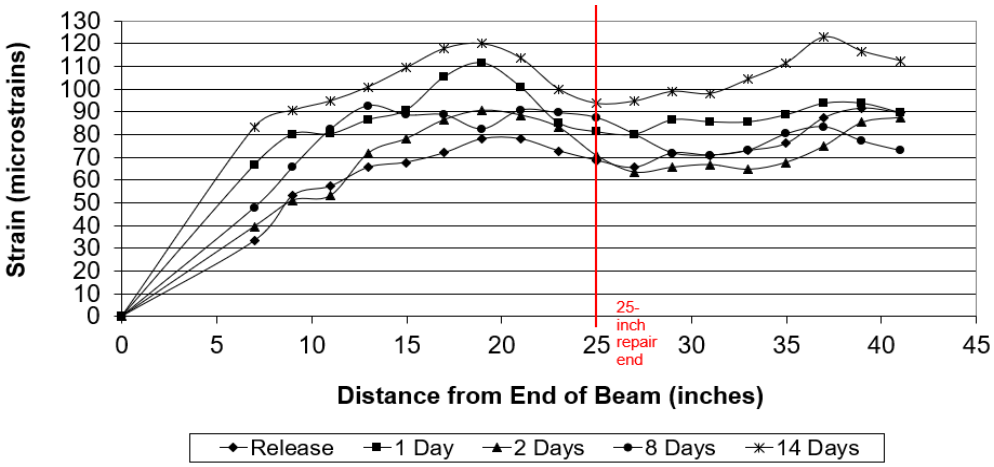

Figure 73. Graph. CSS transfer length plot for Girder 4, north end (2 strands).

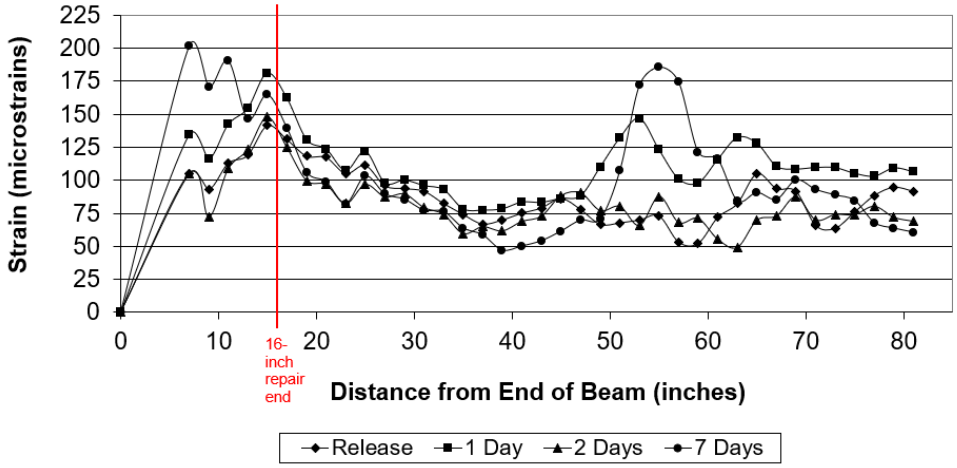

Figure 74. Graph. CSS transfer length plot for Girder 1, north end (4 strands).

CONCRETE SLANT SHEAR CYLINDER TESTS

To test the efficacy of the Sikadur-32 two-part epoxy bonding agent, slant shear cylinders were cast. The focus of these slant shear cylinder tests was to determine the strength of the

bond the fresh SCC mix made to the girder concrete mix. The slant shear cylinders were cast following ASTM C882.[20] The bottom half of the cylinder was cast with top flange repair concrete batches because it best matched the strength of the existing girder concrete. These bottom halves were left to cure at a 30-degree angle on a custom wooden form. To match the 0.25-in. amplitude of the repair surface, the surface of these bottom half cylinders was roughened using a #4 piece of rebar (see figure 75).

Figure 75. Photo. Roughening the surfaces of the bottom half slant shear cylinders, which were cast at a 30-degree angle.

The bottom halves of these cylinders were left to cure in the fog room until a future SCC casting. The day before the SCC casting, 10 bottom half cylinders were taken out of the fog room to allow the surface to dry before applying the Sikadur-32 epoxy coat on half of these the next day. Before completing the top half of the cylinder with SCC mix, a coat of Sikadur-32 was brushed on the 30-degree angled surface of five of the slant shear cylinders (see figure 76).

Figure 76. Photo. Sikadur-32 coat on angled surface of slant shear cylinders.

Only 5 of the 10 slant shear cylinder bottoms had a Sikadur-32 layer. Thus, results from slant shear tests with epoxy and without epoxy could be compared to see which performs best. The bottom half of the cylinder was then placed back into a 3-in. × 6-in. cylinder mold. After approximately 92 days, the mold was filled with the SCC repair mix to complete the full cylinder. The slant shear cylinders were left to cure upright on a level surface upon completion. After 1 day, the 10 specimens were demolded and placed in the fog room until the SCC reached 28-day strength (see figure 77). The slant shear cylinders were tested following ASTM C39.[16]

Data from the strength tests are given in table 11 and table 12 for the cases with and without epoxy, respectively. In the table, A is the minor axis of the elliptical bonding surface, C is the major axis of the elliptical bonding surface, and A_{bs} is the bond surface area. The results show that the cylinders with epoxy performed worse than those without epoxy. These results are addressed further in chapter 10.

Figure 77. Photo. Demolded slant shear cylinders.

Table 11. Concrete strength for shear slant cylinders with epoxy.

Name	A (in.)	C (in.)	A_{bs} (in.^{2})	Maximum Load (lb)	Strength (psi)	Average Strength (psi)
TF-SCC-1E	3.0370	5.4780	13.07	42,084	3,218	2,859
TF-SCC-2E	3.0275	5.3560	12.74	39,636	3,112	
TF-SCC-3E	2.9760	5.5505	12.97	40,012	3,084	
TF-SCC-4E	2.9825	5.2600	12.32	30,796	2,499	
TF-SCC-5E	3.0175	5.4175	12.84	30,581	2,382	

Table 12. Concrete strength for shear slant cylinders without epoxy.

Name	A (in.)	C (in.)	A_{bs} (in.^{2})	Maximum Load (lb)	Strength (psi)	Average Strength (psi)
TF-SCC-1	3.0000	5.6490	13.31	55,364	4,160	3,529
TF-SCC-2	3.0005	5.5735	13.13	41,350	3,148	
TF-SCC-3	2.9920	5.0530	11.87	38,810	3,268	
TF-SCC-4	2.9885	5.3335	12.52	51,064	4,079	
TF-SCC-5	2.9895	5.4085	12.70	37,946	2,988	

CHAPTER 4. FULL-SCALE EXPERIMENTAL TEST SETUP AND EVALUATIONS

As introduced in chapter 1, the four BT-54 girders were constructed, repaired, and tested in this project to determine the efficacy of the various repair techniques. The behavior of the different repair methods is affected by the following overall girder behaviors: flexure, shear, and bond between prestressing strands and the original or repair concrete in the bearing region. The general girder test setup and loading procedure for different girder behaviors is described in this chapter.

OVERVIEW

Loading each girder at the midspan was designed to highlight the flexural response, determine the composite response/interaction between the flange repair and the deck, and determine if delamination cracking occurred in the bottom flange repairs located at or near the midspan. Shear behavior was studied by loading girders with concentrated loads applied at approximately two times their depth from each end. The compression strut developed from the "shear" loading was designed to displace the bottom flange repairs as well as investigate the composite action of the flange repairs near the end of each girder. Bond behavior was most important in girders with repairs made in the bottom flange bearing zones. The bond behavior was studied by measuring external strains at the level of the bottom strands to determine changes in the transfer length of the strands and by measuring strand slip at the exposed ends of those strands. Shear loads close to the ends of the girders created diagonal struts, which exacerbated the bond stresses near the end of the girders.

Some flange repairs were tested separately to determine their flexural and shear ultimate capacities to determine if the repairs were at least as strong as the original flanges. Such flange strength is important to assure that the girder has adequate capacities for all construction loads. These flange strength tests were conducted only on Girder 1 and are presented in chapter 5.

GENERAL GIRDER TEST PROCEDURES

For each test, a string pot was used to measure deflection of the girder under load. Dial gauges were mounted in several locations to measure surface strain, as well as any prestressing strand or repair movement. On Girders 1 and 4, DEMEC gauges were applied at the level of the bottom layer of prestressing strands to measure the transfer and development lengths. Qualitative data, such as crack patterns and visual repair movement, were key components to ensure safe and effective tests.

Each girder was placed into the testing frame via a crane and a roller. A spreader girder was used to transfer load from the actuator to the girder specimen. The spreader girder was chosen to conduct three- and four-point testing. Rollers 12 in. long × 2 in. diameter were placed 4 ft apart to support the spreader girder, with a 12-in. × 24-in. steel plate under each roller and an elastomeric rubber pad between the steel plate and the girder top surface. An overall view of the spreader girder is shown in figure 78.

The girder was placed on 20-in.-long × 2.75-in.-diameter rollers with a 12-in. × 24-in. steel plate between the roller and the girder. The rollers rested on 16-in.-tall × 16-in.-wide × 24-in.-long steel pedestal supports. The girder end boundary conditions are shown in figure 79.

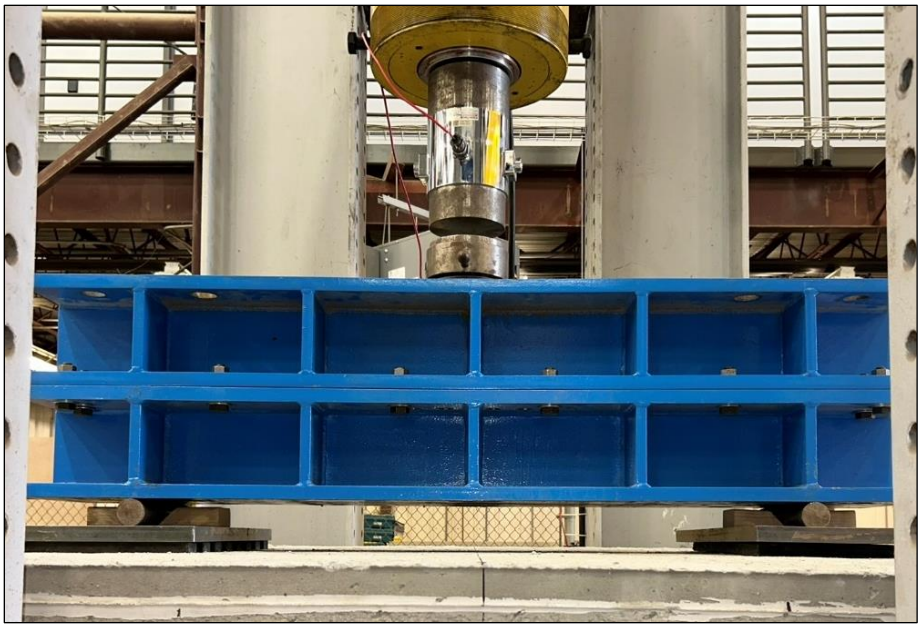

Figure 78. Photo. General spreader girder configuration.

Figure 79. Photo. Girder boundary conditions.

FLEXURAL BEHAVIOR

A collective total of three flexural tests were conducted on the repaired girders. Girders 2, 3, and 4 each had a flexural test because they were the girders that had a deck cast. During and after all flexural tests, no top flange or bottom flange repair failed or spalled. The repairs cracked cohesively with the girder for much of the time. On certain bottom flange repairs, especially the shallow ones, the perimeter of the repair appeared to be detaching from the girder (see chapter 5, chapter 6, chapter 7, and chapter 8 for Girders 1, 2, 3, and 4, respectively, for details). However, the repair was confirmed to not be detached after the girder was unloaded. All the flexural tests were terminated when 95 percent of the calculated ultimate load was reached or once a bulb surface strain of 0.00847 occurred (90 percent of ultimate stress in the prestressing strands, or 243 ksi).

SHEAR BEHAVIOR

A collective total of seven shear tests were conducted on the repaired girders. Girders 2, 3, and 4 each had two shear tests, and Girder 1 only had one shear test. No repair failed or spalled during or after all the shear tests. All the shear tests were stopped when 95 percent of the calculated ultimate shear capacity was reached or once a slip of 0.01 in. occurred at the ends of the prestressing strands. Past research commonly used a 0.01-in. slip as the definition of bond failure.[21]

BOND BEHAVIOR

The bond, transfer, and development lengths of prestressing strands in repaired sections were measured to determine if the repairs would develop transfer of forces from strands to the surrounding girder concrete, as occurs in nondamaged girders. Lack of bond in strand

transfer length regions may result in premature failure of the bearing zones and in poor shear performance of prestressed concrete girders. This bond performance was tested for Girders 1 and 4 through shear tests where the concentrated loads were placed close to the repaired end of each girder.

PERFORMANCE OF REPAIRS

Overall, the repairs acted cohesively with each girder and behaved the same or better than an undamaged girder. Each test was conducted to the safest maximum load, with the goal of reaching yielding of the prestressing strands and verging on the calculated ultimate load. No repair showed signs of major failure, such as extreme cracking or spalling, or dislodgement from the girder. Only repairs in the bearing zone showed poor prestressing bond performance, as discussed in the following chapters.

CHAPTER 5. GIRDER 1 TESTS AND RESULTS

This chapter presents the setup, experiment, and test results for the Girder 1 specimen. Calculations for this girder are given in appendix G.

OVERVIEW

The Girder 1 tests were conducted to ensure proper performance of the one bearing zone repair and three top flange repairs. Girder 1 consisted of different tests than the other three girders because there was no deck cast on the girder. The first test of Grider 1 (Test 1.1.S) was to test the bearing zone repair. The tests following that first test (Tests 1.2.F, 1.3.F, and 1.4.F) were to directly test the top flange repairs with a different top flange test setup (see Top Flange Test Setup). The goal was to test the top flange repair itself because of the difficulty the composite deck created in testing and observing the top flanges during an overall girder test. A matrix of each of the tests on Girder 1 is given in table 13.

Table 13. Girder 1 test matrix.

Test Name	Behavior	Repair(s) Considered
Test 1.1.S	Shear	1.1LBZ
Test 1.2.F	Flexure	1.2LTF
Test 1.3.F	Flexure	1.2LTF
Test 1.4.F	Flexure	1.3LTF, 1.3RTF

TOP FLANGE TEST SETUP

For the top flange tests (Tests 1.2.F, 1.3.F, and 1.4.F), a new setup was used (see figure 80). The top flange test setup consisted of two 46-in.-long W5 × 16 steel shapes spanning across the top flanges with pin and roller supports, which rested on elastomeric bearing pads. The pins for the pin and roller were 2 in. in diameter, resting on a 1-in. plate and 1-in. bearing

pads. The two W5 × 16 shapes were spaced 7 in. apart. On top of the two girders was a 16-in.-deep steel blue pedestal girder to transfer the force from the actuator to the girders. The pin and roller pin supports were centered 3 in. from the edges of the top flange.

Figure 80. Photo. Top flange test setup.

TEST 1.1.S (REPAIR 1.1LBZ) RESULTS

The first test on Girder 1, Test 1.1.S, was a shear test to examine the performance of the bearing zone repair 1.1LBZ and the bond of the strands in that zone. The load point location was 73.5 in. from the center of bearing of the north end of the girder. This distance is referred to as “x1” in the calculations in appendix G. The girder roller supports were centered 7 in. from each end. The spreader beam was used in a three-point bending test configuration, where only one end of the spreader beam was used to transfer the load. The spreader beam configuration for the first test on Girder 1 is shown in figure 81.

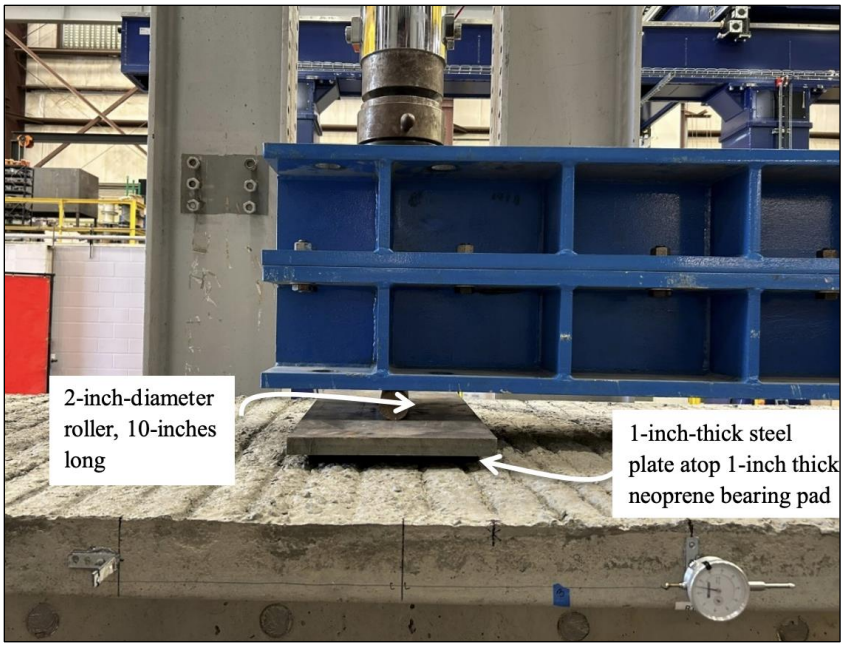

Figure 81. Photo. Test 1.1.S (repair 1.1LBZ) spreader beam configuration.

For each load step, when the load was reached, the pump valves were closed and a brief pause was taken for safety reasons prior to collecting gauge readings. The first diagonal shear cracks occurred at 254 kip (see figure 82 and figure 83). The shear crack width measured 0.00394–0.00591 in. The strut width was 5 in, and the strut angle was between 34 and 35 degrees. Gauge readings were recorded, and no damage was seen in repair 1.1LBZ.

The load was then increased to 303 kip. The shear crack width increased to 0.00787–0.00984 in. These cracks extended into the bulb bearing zone. Cracks on the north end cross-section developed (see figure 84), specifically around the edge of repair 1.1LBZ, measuring 0.0138 in. wide. A strand slip of 0.001 in. was measured in strands LS1 and LS2 (labeled in figure 84).

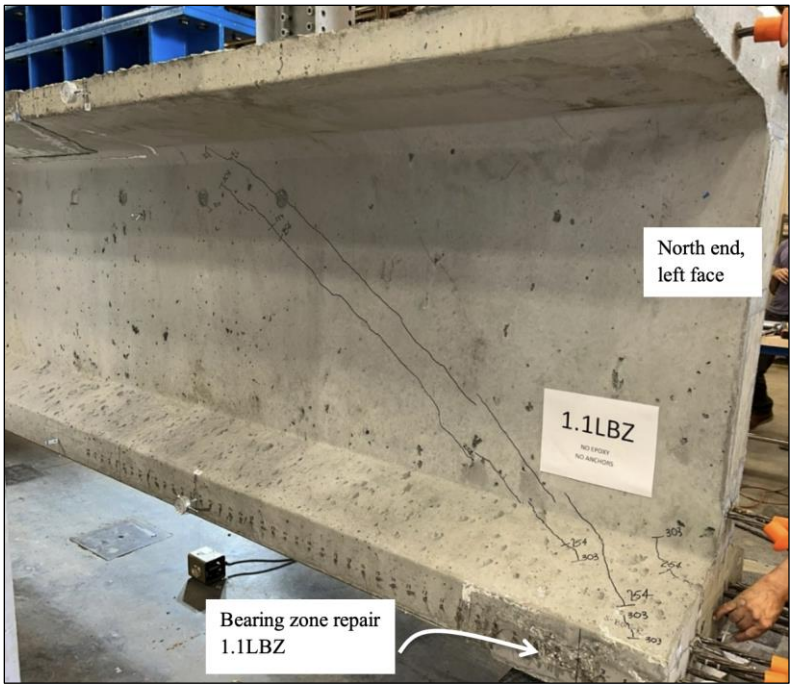

Figure 82. Photo. Test 1.1.S (repair 1.1LBZ) initial shear cracks on the repaired girder side (left face of girder pictured). The repair zone is at the bottom right in this figure. Note that the diagonal cracks and strut orient toward the edge of the bottom flange.

Figure 83. Photo. Test 1.1.S (repair 1.1LBZ) initial shear cracks on the original, nonrepaired girder side (right face of girder pictured). Note that the diagonal cracks orient to a location over the center of the end support.

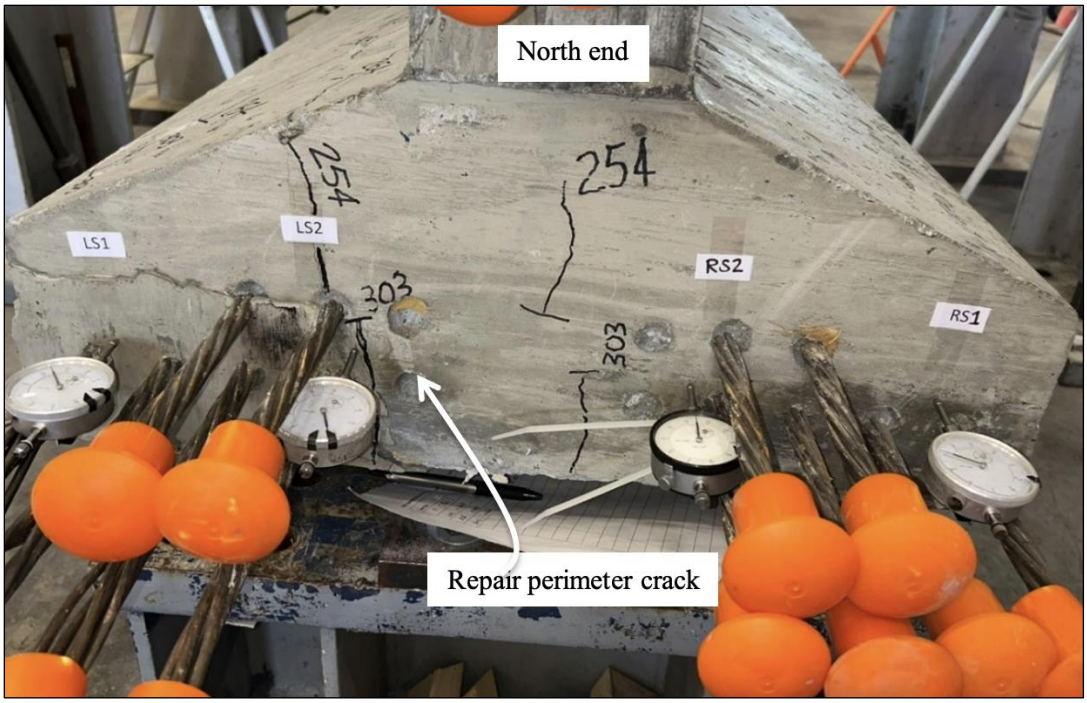

Figure 84. Photo. Test 1.1.S (repair 1.1LBZ) north end cross-section cracks. Note that the crack through label LS2 for the slip dial gauge goes through and around the prestressing strands adjacent to the web. The repair is on the bottom left side of this end view.

Girder 1 was loaded to a final load of 450 kip. A strand slip of 0.038 in. was recorded in strand LS2, which exceeds the 0.01-in. slip limit established in this project as the failure criterion. This prompted the loading to be terminated. The initial shear crack width was 0.0138–0.0177 in., and the secondary shear crack width was 0.00118–0.0138 in. The repair perimeter crack on the north end measured 0.0394 in. wide. The bearing zone cracks at 450 kip are shown in figure 85.

An overall crack pattern from this shear test is shown in figure 86 and figure 87. A residual strength test was done on repair 1.1LBZ. A 16-lb sledgehammer was used to strike the repair approximately 10 times. The only damage observed was pieces of the repair breaking away. Figure 88 shows the aftermath of the residual strength test on repair 1.1LBZ.

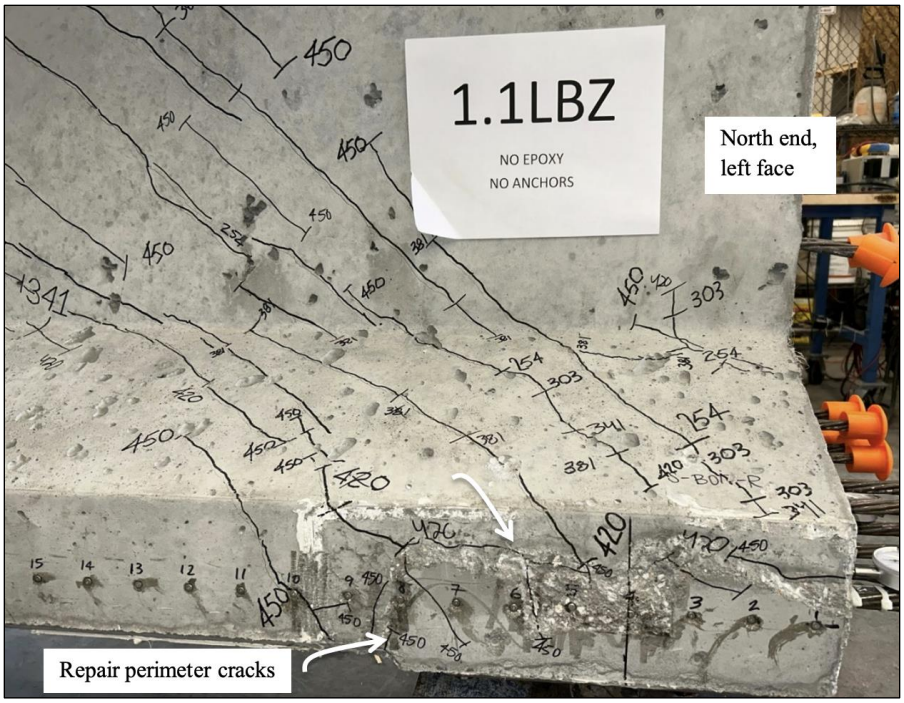

Figure 85. Photo. Test 1.1.S (repair 1.1LBZ) bearing cracks on bulb surface and around perimeter of repair 1.1LBZ at 450 kip (left face of girder pictured).

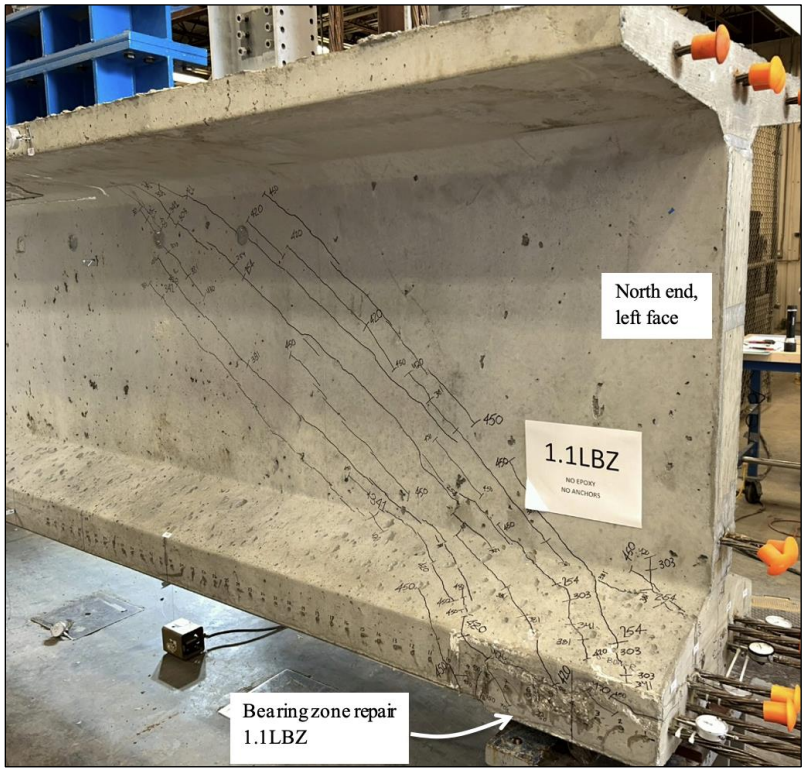

Figure 86. Photo. Test 1.1.S (repair 1.1LBZ) overall crack pattern on repaired girder side at 450 kip (left face of girder pictured).

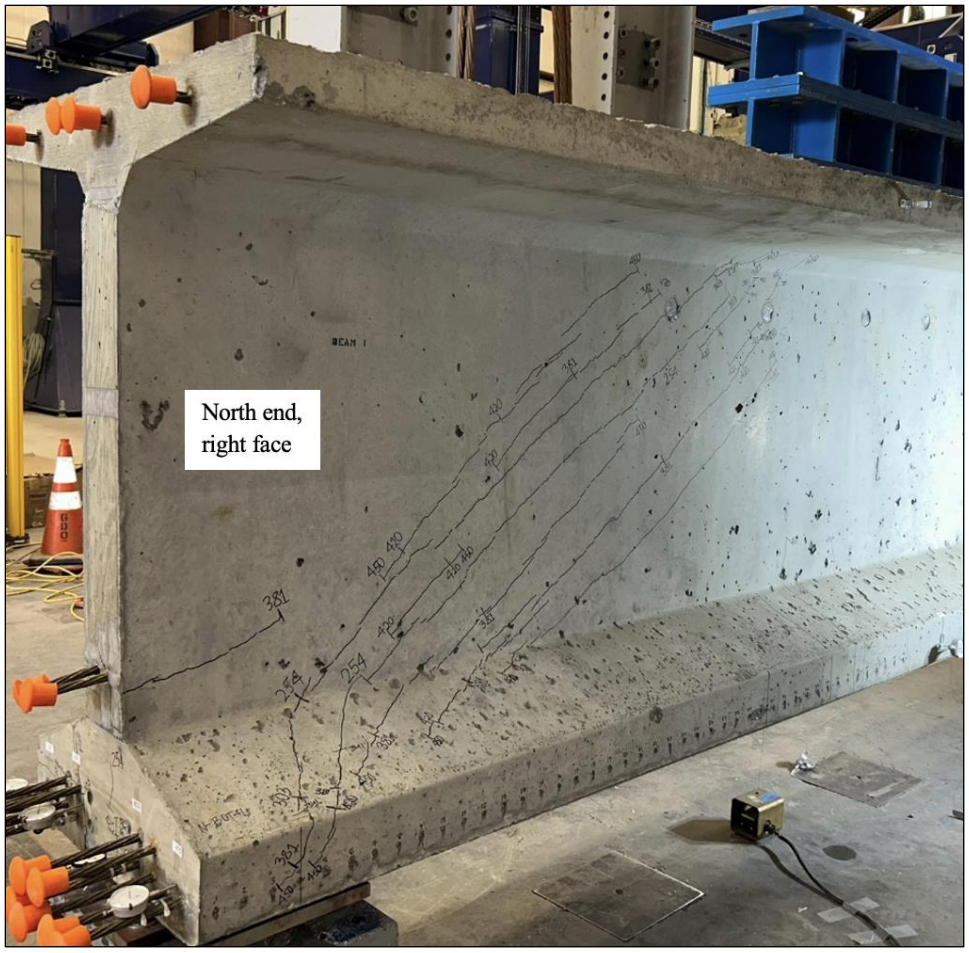

Figure 87. Photo. Test 1.1.S (repair 1.1LBZ) overall crack pattern on original, nonrepaired girder side at 450 kip (right face of girder pictured).

Figure 88. Photo. Test 1.1.S (repair 1.1LBZ) residual strength test using a sledgehammer.

Slight separation of the repair concrete from the original concrete is evident in the photos of the repairs at maximum loads and after residual testing (see figure 85 through figure 88), as cracks formed around the perimeter of the bearing zone repair. It is suspected that bond slip in strand LS2 was exacerbated due to being at the border of the repair.

The load-deflection plot for Test 1.1.S (repair 1.1LBZ) is shown in figure 89. The girder was tested past its elastic point (cracking), resulting in a nonlinear deformation after unloading due to the cracked girder section. The finding of this shear test was that the girder successfully exceeded 90 percent of the maximum load based on the nominal shear capacity (the dashed-dotted line in figure 89). Although repair 1.1LBZ had perimeter cracks, this suggests that the repair did not negatively impact the shear capacity of the nonconforming girder. The girder still performed well past its service load conditions, as shown by this test.

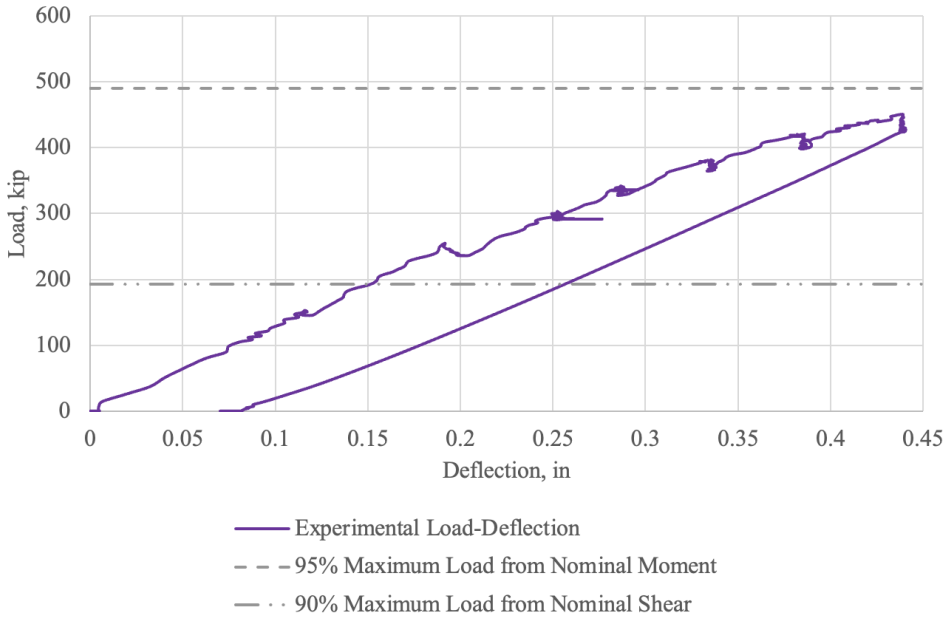

Figure 89. Graph. Test 1.1.S (repair 1.1LBZ) load-deflection plot.

The moment-curvature plot for Test 1.1.S (repair 1.1LBZ) (see figure 90) shows the experimental values obtained from this test. Nonlinear behavior is exhibited after the girder cracked at approximately 1,340 kip-ft.

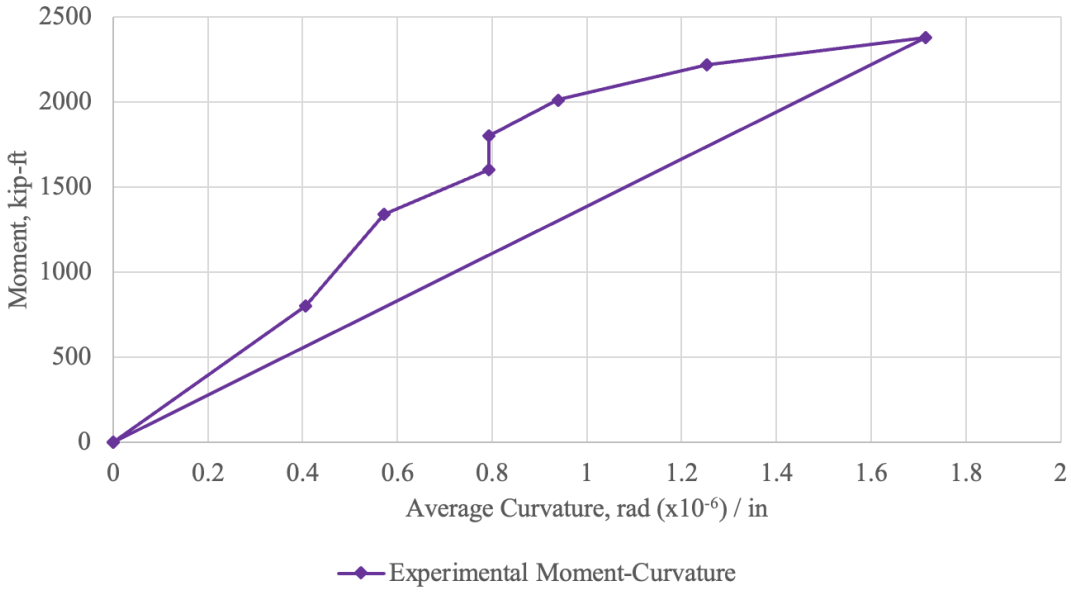

Figure 90. Graph. Test 1.1.S (repair 1.1LBZ) moment-curvature plot.

The load-strand slip plot for Test 1.1.S (repair 1.1LBZ) (see figure 91) shows the strand slip measurements, as well as the nominal capacity loads. Strands LS1 and LS2 exceeded the strand slip limit of 0.01 in. and prompted the termination of loading. This suggests the girder failed in a bond-slip failure caused by shear cracks in the bearing zone extending from the compression strut. Multiple shear cracks passed through the bearing zone, as shown in previous figures.

DEMEC (CSS) measurements were taken at each load interval and plotted. The CSS plot (see figure 92) shows the strand stress at a load prior to maximum and at maximum load. From the plot, it is evident that the strands slipped and lost prestress force at maximum load, as the strand stress at the maximum load dropped below the stress at the load prior to

maximum. As repair 1.1LBZ detached from the girder, additional strand slip was induced, resulting in a loss of stress in the strand at maximum load.

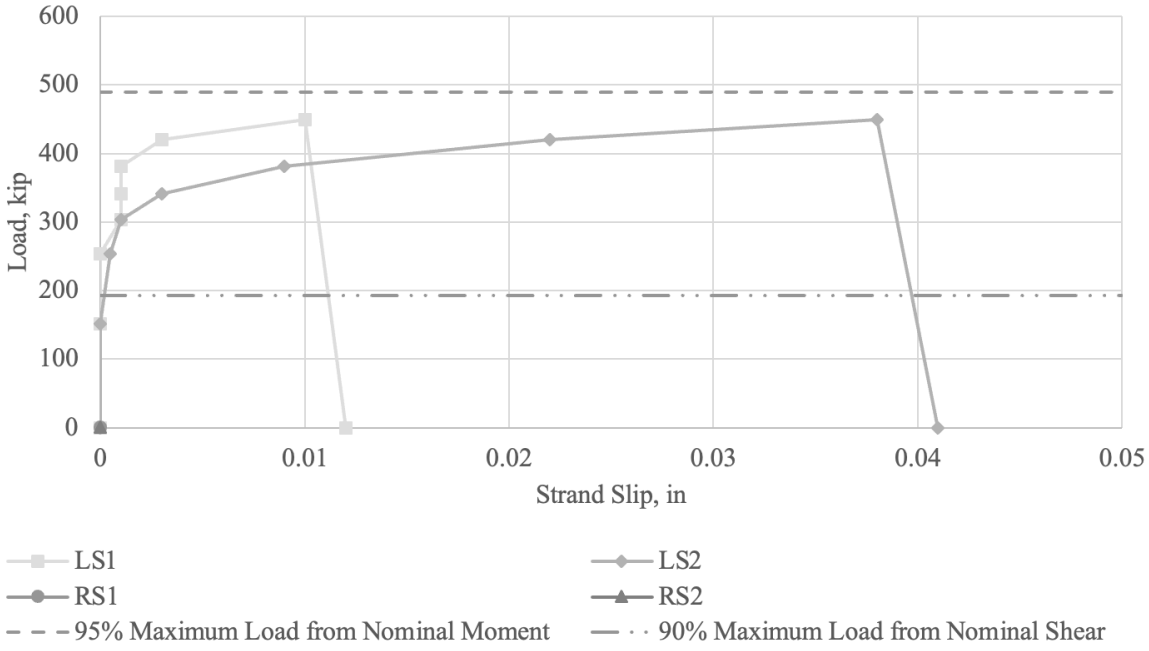

Figure 91. Graph. Test 1.1.S (repair 1.1LBZ) load-strand slip plot.

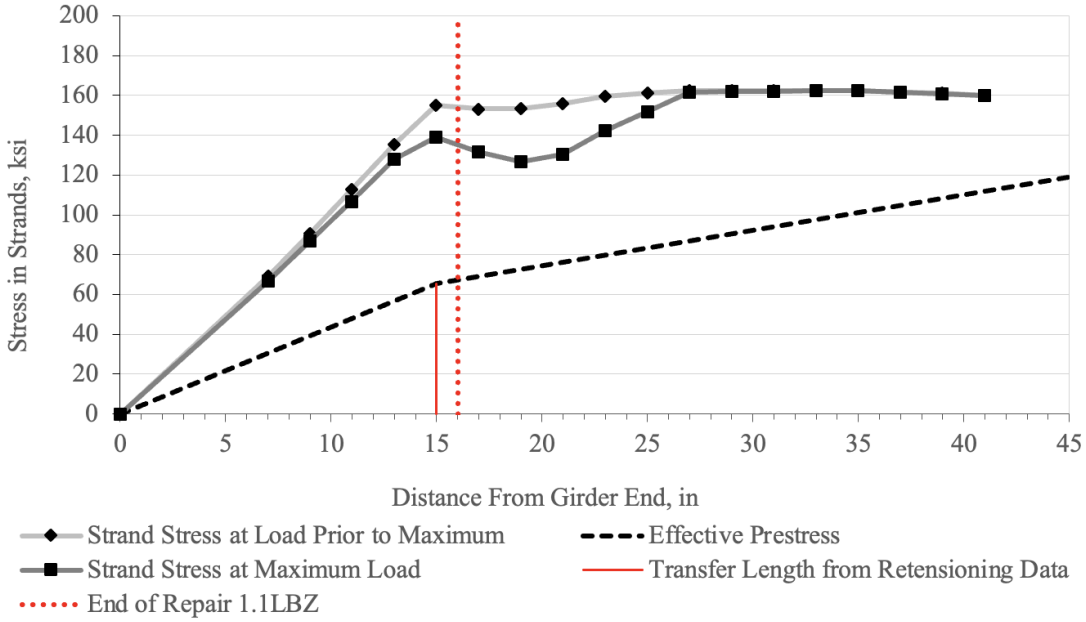

Figure 92. Graph. Test 1.1.S (repair 1.1LBZ) CSS plot: Strand stress vs. distance from girder end.

TEST 1.2.F (REPAIR 1.2LTF) RESULTS

Using the top flange test setup discussed previously (see Top Flange Test Setup), the second test on Girder 1, Test 1.2.F, was a direct top flange test on repair 1.2LTF, located near the edge of the repair closer to the end of the girder. The center of the load point location was 115 in. from the north end of the girder. The top flange flexure setup is shown in figure 93.

The repaired flange was denoted as being located on the left face of the girder, and the original flange was denoted as being located on the right face of the girder. At a load of 15 kip, a new longitudinal flexural crack, near gauge R1 on the right face of the girder, opened 0.002 in. wide. At a load of 30 kip, 45-degree flexural cracks formed on the right side of the flange, which was the original nonrepaired side of the girder flange. These flexural cracks were 0.00984 in. wide, and the longitudinal flexural crack was now 0.0157 in. wide. These cracks can be seen in figure 94 and figure 95.

Figure 93. Photo. Test 1.2.F (repair 1.2LTF) top flange test configuration.

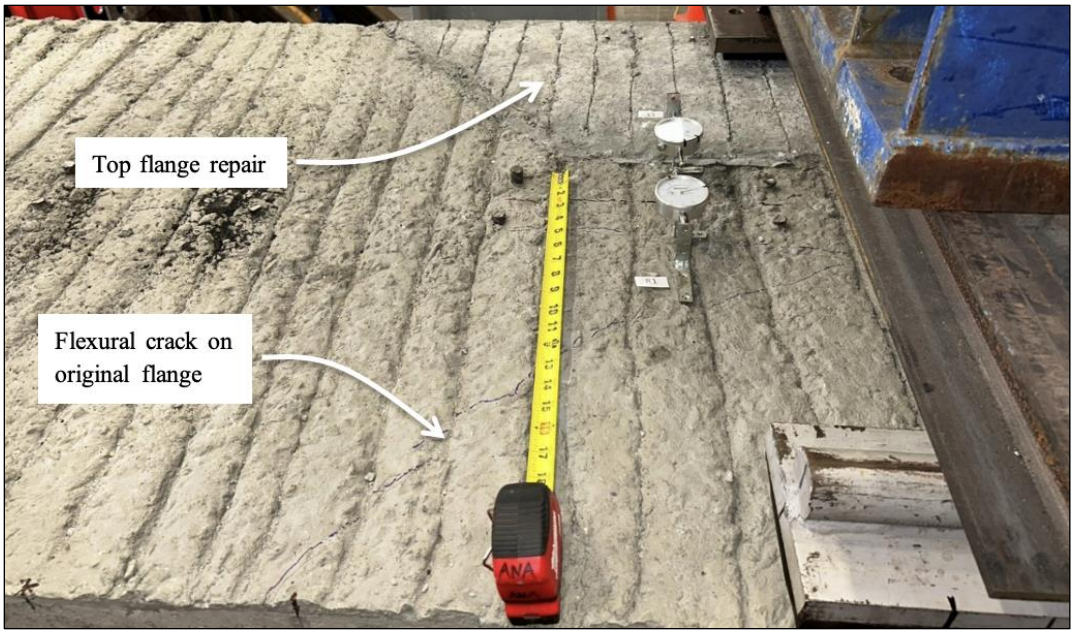

Figure 94. Photo. Test 1.2.F (repair 1.2LTF) top flange flexural cracks on original, nonrepaired flange at 30 kip (from top side).

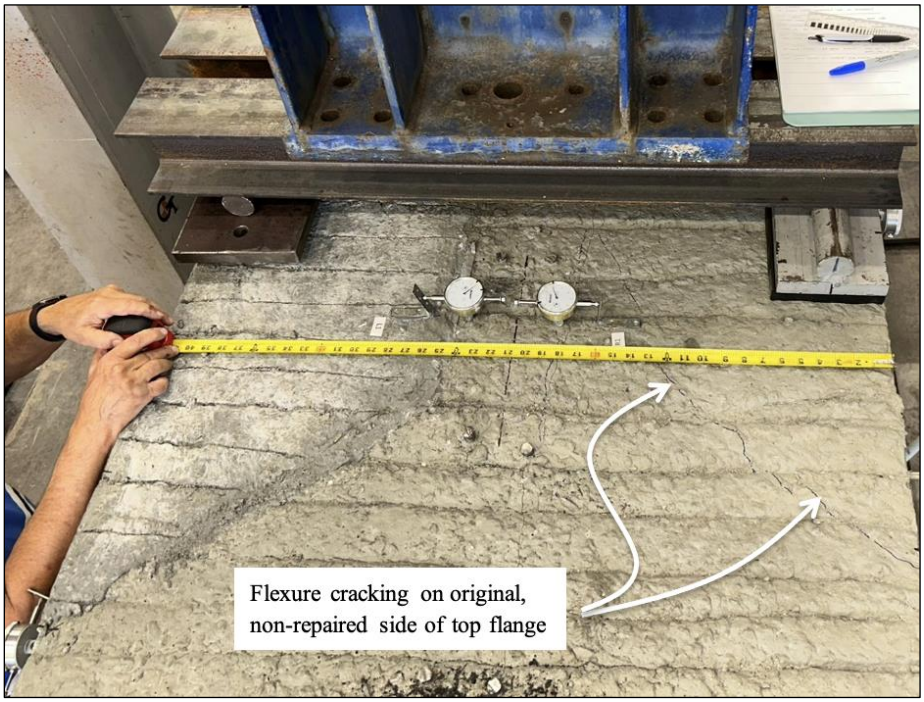

Figure 95. Photo. Test 1.2.F (repair 1.2LTF) top flange flexural cracks on original, nonrepaired flange at 30 kip(from above).

The top flanges were loaded to a final load of 31.4 kip. The original top flange was no longer able to hold a high load; it was deflecting significantly with no increase in loading.

The overall top flange cracks from Test 1.2.F (repair 1.2LTF) can be seen in figure 96. In the figure, the black lines illustrate the girder reinforcement installed at the time of manufacture, the blue lines illustrate the top flange repair post-installed reinforcement, and the red lines illustrate the crack pattern. From this direct top flange test, it was found that the capacity of the top flange repair exceeded that of the original girder top flange. The original top flange was measured to have a maximum flexural crack width of 0.029 in., whereas the top flange repair maximum flexural crack width was only 0.0105 in. under the same loading conditions.

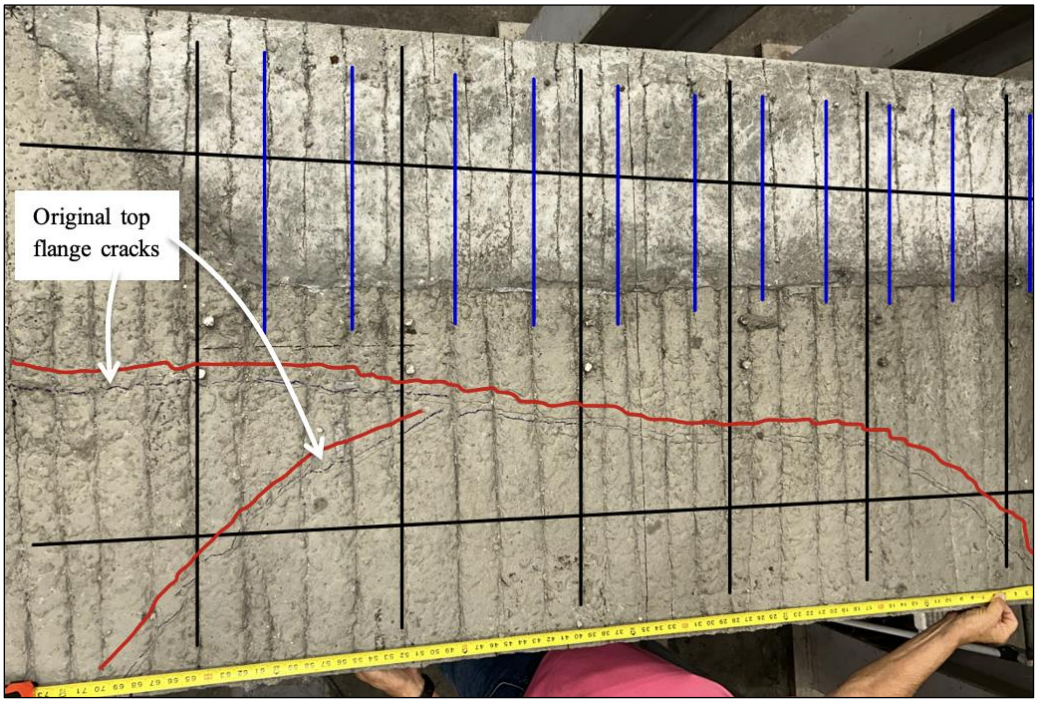

Figure 96. Photo. Test 1.2.F (repair 1.2LTF) overall final top flange crack pattern at maximum 31.4 kip.

TEST 1.3.F (REPAIR 1.2LTF) RESULTS

The third test on Girder 1, Test 1.3.F, was another direct top flange test on repair 1.2LTF, closer to the center of the repair. The load point location was 173.25 in. from the north end of the girder. The top flange test setup for this test is shown in figure 97.

During the loading process, after a load is stopped and the valves are shut on the manual hydraulic pump, the pressure decreases, and the load drops each time. In this test, no cracks were seen in the 5-, 10-, or 15-kip load increments. After loading to 15 kip, the pressure dropped the load to 10 kip. Loading was started again to attempt to load the top flanges to the next interval of 20 kip; however, the original top flange cracked at 13.5 kip while reloading. The crack width was 0.0197–0.0236 in. The shear-flexural cracks are shown in figure 98 and figure 99.

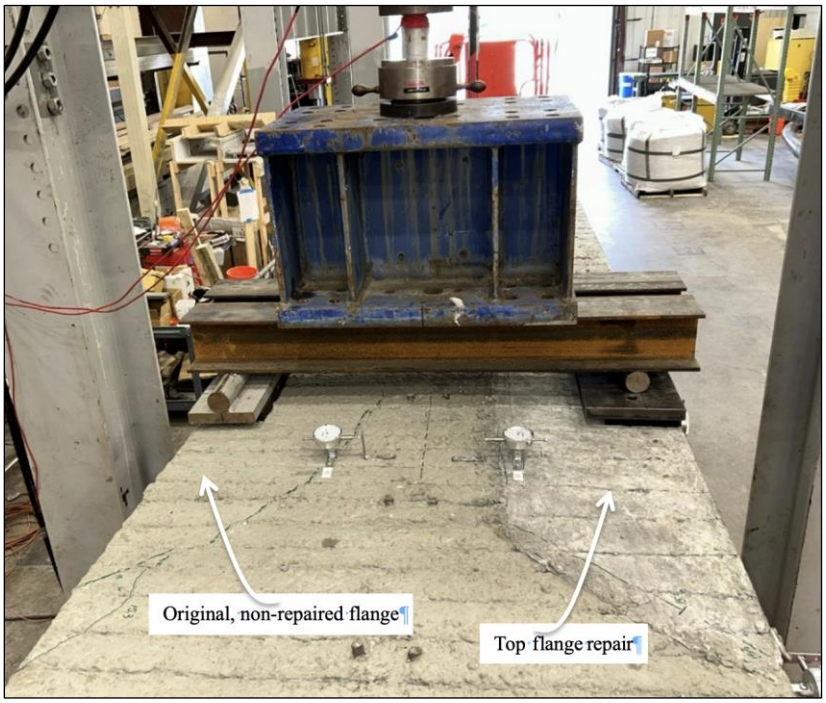

Figure 97. Photo. Test 1.3.F (repair 1.2LTF) top flange configuration.

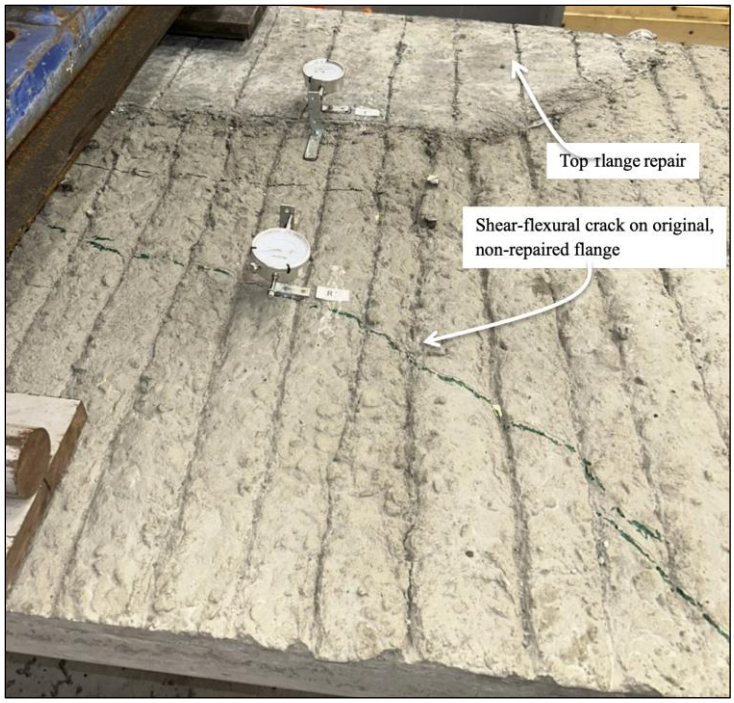

Figure 98. Photo. Test 1.3.F (repair 1.2LTF) shear-flexural cracks at 13.5 kip (right face of girder pictured, south end).

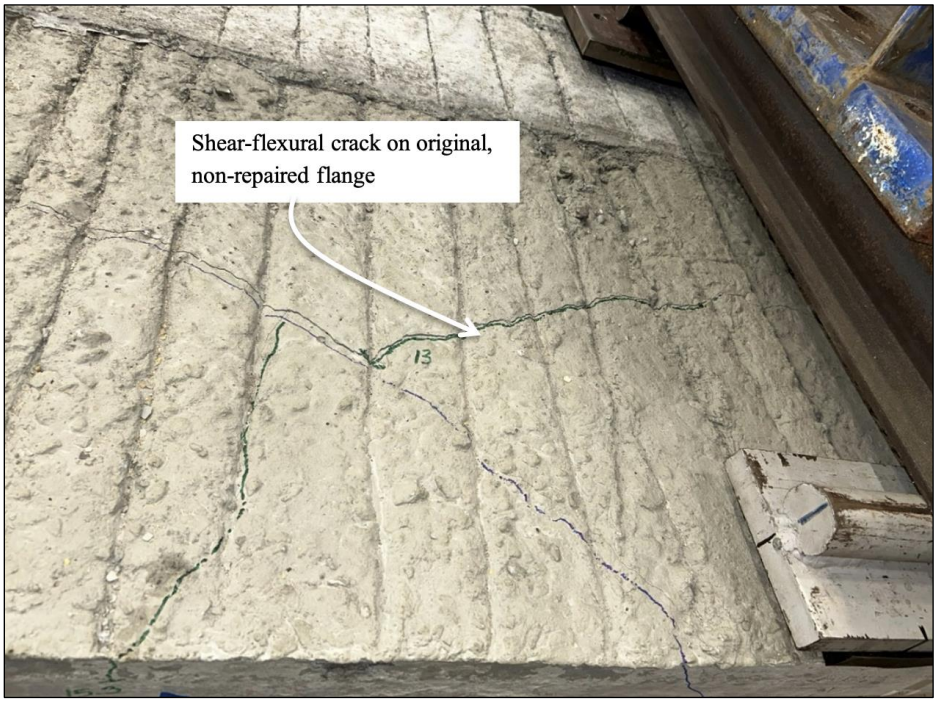

Figure 99. Photo. Test 1.3.F (repair 1.2LTF) shear-flexural cracks at 13.5 kip (right face of girder pictured, north end).

The repair top flange cracked, as well, with a longitudinal flexural crack 0.00591–0.00787 in. wide. Figure 100 provides a top view of the original flange cracks and the repair cracks.

The top flange was then loaded to its final load of 16 kip. Once again, the original top flange was deflecting significantly with no additional load resistance. The overall top flange cracks from Test 1.3.F (repair 1.2LTF) are shown in figure 101. In the figure, the black lines illustrate the girder reinforcement, the blue lines illustrate the top flange repair post-installed reinforcement, and the red lines illustrate the crack pattern. From this test, it was found that the capacity of the top flange repair exceeded that of the original girder top flange, which failed at a moment capacity of 17.3 kip-ft. The repaired flange was measured to have detached only 0.0045 in., whereas the original top flange detached 0.015 in. at the longitudinal flexural crack interface.

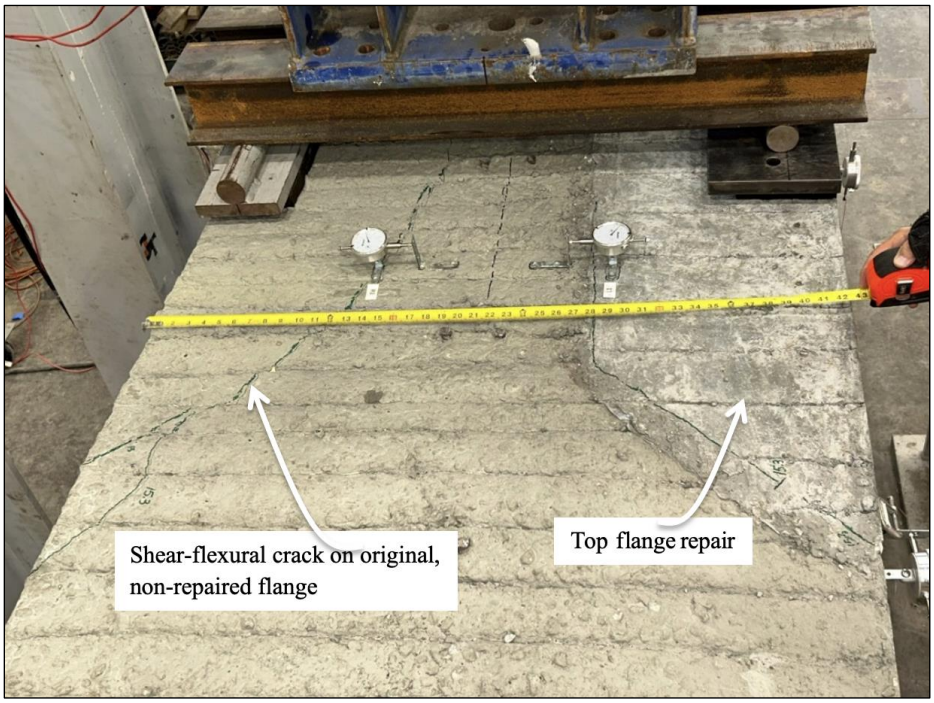

Figure 100. Photo. Test 1.3.F (repair 1.2LTF) shear-flexural cracks at 16 kip.

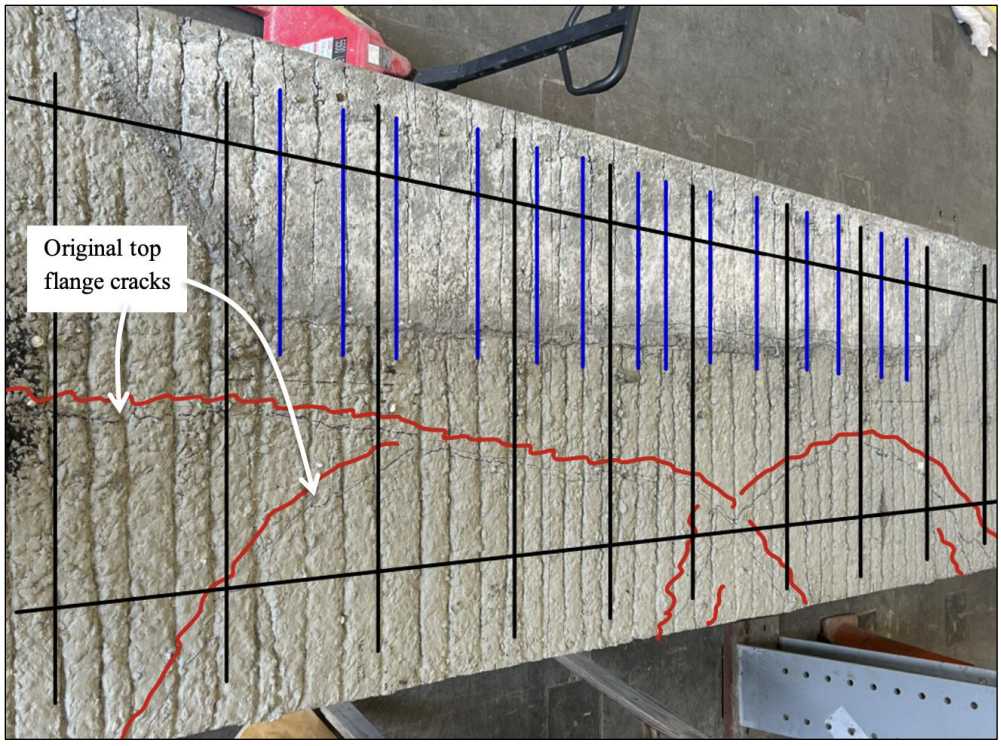

Figure 101. Photo. Test 1.3.F (repair 1.2LTF) overall top flange cracks.

TEST 1.4.F (REPAIR 1.3RTF, 1.3LTF) RESULTS

The fourth and final test on Girder 1, Test 1.4.F, was a direct top flange test on repairs 1.3RTF and 1.3LTF at the midspan of the repairs. As discussed in chapter 4, the repairs were constructed symmetrically on both right and left flanges, and each repair was 6 ft long. Both the right and left repairs used an epoxy bonding agent. The load point location was 123.625 in. from the south end of the girder. The top flange test setup for Test 1.4.F (repair 1.3RTF, 1.3LTF) is shown in figure 102.

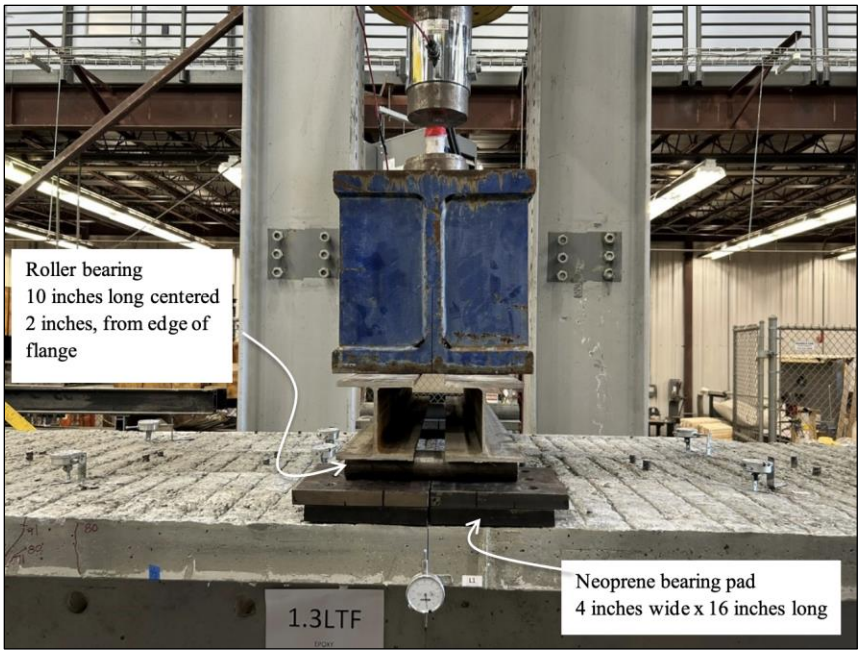

Figure 102. Photo. Test 1.4.F (repair 1.3RTF, 1.3LTF) test configuration.

At a load of 15 kip, a crack formed on the right girder face flange edge, measuring 0.00394 in. wide (see figure 103). A crack near dial gauge L2 (see figure 104) on the corner edge of repair 1.3LTF was seen, as well, measuring 0.00787 in. wide.

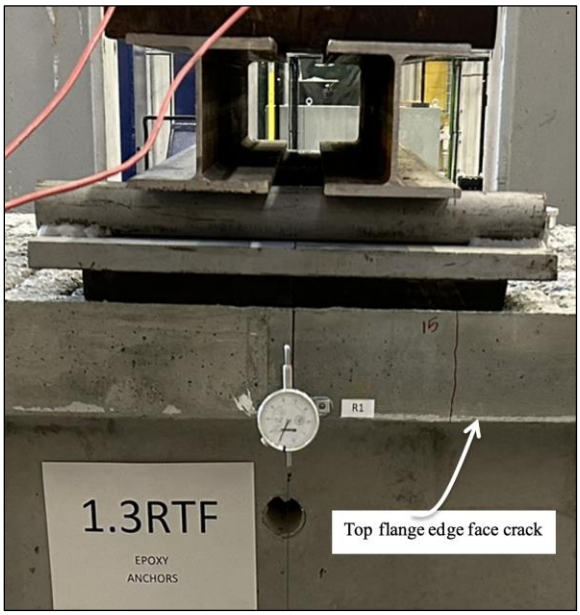

Figure 103. Photo. Test 1.4.F (repair 1.3RTF, 1.3LTF) top flange edge face crack at 15 kip (right face of girder pictured).

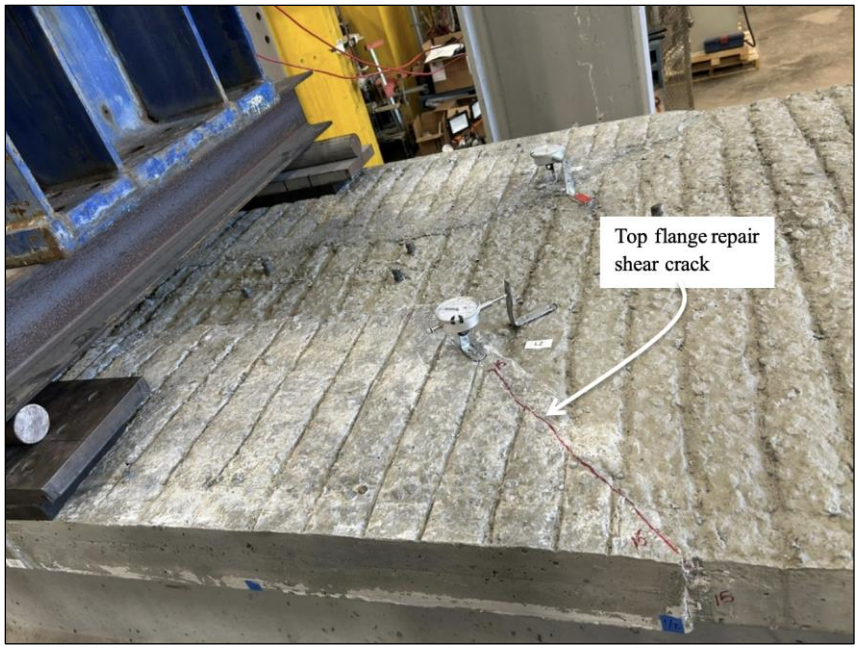

Figure 104. Photo. Test 1.4.F (repair 1.3RTF, 1.3LTF) top flange shear cracks at 15 kip (left face of girder pictured).

The load was then increased to 20 kip. The previous right-side face crack remained the same, and the L2 crack increased to 0.00984 in. wide. Cracks near the R4 gauge and near the L4 gauge were seen, both measuring 0.00394 in. Figure 105 shows the initial L4 crack.

Figure 105. Photo. Test 1.4.F (repair 1.3RTF, 1.3LTF) top flange shear cracks at 20 kip (left face of girder pictured).

The load was then increased to 25 kip. A hairline flexural crack measuring 0.00394 in. wide formed along the longitudinal edge of repair 1.3LTF. The initial right-side face crack now measured 0.00591 in. wide. The previous cracks that had formed remained the same. When the load was increased to 30 kip, no change occurred in the crack widths. However, when the load was increased to 35 kip, a flexural crack on the longitudinal edge of repair 1.3RTF was noticed that measured 0.00591 in.. All other cracks remained the same in width.

The load was then increased to 71 kip. Punching shear cracks formed on both repairs, appearing to propagate from the top flange test setup supports. These two cracks measured 0.00984 in. wide. The left flexural crack measured 0.0177 in., the right-side face crack now measured 0.0177 in., and the L2 crack measured 0.0118 in. The other cracks remained the same in width. The punching shear crack on the left side repair is shown in figure 106.

Figure 106. Photo. Test 1.4.F (repair 1.3RTF, 1.3LTF) top flange shear crack on repair 1.3LTF.

The top flange repairs were loaded to a final load of 80 kip. Loading was terminated at this point due to concerns over reaching failure of the W5 × 16 steel shapes that were part of the top flange test setup. The overall top flange cracks from Test 1.4.F (repair 1.3RTF, 1.3LTF) are shown in figure 107. In the figure, the black lines illustrate the girder reinforcement, the blue lines illustrate the top flange repair post-installed reinforcement, and the red lines illustrate the crack pattern. From this test, it was found that the top flange repairs were able to sustain a 40-kip load, which exceeded the calculated theoretical capacity of 29.4 kip. The two top flange repairs behaved similarly in response to this high load. Detachment of the top flange repairs from the original girder was minimal, with a maximum of 0.022 in. on the longitudinal portion of repair 1.3RTF and a maximum of 0.024 in. on the longitudinal portion of repair 1.3LTF. Due to the top flange repairs being able to sustain a load higher than the theoretical capacity, they exceeded their demand and performed successfully with the girder.

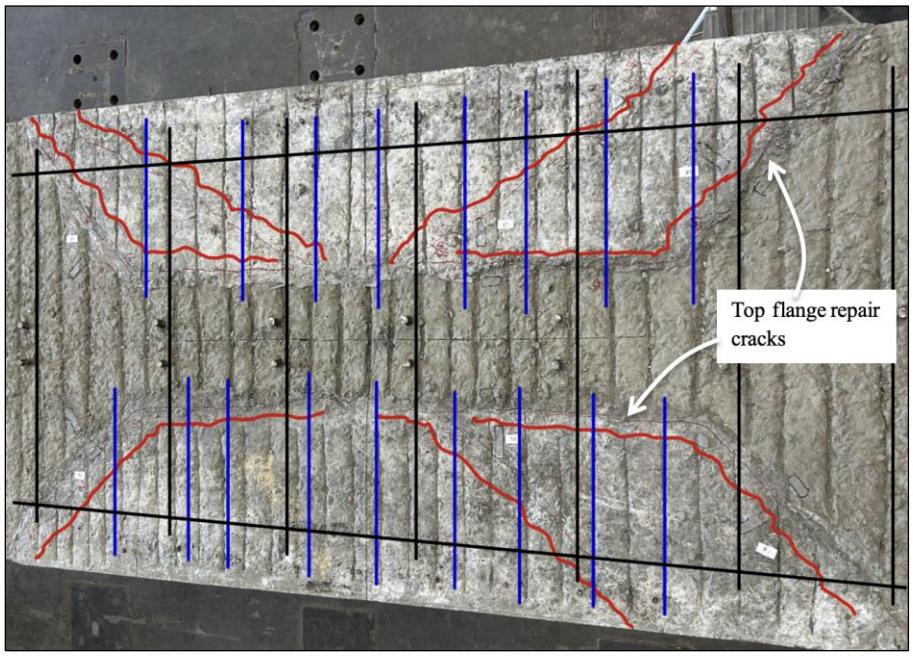

Figure 107. Photo. Test 1.4.F (repair 1.3RTF, 1.3LTF) overall top flange cracks at 80 kip.

CHAPTER 6. GIRDER 2 TESTS AND RESULTS

This chapter presents the setup, experiment, and test results from the Girder 2 test specimen. Calculations for this girder are given in appendix H.

OVERVIEW

A total of three tests were conducted on Girder 2, including a shear test at each end and a flexural test near midspan. The two shear tests were designed to mimic a two-axle American Association of State Highway and Transportation Officials (AASHTO) HS-93 truck load having two concentrated point loads,[22] represented by the spreader beam in a four-point bending test configuration. The flexural test was designed to maximize the tensile stress in repair 2.3RTF and observe the repair performance under this load. A matrix of each of the tests on Girder 2 is given in table 14.

Table 14. Girder 2 test matrix.

Test Name	Behavior	Repair(s) Considered
Test 2.1.S	Shear	2.1RTF, 2.1LTF
Test 2.2.S	Shear	2.2LTF
Test 2.3.F	Flexure	2.3LTF

TEST 2.1.S (REPAIR 2.1RTF, 2.1LTF) RESULTS

The first test on Girder 2, Test 2.1.S, was one of the two shear tests and was designed to test the performance of top flange repairs 2.1RTF and 2.1LTF under a two-axle AASHTO HS-93 truck load.[22] The load point location was 92 in. from the center of bearing of the north end of the girder. This distance is referred to as "x_1" in the calculations in appendix H (a/d = 1.51). The girder supports were centered 7 in. from each end. A spreader beam was

used in a four-point bending test configuration, where the “point” loads were spaced 4 ft apart to match the AASHTO HS-93 truck load wheel spacing (see figure 108).

Figure 108. Photo. Test 2.1.S (repair 2.1RTF, 2.1LTF) spreader beam with two rollers spaced 4 ft apart and 51 in. long.

The load was applied in steps. When either the desired load was reached or a significant crack developed, the pump valves were closed and a brief pause was taken prior to collecting gauge readings. Cracking was first heard and observed at a load of 280 kip. The crack angle was between 35 and 36 degrees from the horizontal. The strut configuration matches that discussed in the commentary for AASHTO Section 5.6.3 Strut-and-Tie Method.[23] The apparent width of the compression strut narrowed as the strut approached the bulb. Gauge readings were recorded, and no damage was seen in repairs 2.1RTF or 2.1LTF, nor in any other top flange repairs on the girder. Shear cracks are shown in figure 109 and figure 110, and end cracking in figure 111.

Figure 109. Photo. Test 2.1.S (repair 2.1RTF, 2.1LTF) shear cracks to the left of repair 2.1RTF (right face of girder pictured).

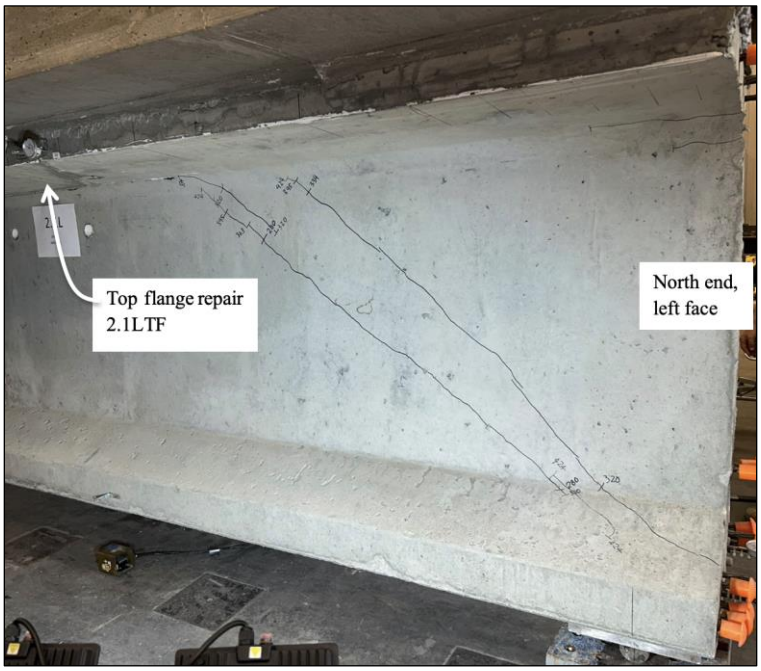

Figure 110. Photo. Test 2.1.S (repair 2.1RTF, 2.1LTF) shear cracks to the right of repair 2.1LTF (left face of girder pictured).

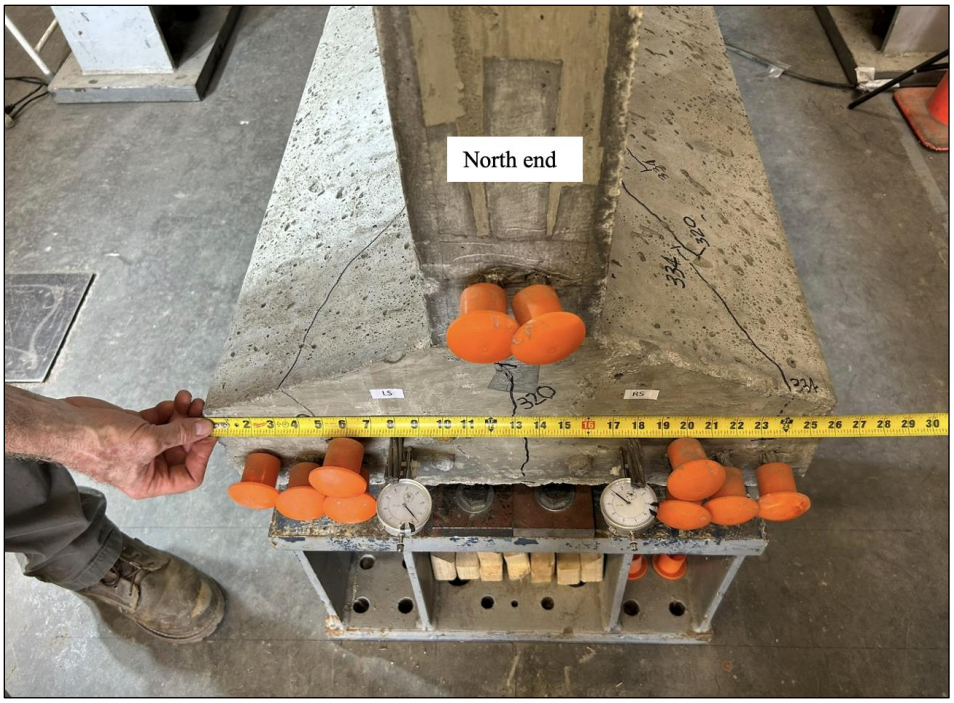

Figure 111. Photo. Test 2.1.S (repair 2.1RTF, 2.1LTF) north end cross-section cracks extending past center of bearing, prompting strand slip failure.

Loading continued to the maximum load of 424 kip. The shear crack width now measured 0.0177 in. Strand slip measured 0.017 in., which was past the slip failure threshold of 0.01 in. Loading was stopped at this point due to strand slip failure and to not prematurely fail the girder before the other tests were conducted. The final shear crack pattern is shown in figure 112 and figure 113. No separation of the repair concrete from the original concrete occurred in any repair. No signs of cracking, debonding, interface shear, or failure in top flange repairs 2.1RTF and 2.1LTF were observed.

Figure 112. Photo. Test 2.1.S (repair 2.1RTF, 2.1LTF) final shear cracks not spreading to top flange repair 2.3RTF at 424 kip (right face of girder pictured).

Figure 113. Photo. Test 2.1.S (repair 2.1RTF, 2.1LTF) final shear cracks not spreading to top flange repair 2.3LTF at 424 kip (left face of girder pictured).

As seen in the load-deflection plot for Test 2.1.S (repair 2.1RTF, 2.1LTF) (see figure 114), the girder was tested past its elastic point (cracking), resulting in a nonlinear deformation after unloading due to the cracked girder section. The finding of this shear test was that the girder sustained a load within 89 percent of the maximum load based on the nominal shear capacity (the dashed-dotted line in figure 114). This suggests that top flange repairs 2.1RTF and 2.1LTF did not negatively impact the shear capacity of the nonconforming girder. The girder performed well past its service load conditions.

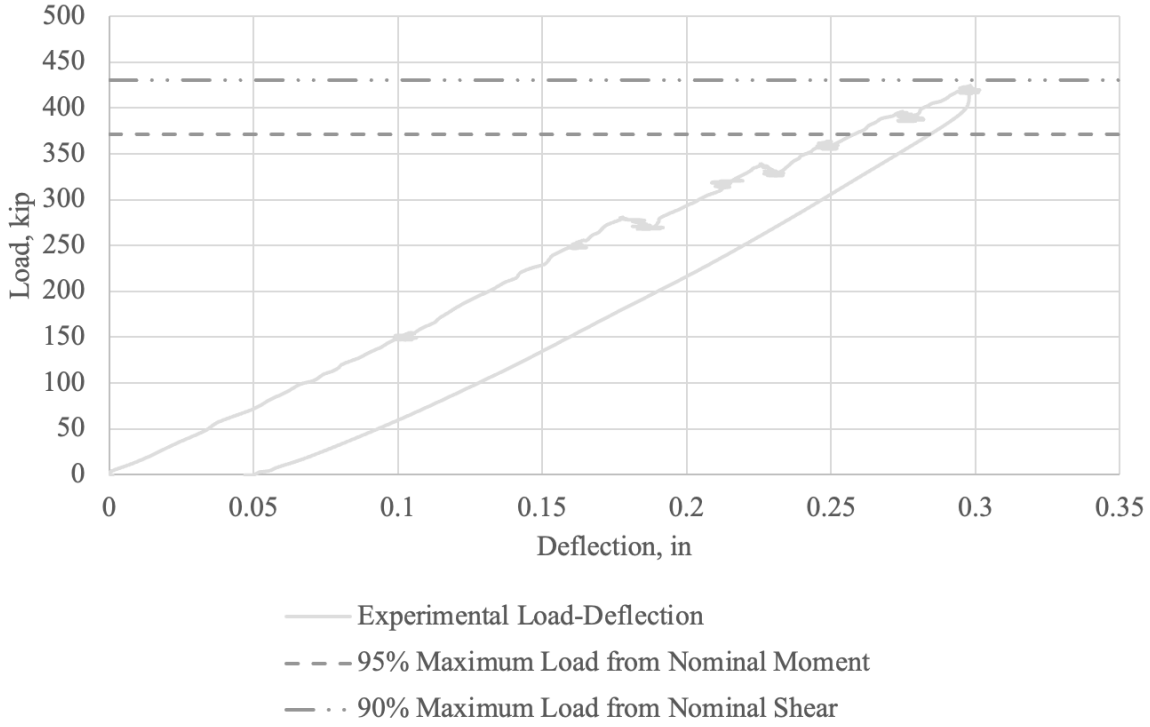

Figure 114. Graph. Test 2.1.S (repair 2.1RTF, 2.1LTF) load-deflection plot.

The moment-curvature plot for Test 2.1.S (repair 2.1RTF, 2.1LTF) (see figure 115) shows the experimental values obtained from this test. Nonlinear behavior is exhibited after the girder cracked at approximately 1,495 kip-ft.

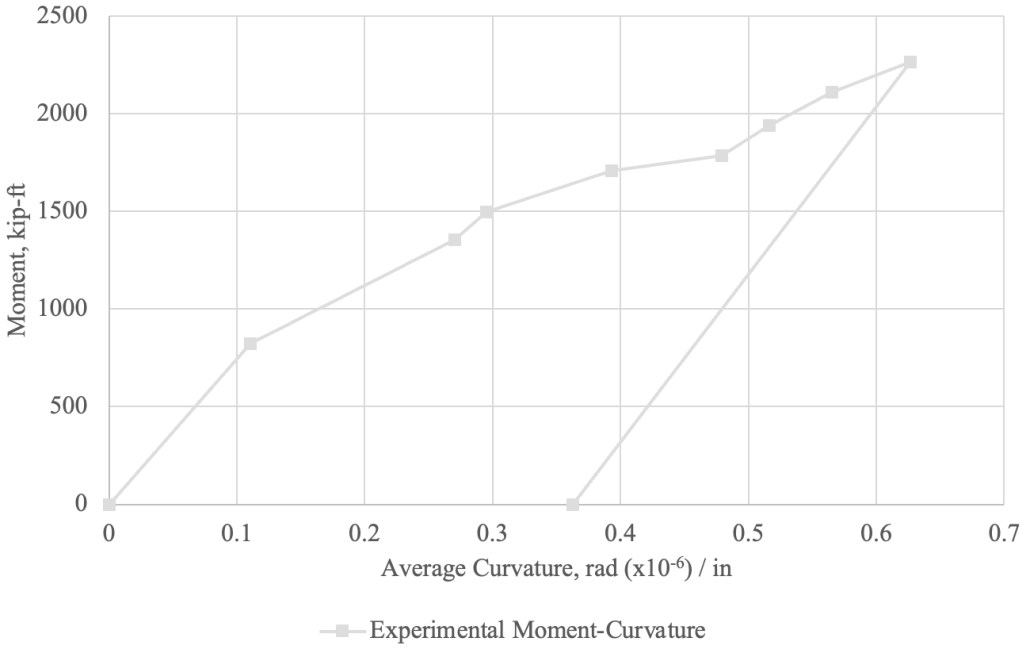

Figure 115. Graph. Test 2.1.S (repair 2.1RTF, 2.1LTF) moment-curvature plot.

The load-strand slip plot for Test 2.1.S (repair 2.1RTF, 2.1LTF) (see figure 116) shows the strand slip measurements, as well as the nominal capacity loads. At a load of 430 kip, strands LS well exceeded the strand slip limit of 0.01 in., which coincides with a load close to 90 percent of the maximum load from nominal shear (the dotted-dashed line in figure 116). This suggests the girder failed due to bond-slip caused by shear cracks through the bearing zone caused by the compression strut. Shear cracks did not spread into the longest top flange repair 2.2LTF.

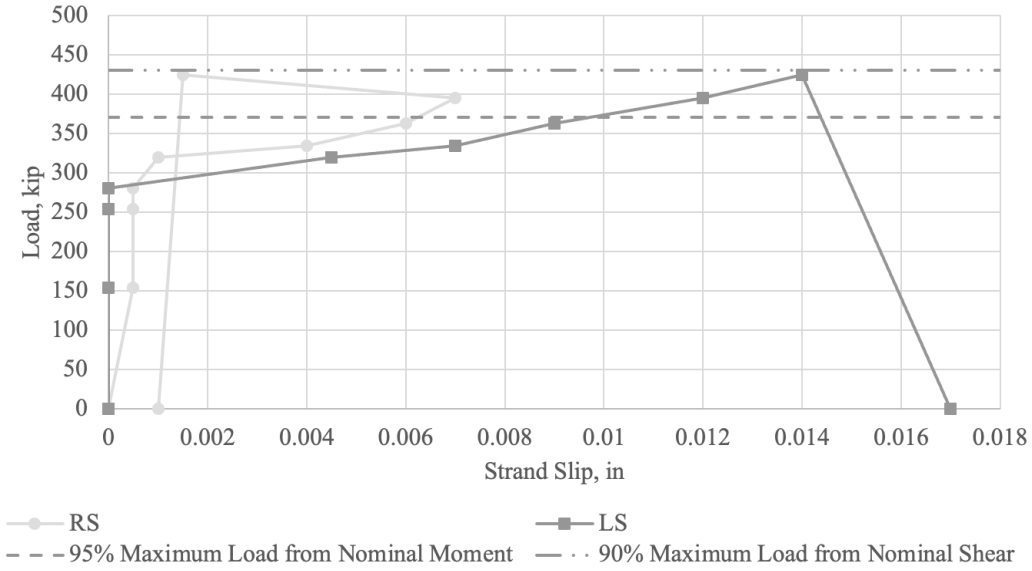

Figure 116. Graph. Test 2.1.S (repair 2.1RTF, 2.1LTF) load-strand slip plot.

TEST 2.2.S (REPAIR 2.2LTF) RESULTS

The second test on Girder 2, Test 2.2.S, was designed to test the performance of top flange repair 2.2LTF under a two-axle AASHTO HS-93 truck load.[(22)] The load point location was 92 in. from the center of bearing of the south end of the girder. This distance is referred to as "x_2" in the appendix H calculations (a/d = 1.51). The girder supports and spreader beam configuration matched the Test 2.1.S (repair 2.1RTF, 2.1LTF) in four-point bending.

As the girder was loaded in steps, the first shear cracks were seen and heard at a load of 281 kip (see figure 117 and figure 118), along with end zone cracking (see figure 119). The shear crack width measured 0.00591 in. The strut width was 10–10.5 in. The strut angle was between 29 and 33 degrees. Gauge readings were taken, and no damage was seen in repair 2.2LTF or any other top flange repairs.

Figure 117. Photo. Test 2.2.S (repair 2.2LTF) initial shear cracks on original, nonrepaired face (right face of girder pictured).

Figure 118. Photo. Test 2.2.S (repair 2.2LTF) shear cracks on repaired face, not extending into top flange repair 2.2LTF (left face of girder pictured).

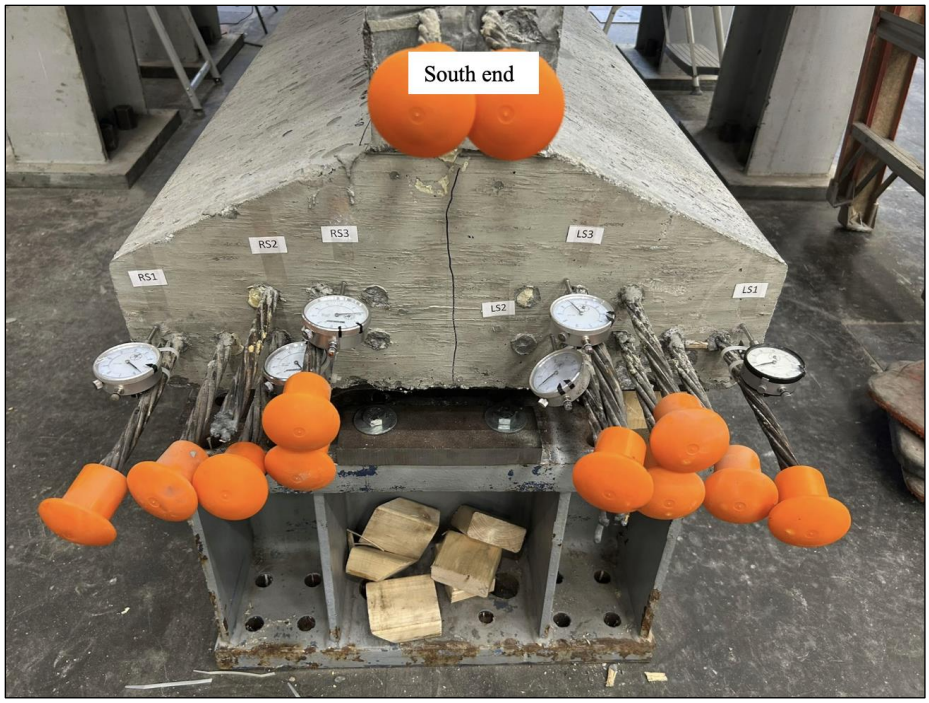

Figure 119. Photo. Test 2.2.S (repair 2.2LTF) south end cross-section crack at 281 kip.

The girder was loaded to a maximum load of 431 kip. More shear cracks formed, measuring 0.00591–0.00787 in. wide. The first shear crack width now measured 0.0157 in., and the slip in the strand measured 0.013 in. in dial gauge LS3. The south end crack width increased to 0.0256 in. The bearing crack width now measured 0.0256 in., and a new bearing crack formed, measuring 0.00787 in. wide (see figure 120). The load was stopped at this point due to strand slip failure and to not prematurely fail the girder before the last test could be conducted. There were no signs of failure in top flange repair 2.2LTF.

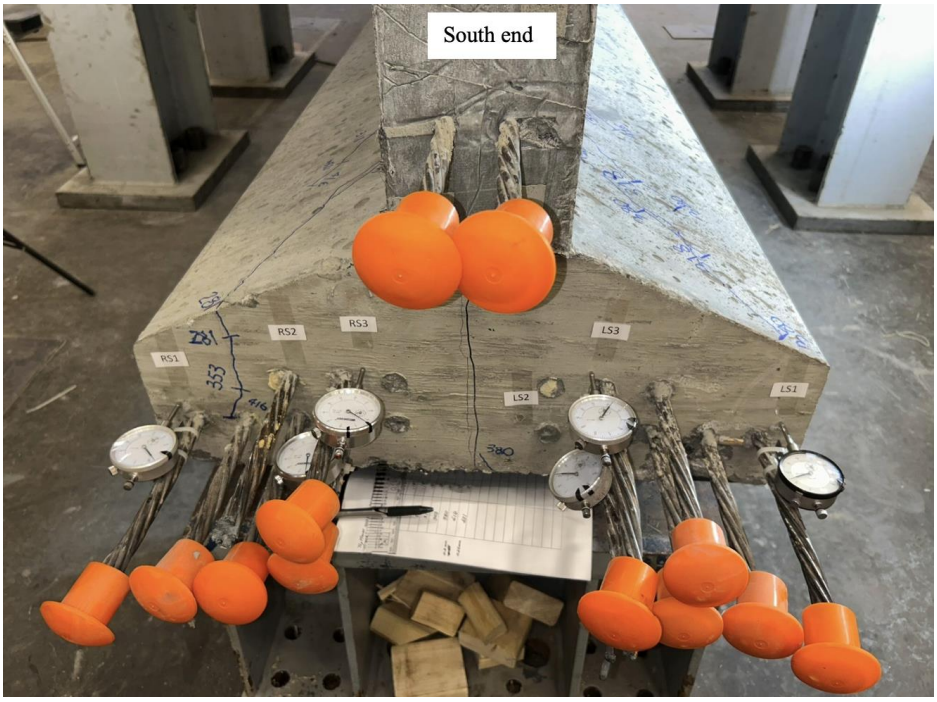

Figure 120. Photo. Test 2.2.S (repair 2.2LTF) south end cross-section vertical cracks at 431 kip.

The final shear crack pattern of Test 2.2.S (repair 2.2LTF) is shown in figure 121 and figure 122. As these overall figures of the repairs at maximum loads show, no separation of the repair concrete from the original concrete occurred in any repair. Diagonal shear cracks were directed at the repair zone; yet, the authors observed no diagonal cracking at the edges of the BT-54 flange or in the cast-in-place deck. No signs of cracking, debonding, interface shear, or failure in top flange repair 2.2LTF were observed.

Figure 121. Photo. Test 2.2.S (repair 2.2LTF) final shear cracks on nonrepaired, original face at 424 kip (right face of girder pictured).

Figure 122. Photo. Test 2.2.S (repair 2.2LTF) final shear cracks on repaired face at 424 kip. The longest top flange repair length is 126 in. (left face of girder pictured).

The load-deflection plot for Test 2.2.S (repair 2.2LTF) is shown in figure 123. The girder behaved in a similar manner to the first shear test on this girder. The finding of this shear test was that the girder successfully exceeded 90 percent of the maximum load based on the nominal shear capacity (the dashed-dotted line in figure 123). This suggests that repair 2.2LTF did not negatively impact the shear capacity of the nonconforming girder. Girder 2 had the longest top flange repair and still performed well past its service load conditions, as shown by this test.

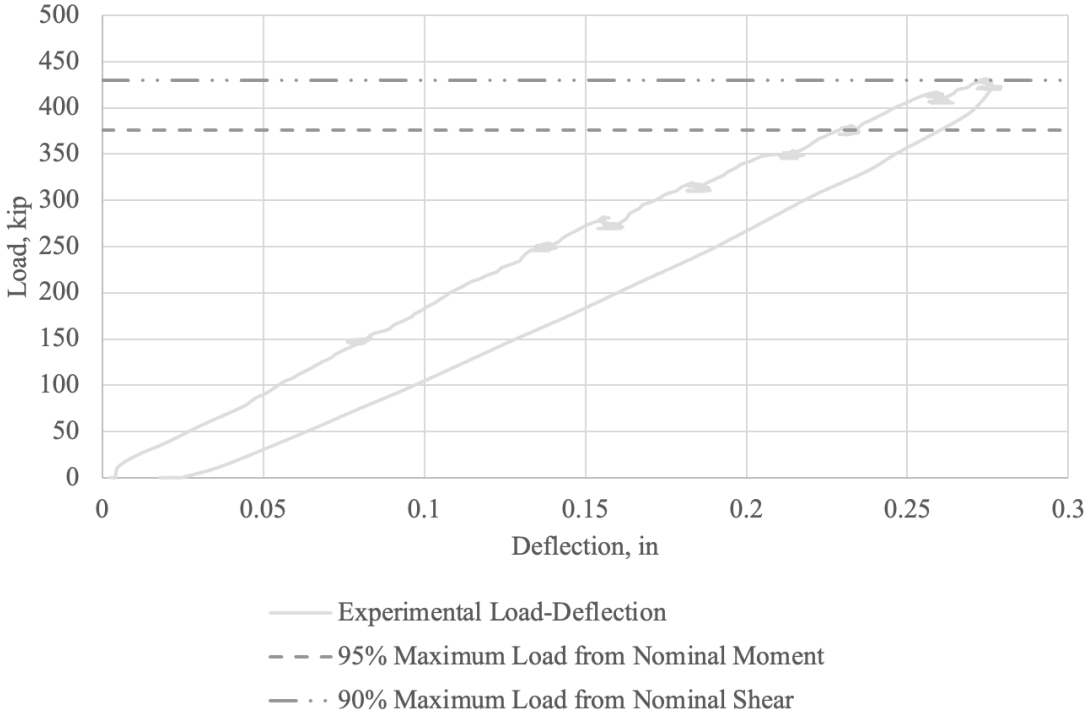

Figure 123. Graph. Test 2.2.S (repair 2.2LTF) load-deflection plot.

The moment-curvature plot for Test 2.2.S (repair 2.2LTF) (see figure 124) shows the experimental values obtained from this test. Nonlinear behavior is exhibited after the girder cracked at approximately 1,500 kip-ft.

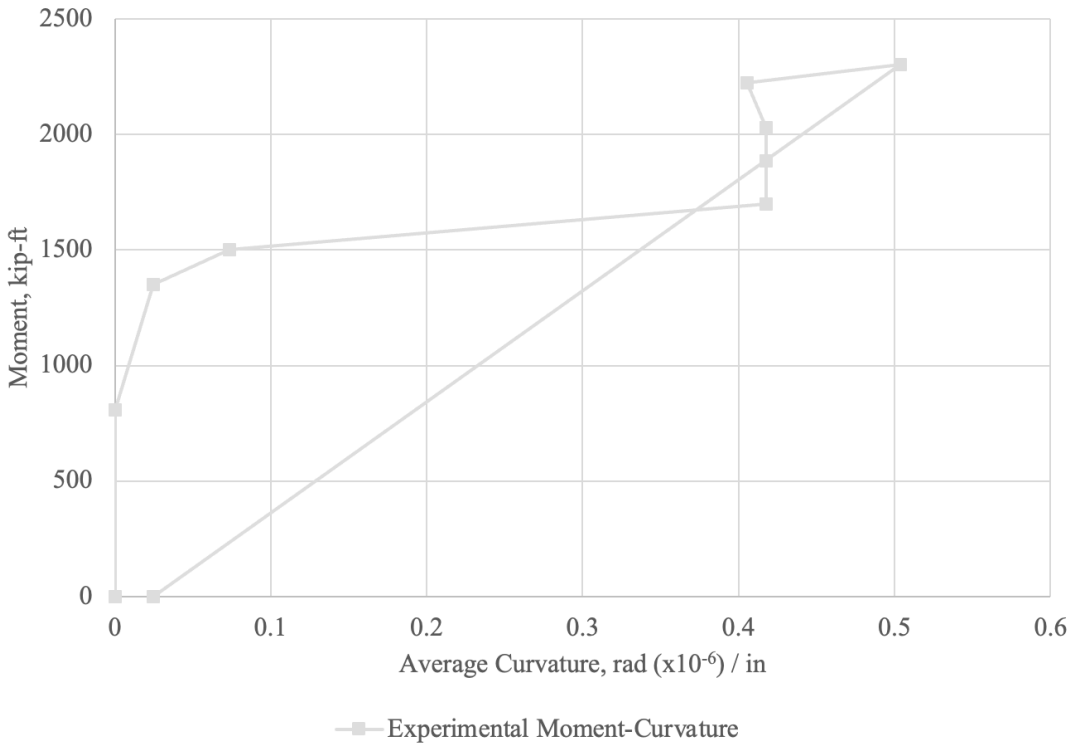

Figure 124. Graph. Test 2.2.S (repair 2.2LTF) moment-curvature plot.

The load-strand slip plot for Test 2.2.S (repair 2.2LTF) (see figure 125) shows the strand slip measurements, as well as the nominal capacity loads. At a load of 500 kip, strands LS2, LS3, and RS3 exceeded the strand slip limit of 0.01 in., which coincides with a load just past 90 percent of the maximum load from nominal shear (the dotted-dashed line in figure 125). This suggests the girder failed as a result of bond-slip caused by shear cracks through the bearing zone caused by the compression strut. Shear cracks did not spread into the longest top flange repair 2.2LTF.

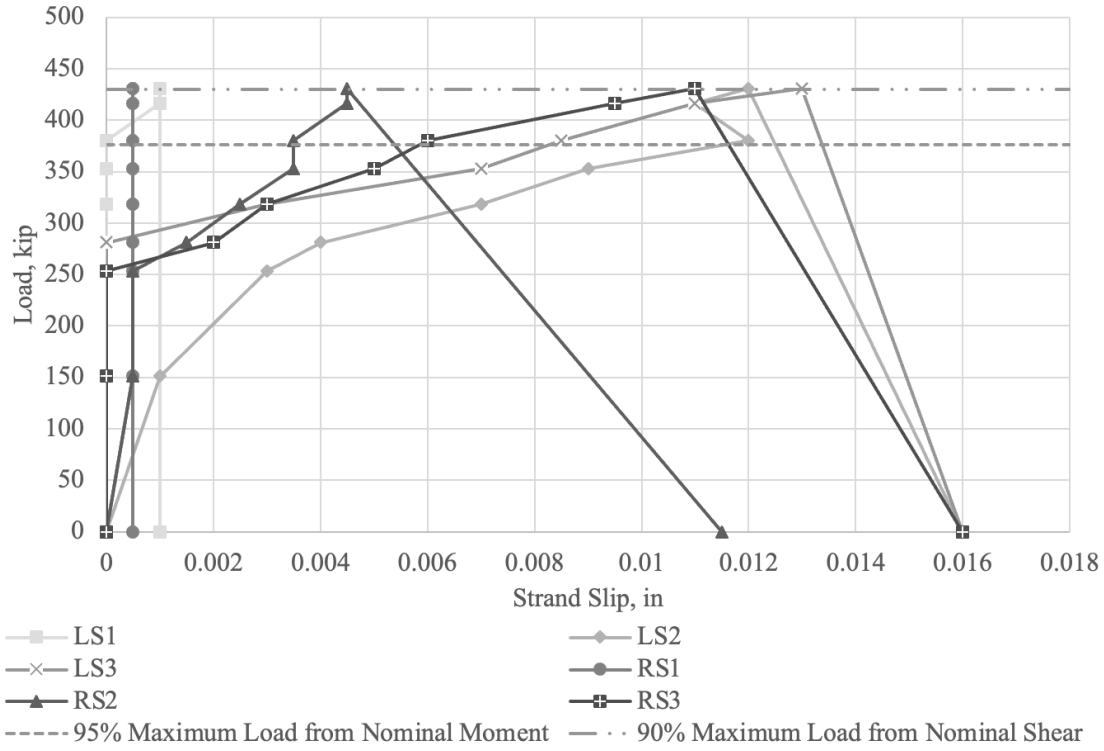

Figure 125. Graph. Test 2.2.S (repair 2.2LTF) load-strand slip plot.

TEST 2.3.F (REPAIR 2.3LTF) RESULTS

The last test on Girder 2, Test 2.3.F, was a flexural, moment capacity test at midspan. This test was designed to observe the performance of top flange repair 2.3LTF by centering the load point over the repair and maximizing the tensile stress experienced by it. The load point location was 263 in. from the center of bearing of the south end of the girder. Theoretical calculations for Girder 2 can be found in appendix H. The girder supports were placed 7 in. from each end. The spreader beam was used in a four-point bending test configuration test (see figure 126). Dial gauges were placed on the bottom flange at the level of the bottom strands and 4 in. below the top of the deck to measure top and bottom strain to enable calculation of girder curvature.

Figure 126. Photo. Test 2.3.F (repair 2.3LTF) spreader beam four-point bending configuration near midspan, simulating a two-axle truck load to create maximum tensile stress in the top flange.

Flexural cracking in the bottom flange occurred at 245 kip, and Figure 127 shows the cracking at 264 kip. At a load of 335 kip, a new shear crack patterned around the tie-down transport holes, near the south end of the girder where the second test took place. Figure 128 and figure 129 show this shear crack pattern that occurred during the midspan loading of Girder 2.

The load was then increased to its final load of 341 kip. After that load, the initial flexural cracks measured 0.0315 in. on the right face of the girder and 0.0591 in. on the left face of the girder. Further, the initial shear-flexural cracks measured 0.0295 in. on both faces of the bulb. The final flexural and shear-flexural crack patterns are shown in figure 130 and figure 131.

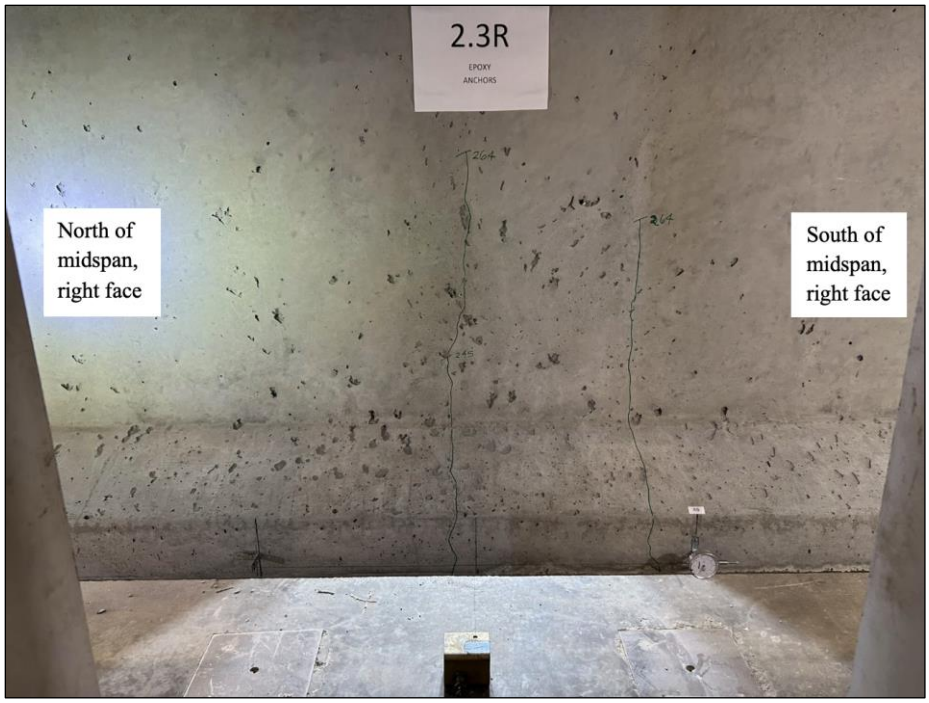

Figure 127. Photo. Test 2.3.F (repair 2.3LTF) flexural cracks at 264 kip (right face of girder pictured).

Figure 128. Photo. Test 2.3.F (repair 2.3LTF) shear cracks through tie-down transport holes toward the midspan of the girder at a 335-kip flexural load, nonrepaired, original face (right face of girder pictured).

Figure 129. Photo. Test 2.3.F (repair 2.3LTF) shear cracks through tie-down holes toward the midspan of the girder at a 335-kip flexural load, repaired face with longest top flange repair of 126 in. (left face of girder pictured).

Figure 130. Photo. Test 2.3.F (repair 2.3LTF) final flexural and shear-flexural cracks on repaired face at 341 kip. Cracks did not extend into top flange repair 2.3RTF (right face of girder pictured).

Figure 131. Photo. Test 2.3.F (repair 2.3LTF) final flexural and shear-flexural cracks on nonrepaired, original face at 341 kip (left face of girder pictured).

As the overall figures of the repairs at maximum loads show, no separation of the repair concrete from the original concrete occurred in any repair (see figure 130 and figure 131). Cracking was arrested in the repair zone due to the longitudinal prestressing strands, the non-prestressed #3 reinforcement (c-bars), and the restraint provided by the cast-in-place concrete deck.

The load-deflection plot for Test 2.3.F (repair 2.3LTF) (see figure 132) shows that the girder was tested well past its elastic point (cracking), resulting in a nonlinear deformation after unloading due to the cracked girder section. The finding of this flexural test was that the girder successfully exceeded 90 percent of the maximum load based on the nominal flexural capacity (the dashed line in figure 132). The girder performed well past its service load conditions, as shown by this test.

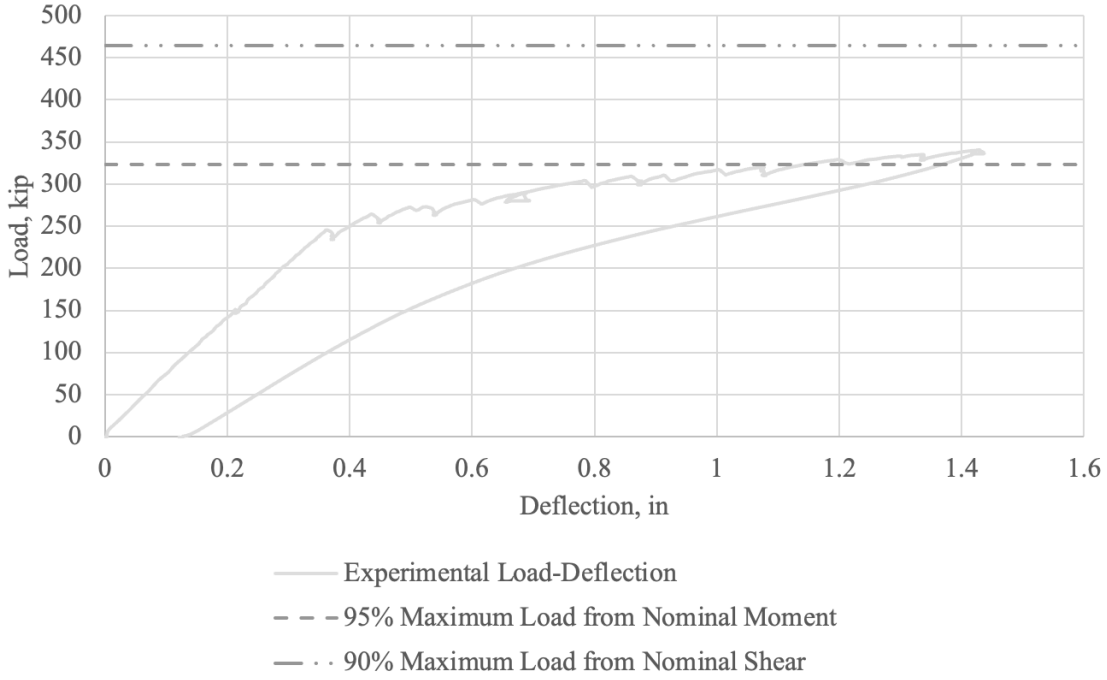

Figure 132. Graph. Test 2.3.F (repair 2.3LTF) load-deflection plot.

The moment-curvature plot for Test 2.3.F (repair 2.3LTF) (see figure 133) shows the experimental values obtained from this test. Nonlinear behavior is exhibited after the girder cracked at approximately 2,470 kip-ft. Based on this plot, the repaired girder exceeded 95 percent of the nominal moment capacity. This suggests that top flange repair 2.3LTF did not negatively impact the capacity of the nonconforming girder.

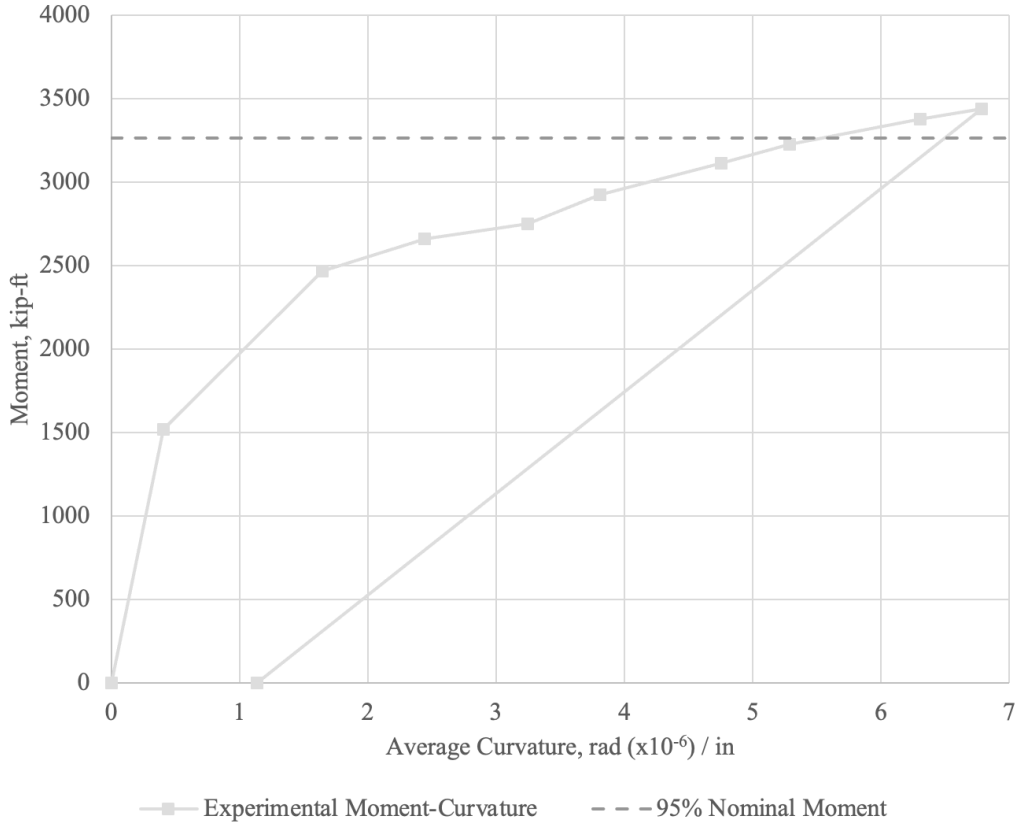

Figure 133. Graph. Test 2.3.F (repair 2.3LTF) moment-curvature plot.

CHAPTER 7. GIRDER 3 TESTS AND RESULTS

This chapter presents the setup, experiment, and test results from the Girder 3 test specimen. Calculations for this girder are given in appendix I.

OVERVIEW

Tests on Girder 3 concentrated on bottom flange repairs located 8.5 ft from the north end, 5.25 ft from the south end, and at midspan. In total, three tests were conducted on Girder 3, as summarized in table 15.

Table 15. Girder 3 test matrix.

Test Name	Behavior	Repair(s) Considered
Test 3.1.S	Shear	3.1RBF, 3.1LBF
Test 3.2.S	Shear	3.2RBF
Test 3.3.F	Flexure	3.3RBF, 3.3LBF

TEST SETUP

As discussed in chapter 2, some bottom flange repairs were just on one side of the girder, whereas others were on both sides. The shear tests at each end were designed to maximize the compression force in the diagonal struts; the total load was concentrated at a single point rather than the previous two-point loads. Such concentration was designed to maximize the stresses in the prestressing strands at and near the ends of the girders, which would create possible bond-slip failures, development length failures in repair patches near the ends, and delamination of repair concrete near the end. The midspan flexural test was designed to determine if the bottom flange patch would dislodge when strand yield strains and large concrete cracks developed.

TEST 3.1.S (REPAIR 3.1RBF, 3.1LBF) RESULTS

The first test on Girder 3, Test 3.1.S, was designed to maximize the compression force in the diagonal strut to observe the performance of repairs 3.1RBF and 3.1LBF under this loading. The load point location was 94.75 in. from the center of bearing of the north end of the girder. This distance is referred to as "x1" in the appendix I calculations (a/d = 1.55). The spreader beam was used in a three-point bending test configuration, where only one end of the spreader beam was used to transfer load. This configuration also maintained the distance from the deck surface to the base of the load cell, alleviating the need to adjust the test setup. The spreader beam configuration for this test is shown in figure 134.

Figure 134. Photo. Test 3.1.S (repair 3.1RBF, 3.1LBF) spreader beam configuration with the hydraulic ram located directly above the load point closest to the north girder bearing.

Upon loading, two diagonal shear cracks were seen at a load of 300 kip. The shear crack width measured 0.00787 in. The strut width was between 9 and 11 in. The crack angles were between 37 and 40 degrees (see figure 135 and figure 136).

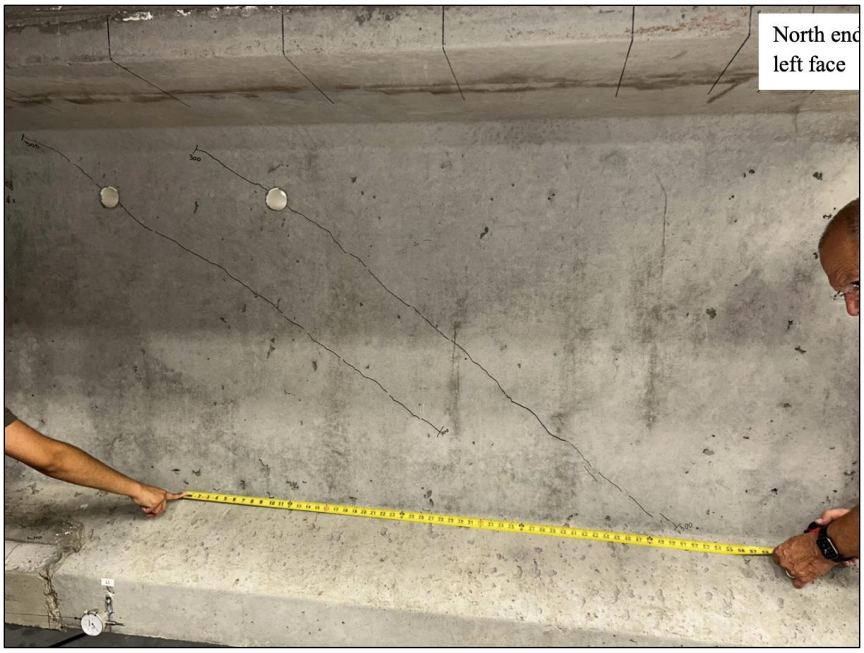

Figure 135. Photo. Test 3.1.S (repair 3.1RBF, 3.1LBF) initial shear cracks (left face of girder pictured).

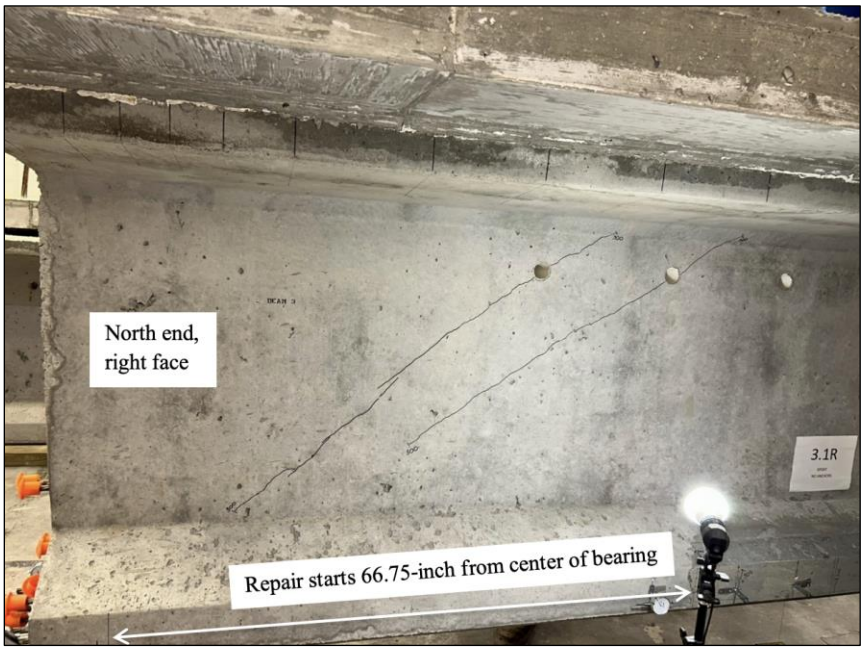

Figure 136. Photo. Test 3.1.S (repair 3.1RBF, 3.1LBF) initial shear cracks (right face of girder pictured).

Gauge readings were recorded, and flexural cracks were seen in repairs 3.3RTF and 3.3LTF at the quarter points. These cracks measured 0.00394–0.00591 in. wide. Flexural cracks occurred at a 325-kip load (see figure 137 and figure 138).

Figure 137. Photo. Test 3.1.S (repair 3.1RBF, 3.1LBF) flexural cracking on midspan repairs at 325 kip (right face of girder pictured).

Figure 138. Photo. Test 3.1.S (repair 3.1RBF, 3.1LBF) flexural cracking on midspan repairs at 325 kip (left face of girder pictured).

At a load of 399 kip, the “bottom” shear crack increased to 0.0157 in. on the right side of the girder. Figure 139 shows the three prominent shear cracks that formed on the right face of the web.

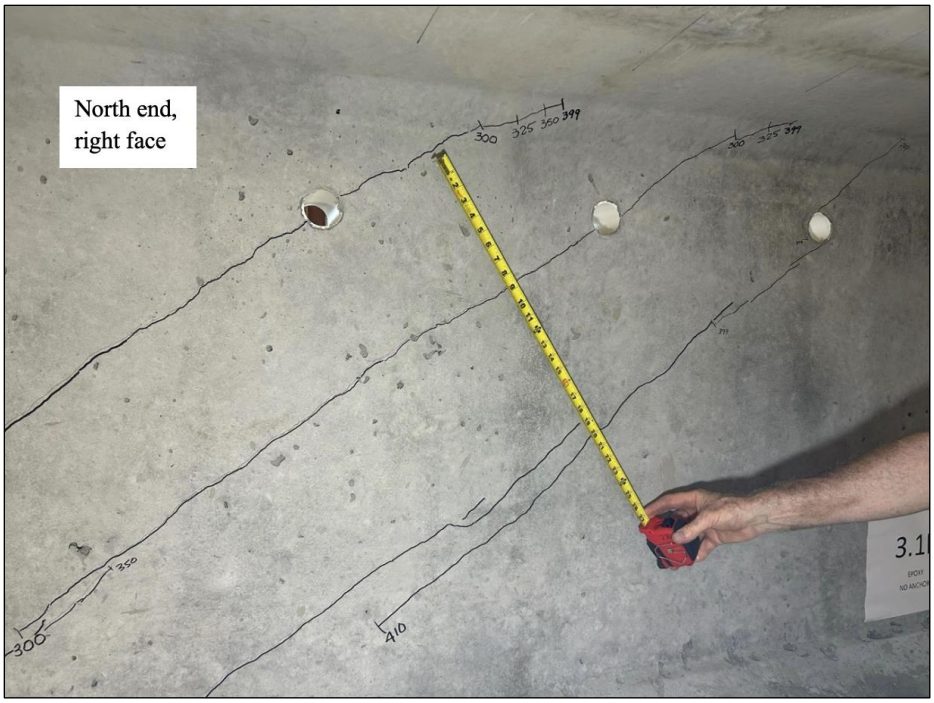

Figure 139. Photo. Test 3.1.S (repair 3.1RBF, 3.1LBF) shear cracks strut width at 410 kip (right face of girder pictured).

At a load of 431 kip, two new short shear cracks, measuring 0.00787 in. wide, formed. A final strand slip of 0.0145 in. was measured in dial gauge RS1, prompting the termination of the test due to bond-slip. Vertical cracks passing through the strands on the end cross-section were observed (see figure 140).

The final crack pattern is shown in figure 141 and figure 142. As these overall figures of the repairs at maximum loads show, no separation of the repair concrete from the original concrete occurred in any repair even though significant cracking occurred in the repair. Crack widths were uniform through the lengths of the repairs, showing that there was no debonding of the prestressing strand. No signs of interface shear cracking or failure of the bottom flange repairs 3.1RBF and 3.1LBF were observed.

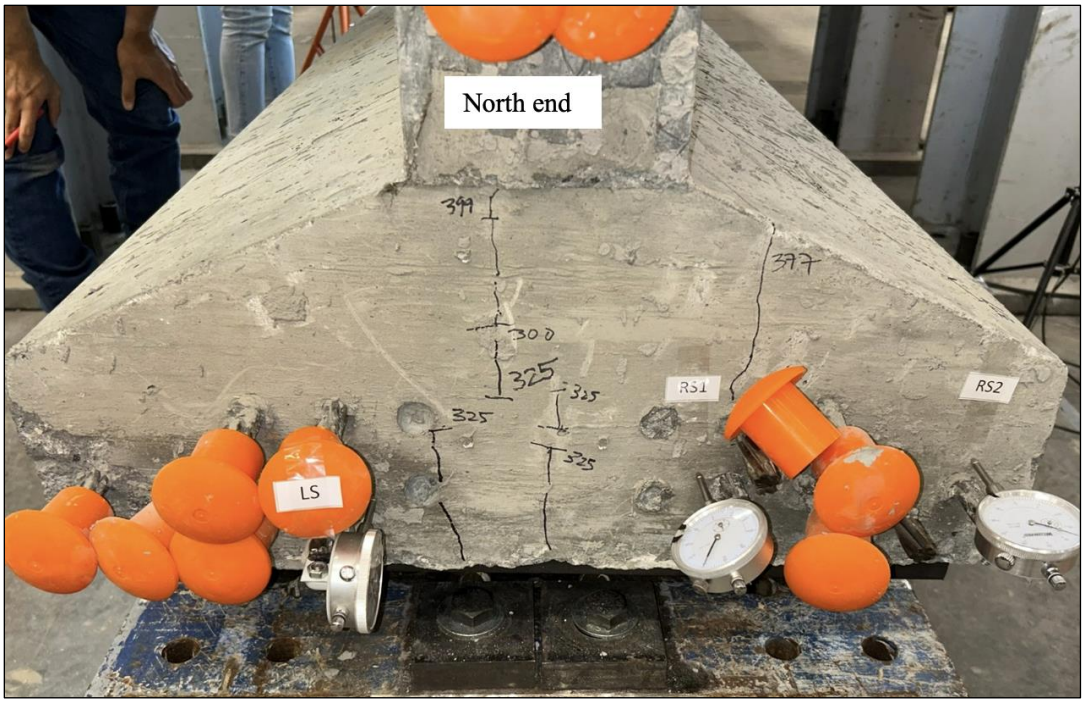

Figure 140. Photo. Test 3.1.S (repair 3.1RBF, 3.1LBF) vertical cracks on north end cross-section at 431 kip; strand slip of 0.0145 in. at dial gauge RS1.

Figure 141. Photo. Test 3.1.S (repair 3.1RBF, 3.1LBF) final crack pattern at 431 kip (right face of girder pictured).

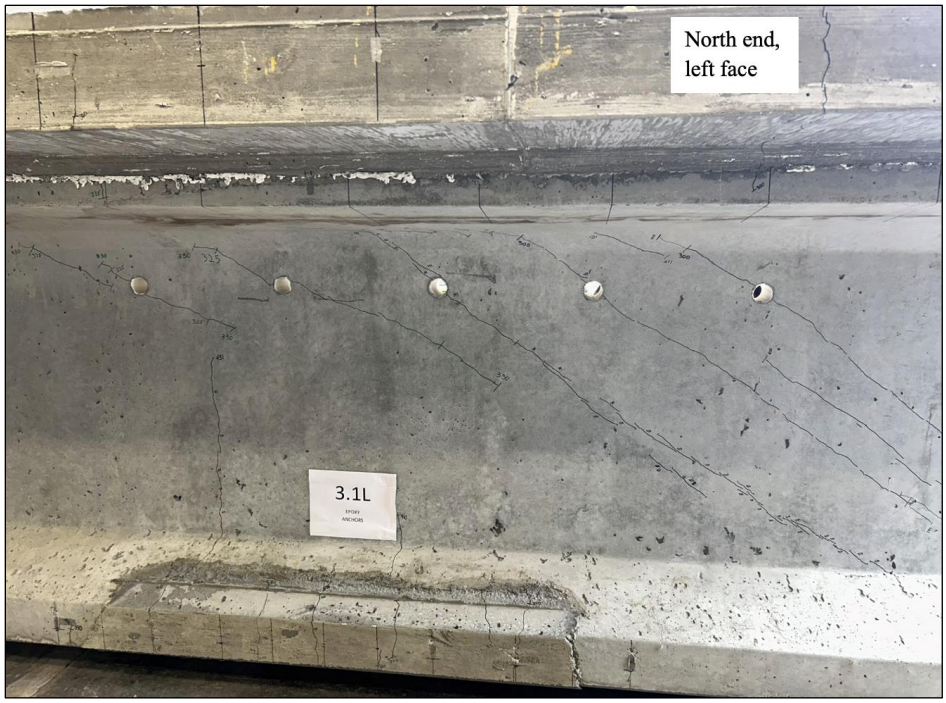

Figure 142. Photo. Test 3.1.S (repair 3.1RBF, 3.1LBF) final crack pattern at 431 kip (left face of girder pictured).

The load-deflection plot for Test 3.1.S (repair 3.1RBF, 3.1LBF) (see figure 143) shows that the girder was tested past its elastic point (cracking), resulting in a nonlinear deformation after unloading due to the cracked girder section. The finding of this shear test was that the girder successfully exceeded 90 percent of the maximum load based on the nominal shear capacity (the dashed-dotted line in figure 143). This suggests that bottom flange repairs 3.1RBF and 3.1LBF did not negatively impact the shear capacity of the nonconforming girder. The girder performed well past its service load conditions, as shown by this test.

The moment-curvature plot for Test 3.1.S (repair 3.1RBF, 3.1LBF) (see figure 144) shows the experimental values obtained from this test. Nonlinear behavior is exhibited after the girder cracked at approximately 1,946 kip-ft.

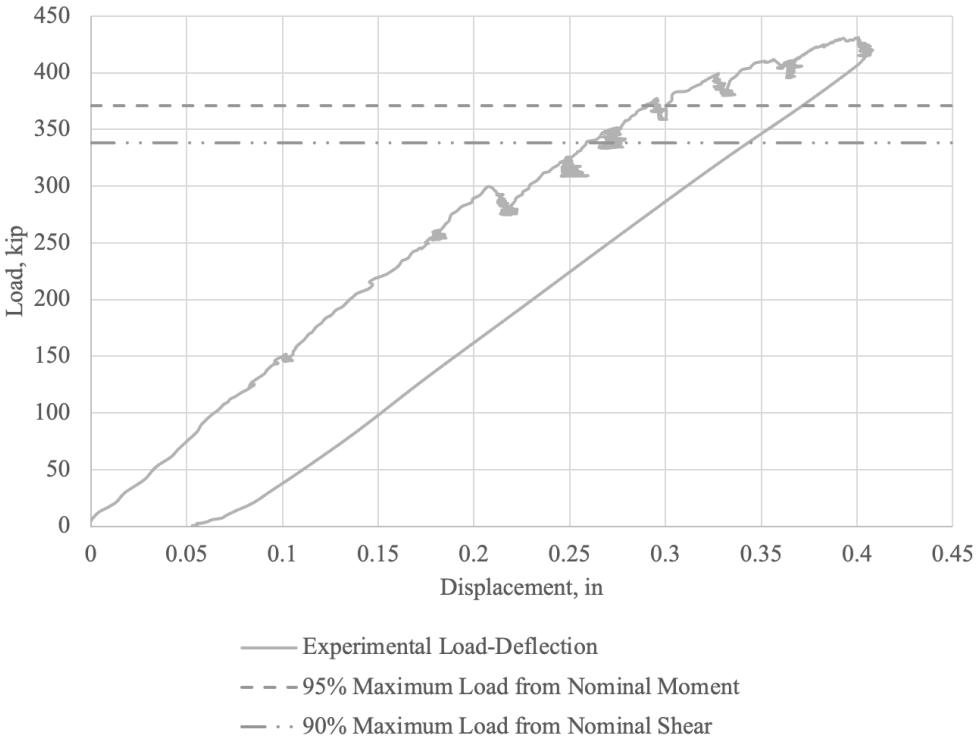

Figure 143. Graph. Test 3.1.S (repair 3.1RBF, 3.1LBF) load-deflection plot.

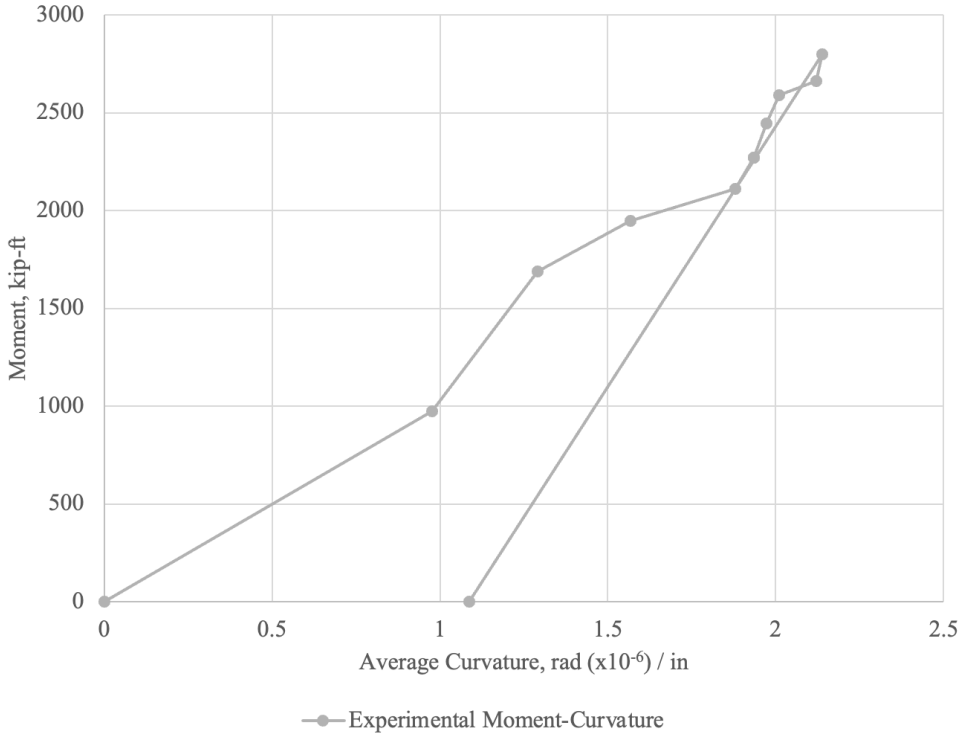

Figure 144. Graph. Test 3.1.S (repair 3.1RBF, 3.1LBF) moment-curvature plot.

The load-strand slip plot for Test 3.1.S (repair 3.1RBF, 3.1LBF) (see figure 145) shows the strand slip measurements, as well as the nominal capacity loads. The strands did not exceed the strand slip limit of 0.01 in. at maximum applied load. However, as the load was removed, the bearings at the end of the girder provided less transverse frictional restraint and allowed the strands to slip farther. This suggests the girder failed in a strand-slip shear nature, as can be confirmed by the load-deflection behavior. Flexural cracks did form in the bottom flange repairs, but 95 percent of the nominal shear capacity was well surpassed.

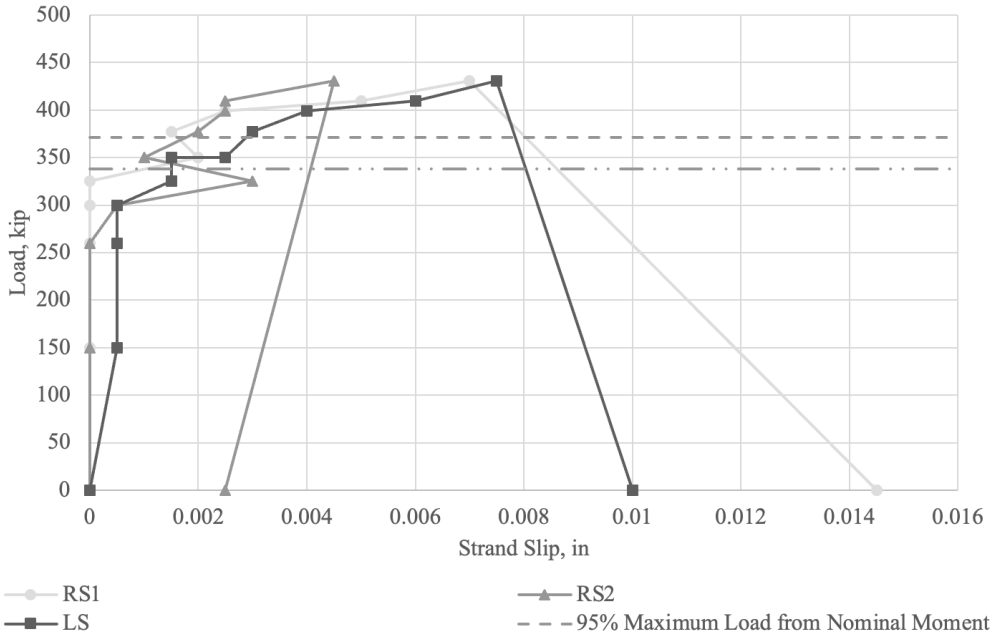

Figure 145. Graph. Test 3.1.S (repair 3.1RBF, 3.1LBF) load-strand slip plot.

TEST 3.2.S (REPAIR 3.2RBF) RESULTS

The second test on Girder 3, Test 3.2.S, was designed to maximize the compression force in the diagonal strut to observe the performance of repair 3.2RBF under this loading. The load point location was 113 in. from the center of bearing of the south end of the girder. This distance is referred to as "x_2" in the appendix I calculations (a/d = 1.85). The girder

supports and spreader beam configuration were the same as that for Test 3.1.S (repair 3.1RBF, 3.1LBF; three-point bending).

At a load of 272 kip, the first diagonal shear cracks were observed, with widths between 0.00394 and 0.00787 in. (see figure 146 and figure 147). The strut width was 10 in. between cracks, and the strut angle was between 27 and 29 degrees.

Flexural cracks also formed on repair 3.2RBF, which were 0.00394 in. wide. Flexural cracking increased at 376 kip (see figure 148 and figure 149).

Figure 146. Photo. Test 3.2.S (repair 3.2RBF) initial shear cracks not going through repair 3.2RBF at 272 kip (right face of girder pictured).

Figure 147. Photo. Test 3.2.S (repair 3.2RBF) initial shear cracks on nonrepaired, original girder face at 272 kip (left face of girder pictured).

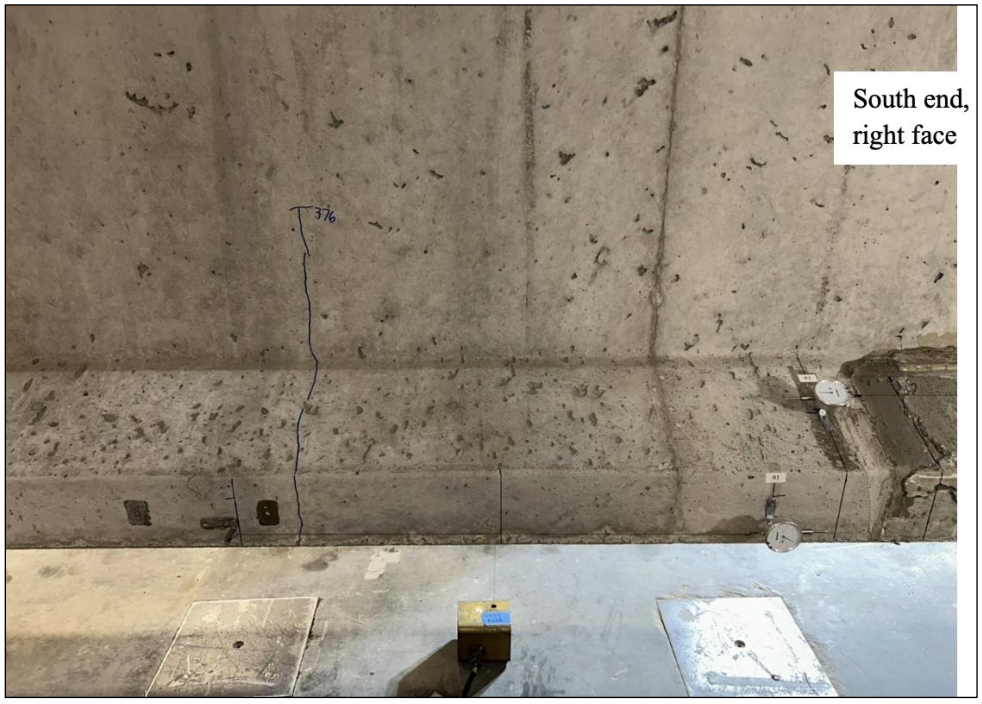

Figure 148. Photo. Test 3.2.S (repair 3.2RBF) flexural cracks toward the midspan, to the left of repair 3.2RBF at 376 kip (right face of girder pictured).

Figure 149. Photo. Test 3.2.S (repair 3.2RBF) flexural cracks toward the midspan, on nonrepaired, original girder face at 376 kip (left face of girder pictured).

At 395 kip, strand slip of 0.010 in. was observed at strand location LS where a vertical crack ran adjacent to the strand. The end cross-section is shown in figure 150.

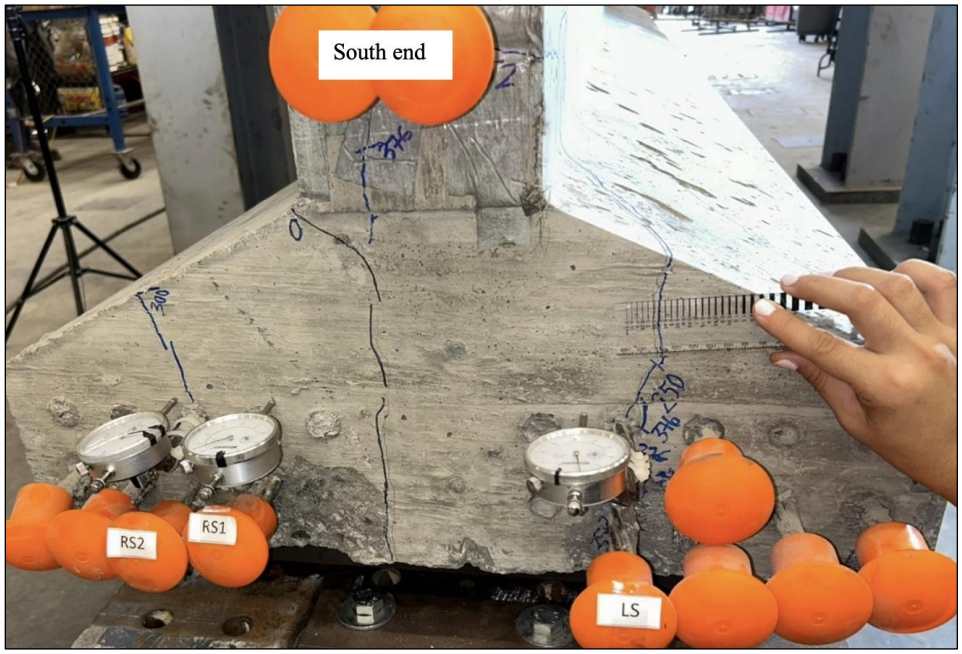

Figure 150. Photo. Test 3.2.S (repair 3.2RBF) south end cross-section crack adjacent to strand LS at 400 kip.

At the maximum load of 410 kip, the initial shear crack on the right side of the girder measured 0.0157 in. and the left crack measured 0.0177 in. Flexural crack width still measured 0.00591–0.00787 in., but the cracks were extending toward the top of the web. Because a strand slip of 0.01 in. had already occurred, loading was terminated at this point to avoid additional girder failure. Figure 151 shows the shear-flexural cracks on the left face of the girder.

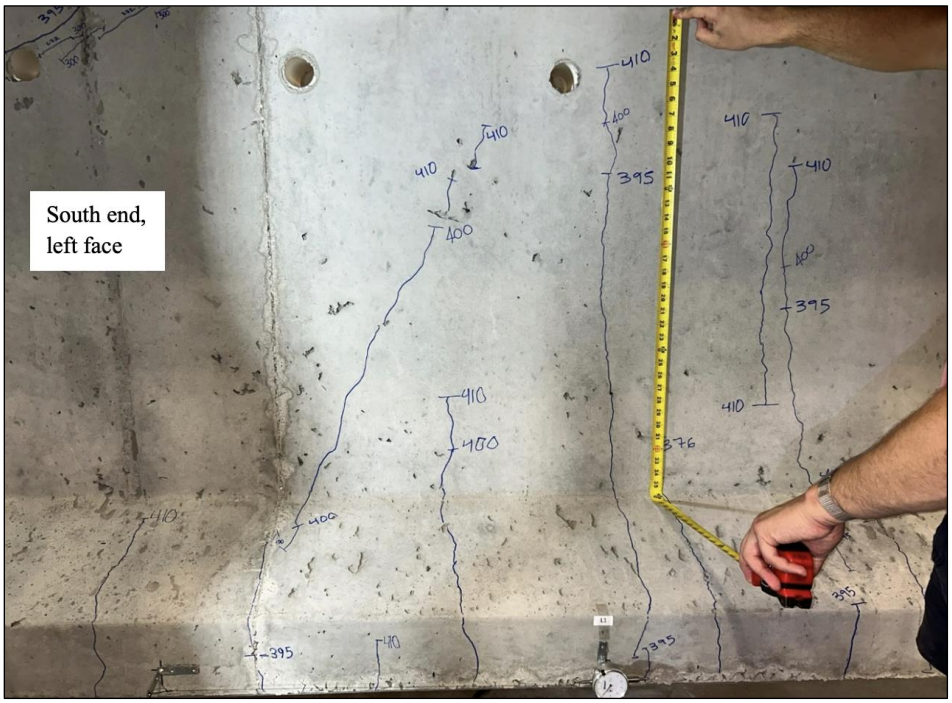

Figure 151. Photo. Test 3.2.S (repair 3.2RBF) shear-flexural cracks located directly under load point at 410 kip (left face of girder pictured).

The final shear crack pattern of both sides of the girder is shown in figure 152 and figure 153. Note the width of the compression struts on each side of the girder and that the center of compression is beyond the center of bearing of the girder. The horizontal component of the compression force in the web was resisted by the tensile forces in the strands across the bottom flange. Because the center of tension in the left and right sides of the bulb was eccentric to the center of compression in the web, transverse tensile forces in

the bottom flange developed; these tensile forces resulted in the end zone cracking, the decrease in bond capacity of the strands, and the resulting bond-slip.

Figure 152. Photo. Test 3.2.S (repair 3.2RBF) final shear cracks on repaired face of the girder at 410 kip (right face of girder pictured).

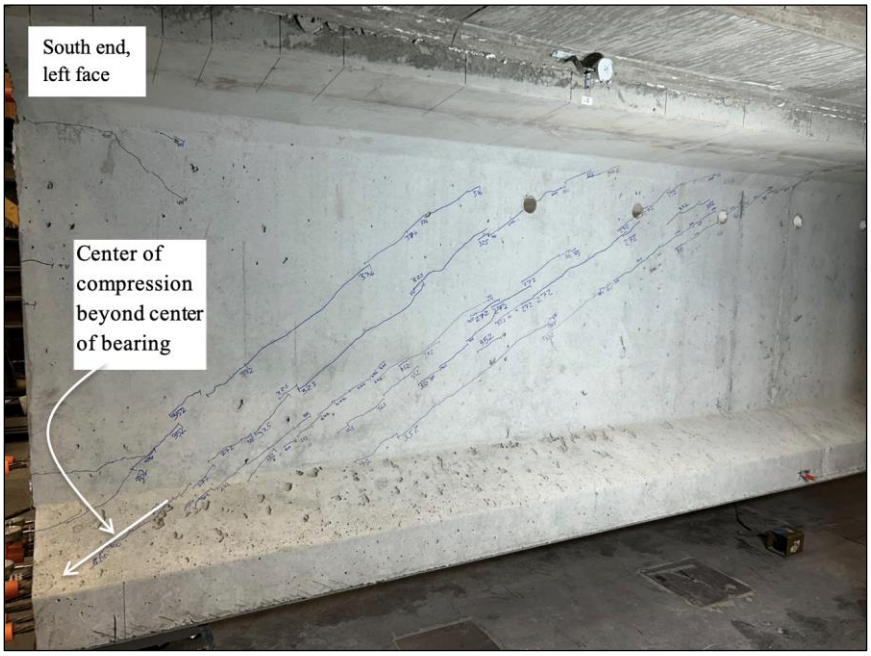

Figure 153. Photo. Test 3.2.S (repair 3.2RBF) final shear cracks on repaired face of the girder at 410 kip (left face of girder pictured).

As the overall figures of the repairs at maximum loads show (see figure 152 and figure 153), no failure of repair 3.2RBF was observed and no separation of the repair concrete from the original was observed. The patch did not dislodge from the bottom of the flange.

The load-deflection plot for Test 3.2.S (repair 3.2RBF) (see figure 154) shows that the girder behaved in a similar manner to the first shear test on this girder. This shear test found that the girder successfully exceeded 90 percent of the maximum load based on the nominal shear capacity (the dashed-dotted line in figure 154). This suggests that bottom flange repair 3.2RBF did not negatively impact the shear capacity of the nonconforming girder. The girder performed well past its service load conditions, as shown by this test.

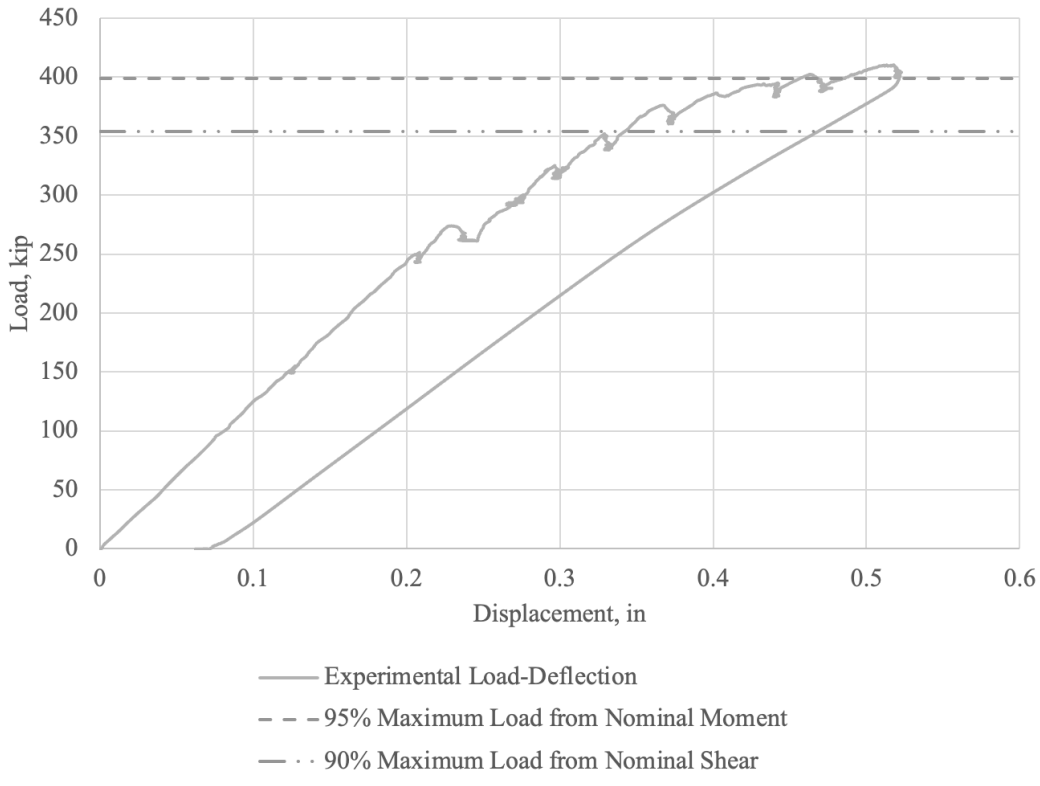

Figure 154. Graph. Test 3.2.S (repair 3.2RBF) load-deflection plot.

The moment-curvature plot for Test 3.2.S (repair 3.2RBF) (see figure 155) shows the experimental values obtained from this test. Nonlinear behavior is exhibited after the girder cracked at approximately 2,017 kip-ft.

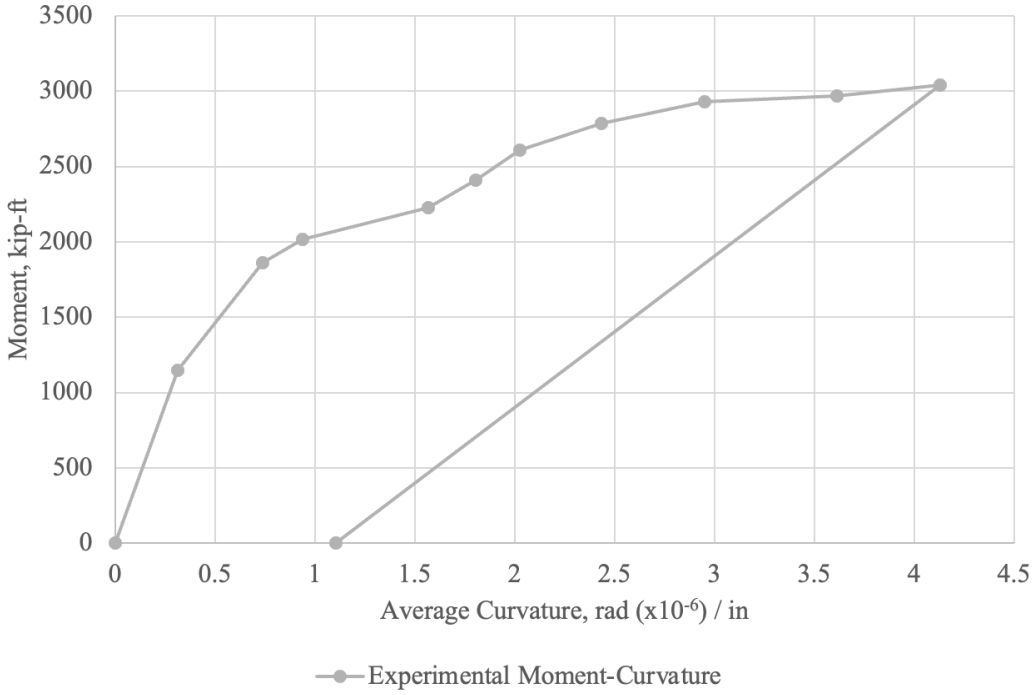

Figure 155. Graph. Test 3.2.S (repair 3.2RBF) moment-curvature plot.

The load-strand slip plot for Test 3.2.S (repair 3.2RBF) (see figure 156) shows the strand slip measurements, as well as the nominal capacity loads. At a load of 376 kip, the strands exceeded the strand slip limit of 0.01 in., which coincides with a load just past 90 percent of the maximum load from nominal shear (the dotted-dashed line in figure 156). This suggests the girder failed in a bond-slip failure caused by shear cracks to the bearing zone inflicted by the compression strut. Flexural cracks did form in the bottom flange repairs, but 95 percent of the nominal flexural capacity was surpassed.

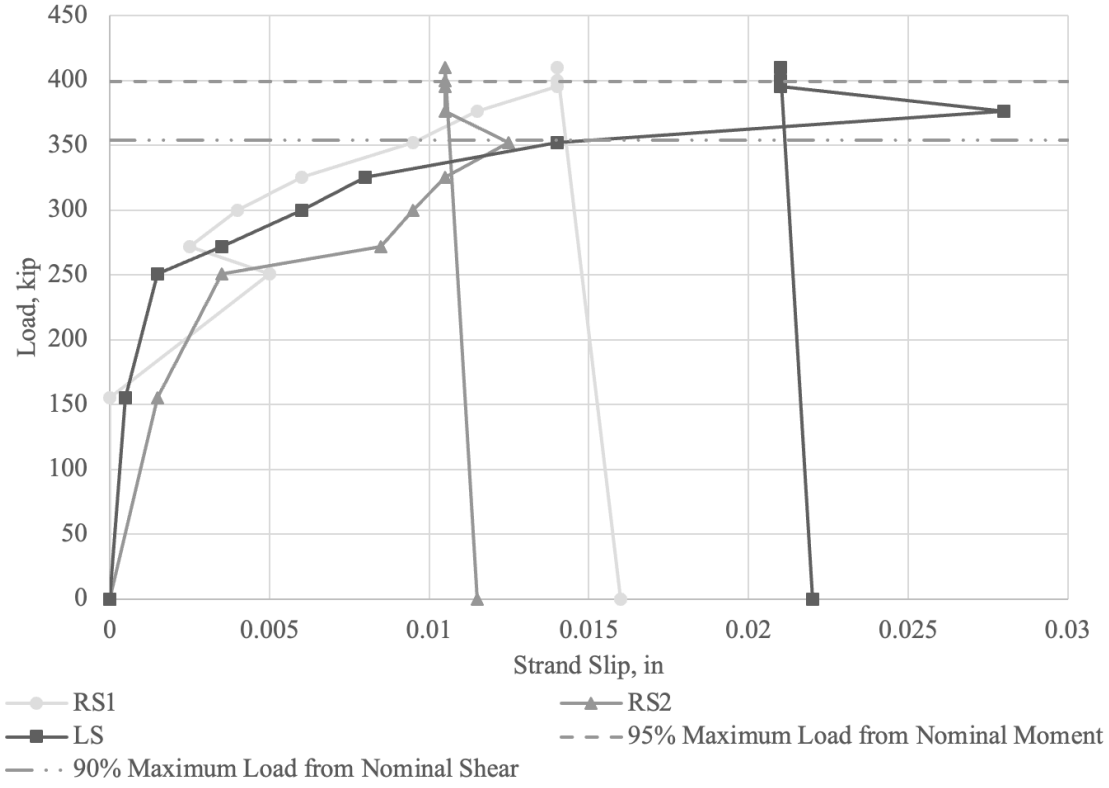

Figure 156. Graph. Test 3.2.S (repair 3.2RBF) load-strand slip plot.

TEST 3.3.F (REPAIR 3.3RBF, 3.3LBF) RESULTS

The last test on Girder 3, Test 3.3.F, was a flexure test, which was designed to observe the performance of midspan repairs 3.3RBF and 3.3LBF under extreme tensile stresses by centering the spreader beam over the repair location. The flexural test used the spreader beam with four-point loading identical to that used for Test 2.3.F. The center of the spreader beam was at midspan, 266 in. from the center of bearing of the south end of the girder. Theoretical calculations for Girder 3 can be found in appendix I.

During the first shear test, flexural cracks had occurred at repairs 3.3RBF and 3.3LBF and measured 0.00394 in. wide. At a load of 200 kip, the old flexural crack widths increased to 0.00591 in. The load was then increased to 240 kip, and new flexural cracks were heard

and seen. These new flexural cracks measured 0.0787 in. wide. Figure 157 and figure 158 show the flexural cracks on the right and left sides of the girder, respectively.

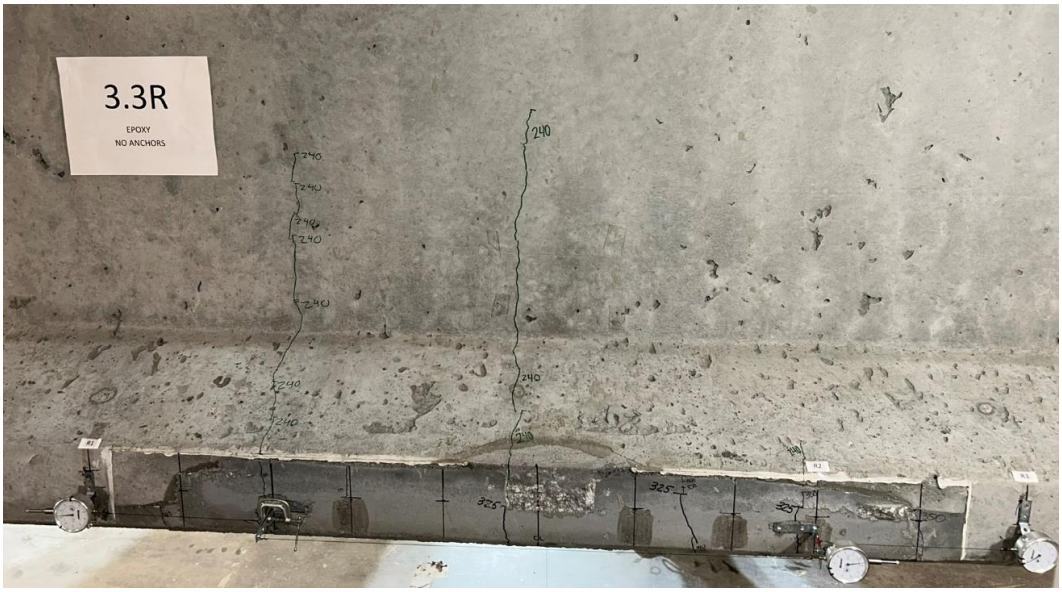

Figure 157. Photo. Test 3.3.F (repair 3.3RBF, 3.3LBF) initial flexural cracks at 240 kip (right face of girder pictured).

Figure 158. Photo. Test 3.3.F (repair 3.3RBF, 3.3LBF) initial flexural cracks extending 15 in. from the top of the bulb at 240 kip (left face of girder pictured).

At a load of 282 kip, shear-flexural cracks started to form, measuring around 0.0118 in. Flexural cracks continued to extend up the web. In the center of the repairs, these cracks measured 0.0157 in. On the outside of the repairs, the cracks measured 0.00984 in. The girder was loaded to a final load of 330 kip. Several new shear-flexural cracks formed, which measured 0.0236 in. The previously formed shear-flexural cracks now measured 0.0256–0.0295 in. On the center of the repair, flexural cracks measured 0.0217–0.0236 in. On the centerline of the overall girder, the flexural cracks still measured 0.0295 in. Figure 159 and figure 160 show the left and right sides, respectively, of the cracking pattern on the girder after this flexural test.

Figure 159. Photo. Test 3.3.F (repair 3.3RBF, 3.3LBF) overall crack pattern at the final load of 330 kip. Extensive flexural cracks occurred in the bottom flange repair (left face of girder pictured).

Figure 160. Photo. Test 3.3.F (repair 3.3RBF, 3.3LBF) overall crack pattern at the final load of 330 kip. Extensive flexural cracks occurred in the bottom flange repair (right face of girder pictured).

As the overall figures of the repairs at maximum loads show (see figure 159 and figure 160), no separation of the repair concrete from the original concrete occurred in any repair, even though significant cracking in the repair was evident. Crack widths were uniform through the lengths of the repairs, showing that there was no debonding of the prestressing strand and that there probably was excellent bond between the repair and the original concrete at the interior side of the original concrete. If there were separation, the exterior strains as shown by cracking would vary significantly.

The load-deflection plot for Test 3.3.F (repair 3.3RBF, 3.3LBF) (see figure 161) shows that the girder was tested well past its elastic point (cracking), resulting in a nonlinear deformation after unloading due to the cracked girder section. The finding of this flexural test was that the girder successfully exceeded 90 percent of the maximum load based on

the nominal flexural capacity (the dashed line in figure 161). The girder performed well past its service load conditions, as shown by this test.

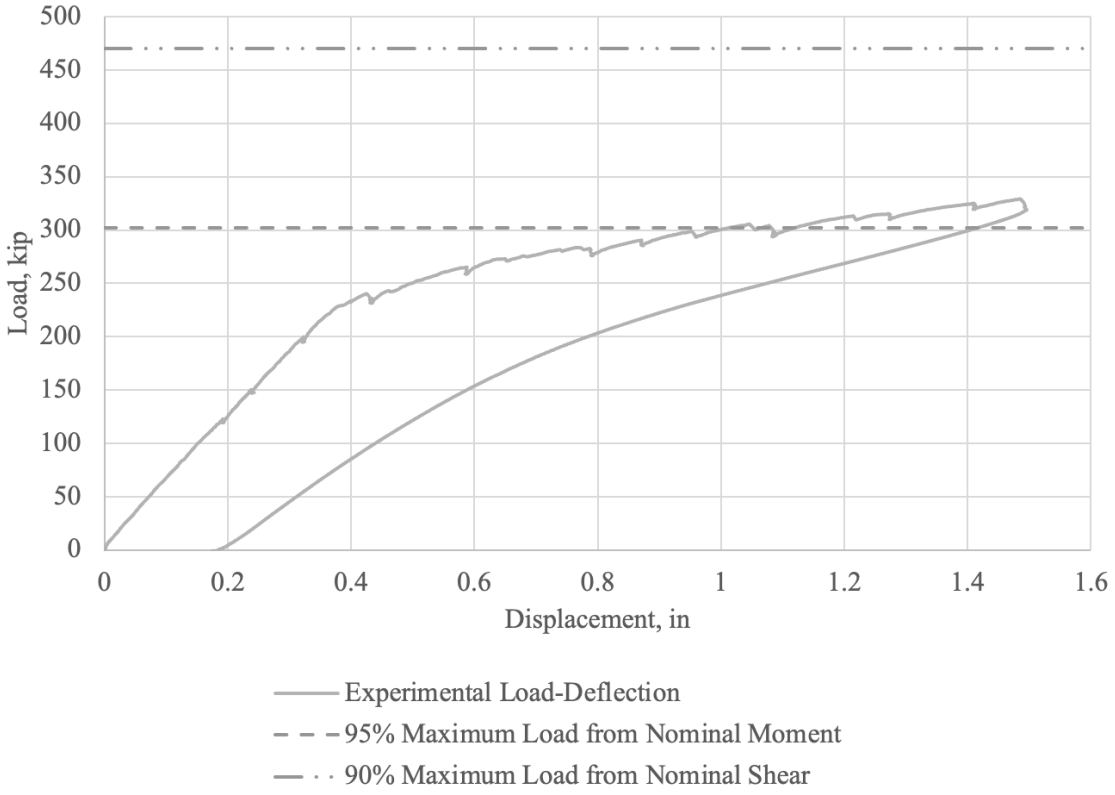

Figure 161. Graph. Test 3.3.F (repair 3.3RBF, 3.3LBF) load-deflection plot.

The moment-curvature plot for Test 3.3.F (repair 3.3RBF, 3.3LBF) (see figure 162) shows the experimental values obtained from this test. Nonlinear behavior is exhibited after the girder cracked at approximately 2,420 kip-ft. Based on this plot, the repaired girder exceeded 95 percent of the nominal moment capacity. This suggests that bottom flange repairs 3.3RBF and 3.3LBF did not negatively impact the capacity of the nonconforming girder, despite being the repairs located at the highest tensile stress location.

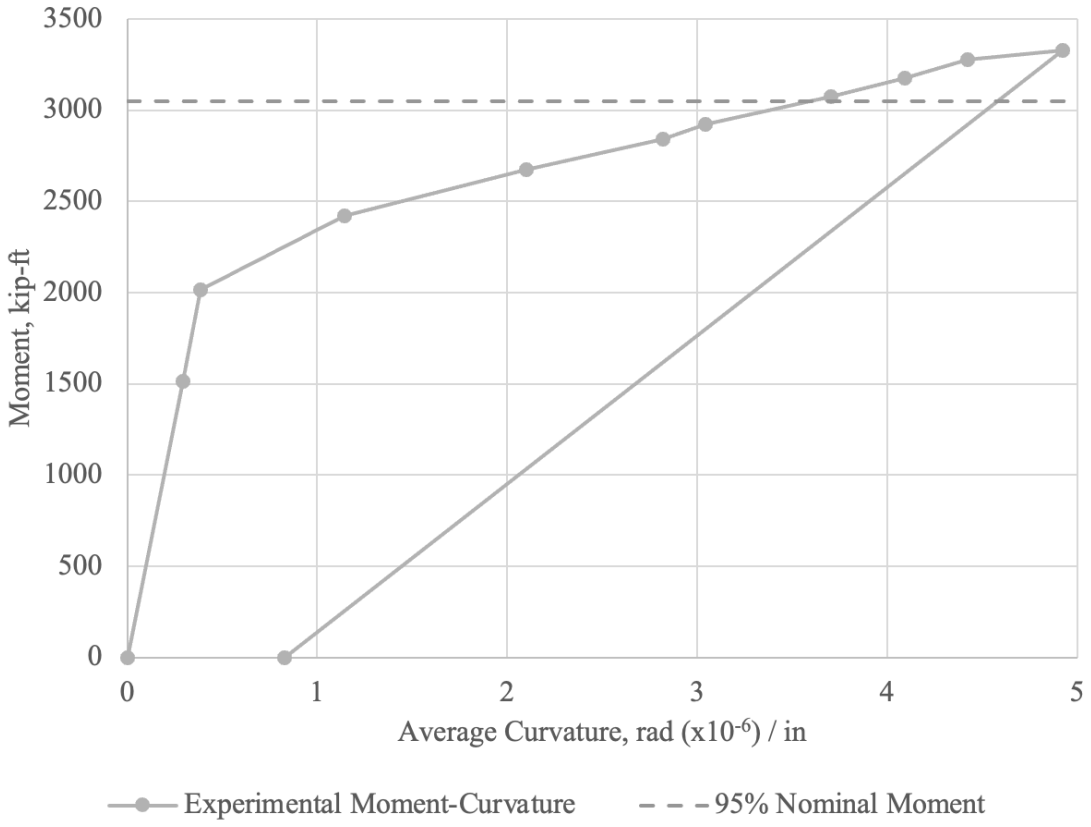

Figure 162. Graph. Test 3.3.F (repair 3.3RBF, 3.3LBF) moment-curvature plot.

CHAPTER 8. GIRDER 4 TESTS AND RESULTS

This chapter presents the setup, experiment, and test results from the Girder 4 test specimen. Calculations for this girder are given in appendix J.

OVERVIEW

A total of three tests were conducted on Girder 4 to evaluate the seven top flange repairs and the three bottom flange repairs. Loading near each end and at midspan allowed for study of the interface shear between the deck and flange to assure that full composite action was achieved and that the flexural and shear capacities were developed. One bottom flange repair near midspan was a shallow repair designed to represent chipping during girder transport; the loss of concrete was below the bottom layer of prestressing strand. The midspan repair was designed to evaluate whether such a shallow repair would remain attached when the girder was loaded to near nominal loads. The final bottom flange repairs were either near or within the bearing zones at the ends of the girder. Those repairs were in areas of high reinforcement congestion; therefore, epoxy bonding agent was not applied.

One purpose of these bearing zone repairs was to determine whether the prestressing strands could be adequately bonded following retensioning so the anticipated transfer and development lengths could be achieved. Surface strain and strand bond-slip measurements were critical for these bearing zone repairs. Repair 4.1LBZ was at the north end bearing zone, on the top surface of the bottom flange with two top row strands that were exposed and retensioned. The other bearing zone repair was 4.2LBZ at the south end, which previously had exposed the bottom of the flange and three bottom row strands. No retensioning was required for that specific repair.

A matrix of the tests performed on Girder 4 is included in table 16.

Table 16. Girder 4 test matrix.

Test Name	Behavior	Repair(s) Considered
Test 4.1.S	Shear	4.1LBZ, 4.1RTF, 4.1LTF, 4.4LTF
Test 4.2.S	Shear	4.2RBZ, 4.2RTF, 4.2RTFE, 4.2LTF
Test 4.3.F	Shear	4.3LTF

TEST 4.1.S (REPAIR 4.1LBZ, 4.1RTF, 4.1LTF, 4.4LTF) RESULTS

The first test on Girder 4, Test 4.1.S, was designed to observe the bearing zone repair performance by focusing the center of the compression strut on the repair and evaluating the behavior of the repair under this high load. This test was also designed to observe the performance of top flange repairs 4.1RTF and 4.1LTF by centering the load point over these repairs and maximizing the tensile stress experienced by them. The load point location was 113 in. from the center of bearing of the north end of the girder. This distance is referred to as "x_1" in the appendix J calculations (a/d = 1.85). The spreader beam was used in a four-point bending test configuration, which was identical to the spreader beam setup for the shear tests on Test 2.1.S (see figure 163).

At a load of 294 kip, two diagonal shear cracks were seen. The shear crack width measured 0.00787 in. The strut width was 9.5–10 in. The crack angles were between 37 and 39 degrees (see figure 164 and figure 165).

Figure 166 shows a close-up of the bearing cracks on repair 4.1LBZ that developed more with each load step. The dial gauges on the extents of each repair measured any separation of the repair from the girder.

Figure 163. Photo. Test 4.1.S (repair 4.1LBZ, 4.1RTF, 4.1LTF, 4.4LTF) general test setup (left face of girder pictured).

Figure 164. Photo. Test 4.1.S (repair 4.1LBZ, 4.1RTF, 4.1LTF, 4.4LTF) initial shear cracks on original, nonrepaired face at 294 kip (right face of girder pictured).

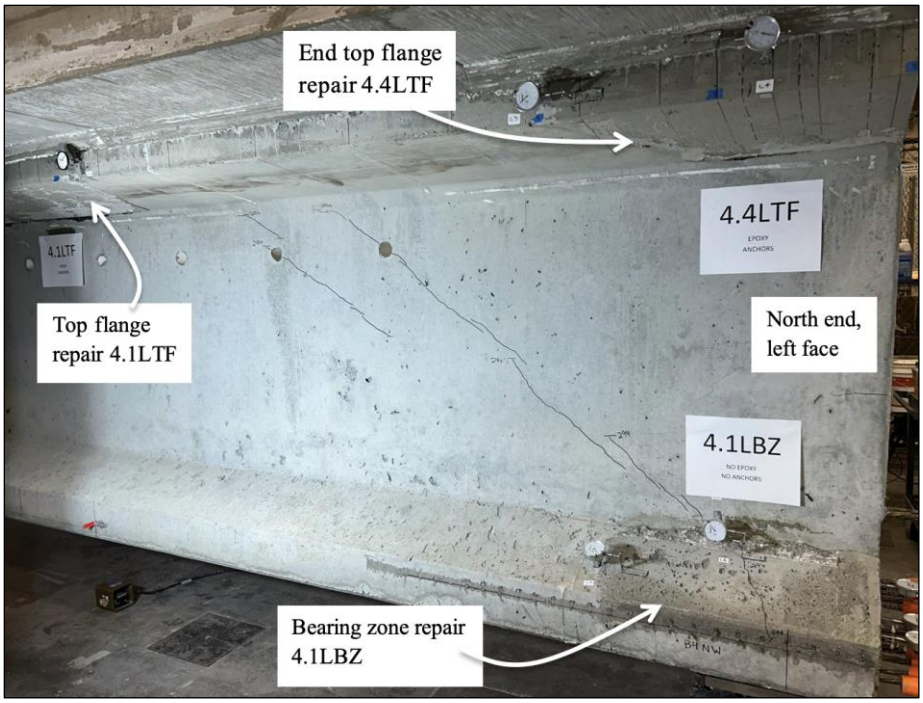

Figure 165. Photo. Test 4.1.S (repair 4.1LBZ, 4.1RTF, 4.1LTF, 4.4LTF) initial shear cracks on repaired face, extending into bottom flange repair 4.1LBZ at 294 kip (left face of girder pictured).

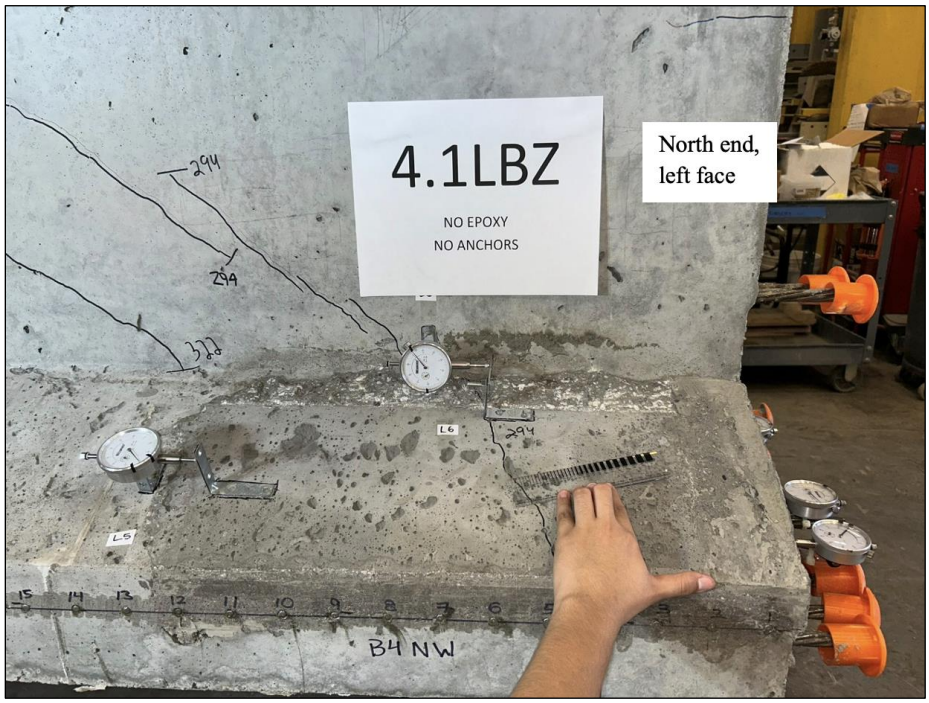

Figure 166. Photo. Test 4.1.S (repair 4.1LBZ, 4.1RTF, 4.1LTF, 4.4LTF) bearing cracks on repair 4.1LBZ at 322 kip (left face of girder pictured). Dial gauges on the strand ends measured the strand slip.

At a load of 394 kip, flexural cracks propagated directly below the load point from the bottom of the girder up toward the spreader beam pin support. They continued to spread up the web after each load step, and their final width measured 0.00787 in. At a load of 470 kip, shear-flexural cracks formed. They formed on both sides of the innermost support of the spreader beam and continued to spread after each load step, with a similar length between them. Their final width measured 0.0256 in. Figure 167 and figure 168 show the flexural and shear-flexural cracks at the final load of 500 kip.

At a load of 368 kip, the first strand slip was seen in strand RS of 0.0015 in. As the compression strut developed and cracks spread into the bearing zone repair 4.1LBZ, the strands continued to slip more, until a maximum final slip failure of 0.026 in. in strand LS1 (the outermost strand in the bearing zone repair).

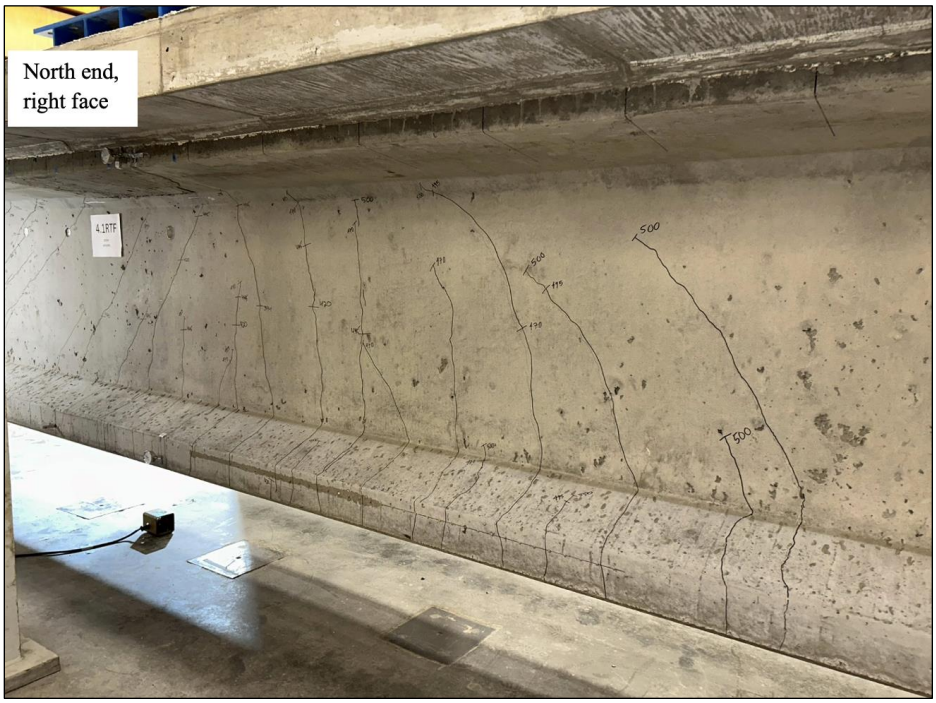

Figure 167. Photo. Test 4.1.S (repair 4.1LBZ, 4.1RTF, 4.1LTF, 4.4LTF) flexural and shear-flexural cracks around the innermost spreader beam support, not extending into repair 4.1RTF at 500 kip (right face of girder pictured).

Figure 168. Photo. Test 4.1.S (repair 4.1LBZ, 4.1RTF, 4.1LTF, 4.4LTF) flexural and shear-flexural cracks around the innermost spreader beam support, not extending into repair 4.1LTF at 500 kip (left face of girder pictured).

The shear cracks continued to spread up the web and into the bearing zone repair 4.1LBZ, and their final width measured 0.0177 in. Figure 169 and figure 170 show the shear cracks at the final load of 500 kip.

As these overall figures of the repairs at maximum loads show, slight separation of the repair concrete from the original concrete was seen, as a crack formed around the edge of the bearing zone repair. It is suspected that bond slip in strand LS1 was exacerbated due to being at the outermost part of the repair.

Figure 169. Photo. Test 4.1.S (repair 4.1LBZ, 4.1RTF, 4.1LTF, 4.4LTF) final shear cracks on top flange repaired face at 500 kip (right face of girder pictured).

Figure 170. Photo. Test 4.1.S (repair 4.1LBZ, 4.1RTF, 4.1LTF, 4.4LTF) final shear cracks on top and bottom flange repaired face at 500 kip (left face of girder pictured).

The load-deflection plot for Test 4.1.S (repair 4.1LBZ, 4.1RTF, 4.1LTF, 4.4LTF) (see figure 171) shows that the girder was tested past its elastic point (cracking), resulting in a nonlinear deformation after unloading due to the cracked girder section. The finding of this shear test was that the girder successfully exceeded 90 percent of the maximum load based on the nominal shear capacity (the dashed-dotted line in figure 171). This suggests that bearing zone repair 4.1LBZ and the top flange repairs did not negatively impact the shear capacity of the nonconforming girder. Girder 4 sustained the maximum load of all tests of 500 kip, proving that it is capable for a girder with many repairs (seven top flange repairs and three bottom flange repairs) to sustain loads well above its service load conditions.

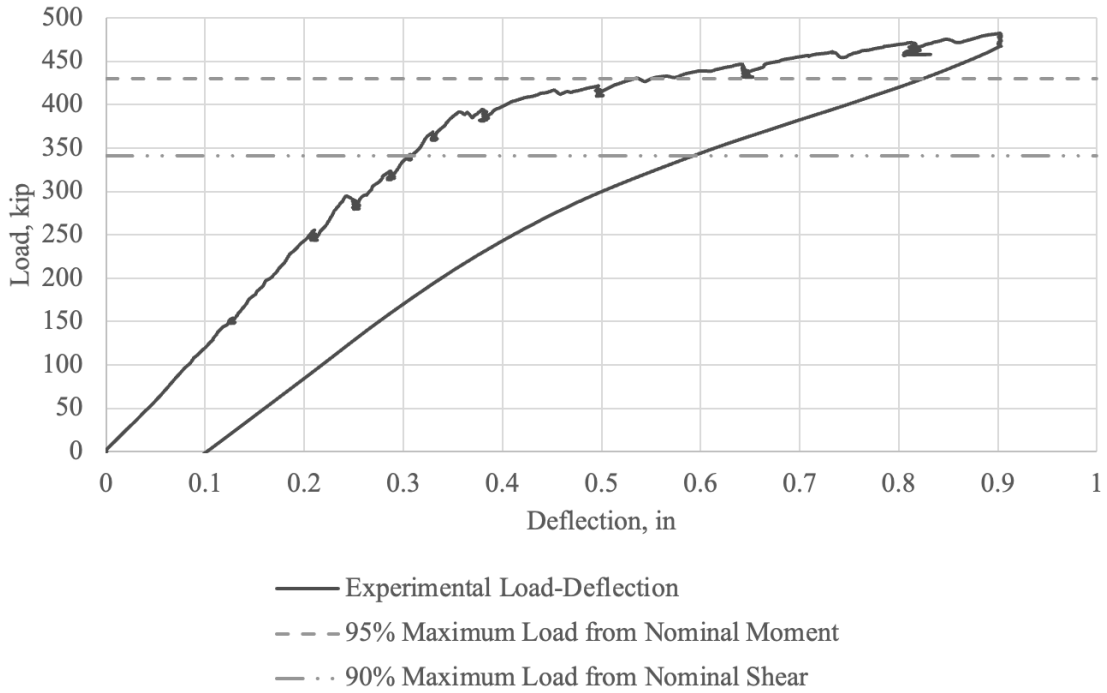

Figure 171. Photo. Test 4.1.S (repair 4.1LBZ, 4.1RTF, 4.1LTF, 4.4LTF) load-deflection plot.

The moment-curvature plot for Test 4.1.S (repair 4.1LBZ, 4.1RTF, 4.1LTF, 4.4LTF) (see figure 172) shows the experimental values obtained from this test. Nonlinear behavior is exhibited after the girder cracked at approximately 1,886 kip-ft.

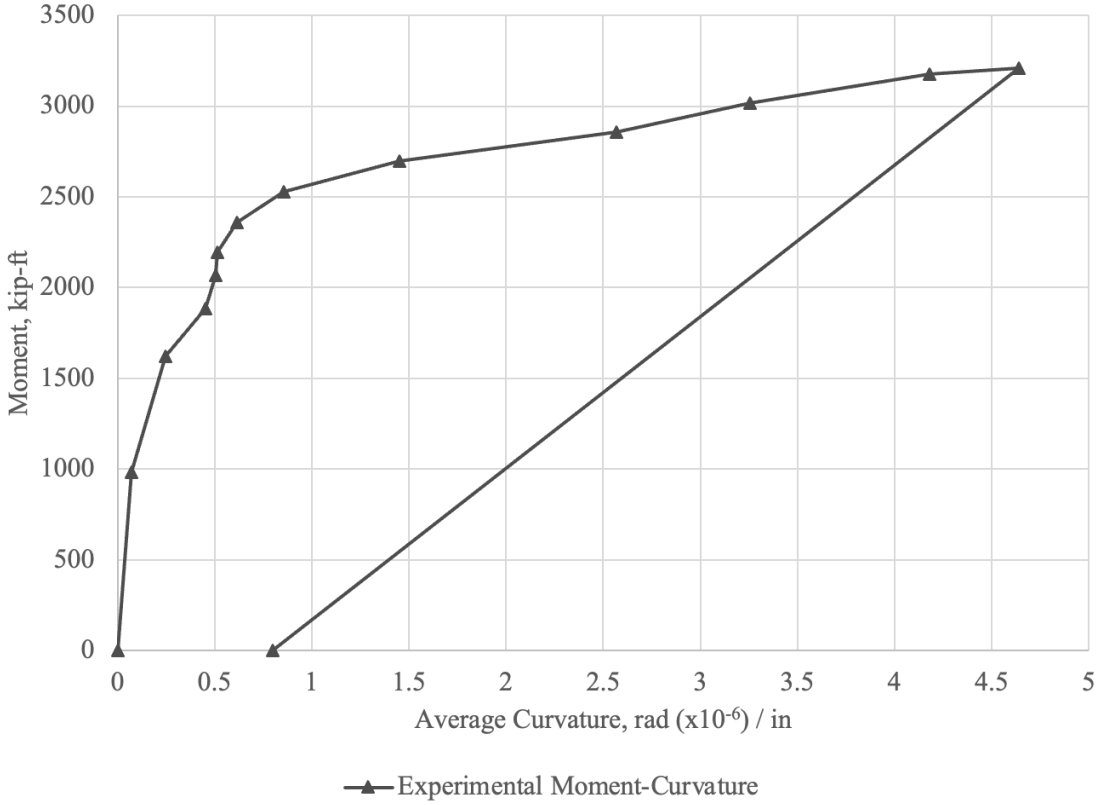

Figure 172. Graph. Test 4.1.S (repair 4.1LBZ, 4.1RTF, 4.1LTF, 4.4LTF) moment-curvature plot.

The load-strand slip plot for Test 4.1.S (repair 4.1LBZ, 4.1RTF, 4.1LTF, 4.4LTF) (see figure 173) shows the strand slip measurements, as well as the nominal capacity loads. At a load of 368 kip, the first strand slip was measured, which is close to 90 percent of the maximum load from nominal shear (the dotted-dashed line in figure 173). Strands LS1 and RS exceeded the strand slip limit of 0.01 in. at a load of 470 kip. The combination of bond-slip and shear-flexural cracks suggests the girder failed in a shear-flexural nature, as can be confirmed by the load-strand slip and load-deflection behavior.

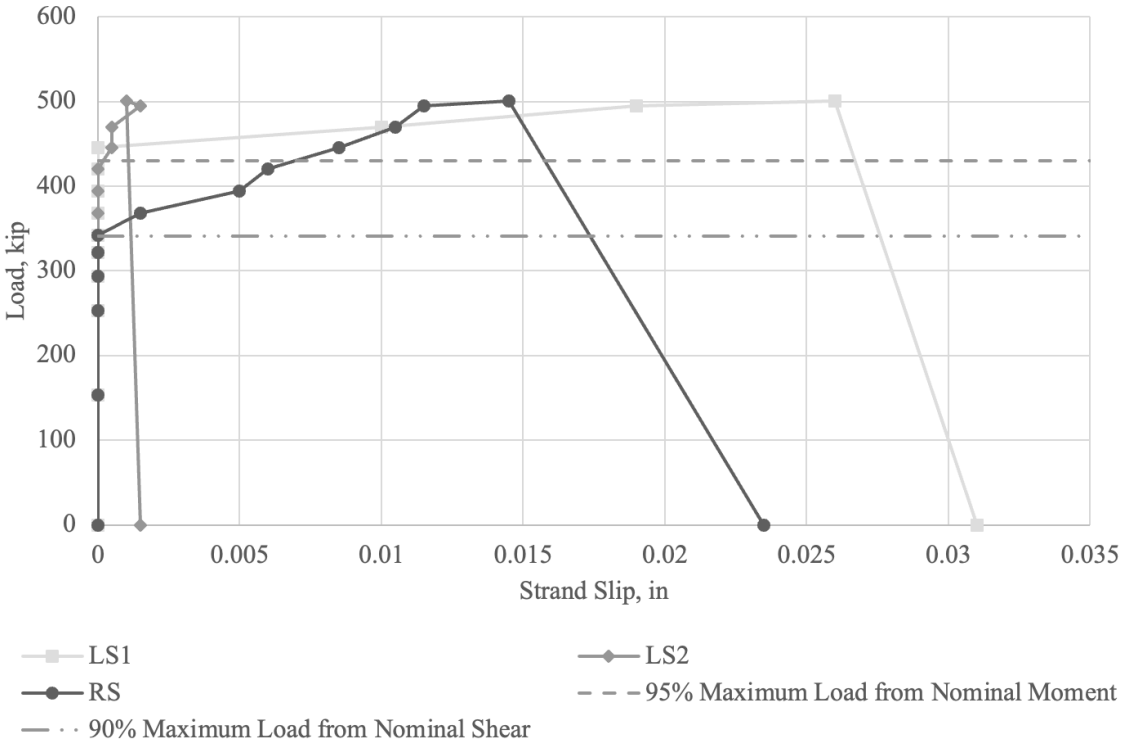

Figure 173. Graph. Test 4.1.S (repair 4.1LBZ, 4.1RTF, 4.1LTF, 4.4LTF) load-strand slip plot.

DEMEC (CSS) measurements were taken at each load interval and plotted. The plot (see figure 174) shows the strand stress at a load prior to maximum and at maximum load. From the plot, the strands do hold their bond until near the end of the repair, where strand slip is seen. As repair 4.1LBZ detached from the girder, strand slip was induced, resulting in a loss of stress in the strand at maximum load at around 23 in. from the end of the girder.

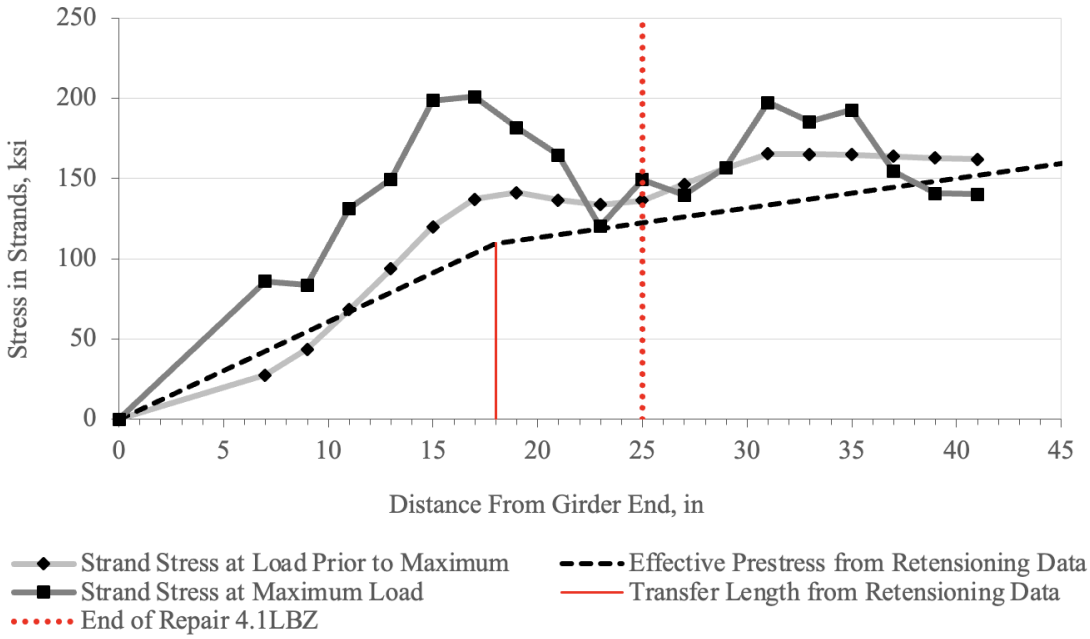

Figure 174. Graph. Test 4.1.S (repair 4.1LBZ, 4.1RTF, 4.1LTF, 4.4LTF) CSS plot; strand stress vs. distance from girder end.

TEST 4.2.S (REPAIR 4.2RBZ, 4.2RTFE, 4.2RTF, 4.2LTF) RESULTS

The second test on Girder 4, Test 4.2.S, was another shear test. It was designed to observe the bearing zone repair 4.2RBZ performance by focusing the center of the compression strut on the repair and seeing the behavior of the repair under this high load. This test was also designed to observe the performance of the smallest top flange repairs 4.2RTF and 4.2LTF by centering the load point over these repairs and maximizing the tensile stress experienced by them. The load point location was 113 in. from the center of bearing of the south end of the girder. This distance is referred to as "x_2" in the appendix J calculations (a/d = 1.85). The girder supports and spreader beam configuration matched the first test on this girder (four-point bending; see figure 163).

Diagonal shear cracks were first observed at a load of 286 kip (see figure 175 and figure 176). The shear crack width measured 0.00787 in. The strut width was 9.5 in. The crack angles were between 35 and 37 degrees.

Further web shear cracking in the web and vertical cracks in the near bearing zone repair was observed at a 314-kip load. The horizontal dial gauges measured 0.0015 in. of separation of the repair concrete from the original at the left vertical end (R3) and top edge (R4) of the 4.2RBZ repair (see figure 177). Shear cracks and tensions cracks formed on repair 4.2RBZ due to the shear force, causing increased tension in the bottom of the girder. These cracks measured 0.00394 in. wide on repair 4.2RBZ at 314 kip.

Figure 175. Photo. Test 4.2.S (repair 4.2RBZ, 4.2RTFE, 4.2RTF, 4.2LTF) initial shear cracks on repaired face at 286 kip (right face of girder pictured).

Figure 176. Photo. Test 4.2.S (repair 4.2RBZ, 4.2RTFE, 4.2RTF, 4.2LTF) initial shear cracks on nonrepaired bottom flange face at 286 kip (left face of girder pictured).

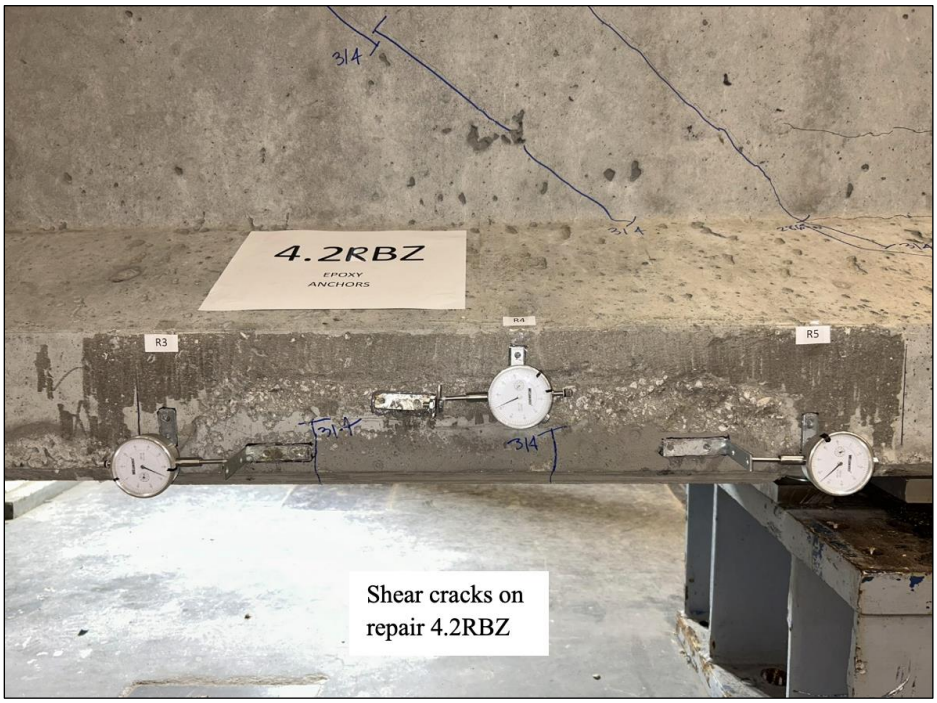

Figure 177. Photo. Test 4.2.S (repair 4.2RBZ, 4.2RTFE, 4.2RTF, 4.2LTF) shear cracks and tension cracking at the base of repair 4.2RBZ at 314 kip (right face of girder pictured).

At a load of 314 kip, south end section cracks were noticed, and a strand slip of 0.0025 in. was measured in dial gauge LS (see figure 178).

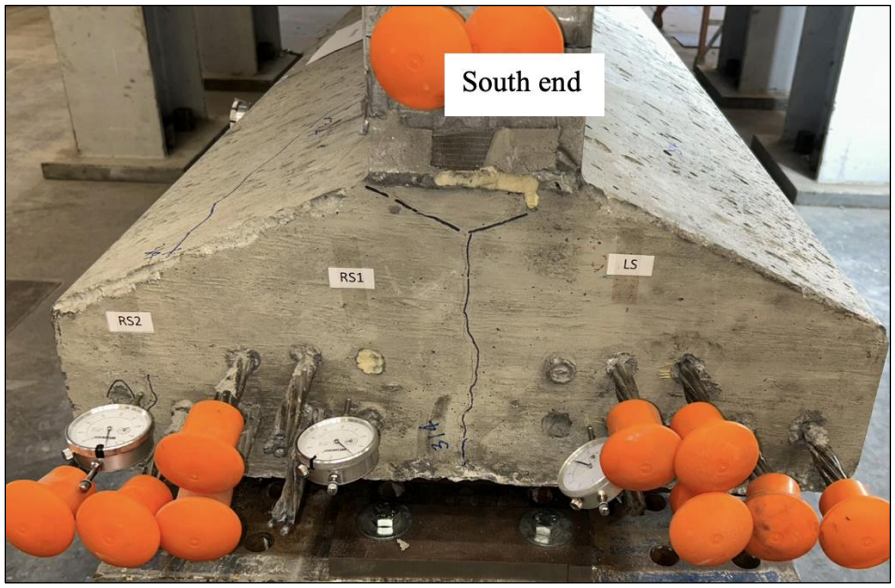

Figure 178. Photo. Test 4.2.S (repair 4.2RBZ, 4.2RTFE, 4.2RTF, 4.2LTF) south end section cracks at 314 kip.

At a load of 411 kip, the first flexural and shear-flexural cracks were seen under the innermost spreader beam support from the bottom flange up the web (see figure 179).

The girder was loaded to a final load of 500 kip. The test was ended at this load due to a strand slip of 0.0275 in. occurring in strand LS, which exceeds the set strand slip limit of 0.01 in. of this project. Some cracks on the perimeter of repair 4.2RBZ were noted, with a maximum of 0.006 in. of separation measured in dial gauge R5. Figure 180 shows one of the researchers pointing at the location of maximum repair detachment for repair 4.2RBZ.

The final shear crack pattern is shown in figure 181 and figure 182. Notably, the compression strut did not pass through repair 4.2LBZ. Also, the crack patterns on each face of the girder were very similar.

Figure 179. Photo. Test 4.2.S (repair 4.2RBZ, 4.2RTFE, 4.2RTF, 4.2LTF) initial flexural and shear-flexural cracks at 411 kip (right face of girder pictured).

Figure 180. Photo. Test 4.2.S (repair 4.2RBZ, 4.2RTFE, 4.2RTF, 4.2LTF) perimeter cracks at 500 kip with a 0.006-in. repair interface crack measured in dial gauge R5, the outermost strand on the right side, and a strand slip of 0.027 in. measured in dial gauge RS1 (right face of girder pictured).

Figure 181. Photo. Test 4.2.S (repair 4.2RBZ, 4.2RTFE, 4.2RTF, 4.2LTF) final shear cracks on top and bottom flange repaired face at 500 kip (right face of girder pictured).

Figure 182. Photo. Test 4.2.S (repair 4.2RBZ, 4.2RTFE, 4.2RTF, 4.2LTF) final shear cracks on top flange repaired face at 500 kip (left face of girder pictured).

The final flexural and shear-flexural crack pattern is shown in figure 183 and figure 184. These cracks propagated below the innermost spreader beam support (the one nearest to the midspan) and around top flange repairs 4.2RTF and 4.2LTF. They only extended slightly into the extents of repair 4.2RTF.

Flexural cracks formed on repair 4.3LBF and extended into shear-flexural cracks up the web (see figure 185). Perimeter cracks formed on repair 4.3LBF, suggesting detachment from the girder and a failure of the concrete bond interface.

Figure 183. Photo. Test 4.2.S (repair 4.2RBZ, 4.2RTFE, 4.2RTF, 4.2LTF) flexural and shear-flexural cracks around the innermost spreader beam support, extending slightly into repair 4.2RTF at 500 kip (right face of girder pictured).

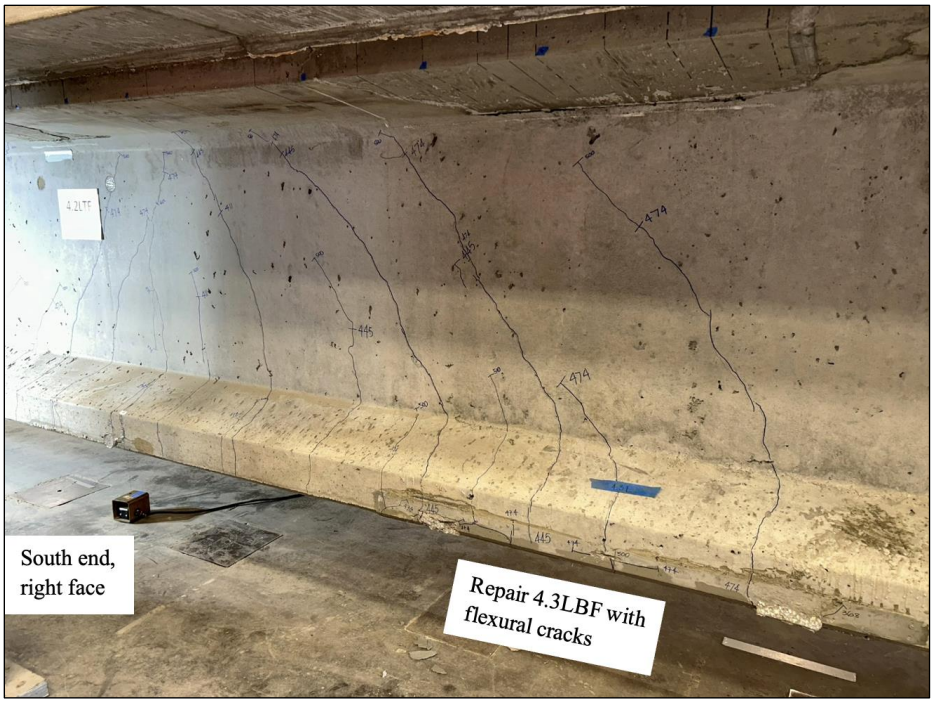

Figure 184. Photo. Test 4.2.S (repair 4.2RBZ, 4.2RTFE, 4.2RTF, 4.2LTF) flexural and shear-flexural cracks around the innermost spreader beam support, not extending into repair 4.2LTF at 500 kip (left face of girder pictured).

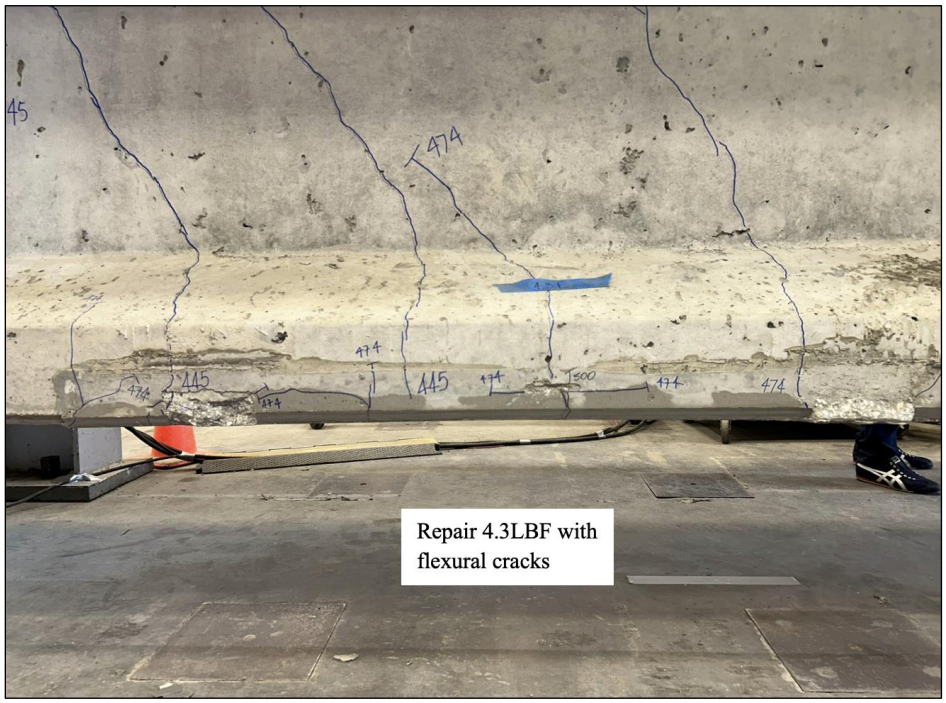

Figure 185. Photo. Test 4.2.S (repair 4.2RBZ, 4.2RTFE, 4.2RTF, 4.2LTF) flexural cracks on repair 4.3LBF at 500 kip. Cracks on the perimeter of the repair formed on the ends and midspan of the repair (left face of girder pictured).

As the overall and close-up figures of the repairs at maximum loads show (see figure 183, figure 184, and figure 185), failure of repairs 4.2LBZ and 4.3LBF was observed; separation of the repair concrete from the original was observed at the ends of 4.2LBZ and at the ends and midspan of 4.3LBF. No failure in the other repairs was observed.

The load-deflection plot for Test 4.2.S (repair 4.2RBZ, 4.2RTFE, 4.2RTF, 4.2LTF) (see figure 186) shows that the girder behaved in a similar manner to the first shear test on this girder. The finding of this shear test was that the girder successfully exceeded 90 percent of the maximum load based on the nominal shear capacity (the dashed-dotted line in figure 186). This suggests that bearing zone repair 4.2RBZ and the top flange repairs did not negatively impact the shear capacity of the nonconforming girder, despite being the girder region with the highest number of repairs. The results of this test further emphasize that it is possible for a girder with a large number of repairs to sustain loads well above its service load conditions.

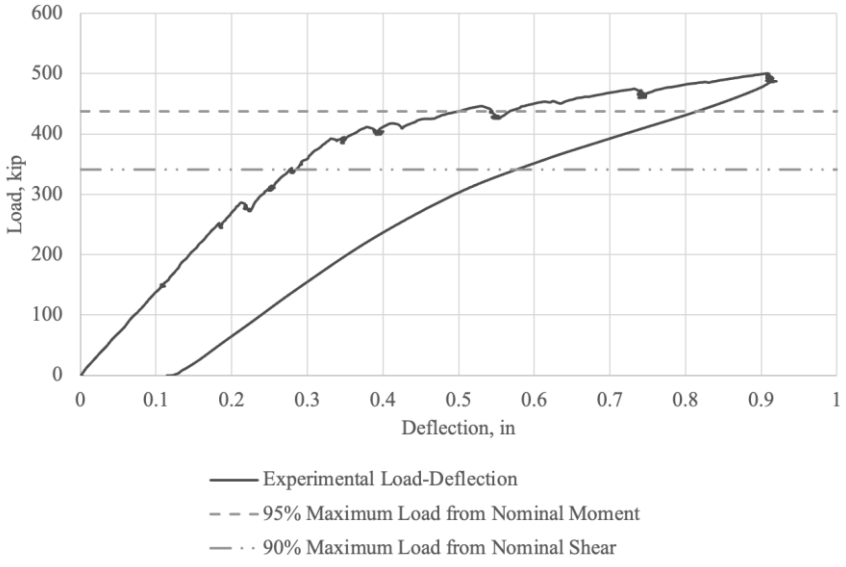

Figure 186. Graph. Test 4.2.S (repair 4.2RBZ, 4.2RTFE, 4.2RTF, 4.2LTF) load-deflection plot.

The moment-curvature plot for Test 4.2.S (repair 4.2RBZ, 4.2RTFE, 4.2RTF, 4.2LTF) (see figure 187) shows the experimental values obtained from this test. Nonlinear behavior is exhibited after the girder cracked at approximately 1,835 kip-ft.

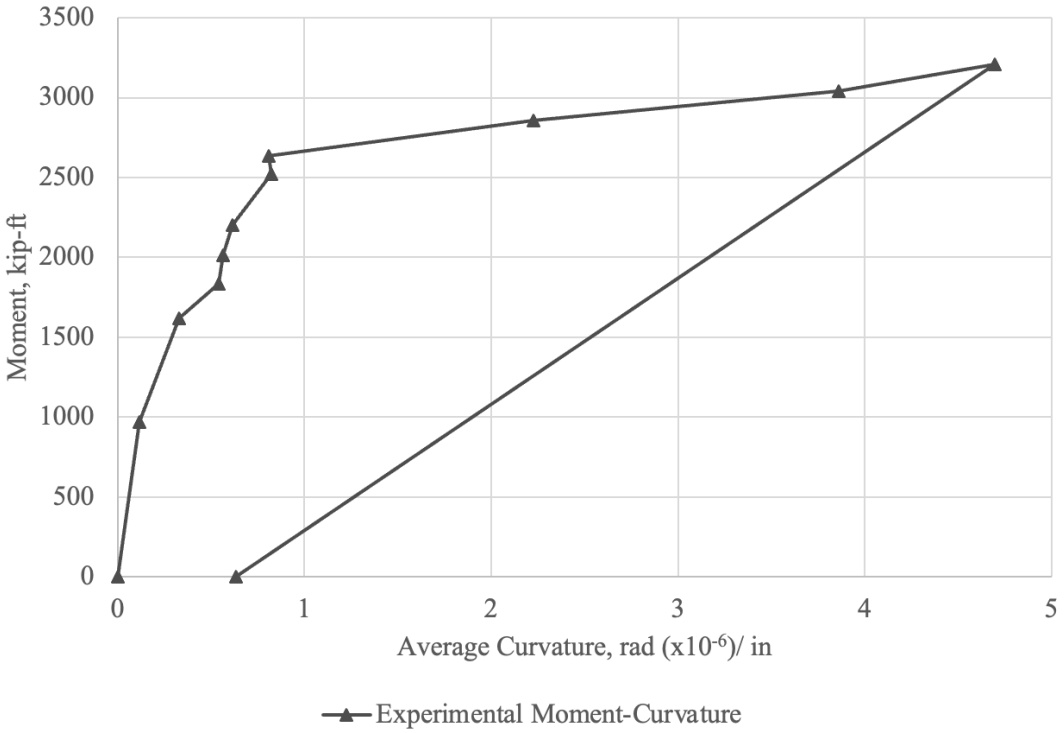

Figure 187. Graph. Test 4.2.S (repair 4.2RBZ, 4.2RTFE, 4.2RTF, 4.2LTF) moment-curvature plot.

The load-strand slip plot for Test 4.2.S (repair 4.2RBZ, 4.2RTFE, 4.2RTF, 4.2LTF) (see figure 188) shows the strand slip measurements, as well as the nominal capacity loads. At a load of 341 kip, the first strand slip was measured, which coincides with 90 percent of the maximum load from nominal shear (the dotted-dashed line in figure 188). Strands LS and RS1 exceeded the strand slip limit of 0.01 in. at a load of 474 kip. The combination of strand slip and shear-flexural cracks suggests the girder failed in a shear-flexural nature, as can be confirmed by the load-strand slip and load-deflection behavior.

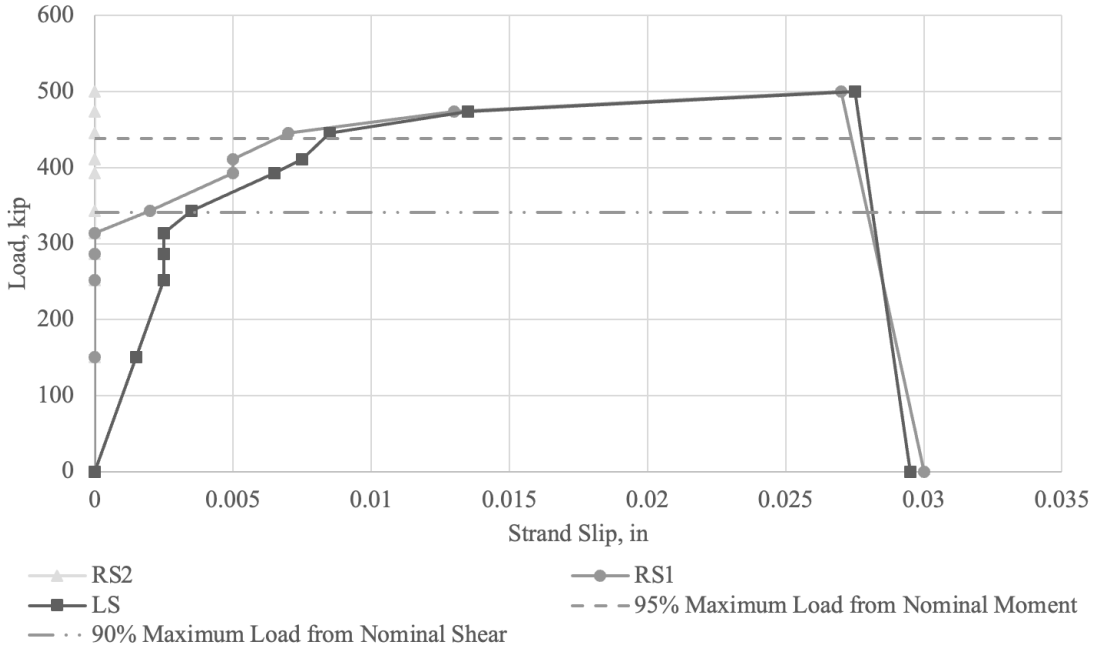

Figure 188. Graph. Test 4.2.S (repair 4.2RBZ, 4.2RTFE, 4.2RTF, 4.2LTF) load-strand slip plot.

TEST 4.3.F (REPAIR 4.3LBF, 4.3LTF) RESULTS

The last test on Girder 4, Test 4.3.F, was a flexure test. It was designed to observe the performance of the shallowest bottom flange repair 4.3LBF and the top flange repair 4.3LTF under high tensile stresses by locating one end of the spreader beam over the center of the repairs. The load point location was 224.5 in. from the center of bearing of the south end of the girder. Theoretical calculations for Girder 4 can be found in appendix J. The spreader beam was used in a four-point bending test configuration, matching the previous two flexural test setups for Girders 2 and 3 (see chapter 6 and chapter 7).

The first flexural and shear-flexural cracks occurred at a load of 280 kip (see figure 189, right side). They measured 0.00984–0.0138 in. wide.

Figure 189. Photo. Test 4.3.F (repair 4.3LBF, 4.3LTF) initial flexural and shear-flexural cracks at 280 kip (left face of girder pictured).

Flexural cracks on the bottom of repair 4.3LBF formed at a load of 280 kip (see figure 190). Their maximum crack width measured 0.0354 in.

The final flexural and shear-flexural crack pattern on Test 4.3.F (repair 4.3LBF, 4.3LTF) is shown in figure 191. The shear-flexural cracks did not extend into repair 4.3LTF but did extend on the opposite girder face of the repair (right face; figure 192). The maximum crack width for flexural cracks was 0.0177 in. and for shear-flexural cracks was 0.0276 in.

Figure 190. Photo. Test 4.3.F (repair 4.3LBF, 4.3LTF) repair 4.3LBF flexural cracks at 320 kip (left face of girder pictured).

Figure 191. Photo. Test 4.3.F (repair 4.3LBF, 4.3LTF) final overall crack pattern on the top and bottom flange repaired girder face after the final load of 331 kip (left face of girder pictured).

Figure 192. Photo. Test 4.3.F (repair 4.3LBF, 4.3LTF) final overall crack pattern on original, nonrepaired girder face after the final load of 331 kip (right face of girder pictured).

As the overall figures of the repairs at maximum loads show (see figure 190, figure 191, and figure 192), no separation of the top flange repair concrete from the original concrete occurred. Some separation was heard when conducting a hammer sounding test on bottom flange repair 4.3LBF. Given that this bottom flange repair is shallow and had no exposed reinforcement to anchor to, it was difficult for the repair to sustain such high tensile stress at the bottom of the beam near midspan. Crack widths were uniform through the lengths of the repairs, showing that there was no debonding of the prestressing strand.

The load-deflection plot for Test 4.3.F (repair 4.3LBF, 4.3LTF) (see figure 193) shows that the girder was tested well past its elastic point (cracking), resulting in a nonlinear deformation after unloading due to the cracked girder section. The finding of this flexural test was that the girder sustained 95 percent of the maximum load based on the nominal

flexural capacity (dashed line in figure 193). The girder performed well past its service load conditions, as shown by this test.

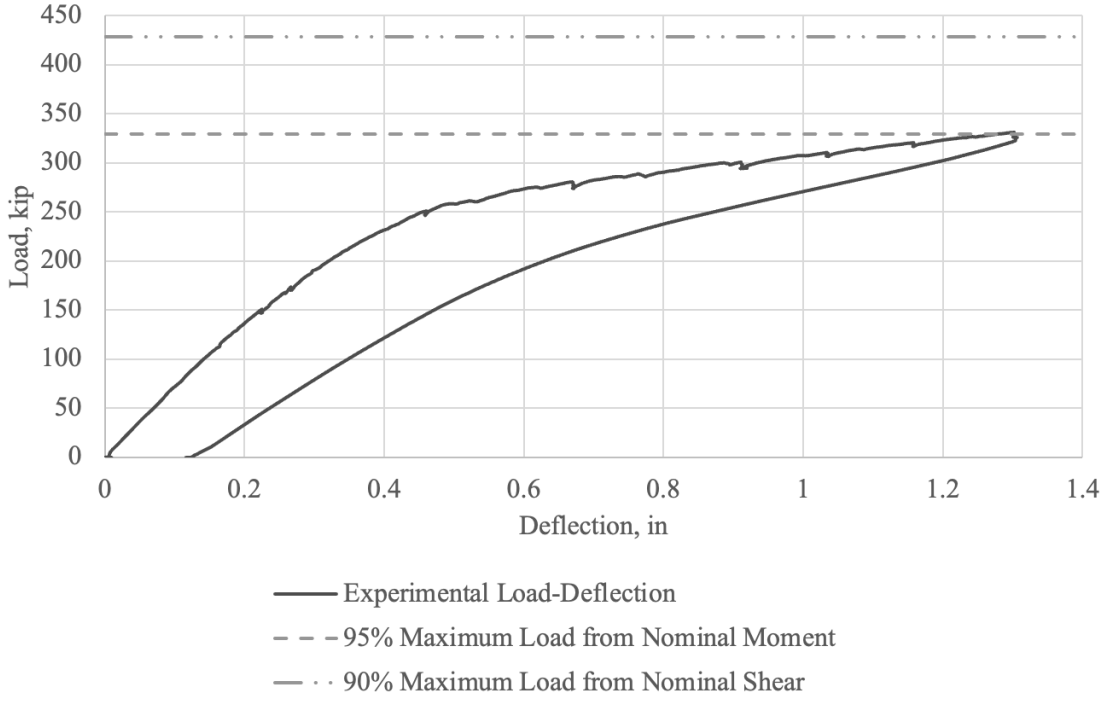

Figure 193. Graph. Test 4.3.F (repair 4.3LBF, 4.3LTF) load-deflection plot.

The moment-curvature plot for Test 4.3.F (repair 4.3LBF, 4.3LTF) (see figure 194) shows the experimental values obtained from this test. Nonlinear behavior is exhibited after the girder cracked at approximately 2,747 kip-ft. Based on this plot, the repaired girder sustained a moment within 94 percent of the nominal moment capacity. This can be explained through the extensive shear-flexural cracks that occurred in the previous shear test on this girder, as described in Test 4.2.S (Repair 4.2RBZ, 4.2RTFE, 4.2RTF, 4.2LTF) ; due to these previous cracks, the moment of inertia of the girder was reduced substantially, leading to the girder being unable to sustain a higher moment in this flexural test.

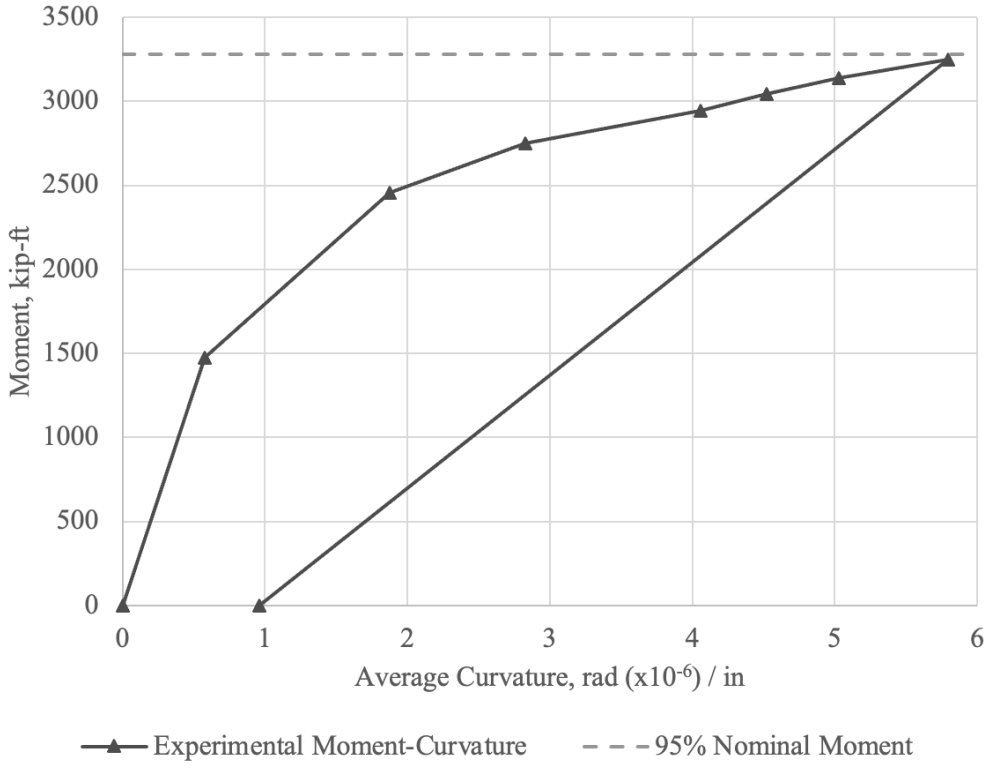

Figure 194. Graph. Test 4.3.F (repair 4.3LBF, 4.3LTF) moment-curvature plot.

CHAPTER 9. DISCUSSION OF RESULTS

FLEXURAL BEHAVIOR

The research team conducted a collective total of three flexural tests on the repaired girders. Girders 2, 3, and 4 each had a flexural test because they were the girders with a deck cast. During and after all flexural tests, no top flange or bottom flange repair failed or spalled. The repairs cracked cohesively with the girder the majority of the time. On certain bottom flange repairs, especially the shallow ones, the perimeter of the repair detached slightly from the girder. All the flexural tests were terminated when 95 percent of the nominal flexural load was reached or when an estimated total bulb surface strain of 0.00847 occurred (i.e., 90 percent of ultimate stress in the prestressing strands, 243 ksi).

A combined moment-curvature plot for the three flexural tests conducted is shown in figure 195. Based on the combined moment-curvature plots, it is evident that the flexural behavior displayed by the three girders is similar in nature. Notably, Test 2.3.F only had top flange repairs, Test 3.3.F only had bottom flange repairs, and Test 4.3.F had a combination of both top and bottom flange repairs.

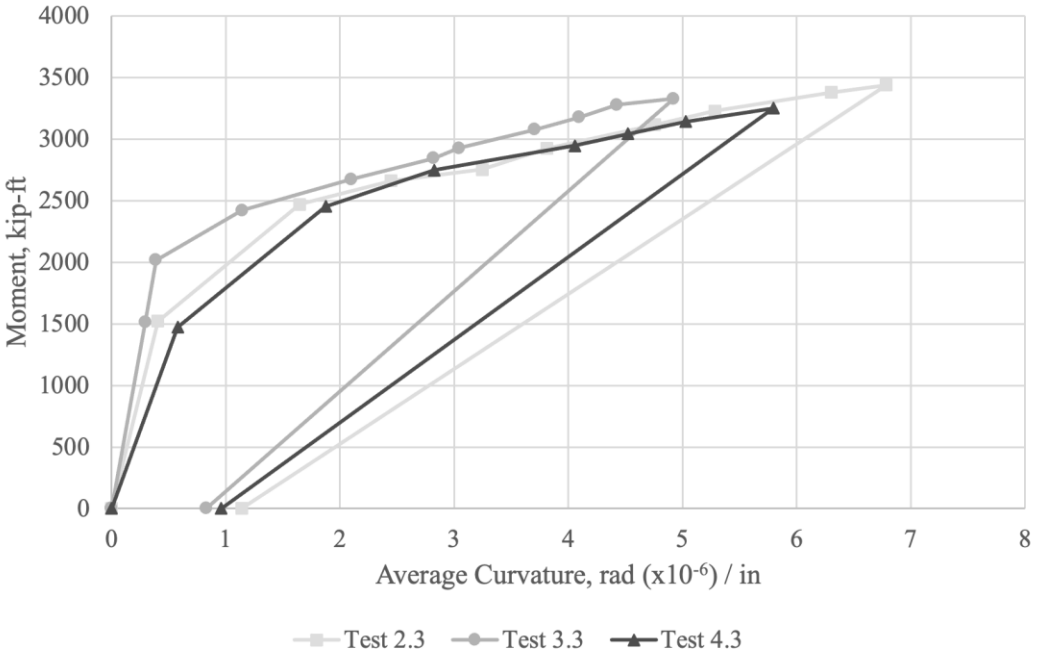

Figure 195. Graph. Combined moment-curvature plots for flexural tests.

SHEAR AND BOND BEHAVIOR

The researchers conducted a collective total of seven shear tests on the repaired girders. Girders 2, 3, and 4 each had two shear tests, whereas Girder 1 had only one shear test. No repair failed or spalled during or after all shear tests. All the shear tests were stopped when 90 percent of the nominal shear capacity was reached or when a slip of 0.01 in. occurred at the ends of the prestressing strands. Past research commonly used a 0.01 in. slip as the definition of bond failure.

The majority of the girders tested during a shear test failed in a bond–strand slip nature. This was caused by the compression strut creating shear cracks through and around the bearing zone. The transfer length of prestressing strands in the repaired sections was measured to determine if the repairs would develop transfer of forces from strands to the surrounding girder concrete as occurs in nondamaged girders. Lack of bond in strand

transfer length regions may result in premature failure of the bearing zones and in poor shear performance of prestressed concrete girders. This bond performance was tested for Girders 1 and 4 through shear tests where the concentrated loads were placed close to the repaired end of each girder.

The CSS plots collected during the north end shear test for Girders 1 and 4 were shown in figure 73 and figure 74. Based on the plots, it is evident that adequate bond between the strand and the concrete was not present in Girder 1 repair 1.1LBZ. For repair 4.1LBZ, the strands did not bond well at the repair/girder interface, as seen at ~23 in. from the north end of the girder.

PERFORMANCE OF REPAIRS

Overall, the repairs acted cohesively with each girder and behaved the same or better than an undamaged girder. Each test was conducted to the safest maximum load with the goal of reaching yielding of the prestressing strands and verging on the nominal capacity load. No repair showed signs of major failure, such as extreme cracking or spalling, or dislodgement from the girder. Only repairs in the bearing zone showed poor prestressing bond performance, as discussed in previous chapters. Table 17 provides a comparison between the nominal load values and the experimental load values from each test. Table 18 provides a comparison between the nominal flexural values and the experimental flexural values from each test.

Table 17. Summary of girder load capacities (nominal and experimental nonconforming).

Test	Test Type	Load Type	Distance from North End to Center of Load (in.)	Maximum Experimental Load (kip)	95% Maximum Load from Nominal Moment (kip)	90% Maximum Load from Nominal Shear (kip)
1.1.S*	Shear	3-point	66.5	450	490	190
2.1.S	Shear	4-point	85	424	371	430
2.2.S	Shear	4-point	99	431	376	430
2.3.F	Flexure	4-point	262	341	323	464
3.1.S	Shear	3-point	87.75	431	371	338
3.2.S	Shear	3-point	120	410	399	354
3.3.F	Flexure	4-point	259	330	302	470
4.1.S	Shear	4-point	106	500	430	341
4.2.S	Shear	4-point	120	500	438	341
4.3.F	Flexure	4-point	300.5	331	329	428

Table 18. Summary of girder flexural capacities (nominal and experimental nonconforming).

Test	Test Type	Maximum Experimental Load (kip)	95% Nominal Flexural Capacity (kip-ft)	Experimental Flexural Capacity (kip-ft)
1.1.S*	Shear	450	2455	2375
2.1.S	Shear	424	2228	2264
2.2.S	Shear	431	2260	2301
2.3.F	Flexure	341	3263	3437
3.1.S	Shear	431	2280	2797
3.2.S	Shear	410	2792	3040
3.3.F	Flexure	330	3048	3327
4.1.S	Shear	500	3013	3208
4.2.S	Shear	500	3063	3208
4.3.F	Flexure	331	3278	3248

* No deck on Girder 1

Based on table 17 and table 18, it can be concluded that most of the repairs meet 95 percent of the nominal flexural capacity and 90 percent of the nominal shear capacity. The only two tests that did not reach 95 percent of the nominal flexural capacity were Tests 1.1.S and 4.3.F. For Test 1.1.S, the bearing zone repair 1.1LBZ was tested and found to not provide a good bond between the strand and the concrete. This provides a sound reason for why the experimental flexural capacity did not meet 95 percent of the nominal flexural capacity. For Test 4.3.F, the girder had already cracked substantially and therefore had a reduced moment of inertia, leading to a slightly lower sustained moment. The only test that did not reach 90 percent of the nominal shear capacity was Test 2.1.S; however, it did sustain 89 percent of the load from nominal shear capacity.

TOP FLANGE REPAIR BEHAVIOR

From the 13 full-scale tests conducted and the 4 direct top flange tests, no signs of top flange repair failure were found. The top flange–focused tests showed that the repaired top flange outperformed the original top flange. The top flange repair capacities are shown in table 19.

Table 19. Summary of girder top flange capacities (no deck).

Test	Test Type	Maximum Experimental Load Per Flange (kip)	Experimental Girder Top Flange Flexural Capacity (kip-ft)	Theoretical Girder Original Top Flange Flexural Capacity (kip-ft)	Theoretical Girder Top Flange Repair Flexural Capacity (kip-ft)
1.2.F	Original Top Flange and Repair Top Flange	15.7	34.0	27.0	53.0
1.3.F	Original Top Flange and Repair Top Flange	8.0	17.3	27.0	53.0
1.4.F	Repair Top Flange and Repair Top Flange	40.0	86.7	–	31.8

– represents not applicable

From table 19, on Test 1.4.F, where two top flange repairs are tested against each other, it was possible to discover that the experimental flexural capacity for these repairs exceeded the theoretical flexural capacity. For Tests 1.2.F and 1.3.F, the same discovery was not possible due to the original top flange failing before the repair.

Under such extreme loads, up to a maximum of two 40-kip concentrated loads, the top flange repairs did not display any signs of failure. Given that the maximum service loads that a typical top flange would experience during its service life are substantially lower than the maximum load tested in this research project, it is safe to conclude that the top flange repairs would provide the maximum demand capacity experienced in the service life of a typical bridge girder.

BOTTOM FLANGE REPAIR BEHAVIOR

From the 13 full-scale tests conducted, 4 of the 9 bottom flange repairs showed signs of failure. These least-performing repairs were 1.1LBZ, 4.1LBZ, 4.2LBZ, and 4.3LBF. In this case, the signs of failure seen were cracks at the repair/girder interface. The repair that performed the worst was repair 4.3LBF, as it showed the highest detachment from the girder and sounded hollow during a concrete soundness test. As mentioned in chapter 9, this repair is situated at the location of maximum tensile stress. This suggests that shallow repairs located at the point of maximum tensile stress will not anchor properly to the girder and pose a potential risk if located above traffic. The poor performance of repairs 1.1LBZ and 4.1LBZ indicates that bottom flange repairs in the bearing zone are not acceptable using current repair technology.

CHAPTER 10. CONCLUSIONS AND RECOMMENDATIONS

CONCLUSIONS

Overall, the repairs performed well during testing and allowed the girders to reach their nominal capacity limits of 95 percent flexural capacity, 90 percent shear capacity, or 0.01-in. strand slip. The top flange repair methods tested in this study perform excellently. Based on the results from the large-scale and top flange–focused tests, the top flange repairs demonstrated greater strength than the original existing girder top flange. As for bottom flange repairs, the bearing zone was the only condition where repairs did not perform to standard. Two of these bearing zone repairs, 1.1LBZ and 4.1LBZ, trialed an untested repair method of retensioning the prestressing strands after transfer. The bearing zone repair performance after testing suggested that adequate bond between the strand and the concrete was not adequately developed in the bearing zone. Furthermore, the shallowest bottom flange repair, 4.3LBF, located in a region of high tensile stress failed prematurely and separated from the girder. All reinforced repair surfaces, whether epoxy coated or not, demonstrated excellent adhesion to the maximum loads achieved, which were to loads equal to or greater than 95 percent of the nominal moment capacity or 90 percent of the nominal shear capacity of the girders tested.

RECOMMENDATIONS

Top Flange Repair Recommendations

From a construction standpoint, the top flange repair method tested in this study is recommended with some adjustments:

- The installation of the c-bars was not difficult; however, finding the perfect placement of the c-bars was difficult, due to a substantial number of stirrups and other reinforcement in the top flange repair area. Also, the decision to bend the rebar into the c-bar shape prior to installation made the rest of the repair process more difficult and required more effort in measurements.

  Recommendation: *An adjusted method that requires less preparation before making the top flange repair would be to simply post-install straight #3 reinforcing bars, wait for the epoxy anchoring agent to cure, and bend the bars to the required shape after it is embedded.*

- The use of the Sikadur-32 two-part epoxy bonding agent should be reconsidered. The slant shear cylinders studied herein where epoxy bonding agent was not used performed as well as the cylinders where the agent was used. During repair, it was difficult to properly coat the repair surface, especially in congested flange areas. Further, the required timing of less than 30 min between placement of the bonding agent and placement of the repair concrete is critical and may be difficult to accomplish in the field. Finally, the application of the bonding agent is costly in labor time and materials.

  Recommendation: *GDOT should consider omitting the use of epoxy bonding agents for concrete repairs if the repair surface is clean, free of laitance and standing water, and intentionally roughened to 0.25-in. amplitude.*

Bottom Flange Repair Recommendations

From a construction standpoint, the bottom flange repair methods (outside the bearing zone) tested in this study are suited for practice with some adjustments:

- The use of chimneys, although successful, can be cumbersome for repairs in need of a quick turnaround.

  Recommendation: *Bottom flange repair regions should have an open top accessible for concrete placement into the void.*

- The use of stainless steel Tapcon screw anchors and galvanized steel wire is recommended with caveats. The Tapcon are designed for concrete compressive strengths up to 5,000 psi; thus, for girders with strengths higher than 5,000 psi, an alternative concrete anchor is suggested. Tapcon were used in this project on girder specimens having a concrete strength higher than 5,000 psi; however, they were difficult to install and required several tries to ensure proper anchorage into the girder concrete. The installation of the 12-gauge galvanized wire was favorable in repairs with little to no exposed reinforcement, as this wire was malleable and did not require embedment into the girder concrete but, rather, coiling around the Tapcon.

  Recommendations: *Future applications should use a combination of stainless steel concrete anchors and stainless steel wire.*

Commentary on the Use of Epoxy Bonding Agents

Due to the heavy use of epoxy bonding agents in this project, their validity and usefulness were questioned, as follows:

- Epoxy is recommended by MNL-137; however, it is very difficult to ensure proper use in a construction environment, as it is time dependent and requires rigid surface preparation.

  Recommendation: *It was difficult to perfect the application of the epoxy bonding agent in a controlled lab environment, so its use in outdoor, weather-dependent construction sites should be reconsidered and avoided when possible.*

- The data from the shear slant cylinder tests suggested that the use of this epoxy bonding agent does not increase the bond strength of the fresh concrete to the existing concrete. On the contrary, the shear slant cylinders that were placed with no epoxy bonding agent were shown to have a higher shear strength than those with the epoxy bonding coat.

  Recommendation: *This result suggests that epoxy bonding agents should not be used in congested and hard-to-reach repair sites.*

Commentary on the Use of SCC and Concrete Repair Mortar

Use of SCC and concrete mortar repair products are recommended with the following adjustments:

- For bottom flange repairs, the use of SCC was successful and is recommended for future applications. It easily flowed through rebar congested areas, and its compressive strength went above the required design strength.

  Recommendation: *It is recommended to practice and perfect successfully flowing SCC batches prior to making a repair with SCC. SCC batches*

require a close watch because the admixtures added and mixing time affect the flowability of the mix.

- The SikaEmaco 425 Gel Patch was not easy to apply over a large surface area. The lack of initial bond of the concrete repair mortar to the repair surface made application very difficult. The mortar required constant manipulation and even the need to be held in place at times.

  Recommendation: *The application of concrete repair mortar is not suggested for repairs with a large surface area, especially if the repair is on a bottom-facing surface. Its use in small surface area repairs may have better performance, but that cannot be concluded from the scope of this research project.*

Commentary on Current SOP

The current GDOT SOP-3[6] does not provide ample guidelines for a time-efficient, successful repair of a nonconforming girder. With the findings from this research project, the research team recommends implementation of a standardized repair procedure for typical nonconformances seen in pre-casting plants.

Recommendation: *Appendix K contains a suggested preliminary repair guide. It is recommended that GDOT build upon this preliminary repair guide with other nonconformance issues that were outside the scope of this research project (e.g., cracks, surface finish, etc.).*

APPENDIX A. NONCONFORMITY PHOTOS

GIRDER 1 NONCONFORMITIES

Figure 196. Photo. Repair 1.1LBZ.

Figure 197. Photo. Repair 1.2LTF.

Figure 198. Photo. Repair 1.3LTF.

Figure 199. Photo. Repair 1.3RTF.

GIRDER 2 NONCONFORMITIES

Figure 200. Photo. Repair 2.1LTF.

Figure 201. Photo. Repair 2.1RTF.

Figure 202. Photo. Repair 2.2LTF.

Figure 203. Photo. Repair 2.3RTF.

GIRDER 3 NONCONFORMITIES

Figure 204. Photo. Repair 3.1LBF.

Figure 205. Photo. Repair 3.1RBF.

Figure 206. Photo. Repair 3.2RBF.

Figure 207. Photo. Repair 3.3LBF.

Figure 208. Photo. Repair 3.3RBF.

GIRDER 4 NONCONFORMITIES

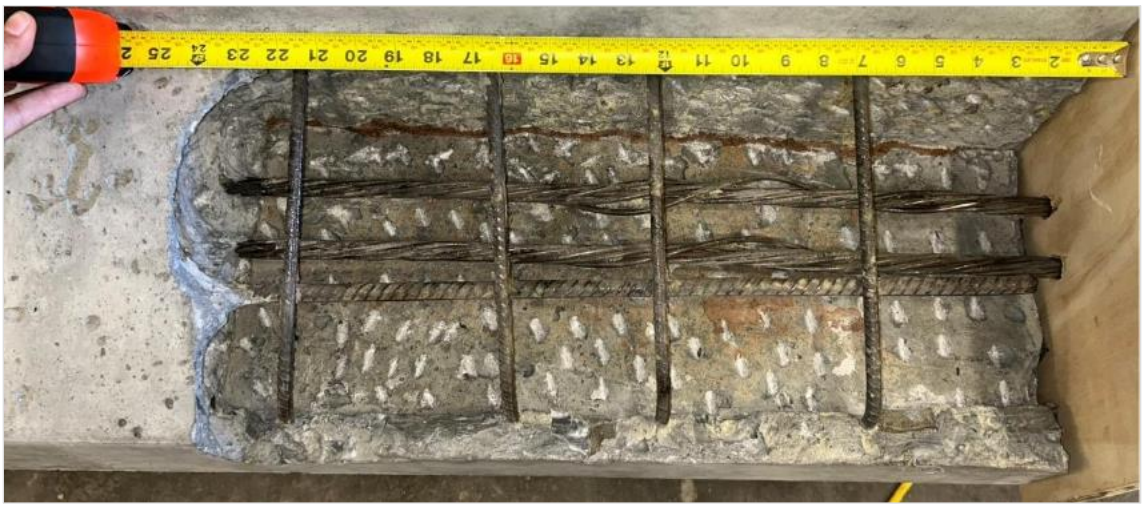

Figure 209. Photo. Repair 4.1LBZ.

Figure 210. Photo. Repair 4.1LTF.

Figure 211. Photo. Repair 4.1RTF.

Figure 212. Photo. Repair 4.2RBZ.

Figure 213. Photo. Repair 4.2LTF.

Figure 214. Photo. Repair 4.2RTF.

Figure 215. Photo. Repair 4.2RTFE.

Figure 216. Photo. Repair 4.3LBF.

Figure 217. Photo. Repair 4.3LTF.

Figure 218. Photo. Repair 4.4LTF.

APPENDIX B. GIRDER DESIGN

RECOMMENDATIONS FOR FUTURE WORK

The purpose of this project was to develop and test repair methods for nonconforming prestressed girders; however, the durability of these repairs was not tested for long-term use. It is recommended that future research be conducted on the long-term performance of these repairs through a cyclic, fatigue loading that reflects girder service conditions.

SCP GIRDER DESIGN DRAWINGS WITH NONCONFORMITIES

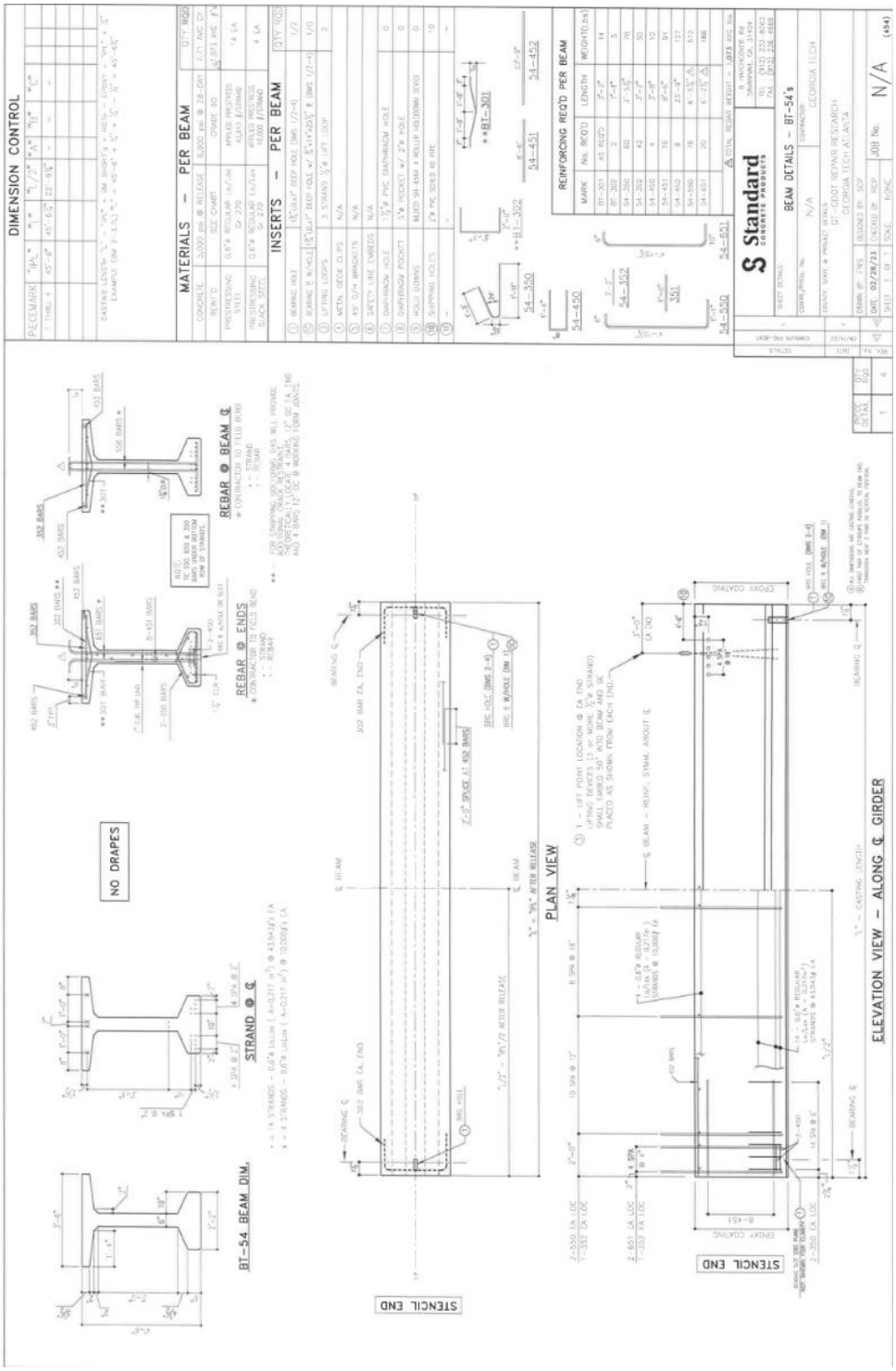

Figure 219. Drawing. SCP Girder Design Drawing 1.

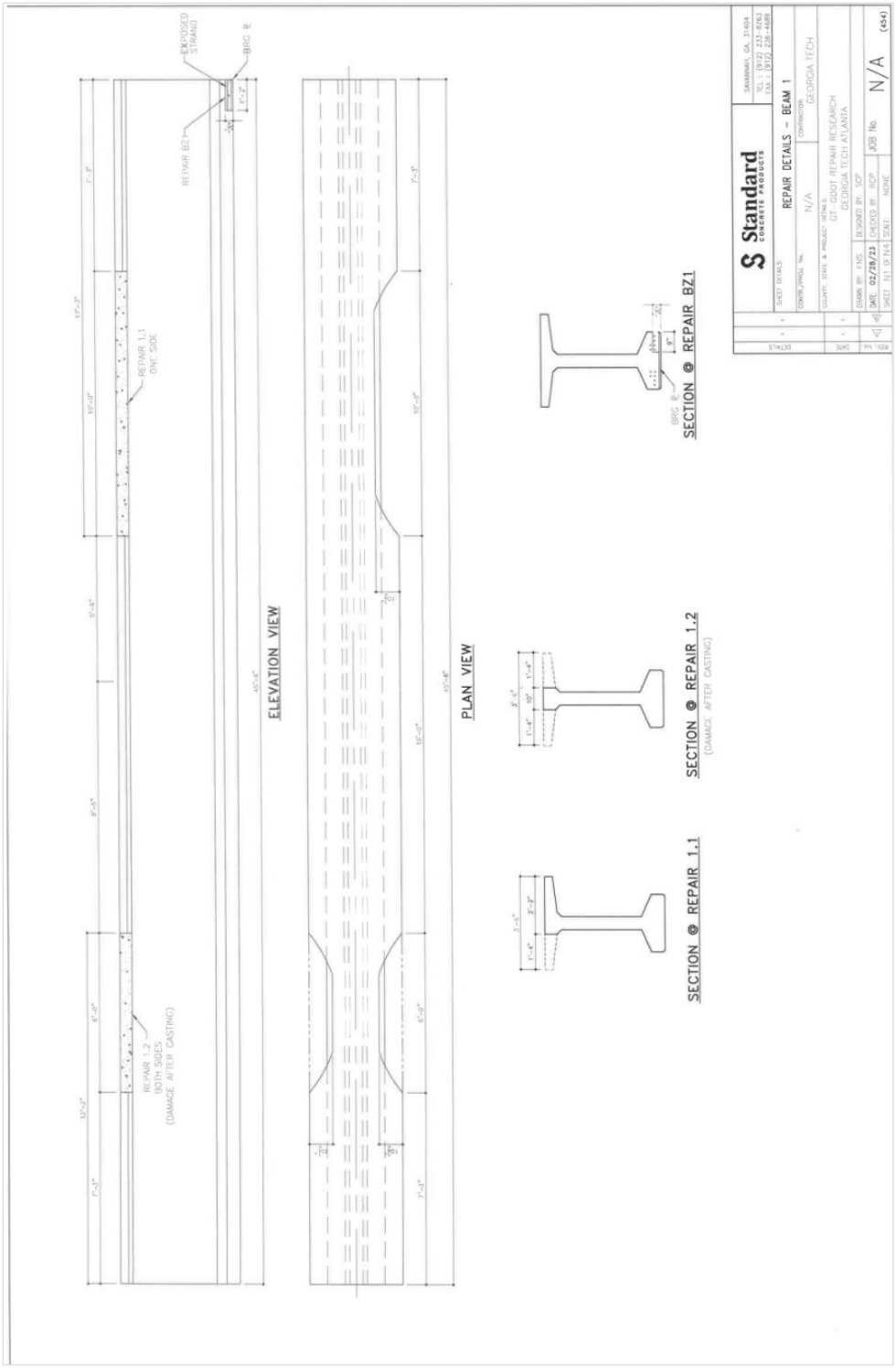

Figure 220. Drawing. SCP Girder Design Drawing 2.

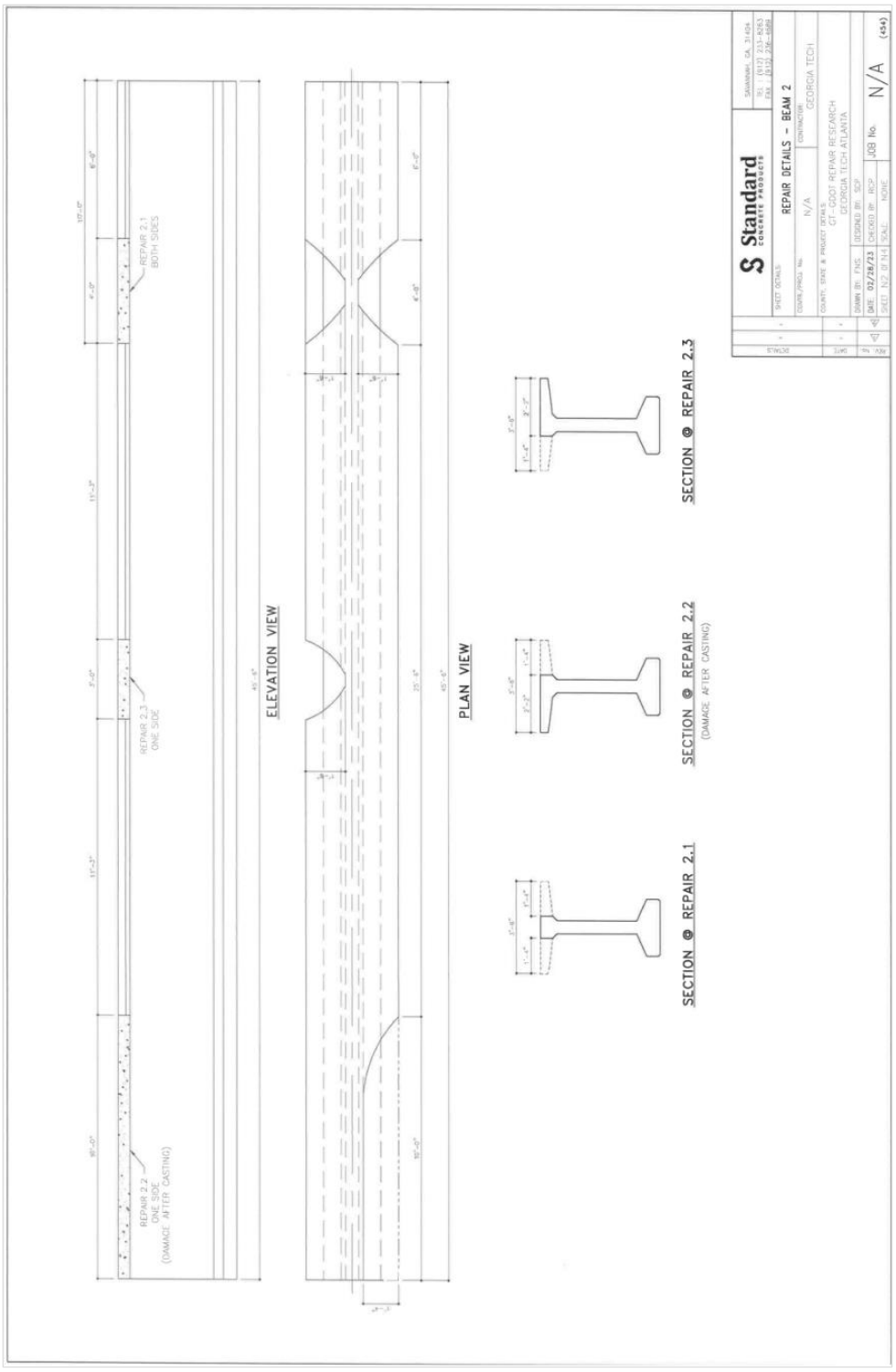

Figure 221. Drawing. SCP Girder Design Drawing 3.

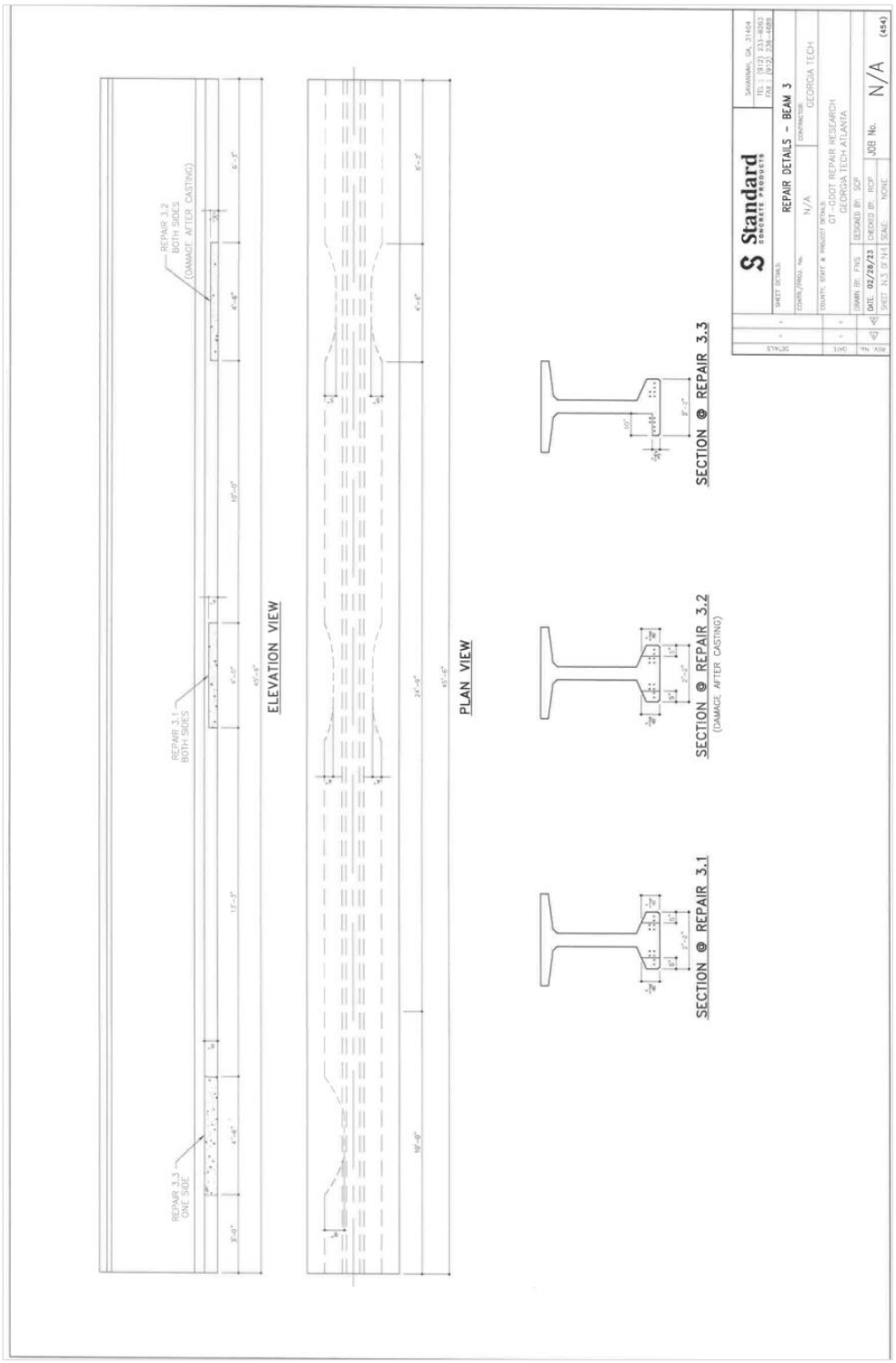

Figure 222. Drawing. SCP Girder Design Drawing 4.

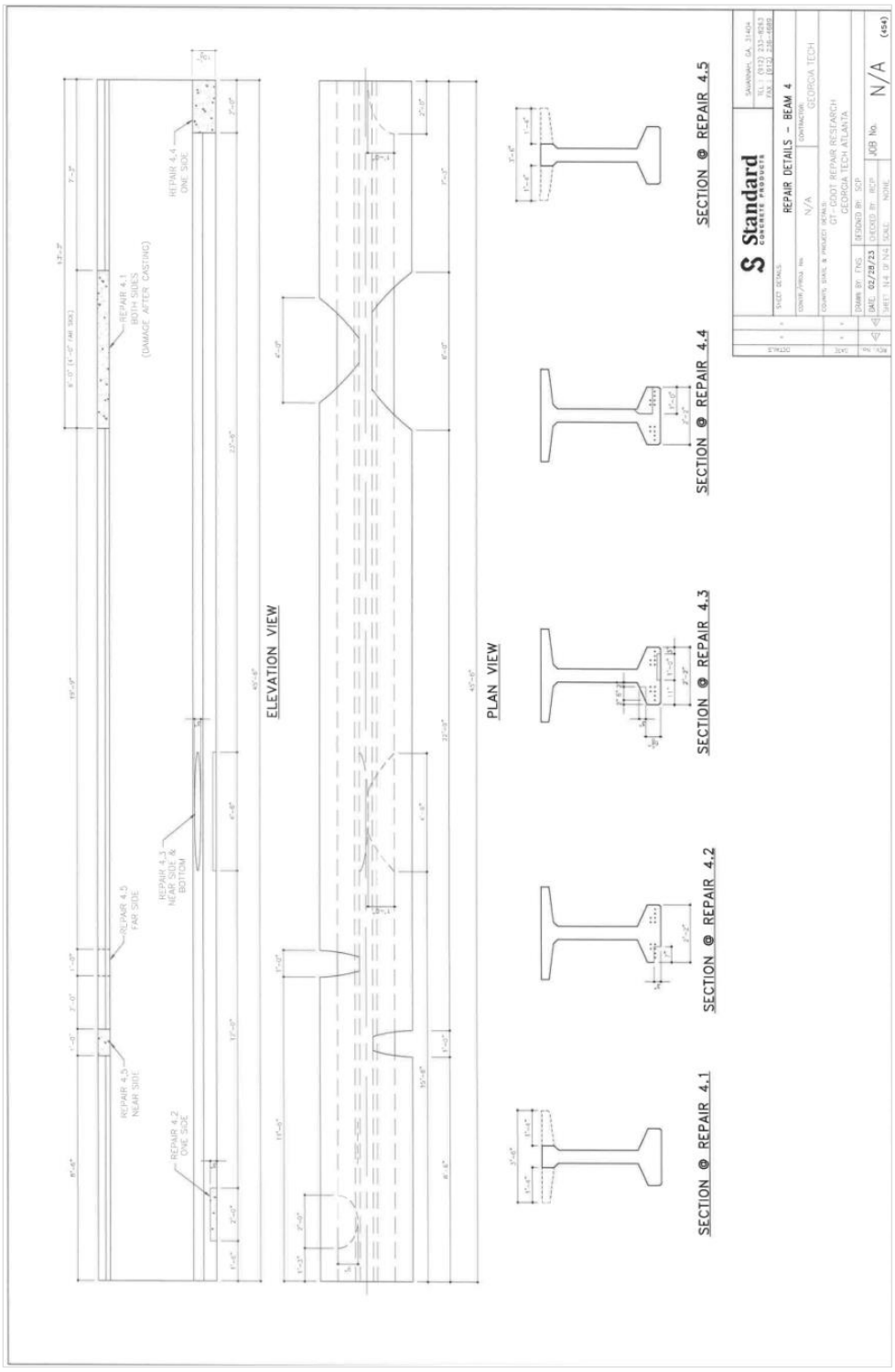

Figure 223. Drawing. SCP Girder Design Drawing 5.

APPENDIX C. GIRDER CONCRETE PROPERTIES

QUALITY CONTROL DEPARTMENT

COUNTY: _____ PROJECT NUMBER: _____ JOB: GT RESEARCH

LAB TEST

CASTING DATE: 5-14-24

TEST	1	2	3	4	5
SLUMP - INCHES					
AIR CONTENT PERCENT					
AMBIENT TEMP. F°					
CONCRETE TEMP. F°					
TIME OF TEST					
BATCH TICKET #					
LOAD #					
WATER CEMENT RATIO					
BED POSITION					

FAR: ____ NEAR: ____ 28 DAY STRENGTH: _____ RELEASE STRENGTH: _____

DATE	TIME	LOAD / FAR	Psi/MPa	LOAD / NEAR	Psi/Mpa
5-15-24	9:37 A.M.	BEAM 1	BEAM 2	BEAM 3	BEAM 4
		9715 PSI	9850 PSI	10085 PSI	8070 PSI
		122,020 lbs	123,716 lbs	126,668 lbs	101,359 lbs

BED: 4

BEAM NUMBERS	
BEAM TYPE	
MIX DESIGN	
UNIT WEIGHT	

COMMENTS: _____

STANDARD CONCRETE PRODUCTS – ATLANTA PLANT SAMPLED BY: _____

Figure 224. Data. SCP full-scale girder concrete compressive strength before cutdown.

Concrete Cylinder Data							
	Name	Diameter (in)	Area (in^2)	Max Load (lbf)	Strength (psi)	**AVG Strength (psi)**	Date
14 DAY	G1-OG-1	4	12.57	152900	12167	**11857**	28-May
	G1-OG-2	4	12.57	145100	11547		
28 DAY	G1-OG-1	4	12.57	162400	12923	**12854**	15-Jun
	G1-OG-2	4	12.57	158400	12605		
	G1-OG-3	4	12.57	163800	13035		
TEST DAY	G1-OG-1	4	12.57	173347	13795	**14342**	9-Jul
	G1-OG-2	4	12.57	179856	14312		
	G1-OG-3	4	12.57	187476	14919		
Concrete Cylinder Data							
	Name	Diameter (in)	Area (in^2)	Max Load (lbf)	Strength (psi)	**AVG Strength (psi)**	Date
14 DAY	G2-OG-1	4	12.57	145300	11563	**11459**	28-May
	G2-OG-2	4	12.57	142700	11356		
28 DAY	G2-OG-1	4	12.57	162700	12947	**12711**	15-Jun
	G2-OG-2	4	12.57	161400	12844		
	G2-OG-3	4	12.57	155100	12342		
TEST DAY	G2-OG-1	4	12.57	187775	14943	**14475**	26-Jun
	G2-OG-2	4	12.57	182964	14560		
	G2-OG-3	4	12.57	174966	13923		
Concrete Cylinder Data							
	Name	Diameter (in)	Area (in^2)	Max Load (lbf)	Strength (psi)	**AVG Strength (psi)**	Date
14 DAY	G3-OG-1	4	12.57	146100	11626	**11658**	28-May
	G3-OG-2	4	12.57	146900	11690		
28 DAY	G3-OG-1	4	12.57	156100	12422	**12323**	15-Jun
	G3-OG-2	4	12.57	153600	12223		
	G3-OG-3	4	12.57	152800	12159		
TEST DAY	G3-OG-1	4	12.57	183839	14629	**14596**	17-Jun
	G3-OG-2	4	12.57	183129	14573		
	G3-OG-3	4	12.57	183300	14587		
Concrete Cylinder Data							
	Name	Diameter (in)	Area (in^2)	Max Load (lbf)	Strength (psi)	**AVG Strength (psi)**	Date
14 DAY	G4-OG-1	4	12.57	117700	9366	**9450**	28-May
	G4-OG-2	4	12.57	119800	9533		
28 DAY	G4-OG-1	4	12.57	118700	9446	**10117**	15-Jun
	G4-OG-2	4	12.57	136300	10846		
	G4-OG-3	4	12.57	126400	10059		
TEST DAY	G4-OG-1	4	12.57	157039	12497	**12619**	24-Jun
	G4-OG-2	4	12.57	159556	12697		
	G4-OG-3	4	12.57	159144	12664		

Figure 225. Data. Full-scale girder concrete compressive strength.

STANDARD CONCRETE PRODUCTS
ATLANTA PLANT

CONCRETE BATCH PLANT
REPORT

DATE 5/14/24
SHEET ___ of ___

Job No. GDOT
Used No. 4
Item No. Research
Mix No. GS0004

Flyash Type ___ Amb. Temp ___ Sand Moistur ___ % Agg. Moisture ___ %
Add Mix 1 WRDA Conc. Temp ___ Cement Type ___
Add Mix 2 ___ HRWR/R ___
Air Ent. ___ ozs
Plant Operator: ___

Batch No.	Control Number	Admix Lbs	Cement Lbs	Stone Lbs	Sand Lbs	Water Gallons	AEA Ozs	Water Red. Plastiment	HRWR/R V2100	Vol. C.Y.	Discharge Time	Notes
1	78585		2415	5680	3370	56	14	90	142	3	2:45	X
2			2425	5580	3380	55	14	92	142	7	3:02	
3			2425	5550	3370	56	14	92	142	10.5	3:15	
4			2430	5630	3380	56	14	92	142	14	3:31	X
5			2425	5570	3380	56	14	92	142	17.5	3:38	
6			2425	5630	3380	56	14	92	142	21	4:06	
7			2415	5600	3380	55	14	92	142	24.5	4:19	X
8			2425	5610	3380	56	14	92	142	28	4:34	
9			2420	5620	3370	57	14	92	142	31.5	4:45	
10			2420	5610	3380	56	14	92	142	35	4:56	X
11			2425	5590	3390	56	14	92	142	38.5	5:08	39
12										42		
13										45.5		
14										49		
15										52.5		
16										56		
17										59.5		
18										63		
19										66.5		
20										70		
21										73.5		
22										77		
23										80.5		
24										84		
25										87.5		
26										91		
27										94.5		
28										98		
29										101.5		
30										105		

Comments: ___

Figure 226. Data. Full-scale girder concrete design mix from SCP.

Figure 227. Data. 0.6-in. strand material testing from SCP.

APPENDIX D. TOP FLANGE REPAIR CONCRETE PROPERTIES

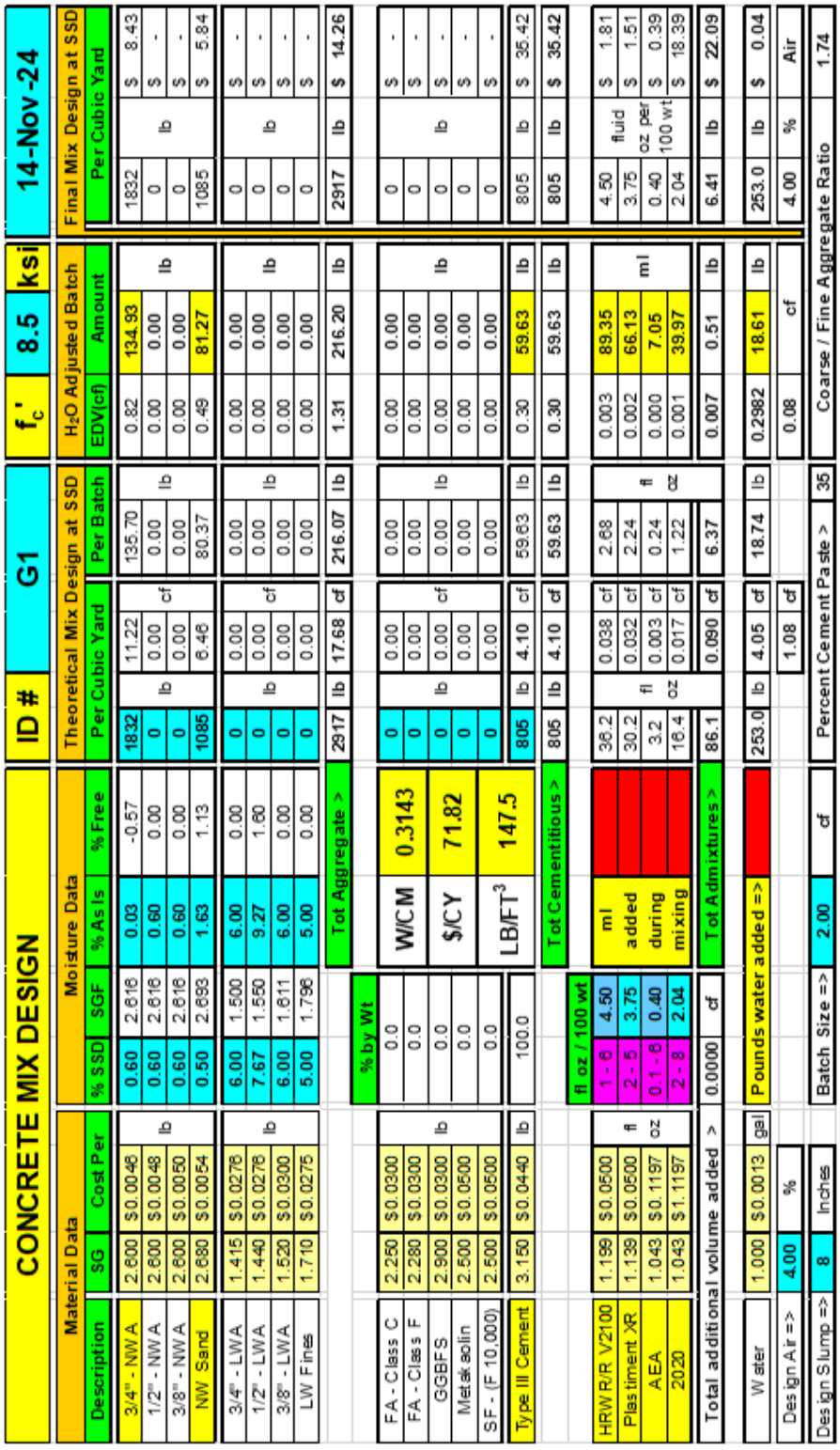

Figure 228. Data. Top flange repair Concrete Mix 1.

CONCRETE MIX DESIGN								ID #	G2		f_c'	8.5	ksi	7-Nov-24		
Material Data			Moisture Data				Theoretical Mix Design at SSD				H_2O Adjusted Batch			Final Mix Design at SSD		
Description	SG	Cost Per	% SSD	SGF	% As Is	% Free	Per Cubic Yard		Per Batch		EDV(cf)	Amount		Per Cubic Yard		
3/4" - NWA	2.600	$0.0046	0.60	2.618	0.03	-0.57	1832	lb	11.22	cf	0.82	134.93	lb	1832	$	8.43
1/2" - NWA	2.600	$0.0048	0.60	2.618	0.60	0.00	0		0.00		0.00	0.00		0	$	-
3/8" - NWA	2.600	$0.0050	0.60	2.618	0.60	0.00	0		0.00		0.00	0.00		0	$	-
NW Sand	2.680	$0.0054	0.50	2.693	2.88	2.38	1085		6.46		0.51	82.28		1085	$	5.84
3/4" - LWA	1.415	$0.0276	6.00	1.500	6.00	0.00	0	lb	0.00	cf	0.00	0.00	lb	0	$	-
1/2" - LWA	1.440	$0.0276	7.67	1.550	9.27	1.60	0		0.00		0.00	0.00		0	$	-
3/8" - LWA	1.520	$0.0300	6.00	1.611	6.00	0.00	0		0.00		0.00	0.00		0	$	-
LW Fines	1.710	$0.0275	5.00	1.796	5.00	0.00	0		0.00		0.00	0.00		0	$	-
					Tot Aggregate >		2917	lb	17.68	cf	1.33	217.21	lb	2917	lb	14.26
			% by Wt													
FA - Class C	2.250	$0.0300	0.0		W/CM	0.3143	0	lb	0.00	cf	0.00	0.00	lb	0	$	-
FA - Class F	2.280	$0.0300	0.0				0		0.00		0.00	0.00		0	$	-
GGBFS	2.900	$0.0300	0.0	lb	$/CY	71.82	0		0.00		0.00	0.00		0	$	-
Metakaolin	2.500	$0.0500	0.0				0		0.00		0.00	0.00		0	$	-
SF - (F 10,000)	2.500	$0.0500	0.0		LB/FT^3	147.5	0		0.00		0.00	0.00		0	$	-
Type III Cement	3.150	$0.0440	100.0	lb			805	lb	4.10	cf	0.30	59.63	lb	805	lb	35.42
					Tot Cementitious >		805	lb	4.10	cf	0.30	59.63	lb	805	lb	35.42
			fl oz / 100 wt													
HRWR/R V2100	1.199	$0.0500	1 - 8	4.50	ml added during mixing		36.2	fl oz	0.038	cf	0.003	79.35	ml	4.50	fluid oz per 100 wt	1.81
Plastiment XR	1.139	$0.0500	2 - 5	3.75			30.2		0.032	cf	0.002	66.13		3.75		1.51
AEA	1.043	$0.1197	0.1 - 8	0.40			3.2		0.003	cf	0.000	7.05		0.40		0.39
2020	1.043	$1.1197	2 - 8	2.04			16.4		0.017	cf	0.001	35.97		2.04		18.39
Total additional volume added >			0.0000	cf	Tot Admixtures >		86.1		0.090	cf	0.007	0.47	lb	6.41	lb	22.09
Water	1.000	$0.0013	gal	Pounds water added =>			253.0	lb	4.05	cf	0.2821	17.61	lb	253.0	lb	0.04
Design Air =>	4.00	%							1.08	cf	0.08	cf		4.00	%	Air
Design Slump =>	8	Inches		Batch Size =>	2.00	cf	Percent Cement Paste >		35		Coarse / Fine Aggregate Ratio			1.74		

Figure 229. Data. Top flange repair Concrete Mix 2.

CONCRETE MIX DESIGN								ID #		G4				f_c'	8.5	ksi	21-Nov-24		
Material Data				Moisture Data				Theoretical Mix Design at SSD						H_2O Adjusted Batch			Final Mix Design at SSD		
Description	SG	Cost Per		% SSD	SGF	% As Is	% Free	Per Cubic Yard				Per Batch		EDV(cf)	Amount		Per Cubic Yard		
3/4" - NWA	2.600	$ 0.0046	lb	0.60	2.616	0.03	-0.57	3220	lb	19.73	cf	238.52	lb	1.44	237.16	lb	3220	lb	$ 14.81
1/2" - NWA	2.600	$ 0.0048		0.60	2.616	0.60	0.00	0		0.00		0.00		0.00	0.00		0		$ -
3/8" - NWA	2.600	$ 0.0050		0.60	2.616	0.60	0.00	0		0.00		0.00		0.00	0.00		0		$ -
NW Sand	2.680	$ 0.0054		0.50	2.693	1.07	0.57	2415		14.37		178.89		1.08	179.90		2415		$ 12.99
3/4" - LWA	1.415	$ 0.0276	lb	6.00	1.500	6.00	0.00	0	lb	0.00	cf	0.00	lb	0.00	0.00	lb	0	lb	$ -
1/2" - LWA	1.440	$ 0.0276		7.67	1.550	9.27	1.60	0		0.00		0.00		0.00	0.00		0		$ -
3/8" - LWA	1.520	$ 0.0300		6.00	1.611	6.00	0.00	0		0.00		0.00		0.00	0.00		0		$ -
LW Fines	1.710	$ 0.0275		5.00	1.796	5.00	0.00	0		0.00		0.00		0.00	0.00		0		$ -
						Tot Aggregate >		5635	lb	34.10	cf	417.41	lb	2.52	417.06	lb	5635	lb	$ 27.80
				% by Wt															
FA - Class C	2.250	$0.0300	lb	0.0		W/CM	-0.9583	0	lb	0.00	cf	0.00	lb	0.00	0.00	lb	0	lb	$ -
FA - Class F	2.280	$0.0300		0.0				0		0.00		0.00		0.00	0.00		0		$ -
GGBFS	2.900	$0.0300		0.0		$/CY	85.20	0		0.00		0.00		0.00	0.00		0		$ -
Metakaolin	2.500	$0.0500		0.0				0		0.00		0.00		0.00	0.00		0		$ -
SF - (F 10,000)	2.500	$0.0500		0.0		LB/FT^3	210.2	0		0.00		0.00		0.00	0.00		0		$ -
Type III Cement	3.150	$ 0.0440	lb	100.0				805	lb	4.10	cf	59.63	lb	0.30	59.63	lb	805	lb	$ 35.42
						Tot Cementitious >		805	lb	4.10	cf	59.63	lb	0.30	59.63	lb	805	lb	$ 35.42
				fl oz / 100 wt															
HRWR/R V2100	1.199	$ 0.0500	fl oz	1 - 6	4.50	ml added during mixing		36.2	fl oz	0.038	cf	2.68	fl oz	0.003	89.35	ml	4.50	fluid oz per 100 wt	$ 1.81
Plastiment XR	1.139	$ 0.0500		2 - 5	3.75			30.2		0.032	cf	2.24		0.002	66.13		3.75		$ 1.51
AEA	1.043	$ 0.1197		0.1 - 6	0.40			3.2		0.003	cf	0.24		0.000	7.05		0.40		$ 0.39
2020	1.043	$ 1.1197		2 - 8	2.04			16.4		0.017	cf	1.22		0.001	39.97		2.04		$ 18.39
Total additional volume added >				0.0000	cf	Tot Admixtures >		86.1		0.090	cf	6.37		0.007	0.51	lb	6.41	lb	$ 22.09
Water	1.000	$0.0013	gal	Pounds water added =>				####	lb	-12.36	cf	-57.15	lb	-0.9103	-56.80	lb	-771.5	lb	$ (0.12)
Design Air =>	4.00	%								1.08	cf			0.08	cf		4.00	%	Air
Design Slump =>	8	Inches		Batch Size =>		2.00	cf	Percent Cement Paste >					-26	Coarse / Fine Aggregate Ratio					1.37

Figure 230. Data. Top flange repair Concrete Mix 3.

Concrete Cylinder Data			Molded on Thursday 14 November 2024 at 12PM				
	Name	Diameter (in)	Area (in^2)	Max Load (lbf)	Strength (psi)	AVG Strength (psi)	Date
24-Hour	G1-TF-B8-1	4	12.57	77469	6165	6334	15-Nov
	G1-TF-B8-2	4	12.57	80736	6425		
	G1-TF-B8-3	4	12.57	80588	6413		
7 DAY	G1-TF-B1-1	4	12.57	131599	10472	10834	21-Nov
	G1-TF-B1-2	4	12.57	137830	10968		
	G1-TF-B1-3	4	12.57	139003	11061		
28 DAY	G1-TF-B1-1	4	12.57	154659	12307	12329	12-Dec
	G1-TF-B1-2	4	12.57	154798	12318		
	G1-TF-B1-3	4	12.57	155339	12361		
	G1-TF-B2-1	4	12.57	147785	11760	11654	
	G1-TF-B2-2	4	12.57	149797	11920		
	G1-TF-B2-3	4	12.57	141762	11281		
	G1-TF-B3-1	4	12.57	151996	12095	11634	
	G1-TF-B3-2	4	12.57	147181	11712		
	G1-TF-B3-3	4	12.57	139407	11094		
	G1-TF-B4-1	4	12.57	151827	12082	11761	
	G1-TF-B4-2	4	12.57	146644	11670		
	G1-TF-B4-3	4	12.57	144890	11530		
	G1-TF-B5-1	4	12.57	145326	11565	11484	
	G1-TF-B5-2	4	12.57	143831	11446		
	G1-TF-B5-3	4	12.57	143783	11442		
	G1-TF-B6-1	4	12.57	146902	11690	11885	13 Dec 8am
	G1-TF-B6-2	4	12.57	150728	11995		
	G1-TF-B6-3	4	12.57	150408	11969		
	G1-TF-B7-1	4	12.57	139055	11066	11228	
	G1-TF-B7-2	4	12.57	138609	11030		
	G1-TF-B7-3	4	12.57	145639	11590		
	G1-TF-B8-1	4	12.57	146977	11696	11252	
	G1-TF-B8-2	4	12.57	138428	11016		
	G1-TF-B8-3	4	12.57	138801	11045		
TEST DAY	G1-TF-B1-1	4	12.57	180268	14345	14042	7-Jul
	G1-TF-B1-2	4	12.57	177519	14127		
	G1-TF-B1-3	4	12.57	171592	13655		
	G1-TF-B2-1	4	12.57	179636	14295	13689	
	G1-TF-B2-2	4	12.57	169336	13475		
	G1-TF-B2-3	4	12.57	167095	13297		
	G1-TF-B3-1	4	12.57	163441	13006	13568	
	G1-TF-B3-2	4	12.57	179308	14269		
	G1-TF-B3-3	4	12.57	168747	13428		
	G1-TF-B4-1	4	12.57	166728	13268	13593	
	G1-TF-B4-2	4	12.57	174361	13875		
	G1-TF-B4-3	4	12.57	171367	13637		
	G1-TF-B5-1	4	12.57	158664	12626	13280	
	G1-TF-B5-2	4	12.57	172333	13714		
	G1-TF-B5-3	4	12.57	169634	13499		
	G1-TF-B6-1	4	12.57	165349	13158	13890	
	G1-TF-B6-2	4	12.57	181352	14432		
	G1-TF-B6-3	4	12.57	176942	14081		
	G1-TF-B7-1	4	12.57	172208	13704	12990	
	G1-TF-B7-2	4	12.57	157697	12549		
	G1-TF-B7-3	4	12.57	159801	12717		
	G1-TF-B8-1	4	12.57	154087	12262	12318	
	G1-TF-B8-2	4	12.57	152600	12144		
	G1-TF-B8-3	4	12.57	157683	12548		

Figure 231. Data. Top flange repair Concrete Strength 1.

Concrete Cylinder Data			Molded on Thursday 7 November 2024 at 12PM				
	Name	Diameter (in)	Area (in^2)	Max Load (lbf)	Strength (psi)	**AVG Strength (psi)**	Date
24-Hour	G2-TF-B6-1	4	12.57	93502	7441	**7473**	8-Nov
	G2-TF-B6-2	4	12.57	96555	7684		
	G2-TF-B6-3	4	12.57	91652	7293		
28 DAY	G2-TF-B1-1	4	12.57	155497	12374	**12374**	5-Dec
	G2-TF-B2-1	4	12.57	160840	12799	**12799**	
	G2-TF-B3-1	4	12.57	155910	12407	**12407**	
	G2-TF-B4-1	4	12.57	160877	12802	**12802**	
	G2-TF-B5-1	4	12.57	156359	12443	**12443**	
	G2-TF-B6-1	4	12.57	153961	12252	**12252**	
TEST DAY	G2-TF-B1-1	4	12.57	176442	14041	**13852**	1-Jul
	G2-TF-B1-2	4	12.57	171688	13662		
	G2-TF-B2-1	4	12.57	180941	14399	**14343**	
	G2-TF-B2-2	4	12.57	179528	14286		
	G2-TF-B3-1	4	12.57	181013	14405	**14748**	
	G2-TF-B3-2	4	12.57	189656	15092		
	G2-TF-B4-1	4	12.57	183748	14622	**15009**	
	G2-TF-B4-2	4	12.57	193472	15396		
	G2-TF-B5-1	4	12.57	182047	14487	**14383**	
	G2-TF-B5-2	4	12.57	179438	14279		
	G2-TF-B6-1	4	12.57	182847	14551	**14318**	
	G2-TF-B6-2	4	12.57	177004	14086		

Figure 232. Data. Top flange repair Concrete Strength 2.

Concrete Cylinder Data			Molded on Thursday 21 November 2024 at 3:30PM				
	Name	Diameter (in)	Area (in^2)	Max Load (lbf)	Strength (psi)	AVG Strength (psi)	Date
24-Hour	G4-TF-B1-1	4	12.57	68991	5490		
	G4-TF-B1-2	4	12.57	81908	6518	6677	22-Nov
	G4-TF-B1-3	4	12.57	85902	6836		
3 DAY	G4-TF-B6-1	4	12.57	127711	10163		
	G4-TF-B6-2	4	12.57	127908	10179	10187	24-Nov
	G4-TF-B6-3	4	12.57	128427	10220		
28 DAY	G4-TF-B1-1	4	12.57	168974	13447		
	G4-TF-B1-2	4	12.57	161719	12869	13634	
	G4-TF-B1-3	4	12.57	183311	14587		
	G4-TF-B2-1	4	12.57	157597	12541		
	G4-TF-B2-2	4	12.57	162819	12957	12689	
	G4-TF-B2-3	4	12.57	157964	12570		
	G4-TF-B3-1	4	12.57	157005	12494		
	G4-TF-B3-2	4	12.57	151555	12060	12534	
	G4-TF-B3-3	4	12.57	163954	13047		
	G4-TF-B4-1	4	12.57	167170	13303		
	G4-TF-B4-2	4	12.57	166888	13281	13239	19-Dec
	G4-TF-B4-3	4	12.57	165036	13133		
	G4-TF-B5-1	4	12.57	158351	12601		
	G4-TF-B5-2	4	12.57	162308	12916	12768	
	G4-TF-B5-3	4	12.57	160685	12787		
	G4-TF-B6-1	4	12.57	153043	12179		
	G4-TF-B6-2	4	12.57	166285	13233	12787	
	G4-TF-B6-3	4	12.57	162741	12951		
	G4-TF-B7-1	4	12.57	166906	13282		
	G4-TF-B7-2	4	12.57	164740	13110	13207	
	G4-TF-B7-3	4	12.57	166260	13231		
TEST DAY	G4-TF-B1-1	4	12.57	150086	11943		
	G4-TF-B1-2	4	12.57	183685	14617	14183	
	G4-TF-B1-3	4	12.57	200931	15990		
	G4-TF-B2-1	4	12.57	185991	14801		
	G4-TF-B2-2	4	12.57	182142	14494	12177	
	G4-TF-B2-3	4	12.57	90934	7236		
	G4-TF-B3-1	4	12.57	171073	13614		
	G4-TF-B3-2	4	12.57	187011	14882	14403	
	G4-TF-B3-3	4	12.57	184882	14712		
	G4-TF-B4-1	4	12.57	182856	14551		
	G4-TF-B4-2	4	12.57	181166	14417	14501	24-Jun
	G4-TF-B4-3	4	12.57	182655	14535		
	G4-TF-B5-1	4	12.57	179331	14271		
	G4-TF-B5-2	4	12.57	180363	14353	14414	
	G4-TF-B5-3	4	12.57	183716	14620		
	G4-TF-B6-1	4	12.57	189501	15080		
	G4-TF-B6-2	4	12.57	176971	14083	15072	
	G4-TF-B6-3	4	12.57	201729	16053		
	G4-TF-B7-1	4	12.57	179692	14299		
	G4-TF-B7-2	4	12.57	182406	14515	14357	
	G4-TF-B7-3	4	12.57	179162	14257		

Figure 233. Data. Top flange repair Concrete Strength 3.

Top Flange Repairs (GIRDER MIX)			
Girder	Repair	Batch	Slump, in
1	1.3RTF	1	8.50
	1.3RTF	2	8.50
	1.3LTF	3	8.25
	1.3LTF	4	9.00
	1.2LTF	5	8.00
	1.2LTF	6	6.00
	1.2LTF	7	8.50
	1.2LTF	8	8.75
2	2.3RTF	1	9.00
	2.1RTF	2	7.00
	2.1LTF	3	3.00
	2.2LTF	4	8.00
	2.2LTF	5	3.50
	2.2LTF	6	3.00
4	4.2RTFE and 4.2RTF	1	11.00
	4.2RTF and 4.2LTF	2	7.75
	4.1RTF and 4.4LTF	3	6.50
	4.1LTF	4	6.75
	4.1LTF	5	6.00
	4.3LTF	6	3.00
	4.3LTF	7	5.00

Figure 234. Data. Top flange repair Concrete Slump.

APPENDIX E. TOP FLANGE DEFLECTION DATA

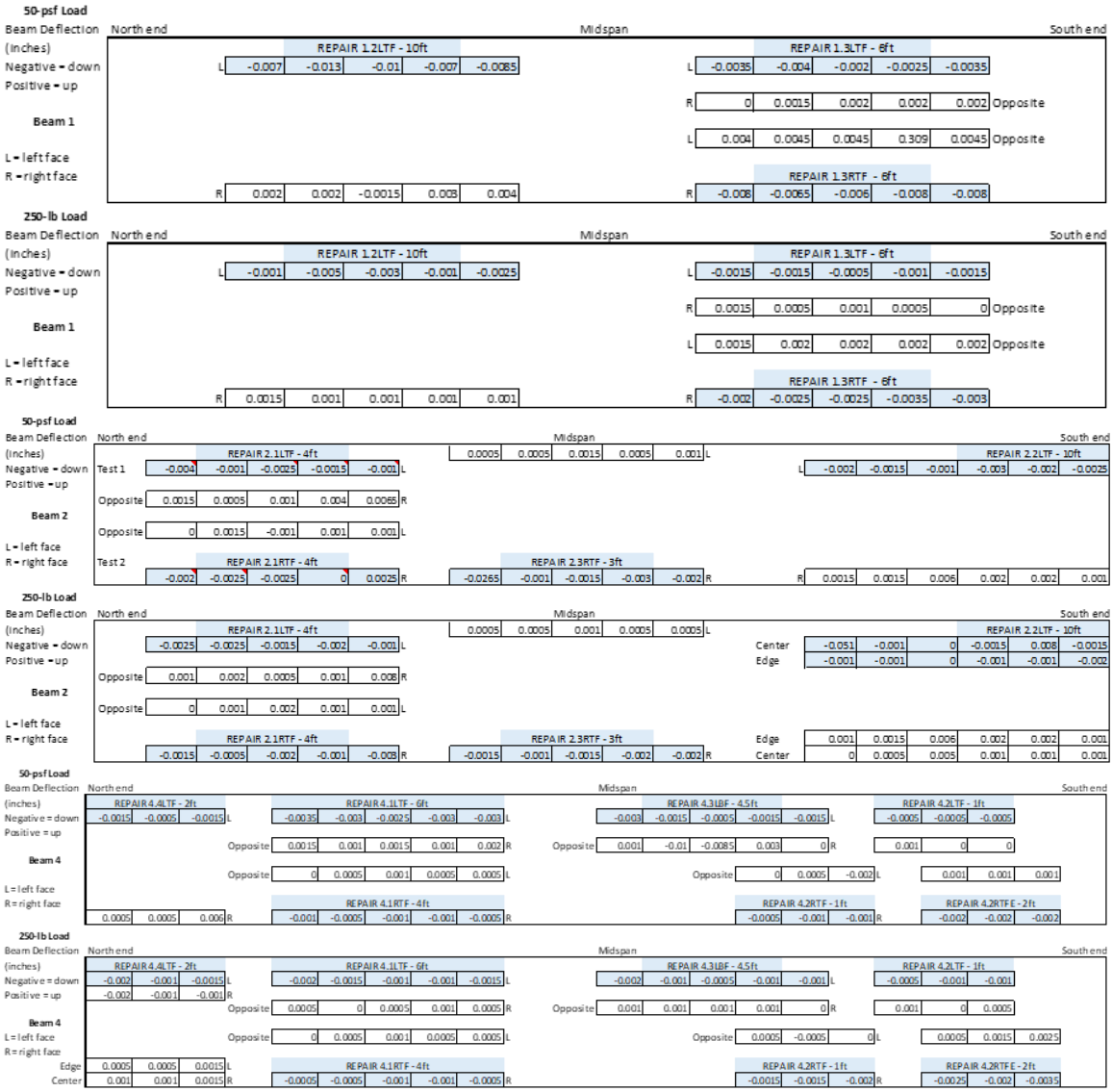

Figure 235. Data. Top flange deflection data.

APPENDIX F. BOTTOM FLANGE REPAIR CONCRETE PROPERTIES

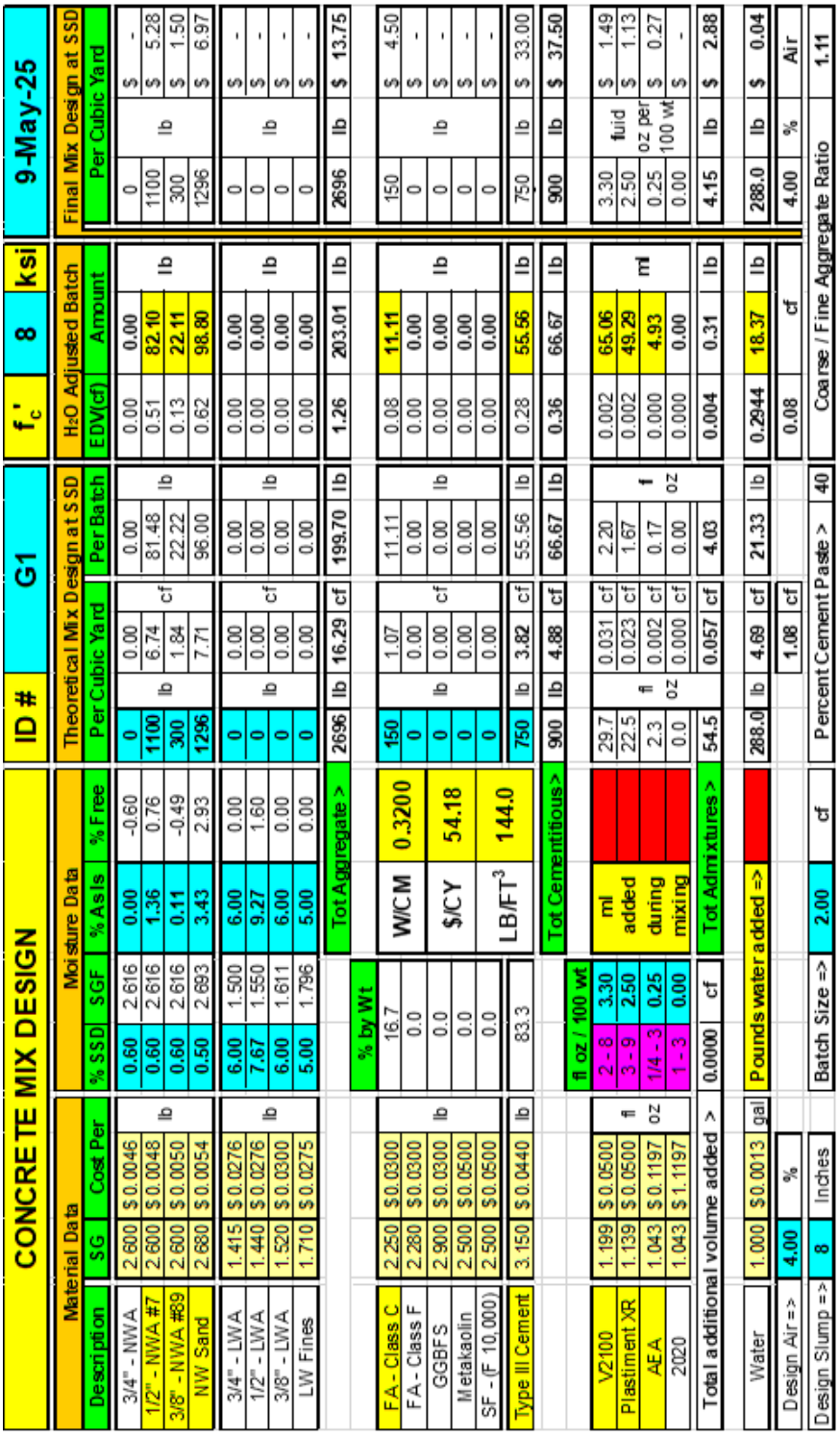

CONCRETE MIX DESIGN								ID #	G1		f_c'	8	ksi	9-May-25		
Material Data			Moisture Data				Theoretical Mix Design at S SD			H2O Adjusted Batch			Final Mix Design at SSD		
Description	SG	Cost Per	% SSD	SGF	% As Is	% Free	Per Cubic Yard		Per Batch	EDV(cf)	Amount		Per Cubic Yard		
3/4" - NWA	2.600	$ 0.0046	0.60	2.616	0.00	-0.60	0		0.00	0.00	0.00		0		$ -
1/2" - NWA #7	2.600	$ 0.0048	0.60	2.616	1.36	0.76	1100	lb	81.48	0.51	82.10	lb	1100	lb	$ 5.28
3/8" - NWA #89	2.600	$ 0.0050	0.60	2.616	0.11	-0.49	300		22.22	0.13	22.11		300		$ 1.50
NW Sand	2.680	$ 0.0054	0.50	2.693	3.43	2.93	1296		96.00	0.62	98.80		1296		$ 6.97
3/4" - LWA	1.415	$ 0.0276	6.00	1.500	6.00	0.00	0		0.00	0.00	0.00		0		$ -
1/2" - LWA	1.440	$ 0.0276	7.67	1.550	9.27	1.60	0	lb	0.00	0.00	0.00	lb	0	lb	$ -
3/8" - LWA	1.520	$ 0.0300	6.00	1.611	6.00	0.00	0		0.00	0.00	0.00		0		$ -
LW Fines	1.710	$ 0.0275	5.00	1.796	5.00	0.00	0	cf	0.00	0.00	0.00		0		$ -
					Tot Aggregate >		2696	lb	16.29 cf	1.26	203.01	lb	2696	lb	$ 13.75
			% by Wt												
FA - Class C	2.250	$ 0.0300	16.7		W/CM	0.3200	150		1.07	0.08	11.11		150		$ 4.50
FA - Class F	2.280	$ 0.0300	0.0				0		0.00	0.00	0.00		0		$ -
GGBFS	2.900	$ 0.0300	0.0	lb	$/CY	54.18	0	lb	0.00 cf	0.00	0.00	lb	0	lb	$ -
Metakaolin	2.500	$ 0.0500	0.0				0		0.00	0.00	0.00		0		$ -
SF - (F 10,000)	2.500	$ 0.0500	0.0		LB/FT^3	144.0	0		0.00	0.00	0.00		0		$ -
Type III Cement	3.150	$ 0.0440	83.3	lb			750	lb	3.82 cf	55.56	lb	0.28	55.56	lb	750	lb	$ 33.00
					Tot Cementitious >		900	lb	4.88 cf	66.67	lb	0.36	66.67	lb	900	lb	$ 37.50
			fl oz / 100 wt													
V2100	1.199	$ 0.0500	2 - 8	3.30	ml		29.7		0.031 cf	2.20		0.002	65.06		3.30	fluid	$ 1.49
Plastiment XR	1.139	$ 0.0500	3 - 9	2.50	added		22.5	fl	0.023 cf	1.67	fl	0.002	49.29	ml	2.50	oz per	$ 1.13
AEA	1.043	$ 0.1197	1/4 - 3	0.25	during		2.3	oz	0.002 cf	0.17	oz	0.000	4.93		0.25	100 wt	$ 0.27
2020	1.043	$ 1.1197	1 - 3	0.00	mixing		0.0		0.000 cf	0.00		0.000	0.00		0.00		$ -
					Tot Admixtures >		54.5		0.057 cf	4.03		0.004	0.31	lb	4.15	lb	$ 2.88
Total additional volume added >			0.0000	cf													
Water	1.000	$ 0.0013	gal	Pounds water added =>			288.0	lb	4.69 cf	21.33	lb	0.2944	18.37	lb	288.0	lb	$ 0.04
Design Air =>	4.00	%															
Design Slump =>	8	Inches		Batch Size =>	2.00	cf			1.08 cf			0.08	cf		4.00	%	Air
									Percent Cement Paste >		40		Coarse / Fine Aggregate Ratio		1.11		

Figure 236. Data. Bottom flange repair Concrete Mix 1.

CONCRETE MIX DESIGN								ID #		G3				f_c'	8	ksi	21-Feb-25		
Material Data				Moisture Data				Theoretical Mix Design at SSD						H_2O Adjusted Batch			Final Mix Design at SSD		
Description	SG	Cost Per		% SSD	SGF	% As Is	% Free	Per Cubic Yard				Per Batch		EDV(cf)	Amount		Per Cubic Yard		
3/4" - NWA	2.600	$0.0046	lb	0.60	2.616	0.00	-0.60	0	lb	0.00	cf	0.00	lb	0.00	0.00	lb	0	lb	$ -
1/2" - NWA #7	2.600	$0.0048		0.60	2.616	1.05	0.45	1100		6.74		81.48		0.51	81.85		1100		$ 5.28
3/8" - NWA #89	2.600	$0.0050		0.60	2.616	1.44	0.84	300		1.84		22.22		0.14	22.41		300		$ 1.50
NW Sand	2.680	$0.0054		0.50	2.693	3.49	2.99	1296		7.71		96.00		0.62	98.86		1296		$ 6.97
3/4" - LWA	1.415	$0.0276	lb	6.00	1.500	6.00	0.00	0	lb	0.00	cf	0.00	lb	0.00	0.00	lb	0	lb	$ -
1/2" - LWA	1.440	$0.0276		7.67	1.550	9.27	1.60	0		0.00		0.00		0.00	0.00		0		$ -
3/8" - LWA	1.520	$0.0300		6.00	1.611	6.00	0.00	0		0.00		0.00		0.00	0.00		0		$ -
LW Fines	1.710	$0.0275		5.00	1.796	5.00	0.00	0		0.00		0.00		0.00	0.00		0		$ -
						Tot Aggregate >		2696	lb	16.29	cf	199.70	lb	1.26	203.11	lb	2696	lb	$ 13.75
				% by Wt															
FA - Class C	2.250	$0.0300	lb	16.7		W/CM	0.3200	150	lb	1.07	cf	11.11	lb	0.08	11.11	lb	150	lb	$ 4.50
FA - Class F	2.280	$0.0300		0.0				0		0.00		0.00		0.00	0.00		0		$ -
GGBFS	2.900	$0.0300		0.0		$/CY	54.18	0		0.00		0.00		0.00	0.00		0		$ -
Metakaolin	2.500	$0.0500		0.0				0		0.00		0.00		0.00	0.00		0		$ -
SF - (F 10,000)	2.500	$0.0500		0.0		LB/FT^3	144.0	0		0.00		0.00		0.00	0.00		0		$ -
Type III Cement	3.150	$0.0440	lb	83.3				750	lb	3.82	cf	55.56	lb	0.28	55.56	lb	750	lb	$ 33.00
						Tot Cementitious>		900	lb	4.88	cf	66.67	lb	0.36	66.67	lb	900	lb	$ 37.50
				fl oz / 100 wt															
V2100	1.199	$0.0500	fl oz	2 - 8	3.30	ml added during mixing		29.7	f oz	0.031	cf	2.20	fl oz	0.002	65.06	ml	3.30	fluid oz per 100 wt	$ 1.49
Plastiment XR	1.139	$0.0500		3 - 9	2.50			22.5		0.023	cf	1.67		0.002	49.29		2.50		$ 1.13
AE A	1.043	$0.1197		1/4 - 3	0.25			2.3		0.002	cf	0.17		0.000	4.93		0.25		$ 0.27
2020	1.043	$1.1197		1 - 3	0.00			0.0		0.000	cf	0.00		0.000	0.00		0.00		$ -
Total additional volume added >				0.0000	cf	Tot Admixtures>		54.5		0.057	cf	4.03		0.004	0.31	lb	4.15	lb	$ 2.88
Water	1.000	$0.0013	gal	Pounds water added =>				288.0	lb	4.69	cf	21.33	lb	0.2928	18.27	lb	288.0	lb	$ 0.04
Design Air =>	4.00	%								1.08	cf			0.08	cf		4.00	%	Air
Design Slump =>	8	Inches		Batch Size =>		2.00	cf	Percent Cement Paste >					40	Coarse / Fine Aggregate Ratio					1.11

Figure 237. Data. Bottom flange repair Concrete Mix 2.

CONCRETE MIX DESIGN				ID #	G4		f'_c	8	ksi	9-Apr-25		
Material Data			Moisture Data			Theoretical Mix Design at SSD			H_2O Adjusted Batch		Final Mix Design at SSD	
Description	SG	Cost Per	% SSD	SGF	% As Is	% Free	Per Cubic Yard	Per Batch	EDV(cf)	Amount	Per Cubic Yard	
3/4" - NWA	2.600	$ 0.0046	0.60	2.616	0.00	-0.60	0	0.00	0.00	0.00	0	$ -
1/2" - NWA #7	2.600	$ 0.0048	0.60	2.616	1.36	0.76	1100	81.48	0.51	82.10	1100	$ 5.28
3/8" - NWA #89	2.600	$ 0.0050	0.60	2.616	0.11	-0.49	300	22.22	0.13	22.11	300	$ 1.50
NW Sand	2.680	$ 0.0054	0.50	2.693	3.43	2.93	1296	96.00	0.62	98.80	1296	$ 6.97
3/4" - LWA	1.415	$ 0.0276	6.00	1.500	6.00	0.00	0	0.00	0.00	0.00	0	$ -
1/2" - LWA	1.440	$ 0.0276	7.67	1.550	9.27	1.60	0	0.00	0.00	0.00	0	$ -
3/8" - LWA	1.520	$ 0.0300	6.00	1.611	6.00	0.00	0	0.00	0.00	0.00	0	$ -
LW Fines	1.710	$ 0.0275	5.00	1.796	5.00	0.00	0	0.00	0.00	0.00	0	$ -
					Tot Aggregate >		2696 lb	16.29 cf	199.70 lb	1.26 cf	203.01 lb	2696 lb $ 13.75
			% by Wt									
FA - Class C	2.250	$ 0.0300	16.7		W/CM	0.3200	150	1.07	11.11	0.08	11.11	150 $ 4.50
FA - Class F	2.280	$ 0.0300	0.0				0	0.00	0.00	0.00	0.00	0 $ -
GGBFS	2.900	$ 0.0300 lb	0.0		$/CY	54.18	0 lb	0.00 cf	0.00 lb	0.00	0.00 lb	0 lb $ -
Metakaolin	2.500	$ 0.0500	0.0				0	0.00	0.00	0.00	0.00	0 $ -
SF - (F 10.000)	2.500	$ 0.0500	0.0		LB/FT^3	144.0	0	0.00	0.00	0.00	0.00	0 $ -
Type III Cement	3.150	$ 0.0440 lb	83.3				750 lb	3.82 cf	55.56 lb	0.28	55.56 lb	750 lb $ 33.00
					Tot Cementitious >		900 lb	4.88 cf	66.67 lb	0.36 cf	66.67 lb	900 lb $ 37.50
			fl oz / 100 wt									
V2100	1.199	$ 0.0500	2 - 8	3.30	ml		29.7	0.031 cf	2.20	0.002	65.06	3.30 fluid $ 1.49
Plastiment XR	1.139	$ 0.0500 fl	3 - 9	2.50	added		22.5	0.023 cf	1.67	0.002	49.29	2.50 oz per $ 1.13
AEA	1.043	$ 0.1197 oz	1/4 - 3	0.25	during		2.3 fl	0.002 cf	0.17 fl	0.000	4.93 ml	0.25 100 wt $ 0.27
2020	1.043	$ 1.1197	1 - 3	0.00	mixing		0.0 oz	0.000 cf	0.00 oz	0.000	0.00	0.00 $ -
					Tot Admixtures >		54.5	0.057 cf	4.03	0.004	0.31 lb	4.15 lb $ 2.88
Total additional volume added >			0.0000	cf								
Water	1.000	$ 0.0013 gal	Pounds water added =>				288.0 lb	4.69 cf	21.33 lb	0.2944	18.37 lb	288.0 lb $ 0.04
Design Air =>	4.00	%						1.08 cf		0.08	cf	4.00 % Air
Design Slump =>	8	Inches	Batch Size =>	2.00	cf		Percent Cement Paste >		40	Coarse / Fine Aggregate Ratio		1.11

Figure 238. Data. Bottom flange repair Concrete Mix 3

Concrete Cylinder Data	Molded on Friday February 21 @am						
	Name	Diameter (in)	Area (in^2)	Max Load (lbf)	Strength (psi)	**AVG Strength (psi)**	
3 DAY	SCC-G3-B1-1	4	12.57	85489	6803	**6803**	24-Feb
	SCC-G3-B1-2	4	12.57				
	SCC-G3-B1-3	4	12.57				
28 DAY	SCC-G3-B1-1	4	12.57	130910	10417	**10357**	21-Mar
	SCC-G3-B1-2	4	12.57	129676	10319		
	SCC-G3-B1-3	4	12.57	129851	10333		
TEST DAY	SCC-G3-B1-1	4	12.57	139406	11094	**11431**	17-Jun
	SCC-G3-B1-2	4	12.57	143475	11417		
	SCC-G3-B1-3	4	12.57	148064	11783		
Concrete Cylinder Data	Molded on Friday February 21 @am						
	Name	Diameter (in)	Area (in^2)	Max Load (lbf)	Strength (psi)	**AVG Strength (psi)**	
28 DAY	SCC-G3-B2-1	4	12.57	125998	10027	**9757**	21-Mar
	SCC-G3-B2-2	4	12.57	117687	9365		
	SCC-G3-B2-3	4	12.57	124160	9880		
TEST DAY	SCC-G3-B2-1	4	12.57	139658	11114	**10448**	17-Jun
	SCC-G3-B2-2	4	12.57	123468	9825		
	SCC-G3-B2-3	4	12.57	130762	10406		
Concrete Cylinder Data	Molded on Friday February 21 @am						
	Name	Diameter (in)	Area (in^2)	Max Load (lbf)	Strength (psi)	**AVG Strength (psi)**	
28 DAY	SCC-G3-B3-1	4	12.57	129426	10299	**10279**	21-Mar
	SCC-G3-B3-2	4	12.57	133078	10590		
	SCC-G3-B3-3	4	12.57	124999	9947		
TEST DAY	SCC-G3-B3-1	4	12.57	139809	11126	**10818**	19-Jun
	SCC-G3-B3-2	4	12.57	131473	10462		
	SCC-G3-B3-3	4	12.57	136536	10865		
Concrete Cylinder Data	Molded on Friday February 21 @am						
	Name	Diameter (in)	Area (in^2)	Max Load (lbf)	Strength (psi)	**AVG Strength (psi)**	
28 DAY	SCC-G3-B4-1	4	12.57	114825	9138	**11040**	21-Mar
	SCC-G3-B4-2	4	12.57	154086	12262		
	SCC-G3-B4-3	4	12.57	147269	11719		
TEST DAY	SCC-G3-B4-1	4	12.57	168124	13379	**13281**	19-Jun
	SCC-G3-B4-2	4	12.57	165738	13189		
	SCC-G3-B4-3	4	12.57	166836	13276		
Concrete Cylinder Data	Molded on Friday February 21 @am						
	Name	Diameter (in)	Area (in^2)	Max Load (lbf)	Strength (psi)	**AVG Strength (psi)**	
28 DAY	SCC-G3-B5-1	4	12.57	137180	10916	**10916**	21-Mar
TEST DAY	SCC-G3-B5-1	4	12.57	132039	10507	**10507**	18-Jun

Figure 239. Data. Bottom flange repair Concrete Strength 1.

Concrete Cylinder Data	Molded on Thursday April 17 @11am					
	Name	Diameter (in)	Area (in^2)	Max Load (lbf)	Strength (psi)	**AVG Strength (psi)**	
24-Hour	SCC-G4-B1-1	4	12.57	89177	7097	**7097**	18-Apr
6 DAY	SCC-G4-B1-1	4	12.57	124400	9899	**9974**	23-Apr
	SCC-G4-B1-2			128902	10258		
	SCC-G4-B1-3			122706	9765		
28 DAY	SCC-G4-B1-1	4	12.57	149045	11861	**11725**	15-May
	SCC-G4-B1-2	4	12.57	145317	11564		
	SCC-G4-B1-3	4	12.57	147660	11750		
TEST DAY	SCC-G4-B1-1	4	12.57	159520	12694	**12602**	24-Jun
	SCC-G4-B1-2	4	12.57	157342	12521		
	SCC-G4-B1-3	4	12.57	158226	12591		
Concrete Cylinder Data	Molded on Thursday April 17 @11am					
	Name	Diameter (in)	Area (in^2)	Max Load (lbf)	Strength (psi)	**AVG Strength (psi)**	
24-Hour	SCC-G4-B2-1	4	12.57	73676	5863	**5863**	18-Apr
6 DAY	SCC-G4-B2-1	4	12.57	104404	8308	**8181**	23-Apr
	SCC-G4-B2-2			105971	8433		
	SCC-G4-B2-3			98056	7803		
28 DAY	SCC-G4-B2-1	4	12.57	127118	10116	**9792**	15-May
	SCC-G4-B2-2	4	12.57	125771	10009		
	SCC-G4-B2-3	4	12.57	116263	9252		
TEST DAY	SCC-G4-B2-1	4	12.57	134367	10693	**11005**	24-Jun
	SCC-G4-B2-2	4	12.57	143744	11439		
	SCC-G4-B2-3	4	12.57	136781	10885		
Concrete Cylinder Data	Molded on Friday May 9 @11am					
	Name	Diameter (in)	Area (in^2)	Max Load (lbf)	Strength (psi)	**AVG Strength (psi)**	
4 DAY	SCC-G1-B1-1	4	12.57	110999	8833	**8677**	13-May
				106290	8458		
				109837	8741		
28 DAY	SCC-G1-B1-1	4	12.57	135396	10774	**10533**	6-Jun
	SCC-G1-B1-2	4	12.57	127521	10148		
	SCC-G1-B1-3	4	12.57	134180	10678		
TEST DAY	SCC-G1-B1-1	4	12.57	145627	11589	**11488**	8-Jul
	SCC-G1-B1-2	4	12.57	145655	11591		
	SCC-G1-B1-3	4	12.57	141821	11286		

Figure 240. Data. Bottom flange repair Concrete Strength 2.

Bottom Flange Repairs (SCC MIX)			
Girder	Repair	Batch	Spread, in
1	1.1LBZ	1	28.00
3	3.1LBF	1	12.50
	3.3LBF	2	21.75
	3.1RBF	3	18.50
	3.3RBF	4	27.00
	3.2RBF	5	29.75
4	4.1LBZ	1	28.00
	4.2LBZ	2	28.00

Figure 241. Data. Bottom flange repair Concrete Slump.

APPENDIX G. GIRDER 1 CALCULATIONS

GDOT Girders: Conforming BT-54 Composite Capacity (Theoretical) Calculations

Variables: **Ana Contreras**

$f_c := 14342$ *girder concrete compressive strength (at time of test)*

$f_{ci} := 9715$ *girder concrete compressive strength (at time of strand release, per SCP)*

$A := 659\ in^2$ *girder cross-sectional area*

$I := 268077\ in^4$ *girder moment of inertia*

$E_c := 57 \cdot \sqrt{f_c} \cdot ksi = 6826.21\ ksi$ *girder modulus of elasticity*

$L := 45.5\ ft$ *girder length*

$h := 54\ in$ *girder height*

$C_b := -27.63\ in$ *girder lower neutral axis distance*

$C_t := h + C_b = 26.37\ in$ *girder upper neutral axis distance*

$S_b := \frac{I}{-C_b} = 9702.39\ in^3$ *girder bottom section modulus*

$S_t := \frac{I}{C_t} = 10165.98\ in^3$ *girder top section modulus*

$e := -19.99\ in$ *girder eccentricity (14 bottom strands, 4 top strands)*

$A_s := 0.217\ in^2$ *strand cross-sectional area (one strand)*

$\#strands := 14$ *number of strands (excluding top 4 strands)*

$A_{ps} := \#strands \cdot A_s = 3.04\ in^2$ *strand total area of steel*

$f_{pu} := 270\ ksi$ *strand ultimate prestressing stress*

$f_y := 0.9 \cdot f_{pu} = 243\ ksi$ *strand yielding prestressing stress (assumed)*

$E_{ps} := 28700\ ksi$ *strand modulus of elasticity*

$F_{se} := 0.75 \cdot f_{pu} \cdot A_s = 43.94\ kip$ *strand effective force (75%)*

Variables:

$f_{cdeck} := 0$ *deck concrete compressive strength (at time of test)*

$h_f := 0$ *deck thickness (no deck for girder 1)*

$E_{cdeck} := 57 \cdot \sqrt{f_{cdeck}} \cdot ksi = 0\ ksi$ *MOE of deck*

$E_{cbeam} := 57 \cdot \sqrt{f_c} \cdot ksi = 6826.21\ ksi$ *MOE of beam*

$\eta := \frac{E_{cdeck}}{E_{cbeam}} = 0$ *modular ratio*

$b_{e1} := \eta \cdot 6\ ft = 0\ ft$ *deck effective width 6-ft (transformed to match strength of beam)*

$A_{deck1} := b_{e1} \cdot h_f = 0\ \frac{1}{ft} \cdot in^2$ *deck cross-sectional area, 8-inch thick section (transformed)*

$b_{e2} := \eta \cdot 42\ in = 0\ in$ *deck effective width 42-inch (transformed to match strength of beam)*

$A_{deck2} := b_{e2} \cdot 1.5\ in = 0\ in^2$ *deck cross-sectional area, 1.5-inch thick section (transformed)*

$\lambda := 1$

$f_r := 7.5 \cdot \lambda \cdot \sqrt{f_c} \cdot psi = 0.9\ ksi$ *rupture stress*

$w := 150\ pcf \cdot A = 686.46\ \frac{lbf}{ft}$ *girder self-weight*

$M_w := \frac{w \cdot L^2}{8} = 177.64\ kip \cdot ft$ *girder self-weight moment*

$w_{deck} := 0\ \frac{lbf}{ft}$ *deck self-weight*

$M_{SD} := \frac{w_{deck} \cdot L^2}{8} = 0\ kip \cdot ft$ *deck self-weight moment*

Variables:

$L_c := L - 14\ in = 44.33\ ft$ *clear distance between end roller supports*

$L_{spr} := 48\ in$ *distance between two point loads (spreader beam roller supports clear distance)*

Test 1.1: $P_{max1} := 450\ kip$

$x_1 := 80.5\ in - 7\ in = 73.5\ in$ *distance from point load to end of beam*

$a_1 := x_1 - \frac{L_{spr}}{2} = 4.13\ ft$

$a_1 = 49.5\ in$ *clear distance from center of north bearing to first point load*

$b_1 := L_c - a_1 - L_{spr} = 36.21\ ft$

$b_1 = 434.5\ in$ *clear distance from center of south bearing to second point load*

Composite Properties Calculations:

Bottom neutral axis distance of composite section

$C_b' := C_b = -27.63\ \textbf{in}$

Top neutral axis distance of composite section

$C_t' := C_t = 26.37\ \textbf{in}$

Moment of inertia of composite section

$I_c' := I = 268077\ \textbf{in}^4$

Cross-sectional area of composite section

$A_c' := A = 659\ \textbf{in}^2$

Radius of gyration of composite section

$r := \sqrt{\frac{I_c'}{A_c'}} = 20.17\ \textbf{in}$ $\qquad r^2 = 406.79\ \textbf{in}^2$

Losses Calculations BT-54 (1/3)

Losses Before Release (10 May 2025)

$f_{pJ} := 0.75 \cdot f_{pu} = 202.5$ ksi

$F_J := f_{pJ} \cdot \#strands \cdot A_s + 40$ kip $= 655.2$ kip total force in all 14 strands (plus 4 top strands @ 10 kips each) at time of tension

Relaxation in Strand, R1 (10 May 2024 to 15 May 2024)

$t1 := 1$ $t2 := 120$ $f_{pi}' := f_{pJ} = 202.5$ ksi

$\Delta f_p R1 := f_{pi}' \cdot \left(\frac{\log(t2) - \log(t1)}{45} \right) \cdot \left(\frac{f_{pi}'}{f_y} - 0.55 \right) = 2.65$ ksi

Losses Just After Release (15 May 2024)

$F_i := \left(f_{pJ} - \Delta f_p R1 \right) \cdot \#strands \cdot A_s = 607.14$ kip

$F_j := 0.9 \cdot F_i = 546.43$ kip *assumed 0.9*

Elastic Shortening in Strand, ES (15 May 2025)

$E_{ps} = 28700$ ksi $f_{ci} = 9715$ $E_{ci} := 57000 \cdot \sqrt{f_{ci}} \cdot psi = 5618.19$ ksi

$\eta_i := \frac{E_{ps}}{E_{ci}} = 5.11$

$f_{cs} := \frac{-F_j}{A} - \frac{F_j \cdot e^2}{I} - \frac{M_w \cdot e}{I} = -1.48$ ksi

$\Delta f_p ES := -\eta_i \cdot f_{cs} = 7.58$ ksi

Losses Calculations BT-54 (2/3)

Losses After ~14 Months (7 July 2025) Note: no deck casted

Creep, CR (15 May 2024 to 7 July 2025)

$K_{cr} := 2$ *for pretensioned members*

$f_{pj} := f_{pJ} - \Delta f_p R1 - \Delta f_p ES = 192.26$ ***ksi***

$P_j := f_{pj} \cdot \#strands \cdot A_s = 584.1$ ***kip***

$f_{cs} := \frac{-P_j}{A} - \frac{P_j \cdot e^2}{I} - \frac{M_w \cdot e}{I} = -1.6$ ***ksi***

$f_{csd} := \frac{-M_{SD} \cdot C_b'}{I_c'} = 0$ ***ksi***

$\Delta f_p CR := 0.80 \left(-K_{cr} \cdot \frac{E_{ps}}{E_c} \left(f_{cs} - f_{csd} \right) \right) = 10.75$ ***ksi*** Note: only 80% of total CR because of 405 day age

Shrinkage, SH (15 May 2024 to 7 July 2025)

$RH := 70$ *relative humidity in Atlanta, GA*

$K_{SH} := 1$ *for pretensioned members*

$V := A \cdot L = 359814$ ***in***^{3} *volume of girder*

$S := 2 \cdot A + 2 \cdot h \cdot L + 26$ ***in*** $\cdot L + 42$ ***in*** $\cdot L = 97414$ ***in***^{2} *approximate surface area of girder*

$\varepsilon_{SH} := 8.2 \cdot 10^{-6} \cdot K_{SH} \cdot \left(1 - \frac{0.06}{in} \cdot \frac{V}{S} \right) (100 - RH) = 0.0001915$

$\Delta f_p SH := \varepsilon_{SH} \cdot E_{ps} = 5.5$ ***ksi***

Relaxation in Strand, R2 (15 May 2024 to 7 July 2025)

$t2 = 120$ $t3 := 10056$ $f_{pi} := f_{pj} = 192.26$ ***ksi***

$\Delta f_p R2 := f_{pi}' \cdot \left(\frac{\log(t3) - \log(t2)}{45} \right) \cdot \left(\frac{f_{pi}'}{f_y} - 0.55 \right) = 1.98$ ***ksi***

Losses Calculations BT-54 (3/3)

Effective Force in Prestress (after losses) 7 July 2025 Test Day

$F_e := \left(f_{pJ} - \Delta f_pR1 - \Delta f_pR2 - \Delta f_pES - \Delta f_pCR - \Delta f_pSH\right) \cdot \#strands \cdot A_s = 528.72$ ***kip***

$Losses := \left(1 - \frac{F_e}{F_J}\right) \cdot 100 = 19.3$ *loss percentage*

$F_{el} := \left(f_{pJ} \cdot \left(1 - \frac{1}{Losses}\right)\right) \cdot A_s = 41.67$ ***kip*** *effective force in individual strand*

$f_{se} := f_{pJ} \cdot \left(1 - \frac{Losses}{100}\right) = 163.41$ ***ksi***

Initial Beam Curvature (1/2):

Curvature due to beam prestress: (negative)

$f_{pe} := f_{se} = 163.41$ **ksi** *refined through previous losses calculations*

$CGS := -C_b + e = 7.64$ **in** *finding CGS from bottom beam*

$\varepsilon_{bi} := \frac{-f_{pe}}{E_{ps}} = -0.0056938$ *strain at CGS due to prestress*

$\varepsilon_{ti} := \frac{\varepsilon_{bi} \cdot C_t}{-e + C_t} = -0.003239$ *strain at top of beam due to prestress*

$h_i := h - CGS = 46.36$ **in** *distance between top of beam and CGS*

$\phi_i := \frac{\varepsilon_{bi} + \varepsilon_{ti}}{h} = -0.0001654 \ \frac{1}{\text{in}}$ *initial (negative) curvature in beam due to prestress*

Initial Beam Curvature (2/2):

Test 1.1:
Curvature due to beam SW: (negative)

$M_{w1} := \frac{w \cdot x_1}{2} \left(L_c - x_1\right) = 80.32\ \textit{kip} \cdot \textit{ft}$ *moment due to beam SW at test location*

$f_{swb1} := \frac{-M_{w1} \cdot e}{I} = 71.88\ \textit{psi}$ *stress at CGS due to beam SW*

$\varepsilon_{swb1} := \frac{f_{swb1}}{E_c} = 0.00001053$ *strain at CGS due to beam SW*

$f_{swt1} := \frac{M_{w1} \cdot C_t}{I} = 94.82\ \textit{psi}$ *stress at top of beam due to beam SW*

$\varepsilon_{swt1} := \frac{f_{swt1}}{E_c} = 0.00001389$ *strain at top of beam due to beam SW*

$h_1 := h - CGS = 46.36\ \textit{in}$ *distance between top of beam and CGS*

$\phi_{1b} := \frac{\varepsilon_{swb1} + \varepsilon_{swt1}}{h_1} = 0.0000005\ \frac{1}{\textit{in}}$ *initial (positive) curvature in beam due to beam SW*

Curvature due to deck SW: (positive)

$M_{SD1} := \frac{w_{deck} \cdot x_1}{2} \left(L_c - x_1\right) = 0\ \textit{kip} \cdot \textit{ft}$ *moment due to deck SW at test location*

$f_{deckswb1} := \frac{-M_{SD1} \cdot e}{I} = 0\ \textit{psi}$ *stress at CGS due to deck SW*

$\varepsilon_{deckswb1} := \frac{f_{deckswb1}}{E_c} = 0$ *strain at CGS due to deck SW*

$f_{deckswt1} := \frac{M_{SD1} \cdot C_t}{I} = 0\ \textit{psi}$ *stress at top of beam due to deck SW*

$\varepsilon_{deckswt1} := \frac{f_{deckswt1}}{E_c} = 0$ *strain at top of beam due to deck SW*

$h_1 = 46.36\ \textit{in}$ *distance between top of beam and CGS*

$\phi_{1d} := \frac{\varepsilon_{deckswb1} + \varepsilon_{deckswt1}}{h_1} = 0\ \frac{1}{\textit{in}}$ *initial (positive) curvature in beam due to deck SW*

$\phi_{initial1} := \phi_{1b} + \phi_{1d} + \phi_i = -0.00016489\ \frac{1}{\textit{in}}$ *total initial (negative) curvature in composite beam prior to Test 2.1*

Cracking Moment:

$$M_{cr} := \frac{f_r \cdot I_c'}{C_b'} = -726.21 \ \textit{kip} \cdot \textit{ft}$$

$$\phi_{cr} := \frac{M_{cr}}{E_c \cdot I_c'} = -0.000004762 \ \frac{1}{\textit{in}}$$

$$M_{cr95} := 0.95 \cdot M_{cr} = -689.9 \ \textit{kip} \cdot \textit{ft}$$

$$\phi_{cr95} := 0.95 \cdot \phi_{cr} = -0.000004524 \ \frac{1}{\textit{in}}$$

Ultimate Moment (1/2):
Test 1.1:

$\varepsilon_{si1} := 0.000656$ *strain measured from test (input)*

$d_1 := h - 2.5\ \textit{in} = 51.5\ \textit{in}$ *depth to centroid of strands from top of composite girder*

$c_1 := 9.3595\ \textit{in}$ *trial and error iterative c value (input until equilibrium)*

$\varepsilon_{s1.1} := -\varepsilon_{bi} + \varepsilon_{si1} = 0.00635$ *strain in lowest strand level at ultimate (test + effective prestress)*

$$\varepsilon_{s2.1} := \frac{\varepsilon_{s1.1} \cdot (d_1 - 2\ \textit{in} - c_1)}{d_1 - c_1} = 0.00605$$ *strain in 2nd strand level at ultimate*

$$\varepsilon_{s3.1} := \frac{\varepsilon_{s1.1} \cdot (d_1 - 12\ \textit{in} - c_1)}{d_1 - c_1} = 0.00454$$ *strain in 3rd strand level at ultimate*

$$\varepsilon_{s4.1} := \frac{\varepsilon_{s1.1} \cdot (d_1 - 49.5\ \textit{in} - c_1)}{d_1 - c_1} = -0.0011089393$$ *strain in top strand level at ultimate*

$$\varepsilon_{c1.1} := \frac{\varepsilon_{si1} \cdot c_1}{d_1 - c_1} = 0.00015$$ *strain at top of top flange at ultimate*

$$\varepsilon_{c2.1} := \frac{\varepsilon_{si1} \cdot (c_1 - 4.5\ \textit{in})}{d_1 - c_1} = 0.0000756477$$ *strain at top of web at ultimate*

$T_{1.1} := 8 \cdot A_s \cdot \varepsilon_{s1.1} \cdot E_{ps} = 316.37\ \textit{kip}$ *tension force from lowest strand level*

$T_{2.1} := 4 \cdot A_s \cdot \varepsilon_{s2.1} \cdot E_{ps} = 150.68\ \textit{kip}$ *tension force from 2nd strand level*

$T_{3.1} := 2 \cdot A_s \cdot \varepsilon_{s3.1} \cdot E_{ps} = 56.57\ \textit{kip}$ *tension force from 3rd strand level*

$\mathbf{T_{4.1}} := \text{if}\left(c_1 > 2.5\ \textit{in}, 0\ \textit{kip}, \left(2 \cdot A_s \cdot \varepsilon_{s4.1} \cdot E_{ps}\right)\right) = 0\ \textit{kip}$

$T_{t1} := T_{1.1} + T_{2.1} + T_{3.1} + \mathbf{T_{4.1}} = 523.61\ \textit{kip}$ *total tension force from prestress*

Ultimate Moment (2/2):

Test 1.1:

$$C_{1.1} := \begin{cases} \text{if } c_1 < 4.5\ \textit{in} \\ \quad \dfrac{\left(\varepsilon_{c1.1}\right) \cdot E_c}{2} \cdot c_1 \cdot 72\ \textit{in} \\ \text{else} \\ \quad \dfrac{\left(\varepsilon_{c1.1} + \varepsilon_{c2.1}\right) \cdot E_c}{2} \cdot c_1 \cdot 72\ \textit{in} \end{cases} = 509.11\ \textit{kip}$$

compression force from 4.5-inch top flange

$$C_{2.1} := \begin{cases} \text{if } c_1 \leq 4.5\ \textit{in} \\ \quad 0\ \textit{kip} \\ \text{else} \\ \quad \dfrac{\left(\varepsilon_{c2.1}\right) \cdot E_c}{2} \cdot c_1 \cdot 6\ \textit{in} \end{cases} = 14.5\ \textit{kip}$$

compression force from web

$$C_{t1} := C_{1.1} + C_{2.1} = 523.61\ \textit{kip}$$

compression force from concrete

$$T_{t1} - C_{t1} = 0.006803\ \textit{kip}$$

equilibrium of forces must = 0 to find c

$$J_{d1} := 63.5\ \textit{in} - \left(\frac{T_{1.1} \cdot 2.5\ \textit{in} + T_{2.1} \cdot 4.5\ \textit{in} + T_{3.1} \cdot 14.5\ \textit{in} + \mathbf{T_{4.1}} \cdot 51.5\ \textit{in}}{T_{t1}} \right) - \frac{c_1}{3} = 56.01\ \textit{in}$$

$$M_{ult1.1} := A_{ps} \cdot \varepsilon_{s1.1} \cdot E_{ps} \cdot \left(J_{d1}\right) = 2584.04\ \textit{kip} \cdot \textit{ft}$$

$$\phi_{ult1.1} := \frac{\varepsilon_{c1.1}}{c_1} = 0.0000156\ \frac{1}{\textit{in}}$$

Theoretical Moment-Curvature Overview:

$M_{cr} = -726.21\ kip \cdot ft$

$\phi_{cr} = -0.000004762\ \frac{1}{in}$

$M_{ult1.1} = 2584.04\ kip \cdot ft$

$\phi_{ult1.1} = 0.000016\ \frac{1}{in}$

Ultimate Loads from Moment Calculations: (four-point bending tests)

Test 1.1:

$a_1 = 4.13\ ft$

$b_1 = 36.21\ ft$

$P_{ult1m} := 2 \cdot \frac{L_c \cdot M_{ult1.1}}{b_1 \cdot (a_1 + L_c - b_1)} = 516.55\ kip$ *ultimate load based on moment capacity*

Theoretical Strut and Tie Cracking Capacity: (1/1) (AASHTO C5.8.2.2-1)

$d := 54\ in + 9.5\ in = 63.5\ in$

$b_w := 6\ in$

$V_{crl} := \left(0.2 - 0.1\left(\frac{a_1}{d}\right)\right) \cdot \sqrt{\frac{f_c}{1000}} \cdot ksi \cdot b_w \cdot d = 176.1\ kip$

Shear Capacity: (1/3)

Prestress Transfer/Development Lengths:

$d_b := 0.6\ in$ *diameter of prestressing strand*

$L_{tr} := min\left(50 \cdot d_b, \left(\frac{f_{pe}}{3000\ psi}\right) \cdot d_b\right) = 30\ in$ *transfer length*

$f_{ps} := \varepsilon_{s1.1} \cdot E_{ps} = 182.24\ ksi$

$L_f := \left(\frac{f_{ps} - f_{pe}}{1000\ psi}\right) \cdot d_b = 11.3\ in$

$L_d := L_{tr} + L_f = 3.44\ ft$ *development length*

V_c **calculation:**

Minimum V_{ci} calculation:

$d_p := \max\left(h - CGS, 0.8\ (h)\right) = 46.36\ in$ *distance from CGS to max compression fiber*

$f_{ce} := f_{pe} = 163.41\ ksi$ *effective prestress stress*

$b_w := 6\ in$ *web width*

$d := d_p = 46.36\ in$ *distance from CGS to max compression fiber*

$f_y := 60\ ksi$ *yield strength of non-prestressed reinforcement*

$A_s := 0.31\ in^2$ *area of non-prestressed longitudinal reinforcement*

$A_{ps} \cdot f_{pe} = 496.44\ kip > 0.4\ \left(A_{ps} \cdot f_{pu} + A_s \cdot f_y\right) = 335.54\ kip$ *ACI 318-19 [22.5.6.3.1]*

$V_{ci} := 2 \cdot \lambda \cdot \sqrt{f_c \cdot psi} \cdot b_w \cdot d = 66.62\ kip$ *flexure-shear strength ACI 318-19 [22.5.6.3.1c]*

V_{cw} calculation:

$f_{pc} := \frac{F_e}{A} = 802.31\ psi$ *compressive stress in concrete at centroid of composite section due to prestress*

$V_{cw} := \left(3.5\ \lambda \cdot \sqrt{f_c \cdot psi} + 0.3\ f_{pc}\right)\ b_w \cdot d_p = 183.54\ kip$ *web-shear strength*

Shear Capacity: (2/3)

V_{ci} calculation Test 1: (using max load from testing)

$a_1 = 49.5\ in$
$b_1 = 434.5\ in$
$x_1 := x_1 - 7\ in = 66.5\ in$

$P_{max1} = 450\ kip$

$V_{d1} := \text{abs}\left(\left(w + w_{deck}\right)\left(\frac{L_c}{2} - x_1\right)\right) = 11.41\ kip$ *shear due to DL (uniform SW beam and SW deck)*

$V_{u1} := \left(\frac{\left(\frac{P_{max1}}{2}\right)}{L_c} \cdot \left(L_c - a_1 + b_1\right)\right) = 387.83\ kip$ *shear due to ultimate load (from test)*

$V_{i1} := V_{u1} - V_{d1} = 376.42\ kip$

$M_{u1} := \frac{\left(\frac{P_{max1}}{2}\right)}{L} \cdot \left(L_c - b_1 + a_1\right) \cdot b_1 = 2193.39\ kip \cdot ft$ *moment due to ultimate load (from test)*

$M_{d1} := \frac{\left(w + w_{deck}\right) \cdot x_1}{2}\left(L_c - x_1\right) = 73.78\ kip \cdot ft$ *moment due to DL (uniform SW beam and SW deck)*

$M_{max1} := M_{u1} - M_{d1} = 2119.61\ kip \cdot ft$

$f_{d1} := \frac{M_{d1} \cdot C_b'}{I_c'} = -91.26\ psi$

$f_{pec} := \frac{F_e}{A_c'} - \frac{F_e \cdot e \cdot C_b'}{I_c'} = -0.29\ ksi$

$M_{cre1} := \left(\frac{I_c'}{C_t'}\right)\left(6\ \lambda \cdot \sqrt{f_c} \cdot psi + f_{pec} - f_{d1}\right) = 442.88\ kip \cdot ft$

$V_{ci1} := 0.6\ \lambda \cdot \sqrt{f_c} \cdot psi \cdot b_w \cdot d_p + V_{d1} + \frac{V_{i1} \cdot M_{cre1}}{M_{max1}} = 110.05\ kip$

$V_{c1} := min\left(V_{cw}, V_{ci1}\right) = 110.05\ kip$ *nominal shear strength provided by concrete for Test 1*

Shear Capacity: (3/3)

V_{se} calculation: (for tests near ends 24-in < x < 144-in)

$s_e := 12\ \textbf{in}$ *spacing for #5 stirrups for 24-in < x < 144-in*

$A_v := 2 \cdot (A_s) = 0.62\ \textbf{in}^2$ *area of shear reinforcement (2#5 bars)*

$V_{se} := \frac{A_s \cdot f_y \cdot d}{s_e} = 71.86\ \textbf{kip}$ *nominal shear strength provided by shear reinforcement (for tests near end)*

V_{sm} calculation: (for tests near midspan 144-in < x < 402-in)

$s_m := 16\ \textbf{in}$ *spacing for #5 stirrups for 144-in < x < 402-in*

$A_v = 0.62\ \textbf{in}^2$ *area of shear reinforcement (2#5 bars)*

$V_{sm} := \frac{A_v \cdot f_y \cdot d}{s_m} = 107.79\ \textbf{kip}$ *nominal shear strength provided by shear reinforcement (for tests near midspan)*

V_n **nominal one-way shear capacity:**

$V_{n1} := V_{c1} + V_{se} = 181.91\ \textbf{kip}$ *nominal shear capacity for Test 1 North end*

Ultimate Loads from Shear Calculations: (four-point bending tests)

Test 1.1:

$a_1 = 4.13\ ft$

$b_1 = 36.21\ ft$

$P_{ult1v} := 2 \cdot \frac{V_{n1} \cdot L_c}{\langle L_c - a_1 + b_1 \rangle} = 211.07\ kip$ *ultimate load based on shear capacity*

Failure Mode Based on Comparing Maximum Load to Maximum Theoretical Capacities:

Test 1 (Shear):

Experimental Maximum Load: $P_{max1} = 450$ ***kip***

Theoretical Maximum Load (Flexure): $P_{ult1m} = 516.55$ ***kip***

Theoretical Maximum Load (Shear): $P_{ult1v} = 211.07$ ***kip***

$x_1 = 66.5$ ***in***

Top Flange Capacity Calculation:

Top Flange Repair: (within 12-ft of either girder end)

$A_{stfr} := 4 \cdot 0.11\ in^2 = 0\ ft^2$

$d := 2.5\ in$

$f_c = 14342$

$f_y = 60\ ksi$

$$a := \frac{A_{stfr} \cdot f_y}{0.85 \cdot f_c \cdot psi \cdot 12\ in} = 0.18\ in$$

$M_{ntfr} := A_{stfr} \cdot f_y \cdot \left(d - \frac{a}{2}\right) = 5.3\ kip \cdot ft$ *moment capacity per foot of top flange repair*

$M_{ntfr6} := 6 \cdot M_{ntfr} = 31.81\ kip \cdot ft$ *moment capacity of 6-ft top flange repair*

$M_{ntfr10} := 10 \cdot M_{ntfr} = 53.01\ kip \cdot ft$ *moment capacity of 10-ft top flange repair*

$$P_{ntfr6} := \frac{M_{ntfr6}}{13\ in} = 29.36\ kip$$ *ultimate load of 6-ft top flange repair*

$$P_{ntfr10} := \frac{M_{ntfr10}}{13\ in} = 48.94\ kip$$ *ultimate load of 10-ft top flange repair*

Original Top Flange: (within 12-ft of either girder end)

$A_{stf} := 2 \cdot 0.11\ in^2 = 0.22\ in^2$

$d = 2.5\ in$

$f_c = 14342$

$f_y = 60\ ksi$

$$a := \frac{A_{stf} \cdot f_y}{0.85 \cdot f_c \cdot psi \cdot 12\ in} = 0.09\ in$$

$M_{ntf} := A_{stf} \cdot f_y \cdot \left(d - \frac{a}{2}\right) = 2.7\ kip \cdot ft$ *moment capacity per foot of original top flange*

$M_{ntf6} := 6 \cdot M_{ntf} = 16.2\ kip \cdot ft$ *moment capacity of 6-ft top flange repair*

$M_{ntf10} := 10 \cdot M_{ntf} = 27\ kip \cdot ft$ *moment capacity of 10-ft top flange repair*

$$P_{ntf6} := \frac{M_{ntf6}}{13\ in} = 14.96\ kip$$ *ultimate load of 6-ft original top flange section*

$$P_{ntf10} := \frac{M_{ntf10}}{13\ in} = 24.93\ kip$$ *ultimate load of 10-ft original top flange section*

APPENDIX H. GIRDER 2 CALCULATIONS

GDOT Girders: Conforming BT-54 Composite Capacity (Theoretical) Calculations

Variables: **Ana Contreras**

$f_c := 14475$ *girder concrete compressive strength (at time of test)*

$f_{ci} := 9850$ *girder concrete compressive strength (at time of strand release, per SCP)*

$A := 659\ in^2$ *girder cross-sectional area*

$I := 268077\ in^4$ *girder moment of inertia*

$E_c := 57 \cdot \sqrt{f_c} \cdot ksi = 6857.79\ ksi$ *girder modulus of elasticity*

$L := 45.5\ ft$ *girder length*

$h := 54\ in$ *girder height*

$C_b := -27.63\ in$ *girder lower neutral axis distance*

$C_t := h + C_b = 26.37\ in$ *girder upper neutral axis distance*

$S_b := \frac{I}{-C_b} = 9702.39\ in^3$ *girder bottom section modulus*

$S_t := \frac{I}{C_t} = 10165.98\ in^3$ *girder top section modulus*

$e := -19.99\ in$ *girder eccentricity (14 bottom strands, 4 top strands)*

$A_s := 0.217\ in^2$ *strand cross-sectional area (one strand)*

$\#strands := 14$ *number of strands (excluding top 4 strands)*

$A_{ps} := \#strands \cdot A_s = 3.04\ in^2$ *strand total area of steel*

$f_{pu} := 270\ ksi$ *strand ultimate prestressing stress*

$f_y := 0.9 \cdot f_{pu} = 243\ ksi$ *strand yielding prestressing stress (assumed)*

$E_{ps} := 28700\ ksi$ *strand modulus of elasticity*

$F_{se} := 0.75 \cdot f_{pu} \cdot A_s = 43.94\ kip$ *strand effective force (75%)*

Variables:

$f_{cdeck} := 9760$ *deck concrete compressive strength (at time of test)*

$h_f := 8\ in$ *deck thickness (not including extra 1.5 inch chamfer)*

$E_{cdeck} := 57 \cdot \sqrt{f_{cdeck}} \cdot ksi = 5631.18\ ksi$ *MOE of deck*

$E_{cbeam} := 57 \cdot \sqrt{f_c} \cdot ksi = 6857.79\ ksi$ *MOE of beam*

$\eta := \frac{E_{cdeck}}{E_{cbeam}} = 0.82$ *modular ratio*

$b_{e1} := \eta \cdot 6\ ft = 4.93\ ft$ *deck effective width 6-ft (transformed to match strength of beam)*

$A_{deck1} := b_{e1} \cdot h_f = 472.97\ in^2$ *deck cross-sectional area, 8-inch thick section (transformed)*

$b_{e2} := \eta \cdot 42\ in = 34.49\ in$ *deck effective width 42-inch (transformed to match strength of beam)*

$A_{deck2} := b_{e2} \cdot 1.5\ in = 51.73\ in^2$ *deck cross-sectional area, 1.5-inch thick section (transformed)*

$\lambda := 1$

$f_r := 7.5 \cdot \lambda \cdot \sqrt{f_c} \cdot psi = 0.9\ ksi$ *rupture stress*

$w := 150\ pcf \cdot A = 686.46\ \frac{lbf}{ft}$ *girder self-weight*

$M_w := \frac{w \cdot L^2}{8} = 177.64\ kip \cdot ft$ *girder self-weight moment*

$w_{deck} := 150\ pcf \cdot ((6\ ft \cdot 8\ in) + (42\ in \cdot 1.5\ in)) = 665.63\ \frac{lbf}{ft}$ *deck self-weight*

$M_{SD} := \frac{w_{deck} \cdot L^2}{8} = 172.25\ kip \cdot ft$ *deck self-weight moment*

Variables:

$L_c := L - 14\ in = 44.33\ ft$ *clear distance between end roller supports*

$L_{spr} := 48\ in$ *distance between two point loads (spreader beam roller supports clear distance)*

Test 2.1: $P_{max1} := 424\ kip$

$x_1 := 99\ in - 7\ in = 92\ in$ *distance from point load to end of beam*

$a_1 := x_1 - \frac{L_{spr}}{2} = 5.67\ ft$

$a_1 = 68\ in$ *clear distance from center of north bearing to first point load*

$b_1 := L_c - a_1 - L_{spr} = 34.67\ ft$

$b_1 = 416\ in$ *clear distance from center of south bearing to second point load*

Test 2.2: $P_{max2} := 431\ kip$

$x_2 := 45.5\ ft - 99\ in - 7\ in = 440\ in$ *distance from point load to end of beam*

$a_2 := x_2 - \frac{L_{spr}}{2} = 34.67\ ft$

$a_2 = 416\ in$ *clear distance from center of north bearing to first point load*

$b_2 := L_c - a_2 - L_{spr} = 5.67\ ft$

$b_2 = 68\ in$ *clear distance from center of south bearing to second point load*

Test 2.3: $P_{max3} := 341\ kip$

$x_3 := L - 270\ in - 7\ in = 269\ in$ *distance from point load to end of beam*

$a_3 := x_3 - \frac{L_{spr}}{2} = 20.42\ ft$

$a_3 = 245\ in$ *clear distance from center of north bearing to first point load*

$b_3 := L_c - a_3 - L_{spr} = 19.92\ ft$

$b_3 = 239\ in$ *clear distance from center of south bearing to second point load*

Composite Properties Calculations:

Bottom neutral axis distance of composite section

$$C_b' := \frac{\left(A_{deck1} \cdot \left(h + 1.5\ in + \frac{h_f}{2}\right)\right) + \left(A_{deck2} \cdot \left(h + \frac{1.5\ in}{2}\right)\right) + \left(A \cdot -C_b\right)}{A_{deck1} + A_{deck2} + A} = 41.55\ in$$

Top neutral axis distance of composite section

$$C_t' := h + h_f + 1.5\ in - C_b' = 21.95\ in$$

Moment of inertia of composite section

$$I_c' := I + A \cdot \left(C_b' + C_b\right)^2 + \frac{b_{e1} \cdot h_f^3}{12} + A_{deck1} \cdot \left(\left(h + 1.5\ in + \frac{h_f}{2}\right) - C_b'\right)^2 + \frac{b_{e2} \cdot (1.5\ in)^3}{12} + A_{deck2} \cdot \left(\left(h + \frac{1.5\ in}{2}\right) - C_b'\right)^2 = 559708.71\ in^4$$

Cross-sectional area of composite section

$$A_c' := A + \left(h_f \cdot b_{e1}\right) + \left(1.5\ in \cdot b_{e2}\right) = 1183.71\ in^2$$

Radius of gyration of composite section

$$r := \sqrt{\frac{I_c'}{A_c'}} = 21.74\ in \qquad r^2 = 472.84\ in^2$$

Top section modulus of composite section (top of precast member)

$$S_{tc} := \frac{I_c'}{C_t'} = 25498.74\ in^3$$

Bottom section modulus of composite section (bottom of precast member)

$$S_{bc} := \frac{I_c'}{C_b'} = 13470.87\ in^3$$

Top section modulus of composite section (top of slab)

$$S_{tcs} := \frac{I_c'}{C_t' + h_f} = 18687.83\ in^3$$

Bottom section modulus of composite section (bottom of slab)

$$S_{bcs} := \frac{I_c'}{C_t'} = 25498.74\ in^3$$

Losses Calculations BT-54 with Composite Deck (1/3)

Losses Before Release (10 May 2025)

$f_{pJ} := 0.75 \cdot f_{pu} = 202.5$ ***ksi***

$F_J := f_{pJ} \cdot \#strands \cdot A_s + 40$ ***kip*** $= 655.2$ ***kip*** total force in all 14 strands (plus 4 top strands @ 10 kips each) at time of tension

Relaxation in Strand, R1 (10 May 2024 to 15 May 2024)

$t1 := 1$ $t2 := 120$ $f_{pi}' := f_{pJ} = 202.5$ ***ksi***

$\Delta f_p R1 := f_{pi}' \cdot \left(\frac{\log(t2) - \log(t1)}{45} \right) \cdot \left(\frac{f_{pi}'}{f_y} - 0.55 \right) = 2.65$ ***ksi***

Losses Just After Release (15 May 2024)

$F_i := \left(f_{pJ} - \Delta f_p R1 \right) \cdot \#strands \cdot A_s = 607.14$ ***kip***

$F_j := 0.9 \cdot F_i = 546.43$ ***kip*** *assumed 0.9*

Elastic Shortening in Strand, ES (15 May 2025)

$E_{ps} = 28700$ ***ksi*** $f_{ci} = 9850$ $E_{ci} := 57000 \cdot \sqrt{f_{ci}} \cdot psi = 5657.09$ ***ksi***

$\eta_i := \frac{E_{ps}}{E_{ci}} = 5.07$

$f_{cs} := \frac{-F_j}{A} - \frac{F_j \cdot e^2}{I} - \frac{M_w \cdot e}{I} = -1.48$ ***ksi***

$\Delta f_p ES := -\eta_i \cdot f_{cs} = 7.53$ ***ksi***

Losses Calculations BT-54 with Composite Deck (2/3)

Losses After ~13 Months (25 June 2025) Note: deck casted on 14 February 2025

Creep, CR (15 May 2024 to 25 June 2025)

$K_{cr} := 2$ *for pretensioned members*

$f_{pj} := f_{pJ} - \Delta f_p R1 - \Delta f_p ES = 192.32$ ***ksi***

$P_j := f_{pj} \cdot \#strands \cdot A_s = 584.26$ ***kip***

$f_{cs} := \frac{-P_j}{A} - \frac{P_j \cdot e^2}{I} - \frac{M_w \cdot e}{I} = -1.6$ ***ksi***

$f_{csd} := \frac{-M_{SD} \cdot C_b'}{I_c'} = -0.15$ ***ksi***

$\Delta f_p CR := 0.80 \left(-K_{cr} \cdot \frac{E_{ps}}{E_c} \left(f_{cs} - f_{csd} \right) \right) = 9.68$ ***ksi*** Note: only 80% of total CR because of 405 day age

Shrinkage, SH (15 May 2024 to 25 June 2025)

$RH := 70$ *relative humidity in Atlanta, GA*

$K_{SH} := 1$ *for pretensioned members*

$V := A \cdot L = 359814$ ***in***^{3} *volume of girder*

$S := 2 \cdot A + 2 \cdot h \cdot L + 26$ ***in*** $\cdot L + 42$ ***in*** $\cdot L = 97414$ ***in***^{2} *approximate surface area of girder*

$\varepsilon_{SH} := 8.2 \cdot 10^{-6} \cdot K_{SH} \cdot \left(1 - \frac{0.06}{in} \cdot \frac{V}{S} \right) (100 - RH) = 0.0001915$

$\Delta f_p SH := \varepsilon_{SH} \cdot E_{ps} = 5.5$ ***ksi***

Relaxation in Strand, R2 (15 May 2024 to 14 February 2025)

$t2 = 120$ $t3 := 6609$ $f_{pi}' := f_{pj} = 192.32$ ***ksi***

$\Delta f_p R2 := f_{pi}' \cdot \left(\frac{\log(t3) - \log(t2)}{45} \right) \cdot \left(\frac{f_{pi}'}{f_y} - 0.55 \right) = 1.8$ ***ksi***

Losses Calculations BT-54 with Composite Deck (3/3)

Relaxation in Strand, R3 (14 February 2024 to 25 June 2025, Deck Casted)

$t3 = 6609$ $t4 := 9744$ $f_{pi}' := f_{pj} - \Delta f_p R2 + f_{csd} \cdot \frac{E_{ps}}{E_c} = 189.88$ ***ksi***

$\Delta f_p R3 := f_{pi}' \cdot \left(\frac{\log(t4) - \log(t3)}{45} \right) \cdot \left(\frac{f_{pi}'}{f_y} - 0.55 \right) = 0.16$ ***ksi***

Effective Force in Prestress (after losses) 25 June 2025 Test Day

$F_e := \left(f_{pJ} - \Delta f_p R1 - \Delta f_p R2 - \Delta f_p R3 - \Delta f_p ES - \Delta f_p CR - \Delta f_p SH \right) \cdot \#strands \cdot A_s = 532.21$ ***kip***

$Losses := \left(1 - \frac{F_e}{F_J} \right) \cdot 100 = 18.77$ *loss percentage*

$F_{ei} := \left(f_{pJ} \cdot \left(1 - \frac{1}{Losses} \right) \right) \cdot A_s = 41.6$ ***kip*** *effective force in individual strand*

$f_{se} := f_{pJ} \cdot \left(1 - \frac{Losses}{100} \right) = 164.49$ ***ksi***

Initial Beam Curvature (1/4):

Curvature due to beam prestress: (negative)

$f_{pe} := f_{se} = 164.49\ ksi$ *refined through previous losses calculations*

$CGS := -C_b + e = 7.64\ in$ *finding CGS from bottom beam*

$\varepsilon_{bi} := \frac{-f_{pe}}{E_{ps}} = -0.0057313$ *strain at CGS due to prestress*

$\varepsilon_{ti} := \frac{\varepsilon_{bi} \cdot C_t}{-e + C_t} = -0.00326$ *strain at top of beam due to prestress*

$h_i := h - CGS = 46.36\ in$ *distance between top of beam and CGS*

$\phi_i := \frac{\varepsilon_{bi} + \varepsilon_{ti}}{h} = -0.0001665\ \frac{1}{in}$ *initial (negative) curvature in beam due to prestress*

Initial Beam Curvature (2/4):

Test 2.1:

Curvature due to beam SW: (negative)

$M_{w1} := \frac{w \cdot x_1}{2} \left(L_c - x_1\right) = 96.49\ \textit{kip} \cdot \textit{ft}$ *moment due to beam SW at test location*

$f_{swb1} := \frac{-M_{w1} \cdot e}{I} = 86.34\ \textit{psi}$ *stress at CGS due to beam SW*

$\varepsilon_{swb1} := \frac{f_{swb1}}{E_c} = 0.00001259$ *strain at CGS due to beam SW*

$f_{swt1} := \frac{M_{w1} \cdot C_t}{I} = 113.89\ \textit{psi}$ *stress at top of beam due to beam SW*

$\varepsilon_{swt1} := \frac{f_{swt1}}{E_c} = 0.00001661$ *strain at top of beam due to beam SW*

$h_1 := h - CGS = 46.36\ \textit{in}$ *distance between top of beam and CGS*

$\phi_{1b} := \frac{\varepsilon_{swb1} + \varepsilon_{swt1}}{h_1} = 0.0000006\ \frac{1}{\textit{in}}$ *initial (positive) curvature in beam due to beam SW*

Curvature due to deck SW: (positive)

$M_{SD1} := \frac{w_{deck} \cdot x_1}{2} \left(L_c - x_1\right) = 93.56\ \textit{kip} \cdot \textit{ft}$ *moment due to deck SW at test location*

$f_{deckswb1} := \frac{-M_{SD1} \cdot e}{I} = 83.72\ \textit{psi}$ *stress at CGS due to deck SW*

$\varepsilon_{deckswb1} := \frac{f_{deckswb1}}{E_c} = 0.00001221$ *strain at CGS due to deck SW*

$f_{deckswt1} := \frac{M_{SD1} \cdot C_t}{I} = 110.44\ \textit{psi}$ *stress at top of beam due to deck SW*

$\varepsilon_{deckswt1} := \frac{f_{deckswt1}}{E_c} = 0.0000161$ *strain at top of beam due to deck SW*

$h_1 = 46.36\ \textit{in}$ *distance between top of beam and CGS*

$\phi_{1d} := \frac{\varepsilon_{deckswb1} + \varepsilon_{deckswt1}}{h_1} = 0.0000006107\ \frac{1}{\textit{in}}$ *initial (positive) curvature in beam due to deck SW*

$\phi_{initial1} := \phi_{1b} + \phi_{1d} + \phi_i = -0.00016527\ \frac{1}{\textit{in}}$ *total initial (negative) curvature in composite beam prior to Test 2.1*

Initial Beam Curvature (3/4):

Test 2.2:
Curvature due to beam SW: (negative)

$M_{w2} := \frac{w \cdot x_2}{2}\left(L_c - x_2\right) = 96.49\ \textit{kip}\cdot\textit{ft}$ *moment due to beam SW at test location*

$f_{swb2} := \frac{-M_{w2}\cdot e}{I} = 86.34\ \textit{psi}$ *stress at CGS due to beam SW*

$\varepsilon_{swb2} := \frac{f_{swb2}}{E_c} = 0.00001259$ *strain at CGS due to beam SW*

$f_{swt2} := \frac{M_{w2}\cdot C_t}{I} = 113.89\ \textit{psi}$ *stress at top of beam due to beam SW*

$\varepsilon_{swt2} := \frac{f_{swt2}}{E_c} = 0.00001661$ *strain at top of beam due to beam SW*

$h_2 := h_1 = 46.36\ \textit{in}$ *distance between top of beam and CGS*

$\phi_{2b} := \frac{\varepsilon_{swb2} + \varepsilon_{swt2}}{h_2} = 0.0000006\ \frac{1}{\textit{in}}$ *initial (positive) curvature in beam due to beam SW*

Curvature due to deck SW: (positive)

$M_{SD2} := \frac{w_{deck}\cdot x_2}{2}\left(L_c - x_2\right) = 93.56\ \textit{kip}\cdot\textit{ft}$ *moment due to deck SW at test location*

$f_{deckswb2} := \frac{-M_{SD2}\cdot e}{I} = 83.72\ \textit{psi}$ *stress at CGS due to deck SW*

$\varepsilon_{deckswb2} := \frac{f_{deckswb2}}{E_c} = 0.00001221$ *strain at CGS due to deck SW*

$f_{deckswt2} := \frac{M_{SD2}\cdot C_t}{I} = 110.44\ \textit{psi}$ *stress at top of beam due to deck SW*

$\varepsilon_{deckswt2} := \frac{f_{deckswt2}}{E_c} = 0.0000161$ *strain at top of beam due to deck SW*

$h_2 = 46.36\ \textit{in}$ *distance between top of beam and CGS*

$\phi_{2d} := \frac{\varepsilon_{deckswb2} + \varepsilon_{deckswt2}}{h_2} = 0.0000006107\ \frac{1}{\textit{in}}$ *initial (positive) curvature in beam due to deck SW*

$\phi_{initial2} := \phi_{2b} + \phi_{2d} + \phi_i = -0.00016527\ \frac{1}{\textit{in}}$ *total initial (negative) curvature in composite beam prior to Test 2.2*

Initial Beam Curvature (4/4):

Test 2.3:

Curvature due to beam SW: (negative)

$M_{w3} := \frac{w \cdot x_1}{2} \left(L_c - x_1\right) = 96.49$ **kip·ft** *moment due to beam SW at test location*

$f_{swb3} := \frac{-M_{w1} \cdot e}{I} = 86.34$ **psi** *stress at CGS due to beam SW*

$\varepsilon_{swb3} := \frac{f_{swb1}}{E_c} = 0.00001259$ *strain at CGS due to beam SW*

$f_{swt3} := \frac{M_{w1} \cdot C_t}{I} = 113.89$ **psi** *stress at top of beam due to beam SW*

$\varepsilon_{swt3} := \frac{f_{swt1}}{E_c} = 0.00001661$ *strain at top of beam due to beam SW*

$h_3 := h_1 = 46.36$ **in** *distance between top of beam and CGS*

$\phi_{3b} := \frac{\varepsilon_{swb3} + \varepsilon_{swt3}}{h_3} = 0.0000006 \frac{1}{\text{in}}$ *initial (positive) curvature in beam due to beam SW*

Curvature due to deck SW: (positive)

$M_{SD3} := \frac{w_{deck} \cdot x_3}{2} \left(L_c - x_3\right) = 163.51$ **kip·ft** *moment due to deck SW at test location*

$f_{deckswb3} := \frac{-M_{SD3} \cdot e}{I} = 146.31$ **psi** *stress at CGS due to deck SW*

$\varepsilon_{deckswb3} := \frac{f_{deckswb3}}{E_c} = 0.00002134$ *strain at CGS due to deck SW*

$f_{deckswt3} := \frac{M_{SD3} \cdot C_t}{I} = 193.01$ **psi** *stress at top of beam due to deck SW*

$\varepsilon_{deckswt3} := \frac{f_{deckswt3}}{E_c} = 0.00002814$ *strain at top of beam due to deck SW*

$h_3 = 46.36$ **in** *distance between top of beam and CGS*

$\phi_{3d} := \frac{\varepsilon_{deckswb3} + \varepsilon_{deckswt3}}{h_3} = 0.0000010673 \frac{1}{\text{in}}$ *initial (positive) curvature in beam due to deck SW*

$\phi_{initial3} := \phi_{3b} + \phi_{3d} + \phi_i = -0.00016481 \frac{1}{\text{in}}$ *total initial (negative) curvature in composite beam prior to Test 2.3*

Cracking Moment:

$$M_{cr} := \frac{f_r \cdot I_c'}{C_b'} = 1012.94 \ \textit{kip} \cdot \textit{ft}$$

$$\phi_{cr} := \frac{M_{cr}}{E_c \cdot I_c'} = 0.000003167 \ \frac{1}{\textit{in}}$$

$$M_{cr95} := 0.95 \cdot M_{cr} = 962.3 \ \textit{kip} \cdot \textit{ft}$$

$$\phi_{cr95} := 0.95 \cdot \phi_{cr} = 0.000003008 \ \frac{1}{\textit{in}}$$

Ultimate Moment (1/9):
Test 2.1:

$\varepsilon_{si1} := 0.000229$ *strain measured from test (input)*

$d_1 := h + h_f + 1.5\ \textit{in} - 2.5\ \textit{in} = 61\ \textit{in}$ *depth to centroid of strands from top of composite girder*

$c_1 := 14.7858\ \textit{in}$ *trial and error iterative c value (input until equilibrium)*

$\varepsilon_{s1.1} := -\varepsilon_{bi} + \varepsilon_{si1} = 0.00596$ *strain in lowest strand level at ultimate (test + effective prestress)*

$\varepsilon_{s2.1} := \frac{\varepsilon_{s1.1} \cdot (d_1 - 2\ \textit{in} - c_1)}{d_1 - c_1} = 0.0057$ *strain in 2nd strand level at ultimate*

$\varepsilon_{s3.1} := \frac{\varepsilon_{s1.1} \cdot (d_1 - 12\ \textit{in} - c_1)}{d_1 - c_1} = 0.00441$ *strain in 3rd strand level at ultimate*

$\varepsilon_{s4.1} := \frac{\varepsilon_{s1.1} \cdot (d_1 - 49.5\ \textit{in} - c_1)}{d_1 - c_1} = -0.0004237746$ *strain in top strand level at ultimate*

$\varepsilon_{c1.1} := \frac{\varepsilon_{si1} \cdot c_1}{d_1 - c_1} = 0.00007$ *strain at top of concrete deck at ultimate*

$\varepsilon_{c2.1} := \frac{\varepsilon_{si1} \cdot (c_1 - 8\ \textit{in})}{d_1 - c_1} = 0.0000336249$ *strain at top of 1.5-inch deck haunch at ultimate*

$\varepsilon_{c3.1} := \frac{\varepsilon_{si1} \cdot (c_1 - 9.5\ \textit{in})}{d_1 - c_1} = 0.0000261921$ *strain at top of top flange at ultimate*

$\varepsilon_{c4.1} := \frac{\varepsilon_{si1} \cdot (c_1 - 14\ \textit{in})}{d_1 - c_1} = 0.0000038938$ *strain at top of web at ultimate*

$T_{1.1} := 8 \cdot A_s \cdot \varepsilon_{s1.1} \cdot E_{ps} = 296.96\ \textit{kip}$ *tension force from lowest strand level*

$T_{2.1} := 4 \cdot A_s \cdot \varepsilon_{s2.1} \cdot E_{ps} = 142.06\ \textit{kip}$ *tension force from 2nd strand level*

$T_{3.1} := 2 \cdot A_s \cdot \varepsilon_{s3.1} \cdot E_{ps} = 54.96\ \textit{kip}$ *tension force from 3rd strand level*

$\mathbf{T_{4.1}} := \text{if}\left(c_1 > 12\ \textit{in}, 0\ \textit{kip}, \left(2 \cdot A_s \cdot \varepsilon_{s4.1} \cdot E_{ps}\right)\right) = 0\ \textit{kip}$ *tension force from top strand level*

$T_{t1} := T_{1.1} + T_{2.1} + T_{3.1} + \mathbf{T_{4.1}} = 493.98\ \textit{kip}$ *total tension force from prestress*

Ultimate Moment (2/9):
Test 2.1:

$$C_{1.1} := \begin{cases} \dfrac{(\varepsilon_{c1.1}) \cdot E_{cdeck}}{2} \cdot c_1 \cdot 72\ in & \text{if } c_1 < 8\ in \\ \dfrac{(\varepsilon_{c1.1} + \varepsilon_{c2.1}) \cdot E_{cdeck}}{2} \cdot c_1 \cdot 72\ in & \text{else} \end{cases} = 320.4\ kip$$

compression force from 8-inch concrete deck

$$C_{2.1} := \begin{cases} 0\ kip & \text{if } c_1 \leq 8\ in \\ \dfrac{(\varepsilon_{c2.1}) \cdot E_{cdeck}}{2} \cdot c_1 \cdot 43.5\ in & \text{else if } 8\ in < c_1 \leq 9.5\ in \\ \dfrac{(\varepsilon_{c2.1} + \varepsilon_{c3.1}) \cdot E_{cdeck}}{2} \cdot c_1 \cdot 43.5\ in & \text{else if } c_1 > 9.5\ in \end{cases} = 108.33\ kip$$

compression force from 1.5-inch concrete deck haunch

$$C_{3.1} := \begin{cases} 0\ kip & \text{if } c_1 \leq 9.5\ in \\ \dfrac{(\varepsilon_{c3.1}) \cdot E_c}{2} \cdot c_1 \cdot 42\ in & \text{else if } 9.5\ in < c_1 \leq 14\ in \\ \dfrac{(\varepsilon_{c3.1} + \varepsilon_{c4.1}) \cdot E_c}{2} \cdot c_1 \cdot 42\ in & \text{else if } c_1 > 14\ in \end{cases} = 64.06\ kip$$

compression force from 4.5-inch top flange

$$C_{4.1} := \begin{cases} 0\ kip & \text{if } c_1 \leq 14\ in \\ \dfrac{(\varepsilon_{c4.1}) \cdot E_c}{2} \cdot c_1 \cdot 6\ in & \text{else} \end{cases} = 1.18\ kip$$

compression force from web

$$C_{t1} := C_{1.1} + C_{2.1} + C_{3.1} + C_{4.1} = 493.97\ kip$$

compression force from concrete

$$T_{t1} - C_{t1} = 0.009487\ kip$$

equilibrium of forces must = 0 to find c

Ultimate Moment (3/9):

Test 2.1:

$$J_{d1} := 63.5\ in - \left(\frac{T_{1.1} \cdot 2.5\ in + T_{2.1} \cdot 4.5\ in + T_{3.1} \cdot 14.5\ in + \mathbf{T_{4.1}} \cdot 51.5\ in}{T_{t1}} \right) - \frac{c_1}{3} = 54.16\ in$$

$$M_{ult2.1} := A_{ps} \cdot \varepsilon_{s1.1} \cdot E_{ps} \cdot \left(J_{d1} \right) = 2345.55\ kip \cdot ft$$

$$\phi_{ult2.1} := \frac{\varepsilon_{c1.1}}{c_1} = 0.000005\ \frac{1}{in}$$

Ultimate Moment (4/9):
Test 2.2:

$\varepsilon_{si2} := 0.000285$ *strain measured from test (input)*

$d_2 := h + h_f + 1.5\ in - 2.5\ in = 61\ in$ *depth to centroid of strands from top of composite girder*

$c_2 := 13.9185\ in$ *trial and error iterative c value (input until equilibrium)*

$\varepsilon_{s1.2} := -\varepsilon_{bi} + \varepsilon_{si2} = 0.006016$ *strain in lowest strand level at ultimate (test + effective prestress)*

$$\varepsilon_{s2.2} := \frac{\varepsilon_{s1.2} \cdot (d_2 - 2\ in - c_2)}{d_2 - c_2} = 0.00576$$ *strain in 2nd strand level at ultimate*

$$\varepsilon_{s3.2} := \frac{\varepsilon_{s1.2} \cdot (d_2 - 12\ in - c_2)}{d_2 - c_2} = 0.00448$$ *strain in 3rd strand level at ultimate*

$$\varepsilon_{s4.2} := \frac{\varepsilon_{s1.2} \cdot (d_2 - 49.5\ in - c_2)}{d_2 - c_2} = -0.0003090483$$ *strain in top strand level at ultimate*

$$\varepsilon_{c1.2} := \frac{\varepsilon_{si2} \cdot c_2}{d_2 - c_2} = 0.00008$$ *strain at top of concrete deck at ultimate*

$$\varepsilon_{c2.2} := \frac{\varepsilon_{si2} \cdot (c_2 - 8\ in)}{d_2 - c_2} = 0.0000358267$$ *strain at top of 1.5-inch deck haunch at ultimate*

$$\varepsilon_{c3.2} := \frac{\varepsilon_{si2} \cdot (c_2 - 9.5\ in)}{d_2 - c_2} = 0.0000267467$$ *strain at top of top flange at ultimate*

$$\varepsilon_{c4.2} := \frac{\varepsilon_{si2} \cdot (c_2 - 14\ in)}{d_2 - c_2} = -0.0000004933$$ *strain at top of web at ultimate*

$T_{1.2} := 8 \cdot A_s \cdot \varepsilon_{s1.2} \cdot E_{ps} = 299.75\ kip$ *tension force from lowest strand level*

$T_{2.2} := 4 \cdot A_s \cdot \varepsilon_{s2.2} \cdot E_{ps} = 143.51\ kip$ *tension force from 2nd strand level*

$T_{3.2} := 2 \cdot A_s \cdot \varepsilon_{s3.2} \cdot E_{ps} = 55.84\ kip$ *tension force from 3rd strand level*

$\mathbf{T_{4.2}} := \text{if}\left(c_2 > 12\ in, 0\ kip, \left(2 \cdot A_s \cdot \varepsilon_{s4.2} \cdot E_{ps}\right)\right) = 0\ kip$ *tension force from top strand level*

$T_{t2} := T_{1.2} + T_{2.2} + T_{3.2} + \mathbf{T_{4.2}} = 499.1\ kip$ *total tension force from prestress*

Ultimate Moment (5/9):
Test 2.2:

$$C_{1.2} := \text{if } c_2 < 8\ in \quad \left\| \frac{(\varepsilon_{c1.2}) \cdot E_{cdeck}}{2} \cdot c_2 \cdot 72\ in \right. \quad \text{else} \quad \left\| \frac{(\varepsilon_{c1.2} + \varepsilon_{c2.2}) \cdot E_{cdeck}}{2} \cdot c_2 \cdot 72\ in \right. = 338.82\ kip$$

compression force from 8-inch concrete deck

$$C_{2.2} := \text{if } c_2 \leq 8\ in \quad \| 0\ kip \quad \text{else if } 8\ in < c_2 \leq 9.5\ in \quad \left\| \frac{(\varepsilon_{c2.2}) \cdot E_{cdeck}}{2} \cdot c_2 \cdot 43.5\ in \right. \quad \text{else if } c_2 > 9.5\ in \quad \left\| \frac{(\varepsilon_{c2.2} + \varepsilon_{c3.2}) \cdot E_{cdeck}}{2} \cdot c_2 \cdot 43.5\ in \right. = 106.67\ kip$$

compression force from 1.5-inch concrete deck haunch

$$C_{3.2} := \text{if } c_2 \leq 9.5\ in \quad \| 0\ kip \quad \text{else if } 9.5\ in < c_2 \leq 14\ in \quad \left\| \frac{(\varepsilon_{c3.2}) \cdot E_c}{2} \cdot c_2 \cdot 42\ in \right. \quad \text{else if } c_2 > 14\ in \quad \left\| \frac{(\varepsilon_{c3.2} + \varepsilon_{c4.2}) \cdot E_c}{2} \cdot c_2 \cdot 42\ in \right. = 53.61\ kip$$

compression force from 4.5-inch top flange

$$C_{4.2} := \text{if } c_2 \leq 14\ in \quad \| 0\ kip \quad \text{else} \quad \left\| \frac{(\varepsilon_{c4.2}) \cdot E_c}{2} \cdot c_2 \cdot 6\ in \right. = 0\ kip$$

compression force from web

$$C_{t2} := C_{1.2} + C_{2.2} + C_{3.2} + C_{4.2} = 499.1\ kip$$

compression force from concrete

$$T_{t2} - C_{t2} = 0.000438\ kip$$

equilibrium of forces must = 0 to find c

Ultimate Moment (6/9):

Test 2.2:

$$J_{d2} := 63.5\ in - \left(\frac{T_{1.2} \cdot 2.5\ in + T_{2.2} \cdot 4.5\ in + T_{3.2} \cdot 14.5\ in + \mathbf{T_{4.2}} \cdot 51.5\ in}{T_{t2}} \right) - \frac{c_2}{3} = 54.44\ in$$

$$M_{ult2.2} := A_{ps} \cdot \varepsilon_{s1.2} \cdot E_{ps} \cdot \langle J_{d2} \rangle = 2379.91\ kip \cdot ft$$

$$\phi_{ult2.2} := \frac{\varepsilon_{c1.2}}{c_2} = 0.0000061\ \frac{1}{in}$$

Ultimate Moment (7/9):
Test 2.3:

$\varepsilon_{si3} := 0.002729$ *strain measured from test (input)*

$d_3 := h + h_f + 1.5\ \textit{in} - 2.5\ \textit{in} = 61\ \textit{in}$ *depth to centroid of strands from top of composite girder*

$c_3 := 8.13956\ \textit{in}$ *trial and error iterative c value (input until equilibrium)*

$\varepsilon_{s1.3} := -\varepsilon_{bi} + \varepsilon_{si3} = 0.00846$ *strain in lowest strand level at ultimate (test + effective prestress)*

$\varepsilon_{s2.3} := \frac{\varepsilon_{s1.3} \cdot (d_3 - 2\ \textit{in} - c_3)}{d_3 - c_3} = 0.00814$ *strain in 2nd strand level at ultimate*

$\varepsilon_{s3.3} := \frac{\varepsilon_{s1.3} \cdot (d_3 - 12\ \textit{in} - c_3)}{d_3 - c_3} = 0.00654$ *strain in 3rd strand level at ultimate*

$\varepsilon_{s4.3} := \frac{\varepsilon_{s1.3} \cdot (d_3 - 49.5\ \textit{in} - c_3)}{d_3 - c_3} = 0.0005378385$ *strain in top strand level at ultimate*

$\varepsilon_{c1.3} := \frac{\varepsilon_{si3} \cdot c_3}{d_3 - c_3} = 0.00042$ *strain at top of concrete deck at ultimate*

$\varepsilon_{c2.3} := \frac{\varepsilon_{si3} \cdot (c_3 - 8\ \textit{in})}{d_3 - c_3} = 0.000007205$ *strain at top of 1.5-inch deck haunch at ultimate*

$\varepsilon_{c3.3} := \frac{\varepsilon_{si3} \cdot (c_3 - 9.5\ \textit{in})}{d_3 - c_3} = -0.0000702348$ *strain at top of top flange at ultimate*

$\varepsilon_{c4.3} := \frac{\varepsilon_{si3} \cdot (c_3 - 14\ \textit{in})}{d_3 - c_3} = -0.0003025541$ *strain at top of web at ultimate*

$T_{1.3} := 8 \cdot A_s \cdot \varepsilon_{s1.3} \cdot E_{ps} = 421.52\ \textit{kip}$ *tension force from lowest strand level*

$T_{2.3} := 4 \cdot A_s \cdot \varepsilon_{s2.3} \cdot E_{ps} = 202.79\ \textit{kip}$ *tension force from 2nd strand level*

$T_{3.3} := 2 \cdot A_s \cdot \varepsilon_{s3.3} \cdot E_{ps} = 81.46\ \textit{kip}$ *tension force from 3rd strand level*

$\mathbf{T_{4.3}} := \text{if}\left(c_3 \geq 12\ \textit{in}, 0\ \textit{kip}, \left(2 \cdot A_s \cdot \varepsilon_{s4.3} \cdot E_{ps}\right)\right) = 6.7\ \textit{kip}$ *tension force from top strand level*

$T_{t3} := T_{1.3} + T_{2.3} + T_{3.3} + \mathbf{T_{4.3}} = 712.46\ \textit{kip}$ *total tension force from prestress*

Ultimate Moment (8/9):
Test 2.3:

$$C_{1.3} := \text{if } c_3 < 8\ in \quad \left\| \frac{(\varepsilon_{c1.3}) \cdot E_{cdeck}}{2} \cdot c_3 \cdot 72\ in \right. \quad \text{else} \quad \left\| \frac{(\varepsilon_{c1.3} + \varepsilon_{c2.3}) \cdot E_{cdeck}}{2} \cdot c_3 \cdot 72\ in \right. = 705.28\ kip$$

compression force from 8-inch concrete deck

$$C_{2.3} := \text{if } c_3 \leq 8\ in \quad \| 0\ kip \quad \text{else if } 8\ in < c_3 \leq 9.5\ in \quad \left\| \frac{(\varepsilon_{c2.3}) \cdot E_{cdeck}}{2} \cdot c_3 \cdot 43.5\ in \right. \quad \text{else if } c_3 > 9.5\ in \quad \left\| \frac{(\varepsilon_{c2.3} + \varepsilon_{c3.3}) \cdot E_{cdeck}}{2} \cdot c_3 \cdot 43.5\ in \right. = 7.18\ kip$$

compression force from 1.5-inch concrete deck haunch

$$C_{3.3} := \text{if } c_3 \leq 9.5\ in \quad \| 0\ kip \quad \text{else if } 9.5\ in < c_3 \leq 14\ in \quad \left\| \frac{(\varepsilon_{c3.3}) \cdot E_c}{2} \cdot c_3 \cdot 42\ in \right. \quad \text{else if } c_3 > 14\ in \quad \left\| \frac{(\varepsilon_{c3.3} + \varepsilon_{c4.3}) \cdot E_c}{2} \cdot c_3 \cdot 42\ in \right. = 0\ kip$$

compression force from 4.5-inch top flange

$$C_{4.3} := \text{if } c_3 \leq 14\ in \quad \| 0\ kip \quad \text{else} \quad \left\| \frac{(\varepsilon_{c4.3}) \cdot E_c}{2} \cdot c_3 \cdot 6\ in \right. = 0\ kip$$

compression force from web

$$C_{t3} := C_{1.3} + C_{2.3} + C_{3.3} + C_{4.3} = 712.46\ kip$$

compression force from concrete

$$T_{t3} - C_{t3} = 0.001871\ kip$$

equilibrium of forces must = 0 to find c

Ultimate Moment (9/9):

Test 2.3:

$$J_{d3} := 63.5\ in - \left(\frac{T_{1.3} \cdot 2.5\ in + T_{2.3} \cdot 4.5\ in + T_{3.3} \cdot 14.5\ in + \mathbf{T_{4.3}} \cdot 51.5\ in}{T_{t3}} \right) - \frac{c_3}{3} = 55.88\ in$$

$$M_{ult2.3} := A_{ps} \cdot \varepsilon_{s1.3} \cdot E_{ps} \cdot (J_{d3}) = 3435.33\ kip \cdot ft$$

$$\phi_{ult2.3} := \frac{\varepsilon_{c1.3}}{c_3} = 0.0000516\ \frac{1}{in}$$

Theoretical Moment-Curvature Overview:

$M_{cr} = 1012.94\ kip \cdot ft$ $M_{ult2.2} = 2379.91\ kip \cdot ft$

$\phi_{cr} = 0.000003167\ \frac{1}{in}$ $\phi_{ult2.2} = 0.000006\ \frac{1}{in}$

$M_{ult2.1} = 2345.55\ kip \cdot ft$ $M_{ult2.3} = 3435.33\ kip \cdot ft$

$\phi_{ult2.1} = 0.000005\ \frac{1}{in}$ $\phi_{ult2.3} = 0.000052\ \frac{1}{in}$

Ultimate Loads from Moment Calculations: (four-point bending tests)

Test 2.1:

$a_1 = 5.67\ ft$

$b_1 = 34.67\ ft$

$P_{ult1m} := 2 \cdot \frac{L_c \cdot M_{ult2.1}}{b_1 \cdot (a_1 + L_c - b_1)} = 391.25\ kip$ *ultimate load based on moment capacity*

Test 2.2:

$a_2 = 34.67\ ft$

$b_2 = 5.67\ ft$

$P_{ult2m} := 2 \cdot \frac{L_c \cdot M_{ult2.2}}{a_2 \cdot (b_2 + L_c - a_2)} = 396.98\ kip$ *ultimate load based on moment capacity*

Test 2.3:

$a_3 = 20.42\ ft$

$b_3 = 19.92\ ft$

$P_{ult3m} := 2 \cdot \frac{L_c \cdot M_{ult2.3}}{a_3 \cdot (b_3 + L_c - a_3)} = 340.36\ kip$ *ultimate load based on moment capacity*

Theoretical Strut and Tie Cracking Capacity: (1/) (AASHTO C5.8.2.2-1)

$d := 54\ in + 9.5\ in = 63.5\ in$

$b_w := 6\ in$

$V_{cr1} := \left(0.2 - 0.1\left(\frac{a_1}{d}\right)\right) \cdot \sqrt{\frac{f_c}{1000}} \cdot ksi \cdot b_w \cdot d = 134.68\ kip$

$V_{cr2} := \left(0.2 - 0.1\left(\frac{L_c - L_{spr} - a_2}{d}\right)\right) \cdot \sqrt{\frac{f_c}{1000}} \cdot ksi \cdot b_w \cdot d = 134.68\ kip$

$V_{cr3} := \max\left(\left(0.2 - 0.1\left(\frac{L_c - L_{spr} - a_3}{d}\right)\right), 0.0632\right) \cdot \sqrt{\frac{f_c}{1000}} \cdot ksi \cdot b_w \cdot d = 91.61\ kip$

Shear Capacity: (1/5)

Prestress Transfer/Development Lengths:

$d_b := 0.6\ in$ *diameter of prestressing strand*

$L_{tr} := min\left(50 \cdot d_b, \left(\frac{f_{pe}}{3000\ psi}\right) \cdot d_b\right) = 30\ in$ *transfer length*

$f_{ps} := \varepsilon_{s1.3} \cdot E_{ps} = 242.81\ ksi$

$L_f := \left(\frac{f_{ps} - f_{pe}}{1000\ psi}\right) \cdot d_b = 46.99\ in$

$L_d := L_{tr} + L_f = 6.42\ ft$ *development length*

V_c calculation:

Minimum V_{ci} calculation:

$d_p := \max\left(h + h_f + 1.5\ in - CGS, 0.8\ \left(h + h_f + 1.5\ in\right)\right) = 55.86\ in$ *distance from CGS to max compression fiber*

$f_{ce} := f_{pe} = 164.49\ ksi$ *effective prestress stress*

$b_w := 6\ in$ *web width*

$d := d_p = 55.86\ in$ *distance from CGS to max compression fiber*

$f_y := 60\ ksi$ *yield strength of non-prestressed reinforcement*

$A_s := 0.31\ in^2$ *area of non-prestressed longitudinal reinforcement*

$A_{ps} \cdot f_{pe} = 499.72\ kip > 0.4\ \left(A_{ps} \cdot f_{pu} + A_s \cdot f_y\right) = 335.54\ kip$ *ACI 318-19 [22.5.6.3.1]*

$V_{ci} := 2 \cdot \lambda \cdot \sqrt{f_c \cdot psi} \cdot b_w \cdot d = 80.65\ kip$ *flexure-shear strength ACI 318-19 [22.5.6.3.1c]*

V_{cw} calculation:

$f_{pc} := \frac{F_e}{A} = 807.6\ psi$ *compressive stress in concrete at centroid of beam due to prestress*

$V_{cw} := \left(3.5\ \lambda \cdot \sqrt{f_c \cdot psi} + 0.3\ f_{pc}\right)\ b_w \cdot d_p = 222.34\ kip$ *web-shear strength*

Shear Capacity: (2/5)

$a_1 = 68\ in$
$b_1 = 416\ in$
$x_1 := x_1 - 7\ in = 85\ in$

V_{ci} calculation Test 1: (using max load from testing)

$P_{max1} = 424\ kip$

$V_{d1} := \text{abs}\left(\left(w + w_{deck}\right)\left(\frac{L_c}{2} - x_1\right)\right) = 20.39\ kip$ *shear due to DL (uniform SW beam and SW deck)*

$V_{u1} := \left(\frac{\left(\frac{P_{max1}}{2}\right)}{L_c} \cdot \left(L_c - a_1 + b_1\right)\right) = 350.68\ kip$ *shear due to ultimate load (from test)*

$V_{i1} := V_{u1} - V_{d1} = 330.28\ kip$

$M_{u1} := \frac{\left(\frac{P_{max1}}{2}\right)}{L} \cdot \left(L_c - b_1 + a_1\right) \cdot b_1 = 2476.7\ kip \cdot ft$ *moment due to ultimate load (from test)*

$M_{d1} := \frac{\left(w + w_{deck}\right) \cdot x_1}{2}\left(L_c - x_1\right) = 178.38\ kip \cdot ft$ *moment due to DL (uniform SW beam and SW deck*

$M_{max1} := M_{u1} - M_{d1} = 2298.32\ kip \cdot ft$

$f_{d1} := \frac{M_{d1} \cdot C_b'}{I_c'} = 158.9\ psi$

$f_{pec} := \frac{F_e}{A_c'} - \frac{F_e \cdot e \cdot C_b'}{I_c'} = 1.24\ ksi$

$M_{cre1} := \left(\frac{I_c'}{C_b'}\right)\left(6\ \lambda \cdot \sqrt{f_c} \cdot psi + f_{pec} - f_{d1}\right) = 2023.27\ kip \cdot ft$

$V_{ci1} := 0.6\ \lambda \cdot \sqrt{f_c} \cdot psi \cdot b_w \cdot d_p + V_{d1} + \frac{V_{i1} \cdot M_{cre1}}{M_{max1}} = 335.34\ kip$

$V_{c1} := min\left(V_{cw}, V_{ci1}\right) = 222.34\ kip$ *nominal shear strength provided by concrete for Test 1*

Shear Capacity: (3/5)

$a_2 = 416\ in$
$b_2 = 68\ in$
$x_2 := x_2 - 7\ in = 433\ in$

V_{ci} calculation Test 2: (using max load from testing)

$P_{max2} = 431\ kip$

$V_{d2} := \text{abs}\left(\left(w + w_{deck}\right)\left(\frac{L_c}{2} - x_2\right)\right) = 18.82\ kip$ *shear due to DL (uniform SW beam and SW deck)*

$V_{u2} := \left(\frac{\left(\frac{P_{max2}}{2}\right)}{L_c} \cdot \left(L_c - b_2 + a_2\right)\right) = 356.47\ kip$ *shear due to ultimate load (from test)*

$V_{i2} := V_{u2} - V_{d2} = 337.65\ kip$

$M_{u2} := \frac{\left(\frac{P_{max2}}{2}\right)}{L} \cdot \left(L_c - a_2 + b_2\right) \cdot a_2 = 2517.59\ kip \cdot ft$ *moment due to ultimate load (from test)*

$M_{d2} := \frac{\left(w + w_{deck}\right) \cdot x_2}{2}\left(L_c - x_2\right) = 201.25\ kip \cdot ft$ *moment due to DL (uniform SW beam and SW deck)*

$M_{max2} := M_{u2} - M_{d2} = 2316.34\ kip \cdot ft$

$f_{d2} := \frac{M_{d2} \cdot C_b'}{I_c'} = 179.27\ psi$

$M_{cre2} := \left(\frac{I_c'}{C_b'}\right)\left(6\ \lambda \cdot \sqrt{f_c} \cdot psi + f_{pec} - f_{d2}\right) = 2000.4\ kip \cdot ft$

$V_{ci2} := 0.6\ \lambda \cdot \sqrt{f_c} \cdot psi \cdot b_w \cdot d_p + V_{d2} + \frac{V_{i2} \cdot M_{cre2}}{M_{max2}} = 334.61\ kip$

$V_{c2} := min\left(V_{cw}, V_{ci2}\right) = 222.34\ kip$ *nominal shear strength provided by concrete for Test 2*

Shear Capacity: (4/5)

V_{ci} calculation Test 3: (using max load from testing)

$a_3 = 245\ in$
$b_3 = 239\ in$
$x_3 := x_3 - 7\ in = 262\ in$

$P_{max3} = 341\ kip$

$V_{d3} := \text{abs}\left(\left(w + w_{deck}\right)\left(\frac{L_c}{2} - x_3\right)\right) = 0.45\ kip$ *shear due to DL (uniform SW beam and SW deck)*

$V_{u3} := \left(\frac{\left(\frac{P_{max3}}{2}\right)}{L_c} \cdot \left(L_c - b_3 + a_3\right)\right) = 172.42\ kip$ *shear due to ultimate load (from test)*

$V_{i3} := V_{u3} - V_{d3} = 171.97\ kip$

$M_{u3} := \frac{\left(\frac{P_{max3}}{2}\right)}{L} \cdot \left(L_c - a_3 + b_3\right) \cdot a_3 = 3353.53\ kip \cdot ft$ *moment due to ultimate load (from test)*

$M_{d3} := \frac{\left(w + w_{deck}\right) \cdot x_3}{2}\left(L_c - x_3\right) = 332.11\ kip \cdot ft$ *moment due to DL (uniform SW beam and SW deck)*

$M_{max3} := M_{u3} - M_{d3} = 3021.43\ kip \cdot ft$

$f_{d3} := \frac{M_{d3} \cdot C_b'}{I_c'} = 295.84\ psi$

$M_{cre3} := \left(\frac{I_c'}{C_b'}\right)\left(6\ \lambda \cdot \sqrt{f_c} \cdot psi + f_{pec} - f_{d3}\right) = 1869.54\ kip \cdot ft$

$V_{ci3} := 0.6\ \lambda \cdot \sqrt{f_c} \cdot psi \cdot b_w \cdot d_p + V_{d3} + \frac{V_{i3} \cdot M_{cre3}}{M_{max3}} = 131.05\ kip$

$V_{c3} := min\left(V_{cw}, V_{ci3}\right) = 131.05\ kip$ *nominal shear strength provided by concrete for Test 3*

Shear Capacity: (5/5)

V_{se} calculation: (for tests near ends 24-in < x < 144-in)

$s_e := 12\ \textit{in}$ *spacing for #5 stirrups for 24-in < x < 144-in*

$A_v := 2 \cdot (A_s) = 0.62\ \textit{in}^2$ *area of shear reinforcement (2#5 bars)*

$V_{se} := \frac{A_v \cdot f_y \cdot d}{s_e} = 173.17\ \textit{kip}$ *nominal shear strength provided by shear reinforcement (for tests near end)*

V_{sm} calculation: (for tests near midspan 144-in < x < 402-in)

$s_m := 16\ \textit{in}$ *spacing for #5 stirrups for 144-in < x < 402-in*

$A_v = 0.62\ \textit{in}^2$ *area of shear reinforcement (2#5 bars)*

$V_{sm} := \frac{A_v \cdot f_y \cdot d}{s_m} = 129.87\ \textit{kip}$ *nominal shear strength provided by shear reinforcement (for tests near midspan)*

V_n **nominal one-way shear capacity:**

$V_{n1} := V_{c1} + V_{se} = 395.5\ \textit{kip}$ *nominal shear capacity for Test 1 North end*

$V_{n2} := V_{c2} + V_{se} = 395.5\ \textit{kip}$ *nominal shear capacity for Test 2 South end*

$V_{n3} := V_{c3} + V_{sm} = 260.93\ \textit{kip}$ *nominal shear capacity for Test 3 near midspan*

Ultimate Loads from Shear Calculations: (four-point bending tests)

Test 2.1:

$a_1 = 5.67\ ft$

$b_1 = 34.67\ ft$

$P_{ult1v} := 2 \cdot \frac{V_{n1} \cdot L_c}{(L_c - a_1 + b_1)} = 478.2\ kip$ *ultimate load based on shear capacity*

Test 2.2:

$a_2 = 34.67\ ft$

$b_2 = 5.67\ ft$

$P_{ult2v} := 2 \cdot \frac{V_{n2} \cdot L_c}{(L_c - b_2 + a_2)} = 478.2\ kip$ *ultimate load based on shear capacity*

Test 2.3:

$a_3 = 20.42\ ft$

$b_3 = 19.92\ ft$

$P_{ult3v} := 2 \cdot \frac{V_{n3} \cdot L_c}{(L_c - b_3 + a_3)} = 516.04\ kip$ *ultimate load based on shear capacity*

Failure Mode Based on Comparing Maximum Load to Maximum Theoretical Capacities:

	Test 1 (Shear):	Test 2 (Shear):	Test 3 (Flexure):
Experimental Maximum Load:	$P_{max1} = 424$ ***kip***	$P_{max2} = 431$ ***kip***	$P_{max3} = 341$ ***kip***
Theoretical Maximum Load (Flexure):	$P_{ult1m} = 391.25$ ***kip***	$P_{ult2m} = 396.98$ ***kip***	$P_{ult3m} = 340.36$ ***kip***
Theoretical Maximum Load (Shear):	$P_{ult1v} = 478.2$ ***kip***	$P_{ult2v} = 478.2$ ***kip***	$P_{ult3v} = 516.04$ ***kip***
	$x_1 = 85$ ***in***	$L_c - x_2 = 99$ ***in***	$x_3 = 262$ ***in***

APPENDIX I. GIRDER 3 CALCULATIONS

GDOT Girders: Conforming BT-54 Composite Capacity (Theoretical) Calculations

Variables: **Ana Contreras**

$f_c := 14596$ *girder concrete compressive strength (at time of test)*

$f_{ci} := 10085$ *girder concrete compressive strength (at time of strand release, per SCP)*

$A := 659\ in^2$ *girder cross-sectional area*

$I := 268077\ in^4$ *girder moment of inertia*

$E_c := 57 \cdot \sqrt{f_c} \cdot ksi = 6886.39\ ksi$ *girder modulus of elasticity*

$L := 45.5\ ft$ *girder length*

$h := 54\ in$ *girder height*

$C_b := -27.63\ in$ *girder lower neutral axis distance*

$C_t := h + C_b = 26.37\ in$ *girder upper neutral axis distance*

$S_b := \frac{I}{-C_b} = 9702.39\ in^3$ *girder bottom section modulus*

$S_t := \frac{I}{C_t} = 10165.98\ in^3$ *girder top section modulus*

$e := -19.99\ in$ *girder eccentricity (14 bottom strands, 4 top strands)*

$A_s := 0.217\ in^2$ *strand cross-sectional area (one strand)*

$\#strands := 14$ *number of strands (excluding top 4 strands)*

$A_{ps} := \#strands \cdot A_s = 3.04\ in^2$ *strand total area of steel*

$f_{pu} := 270\ ksi$ *strand ultimate prestressing stress*

$f_y := 0.9 \cdot f_{pu} = 243\ ksi$ *strand yielding prestressing stress (assumed)*

$E_{ps} := 28700\ ksi$ *strand modulus of elasticity*

$F_{se} := 0.75 \cdot f_{pu} \cdot A_s = 43.94\ kip$ *strand effective force (75%)*

Variables:

$f_{cdeck} := 6951$ *deck concrete compressive strength (at time of test)*

$h_f := 8\ in$ *deck thickness (not including extra 1.5 inch chamfer)*

$E_{cdeck} := 57 \cdot \sqrt{f_{cdeck}} \cdot ksi = 4752.24\ ksi$ *MOE of deck*

$E_{cbeam} := 57 \cdot \sqrt{f_c} \cdot ksi = 6886.39\ ksi$ *MOE of beam*

$\eta := \frac{E_{cdeck}}{E_{cbeam}} = 0.69$ *modular ratio*

$b_{e1} := \eta \cdot 6\ ft = 4.14\ ft$ *deck effective width 6-ft (transformed to match strength of beam)*

$A_{deck1} := b_{e1} \cdot h_f = 397.49\ in^2$ *deck cross-sectional area, 8-inch thick section (transformed)*

$b_{e2} := \eta \cdot 42\ in = 28.98\ in$ *deck effective width 42-inch (transformed to match strength of beam)*

$A_{deck2} := b_{e2} \cdot 1.5\ in = 43.48\ in^2$ *deck cross-sectional area, 1.5-inch thick section (transformed)*

$\lambda := 1$

$f_r := 7.5 \cdot \lambda \cdot \sqrt{f_c} \cdot psi = 0.91\ ksi$ *rupture stress*

$w := 150\ pcf \cdot A = 686.46\ \frac{lbf}{ft}$ *girder self-weight*

$M_w := \frac{w \cdot L^2}{8} = 177.64\ kip \cdot ft$ *girder self-weight moment*

$w_{deck} := 150\ pcf \cdot ((6\ ft \cdot 8\ in) + (42\ in \cdot 1.5\ in)) = 665.63\ \frac{lbf}{ft}$ *deck self-weight*

$M_{SD} := \frac{w_{deck} \cdot L^2}{8} = 172.25\ kip \cdot ft$ *deck self-weight moment*

Composite Properties Calculations:

Bottom neutral axis distance of composite section

$$C_b' := \frac{\left(A_{deck1} \cdot \left(h + 1.5\ in + \frac{h_f}{2}\right)\right) + \left(A_{deck2} \cdot \left(h + \frac{1.5\ in}{2}\right)\right) + \left(A \cdot -C_b\right)}{A_{deck1} + A_{deck2} + A} = 40.22\ in$$

Top neutral axis distance of composite section

$$C_t' := h + h_f + 1.5\ in - C_b' = 23.28\ in$$

Moment of inertia of composite section

$$I_c' := I + A \cdot \left(C_b' + C_b\right)^2 + \frac{b_{e1} \cdot h_f^3}{12} + A_{deck1} \cdot \left(\left(h + 1.5\ in + \frac{h_f}{2}\right) - C_b'\right)^2 + \frac{b_{e2} \cdot (1.5\ in)^3}{12} + A_{deck2} \cdot \left(\left(h + \frac{1.5\ in}{2}\right) - C_b'\right)^2 = 531595.96\ in^4$$

Cross-sectional area of composite section

$$A_c' := A + \left(h_f \cdot b_{e1}\right) + \left(1.5\ in \cdot b_{e2}\right) = 1099.97\ in^2$$

Radius of gyration of composite section

$$r := \sqrt{\frac{I_c'}{A_c'}} = 21.98\ in \qquad r^2 = 483.28\ in^2$$

Top section modulus of composite section (top of precast member)

$$S_{tc} := \frac{I_c'}{C_t'} = 22833.59\ in^3$$

Bottom section modulus of composite section (bottom of precast member)

$$S_{bc} := \frac{I_c'}{C_b'} = 13217.64\ in^3$$

Top section modulus of composite section (top of slab)

$$S_{tcs} := \frac{I_c'}{C_t' + h_f} = 16994.04\ in^3$$

Bottom section modulus of composite section (bottom of slab)

$$S_{bcs} := \frac{I_c'}{C_t'} = 22833.59\ in^3$$

Losses Calculations BT-54 with Composite Deck (1/3)

Losses Before Release (10 May 2025)

$f_{pJ} := 0.75 \cdot f_{pu} = 202.5$ ksi

$F_J := f_{pJ} \cdot \#strands \cdot A_s + 40$ kip $= 655.2$ kip total force in all 14 strands (plus 4 top strands @ 10 kips each) at time of tension

Relaxation in Strand, R1 (10 May 2024 to 15 May 2024)

$t1 := 1$ $t2 := 120$ $f_{pi}' := f_{pJ} = 202.5$ ksi

$\Delta f_pR1 := f_{pi}' \cdot \left(\frac{\log(t2) - \log(t1)}{45} \right) \cdot \left(\frac{f_{pi}'}{f_y} - 0.55 \right) = 2.65$ ksi

Losses Just After Release (15 May 2024)

$F_i := \left(f_{pJ} - \Delta f_pR1 \right) \cdot \#strands \cdot A_s = 607.14$ kip

$F_j := 0.9 \cdot F_i = 546.43$ kip *assumed 0.9*

Elastic Shortening in Strand, ES (15 May 2025)

$E_{ps} = 28700$ ksi $f_{ci} = 10085$ $E_{ci} := 57000 \cdot \sqrt{f_{ci}} \cdot psi = 5724.17$ ksi

$\eta_i := \frac{E_{ps}}{E_{ci}} = 5.01$

$f_{cs} := \frac{-F_j}{A} - \frac{F_j \cdot e^2}{I} - \frac{M_w \cdot e}{I} = -1.48$ ksi

$\Delta f_pES := -\eta_i \cdot f_{cs} = 7.44$ ksi

Losses Calculations BT-54 with Composite Deck (2/3)

Losses After ~13 Months (10 June 2025) Note: deck casted on 14 February 2025

Creep, CR (15 May 2024 to 10 June 2025)

$K_{cr} := 2$ *for pretensioned members*

$f_{pj} := f_{pJ} - \Delta f_p R1 - \Delta f_p ES = 192.4$ ***ksi***

$P_j := f_{pj} \cdot \#strands \cdot A_s = 584.53$ ***kip***

$f_{cs} := \frac{-P_j}{A} - \frac{P_j \cdot e^2}{I} - \frac{M_w \cdot e}{I} = -1.6$ ***ksi***

$f_{csd} := \frac{-M_{SD} \cdot C_b'}{I_c'} = -0.16$ ***ksi***

$\Delta f_p CR := 0.80 \left(-K_{cr} \cdot \frac{E_{ps}}{E_c} \left(f_{cs} - f_{csd} \right) \right) = 9.62$ ***ksi*** Note: only 80% of total CR because of 405 day age

Shrinkage, SH (15 May 2024 to 10 June 2025)

$RH := 70$ *relative humidity in Atlanta, GA*

$K_{SH} := 1$ *for pretensioned members*

$V := A \cdot L = 359814$ ***in***^{3} *volume of girder*

$S := 2 \cdot A + 2 \cdot h \cdot L + 26$ ***in*** $\cdot L + 42$ ***in*** $\cdot L = 97414$ ***in***^{2} *approximate surface area of girder*

$\varepsilon_{SH} := 8.2 \cdot 10^{-6} \cdot K_{SH} \cdot \left(1 - \frac{0.06}{in} \cdot \frac{V}{S} \right) (100 - RH) = 0.0001915$

$\Delta f_p SH := \varepsilon_{SH} \cdot E_{ps} = 5.5$ ***ksi***

Relaxation in Strand, R2 (15 May 2024 to 28 February 2025)

$t2 = 120$ $t3 := 6937$ $f_{pi}' := f_{pj} = 192.4$ ***ksi***

$\Delta f_p R2 := f_{pi}' \cdot \left(\frac{\log(t3) - \log(t2)}{45} \right) \cdot \left(\frac{f_{pi}'}{f_y} - 0.55 \right) = 1.82$ ***ksi***

Losses Calculations BT-54 with Composite Deck (3/3)

Relaxation in Strand, R3 (28 February 2024 to 10 June 2025, Deck Casted)

$t3 = 6937$ $t4 := 9384$ $f_{pi} := f_{pj} - \Delta f_p R2 + f_{csd} \cdot \frac{E_{ps}}{E_c} = 189.93$ ***ksi***

$\Delta f_p R3 := f_{pi}' \cdot \left(\frac{\log(t4) - \log(t3)}{45} \right) \cdot \left(\frac{f_{pi}'}{f_y} - 0.55 \right) = 0.13$ ***ksi***

Effective Force in Prestress (after losses) 10 June 2025 Test Day

$F_e := \left(f_{pJ} - \Delta f_p R1 - \Delta f_p R2 - \Delta f_p R3 - \Delta f_p ES - \Delta f_p CR - \Delta f_p SH \right) \cdot \#strands \cdot A_s = 532.68$ ***kip***

$Losses := \left(1 - \frac{F_e}{F_J} \right) \cdot 100 = 18.7$ *loss percentage*

$F_{el} := \left(f_{pJ} \cdot \left(1 - \frac{1}{Losses} \right) \right) \cdot A_s = 41.59$ ***kip*** *effective force in individual strand*

$f_{se} := f_{pJ} \cdot \left(1 - \frac{Losses}{100} \right) = 164.63$ ***ksi***

Initial Beam Curvature (1/4):

Curvature due to beam prestress: (negative)

$f_{pe} := f_{se} = 164.63\ ksi$ *refined through previous losses calculations*

$CGS := -C_b + e = 7.64\ in$ *finding CGS from bottom beam*

$\varepsilon_{bi} := \frac{-f_{pe}}{E_{ps}} = -0.0057363$ *strain at CGS due to prestress*

$\varepsilon_{ti} := \frac{\varepsilon_{bi} \cdot C_t}{-e + C_t} = -0.003263$ *strain at top of beam due to prestress*

$h_i := h - CGS = 46.36\ in$ *distance between top of beam and CGS*

$\phi_i := \frac{\varepsilon_{bi} + \varepsilon_{ti}}{h} = -0.0001667\ \frac{1}{in}$ *initial (negative) curvature in beam due to prestress*

Initial Beam Curvature (2/4):

Test 3.1:
Curvature due to beam SW: (negative)

$M_{w1} := \frac{w \cdot x_1}{2} \left(L_c - x_1\right) = 98.75\ \textbf{kip} \cdot \textbf{ft}$ *moment due to beam SW at test location*

$f_{swb1} := \frac{-M_{w1} \cdot e}{I} = 88.36\ \textbf{psi}$ *stress at CGS due to beam SW*

$\varepsilon_{swb1} := \frac{f_{swb1}}{E_c} = 0.00001283$ *strain at CGS due to beam SW*

$f_{swt1} := \frac{M_{w1} \cdot C_t}{I} = 116.56\ \textbf{psi}$ *stress at top of beam due to beam SW*

$\varepsilon_{swt1} := \frac{f_{swt1}}{E_c} = 0.00001693$ *strain at top of beam due to beam SW*

$h_1 := h - CGS = 46.36\ \textbf{in}$ *distance between top of beam and CGS*

$\phi_{1b} := \frac{\varepsilon_{swb1} + \varepsilon_{swt1}}{h_1} = 0.0000006\ \frac{1}{\textbf{in}}$ *initial (positive) curvature in beam due to beam SW*

Curvature due to deck SW: (positive)

$M_{SD1} := \frac{w_{deck} \cdot x_1}{2} \left(L_c - x_1\right) = 95.75\ \textbf{kip} \cdot \textbf{ft}$ *moment due to deck SW at test location*

$f_{deckswb1} := \frac{-M_{SD1} \cdot e}{I} = 85.68\ \textbf{psi}$ *stress at CGS due to deck SW*

$\varepsilon_{deckswb1} := \frac{f_{deckswb1}}{E_c} = 0.00001244$ *strain at CGS due to deck SW*

$f_{deckswt1} := \frac{M_{SD1} \cdot C_t}{I} = 113.03\ \textbf{psi}$ *stress at top of beam due to deck SW*

$\varepsilon_{deckswt1} := \frac{f_{deckswt1}}{E_c} = 0.00001641$ *strain at top of beam due to deck SW*

$h_1 = 46.36\ \textbf{in}$ *distance between top of beam and CGS*

$\phi_{1d} := \frac{\varepsilon_{deckswb1} + \varepsilon_{deckswt1}}{h_1} = 0.0000006224\ \frac{1}{\textbf{in}}$ *initial (positive) curvature in beam due to deck SW*

$\phi_{initial1} := \phi_{1b} + \phi_{1d} + \phi_i = -0.00016539\ \frac{1}{\textbf{in}}$ *total initial (negative) curvature in composite beam prior to Test 3.1*

Initial Beam Curvature (3/4):

Test 3.2:
Curvature due to beam SW: (negative)

$M_{w2} := \frac{w \cdot x_2}{2}\left(L_c - x_2\right) = 112.85\ \textit{kip} \cdot \textit{ft}$ *moment due to beam SW at test location*

$f_{swb2} := \frac{-M_{w2} \cdot e}{I} = 100.98\ \textit{psi}$ *stress at CGS due to beam SW*

$\varepsilon_{swb2} := \frac{f_{swb2}}{E_c} = 0.00001466$ *strain at CGS due to beam SW*

$f_{swt2} := \frac{M_{w2} \cdot C_t}{I} = 133.21\ \textit{psi}$ *stress at top of beam due to beam SW*

$\varepsilon_{swt2} := \frac{f_{swt2}}{E_c} = 0.00001934$ *strain at top of beam due to beam SW*

$h_2 := h_1 = 46.36\ \textit{in}$ *distance between top of beam and CGS*

$\phi_{2b} := \frac{\varepsilon_{swb2} + \varepsilon_{swt2}}{h_2} = 0.0000007\ \frac{1}{\textit{in}}$ *initial (positive) curvature in beam due to beam SW*

Curvature due to deck SW: (positive)

$M_{SD2} := \frac{w_{deck} \cdot x_2}{2}\left(L_c - x_2\right) = 109.43\ \textit{kip} \cdot \textit{ft}$ *moment due to deck SW at test location*

$f_{deckswb2} := \frac{-M_{SD2} \cdot e}{I} = 97.92\ \textit{psi}$ *stress at CGS due to deck SW*

$\varepsilon_{deckswb2} := \frac{f_{deckswb2}}{E_c} = 0.00001422$ *strain at CGS due to deck SW*

$f_{deckswt2} := \frac{M_{SD2} \cdot C_t}{I} = 129.17\ \textit{psi}$ *stress at top of beam due to deck SW*

$\varepsilon_{deckswt2} := \frac{f_{deckswt2}}{E_c} = 0.00001876$ *strain at top of beam due to deck SW*

$h_2 = 46.36\ \textit{in}$ *distance between top of beam and CGS*

$\phi_{2d} := \frac{\varepsilon_{deckswb2} + \varepsilon_{deckswt2}}{h_2} = 0.0000007113\ \frac{1}{\textit{in}}$ *initial (positive) curvature in beam due to deck SW*

$\phi_{initial2} := \phi_{2b} + \phi_{2d} + \phi_i = -0.00016521\ \frac{1}{\textit{in}}$ *total initial (negative) curvature in composite beam prior to Test 3.2*

Initial Beam Curvature (4/4):

Test 3.3:
Curvature due to beam SW: (negative)

$M_{w3} := \frac{w \cdot x_1}{2}\left(L_c - x_1\right) = 98.75\ \textit{kip} \cdot \textit{ft}$ *moment due to beam SW at test location*

$f_{swb3} := \frac{-M_{w1} \cdot e}{I} = 88.36\ \textit{psi}$ *stress at CGS due to beam SW*

$\varepsilon_{swb3} := \frac{f_{swb1}}{E_c} = 0.00001283$ *strain at CGS due to beam SW*

$f_{swt3} := \frac{M_{w1} \cdot C_t}{I} = 116.56\ \textit{psi}$ *stress at top of beam due to beam SW*

$\varepsilon_{swt3} := \frac{f_{swt1}}{E_c} = 0.00001693$ *strain at top of beam due to beam SW*

$h_3 := h_1 = 46.36\ \textit{in}$ *distance between top of beam and CGS*

$\phi_{3b} := \frac{\varepsilon_{swb3} + \varepsilon_{swt3}}{h_3} = 0.0000006\ \frac{1}{\textit{in}}$ *initial (positive) curvature in beam due to beam SW*

Curvature due to deck SW: (positive)

$M_{SD3} := \frac{w_{deck} \cdot x_3}{2}\left(L_c - x_3\right) = 163.53\ \textit{kip} \cdot \textit{ft}$ *moment due to deck SW at test location*

$f_{deckswb3} := \frac{-M_{SD3} \cdot e}{I} = 146.33\ \textit{psi}$ *stress at CGS due to deck SW*

$\varepsilon_{deckswb3} := \frac{f_{deckswb3}}{E_c} = 0.00002125$ *strain at CGS due to deck SW*

$f_{deckswt3} := \frac{M_{SD3} \cdot C_t}{I} = 193.03\ \textit{psi}$ *stress at top of beam due to deck SW*

$\varepsilon_{deckswt3} := \frac{f_{deckswt3}}{E_c} = 0.00002803$ *strain at top of beam due to deck SW*

$h_3 = 46.36\ \textit{in}$ *distance between top of beam and CGS*

$\phi_{3d} := \frac{\varepsilon_{deckswb3} + \varepsilon_{deckswt3}}{h_3} = 0.000001063\ \frac{1}{\textit{in}}$ *initial (positive) curvature in beam due to deck SW*

$\phi_{initial3} := \phi_{3b} + \phi_{3d} + \phi_i = -0.00016495\ \frac{1}{\textit{in}}$ *total initial (negative) curvature in composite beam prior to Test 3.3*

Cracking Moment:

$$M_{cr} := \frac{f_r \cdot I_c'}{C_b'} = 998.05 \ \textit{kip} \cdot \textit{ft}$$

$$\phi_{cr} := \frac{M_{cr}}{E_c \cdot I_c'} = 0.000003272 \ \frac{1}{\textit{in}}$$

$$M_{cr95} := 0.95 \cdot M_{cr} = 948.14 \ \textit{kip} \cdot \textit{ft}$$

$$\phi_{cr95} := 0.95 \cdot \phi_{cr} = 0.000003108 \ \frac{1}{\textit{in}}$$

Ultimate Moment (1/9):
Test 3.1:

$\varepsilon_{si1} := 0.000333$ *strain measured from test (input)*

$d_1 := h + h_f + 1.5\ in - 2.5\ in = 61\ in$ *depth to centroid of strands from top of composite girder*

$c_1 := 13.92996\ in$ *trial and error iterative c value (input until equilibrium)*

$\varepsilon_{s1.1} := -\varepsilon_{bi} + \varepsilon_{si1} = 0.006069$ *strain in lowest strand level at ultimate (test + effective prestress)*

$\varepsilon_{s2.1} := \frac{\varepsilon_{s1.1} \cdot (d_1 - 2\ in - c_1)}{d_1 - c_1} = 0.00581$ *strain in 2nd strand level at ultimate*

$\varepsilon_{s3.1} := \frac{\varepsilon_{s1.1} \cdot (d_1 - 12\ in - c_1)}{d_1 - c_1} = 0.00452$ *strain in 3rd strand level at ultimate*

$\varepsilon_{s4.1} := \frac{\varepsilon_{s1.1} \cdot (d_1 - 49.5\ in - c_1)}{d_1 - c_1} = -0.000313326$ *strain in top strand level at ultimate*

$\varepsilon_{c1.1} := \frac{\varepsilon_{si1} \cdot c_1}{d_1 - c_1} = 0.0001$ *strain at top of concrete deck at ultimate*

$\varepsilon_{c2.1} := \frac{\varepsilon_{si1} \cdot (c_1 - 8\ in)}{d_1 - c_1} = 0.0000419519$ *strain at top of 1.5-inch deck haunch at ultimate*

$\varepsilon_{c3.1} := \frac{\varepsilon_{si1} \cdot (c_1 - 9.5\ in)}{d_1 - c_1} = 0.00003134$ *strain at top of top flange at ultimate*

$\varepsilon_{c4.1} := \frac{\varepsilon_{si1} \cdot (c_1 - 14\ in)}{d_1 - c_1} = -0.0000004955$ *strain at top of web at ultimate*

$T_{1.1} := 8 \cdot A_s \cdot \varepsilon_{s1.1} \cdot E_{ps} = 302.39\ kip$ *tension force from lowest strand level*

$T_{2.1} := 4 \cdot A_s \cdot \varepsilon_{s2.1} \cdot E_{ps} = 144.77\ kip$ *tension force from 2nd strand level*

$T_{3.1} := 2 \cdot A_s \cdot \varepsilon_{s3.1} \cdot E_{ps} = 56.33\ kip$ *tension force from 3rd strand level*

$\mathbf{T_{4.1}} := \mathbf{if}\left(c_1 > 12\ in, 0\ kip, \left(2 \cdot A_s \cdot \varepsilon_{s4.1} \cdot E_{ps}\right)\right) = 0\ kip$ *tension force from top strand level*

$T_{t1} := T_{1.1} + T_{2.1} + T_{3.1} + \mathbf{T_{4.1}} = 503.49\ kip$ *total tension force from prestress*

Ultimate Moment (2/9):
Test 3.1:

$$C_{1.1} := \begin{cases} \dfrac{(\varepsilon_{c1.1}) \cdot E_{cdeck}}{2} \cdot c_1 \cdot 72\ in & \text{if } c_1 < 8\ in \\ \dfrac{(\varepsilon_{c1.1} + \varepsilon_{c2.1}) \cdot E_{cdeck}}{2} \cdot c_1 \cdot 72\ in & \text{else} \end{cases} = 334.83\ kip$$

compression force from 8-inch concrete deck

$$C_{2.1} := \begin{cases} 0\ kip & \text{if } c_1 \le 8\ in \\ \dfrac{(\varepsilon_{c2.1}) \cdot E_{cdeck}}{2} \cdot c_1 \cdot 43.5\ in & \text{else if } 8\ in < c_1 \le 9.5\ in \\ \dfrac{(\varepsilon_{c2.1} + \varepsilon_{c3.1}) \cdot E_{cdeck}}{2} \cdot c_1 \cdot 43.5\ in & \text{else if } c_1 > 9.5\ in \end{cases} = 105.53\ kip$$

compression force from 1.5-inch concrete deck haunch

$$C_{3.1} := \begin{cases} 0\ kip & \text{if } c_1 \le 9.5\ in \\ \dfrac{(\varepsilon_{c3.1}) \cdot E_c}{2} \cdot c_1 \cdot 42\ in & \text{else if } 9.5\ in < c_1 \le 14\ in \\ \dfrac{(\varepsilon_{c3.1} + \varepsilon_{c4.1}) \cdot E_c}{2} \cdot c_1 \cdot 42\ in & \text{else if } c_1 > 14\ in \end{cases} = 63.13\ kip$$

compression force from 4.5-inch top flange

$$C_{4.1} := \begin{cases} 0\ kip & \text{if } c_1 \le 14\ in \\ \dfrac{(\varepsilon_{c4.1}) \cdot E_c}{2} \cdot c_1 \cdot 6\ in & \text{else} \end{cases} = 0\ kip$$

compression force from web

$$C_{t1} := C_{1.1} + C_{2.1} + C_{3.1} + C_{4.1} = 503.49\ kip$$

compression force from concrete

$$T_{t1} - C_{t1} = -0.00094\ kip$$

equilibrium of forces must = 0 to find c

Ultimate Moment (3/9):

Test 3.1:

$$J_{d1} := 63.5\ in - \left(\frac{T_{1.1} \cdot 2.5\ in + T_{2.1} \cdot 4.5\ in + T_{3.1} \cdot 14.5\ in + \mathbf{T_{4.1}} \cdot 51.5\ in}{T_{t1}} \right) - \frac{c_1}{3} = 54.44\ in$$

$$M_{ult3.1} := A_{ps} \cdot \varepsilon_{s1.1} \cdot E_{ps} \cdot \left(J_{d1} \right) = 2400.72\ kip \cdot ft$$

$$\phi_{ult3.1} := \frac{\varepsilon_{c1.1}}{c_1} = 0.0000071\ \frac{1}{in}$$

Ultimate Moment (4/9):
Test 3.2:

$\varepsilon_{si2} := 0.001542$ *strain measured from test (input)*

$d_2 := h + h_f + 1.5\ in - 2.5\ in = 61\ in$ *depth to centroid of strands from top of composite girder*

$c_2 := 9.6113\ in$ *trial and error iterative c value (input until equilibrium)*

$\varepsilon_{s1.2} := -\varepsilon_{bi} + \varepsilon_{si2} = 0.007278$ *strain in lowest strand level at ultimate (test + effective prestress)*

$$\varepsilon_{s2.2} := \frac{\varepsilon_{s1.2} \cdot \langle d_2 - 2\ in - c_2 \rangle}{d_2 - c_2} = 0.007$$ *strain in 2nd strand level at ultimate*

$$\varepsilon_{s3.2} := \frac{\varepsilon_{s1.2} \cdot \langle d_2 - 12\ in - c_2 \rangle}{d_2 - c_2} = 0.00558$$ *strain in 3rd strand level at ultimate*

$$\varepsilon_{s4.2} := \frac{\varepsilon_{s1.2} \cdot \langle d_2 - 49.5\ in - c_2 \rangle}{d_2 - c_2} = 0.0002675026$$ *strain in top strand level at ultimate*

$$\varepsilon_{c1.2} := \frac{\varepsilon_{si2} \cdot c_2}{d_2 - c_2} = 0.00029$$ *strain at top of concrete deck at ultimate*

$$\varepsilon_{c2.2} := \frac{\varepsilon_{si2} \cdot \langle c_2 - 8\ in \rangle}{d_2 - c_2} = 0.0000483496$$ *strain at top of 1.5-inch deck haunch at ultimate*

$$\varepsilon_{c3.2} := \frac{\varepsilon_{si2} \cdot \langle c_2 - 9.5\ in \rangle}{d_2 - c_2} = 0.0000033397$$ *strain at top of top flange at ultimate*

$$\varepsilon_{c4.2} := \frac{\varepsilon_{si2} \cdot \langle c_2 - 14\ in \rangle}{d_2 - c_2} = -0.00013169$$ *strain at top of web at ultimate*

$T_{1.2} := 8 \cdot A_s \cdot \varepsilon_{s1.2} \cdot E_{ps} = 362.63\ kip$ *tension force from lowest strand level*

$T_{2.2} := 4 \cdot A_s \cdot \varepsilon_{s2.2} \cdot E_{ps} = 174.26\ kip$ *tension force from 2nd strand level*

$T_{3.2} := 2 \cdot A_s \cdot \varepsilon_{s3.2} \cdot E_{ps} = 69.49\ kip$ *tension force from 3rd strand level*

$\mathbf{T_{4.2}} := \mathbf{if}\left(c_2 > 12\ in, 0\ kip, \left(2 \cdot A_s \cdot \varepsilon_{s4.2} \cdot E_{ps}\right)\right) = 3.33\ kip$ *tension force from top strand level*

$T_{t2} := T_{1.2} + T_{2.2} + T_{3.2} + \mathbf{T_{4.2}} = 609.71\ kip$ *total tension force from prestress*

Ultimate Moment (5/9):
Test 3.2:

$$C_{1.2} := \begin{cases} \text{if } c_2 < 8\ \textit{in} \\ \quad \dfrac{(\varepsilon_{c1.2}) \cdot E_{cdeck}}{2} \cdot c_2 \cdot 72\ \textit{in} \\ \text{else} \\ \quad \dfrac{(\varepsilon_{c1.2} + \varepsilon_{c2.2}) \cdot E_{cdeck}}{2} \cdot c_2 \cdot 72\ \textit{in} \end{cases} = 553.72\ \textit{kip}$$

compression force from 8-inch concrete deck

$$C_{2.2} := \begin{cases} \text{if } c_2 \leq 8\ \textit{in} \\ \quad 0\ \textit{kip} \\ \text{else if } 8\ \textit{in} < c_2 \leq 9.5\ \textit{in} \\ \quad \dfrac{(\varepsilon_{c2.2}) \cdot E_{cdeck}}{2} \cdot c_2 \cdot 43.5\ \textit{in} \\ \text{else if } c_2 > 9.5\ \textit{in} \\ \quad \dfrac{(\varepsilon_{c2.2} + \varepsilon_{c3.2}) \cdot E_{cdeck}}{2} \cdot c_2 \cdot 43.5\ \textit{in} \end{cases} = 51.35\ \textit{kip}$$

compression force from 1.5-inch concrete deck haunch

$$C_{3.2} := \begin{cases} \text{if } c_2 \leq 9.5\ \textit{in} \\ \quad 0\ \textit{kip} \\ \text{else if } 9.5\ \textit{in} < c_2 \leq 14\ \textit{in} \\ \quad \dfrac{(\varepsilon_{c3.2}) \cdot E_c}{2} \cdot c_2 \cdot 42\ \textit{in} \\ \text{else if } c_2 > 14\ \textit{in} \\ \quad \dfrac{(\varepsilon_{c3.2} + \varepsilon_{c4.2}) \cdot E_c}{2} \cdot c_2 \cdot 42\ \textit{in} \end{cases} = 4.64\ \textit{kip}$$

compression force from 4.5-inch top flange

$$C_{4.2} := \begin{cases} \text{if } c_2 \leq 14\ \textit{in} \\ \quad 0\ \textit{kip} \\ \text{else} \\ \quad \dfrac{(\varepsilon_{c4.2}) \cdot E_c}{2} \cdot c_2 \cdot 6\ \textit{in} \end{cases} = 0\ \textit{kip}$$

compression force from web

$C_{t2} := C_{1.2} + C_{2.2} + C_{3.2} + C_{4.2} = 609.72\ \textit{kip}$ *compression force from concrete*

$T_{t2} - C_{t2} = -0.007294\ \textit{kip}$ *equilibrium of forces must = 0 to find c*

Ultimate Moment (6/9):

Test 3.2:

$$J_{d2} := 63.5\ in - \left(\frac{T_{1.2} \cdot 2.5\ in + T_{2.2} \cdot 4.5\ in + T_{3.2} \cdot 14.5\ in + \mathbf{T_{4.2}} \cdot 51.5\ in}{T_{t2}} \right) - \frac{c_2}{3} = 55.59\ in$$

$$M_{ult3.2} := A_{ps} \cdot \varepsilon_{s1.2} \cdot E_{ps} \cdot (J_{d2}) = 2939.76\ kip \cdot ft$$

$$\phi_{ult3.2} := \frac{\varepsilon_{c1.2}}{c_2} = 0.00003\ \frac{1}{in}$$

Ultimate Moment (7/9):
Test 3.3:

$\varepsilon_{si3} := 0.002188$ *strain measured from test (input)*

$d_3 := h + h_f + 1.5\ in - 2.5\ in = 61\ in$ *depth to centroid of strands from top of composite girder*

$c_3 := 8.91606\ in$ *trial and error iterative c value (input until equilibrium)*

$\varepsilon_{s1.3} := -\varepsilon_{bi} + \varepsilon_{si3} = 0.007924$ *strain in lowest strand level at ultimate (test + effective prestress)*

$\varepsilon_{s2.3} := \frac{\varepsilon_{s1.3} \cdot (d_3 - 2\ in - c_3)}{d_3 - c_3} = 0.00762$ *strain in 2nd strand level at ultimate*

$\varepsilon_{s3.3} := \frac{\varepsilon_{s1.3} \cdot (d_3 - 12\ in - c_3)}{d_3 - c_3} = 0.0061$ *strain in 3rd strand level at ultimate*

$\varepsilon_{s4.3} := \frac{\varepsilon_{s1.3} \cdot (d_3 - 49.5\ in - c_3)}{d_3 - c_3} = 0.0003931353$ *strain in top strand level at ultimate*

$\varepsilon_{c1.3} := \frac{\varepsilon_{si3} \cdot c_3}{d_3 - c_3} = 0.00037$ *strain at top of concrete deck at ultimate*

$\varepsilon_{c2.3} := \frac{\varepsilon_{si3} \cdot (c_3 - 8\ in)}{d_3 - c_3} = 0.0000384829$ *strain at top of 1.5-inch deck haunch at ultimate*

$\varepsilon_{c3.3} := \frac{\varepsilon_{si3} \cdot (c_3 - 9.5\ in)}{d_3 - c_3} = -0.0000245308$ *strain at top of top flange at ultimate*

$\varepsilon_{c4.3} := \frac{\varepsilon_{si3} \cdot (c_3 - 14\ in)}{d_3 - c_3} = -0.0002135718$ *strain at top of web at ultimate*

$T_{1.3} := 8 \cdot A_s \cdot \varepsilon_{s1.3} \cdot E_{ps} = 394.82\ kip$ *tension force from lowest strand level*

$T_{2.3} := 4 \cdot A_s \cdot \varepsilon_{s2.3} \cdot E_{ps} = 189.83\ kip$ *tension force from 2nd strand level*

$T_{3.3} := 2 \cdot A_s \cdot \varepsilon_{s3.3} \cdot E_{ps} = 75.96\ kip$ *tension force from 3rd strand level*

$\mathbf{T_{4.3}} := \mathbf{if}\left(c_3 \geq 12\ in, 0\ kip, \left(2 \cdot A_s \cdot \varepsilon_{s4.3} \cdot E_{ps}\right)\right) = 4.9\ kip$ *tension force from top strand level*

$T_{t3} := T_{1.3} + T_{2.3} + T_{3.3} + \mathbf{T_{4.3}} = 665.5\ kip$ *total tension force from prestress*

Ultimate Moment (8/9):
Test 3.3:

$$C_{1.3} := \text{if } c_3 < 8\ in \quad \left\| \frac{(\varepsilon_{c1.3}) \cdot E_{cdeck}}{2} \cdot c_3 \cdot 72\ in \right. \quad \text{else} \quad \left\| \frac{(\varepsilon_{c1.3} + \varepsilon_{c2.3}) \cdot E_{cdeck}}{2} \cdot c_3 \cdot 72\ in \right. = 630.03\ kip$$

compression force from 8-inch concrete deck

$$C_{2.3} := \text{if } c_3 \leq 8\ in \quad \| 0\ kip \quad \text{else if } 8\ in < c_3 \leq 9.5\ in \quad \left\| \frac{(\varepsilon_{c2.3}) \cdot E_{cdeck}}{2} \cdot c_3 \cdot 43.5\ in \right. \quad \text{else if } c_3 > 9.5\ in \quad \left\| \frac{(\varepsilon_{c2.3} + \varepsilon_{c3.3}) \cdot E_{cdeck}}{2} \cdot c_3 \cdot 43.5\ in \right. = 35.46\ kip$$

compression force from 1.5-inch concrete deck haunch

$$C_{3.3} := \text{if } c_3 \leq 9.5\ in \quad \| 0\ kip \quad \text{else if } 9.5\ in < c_3 \leq 14\ in \quad \left\| \frac{(\varepsilon_{c3.3}) \cdot E_c}{2} \cdot c_3 \cdot 42\ in \right. \quad \text{else if } c_3 > 14\ in \quad \left\| \frac{(\varepsilon_{c3.3} + \varepsilon_{c4.3}) \cdot E_c}{2} \cdot c_3 \cdot 42\ in \right. = 0\ kip$$

compression force from 4.5-inch top flange

$$C_{4.3} := \text{if } c_3 \leq 14\ in \quad \| 0\ kip \quad \text{else} \quad \left\| \frac{(\varepsilon_{c4.3}) \cdot E_c}{2} \cdot c_3 \cdot 6\ in \right. = 0\ kip$$

compression force from web

$$C_{t3} := C_{1.3} + C_{2.3} + C_{3.3} + C_{4.3} = 665.5\ kip$$

compression force from concrete

$$T_{t3} - C_{t3} = 0.003919\ kip$$

equilibrium of forces must = 0 to find c

Ultimate Moment (9/9):

Test 3.3:

$$J_{d3} := 63.5\ in - \left(\frac{T_{1.3} \cdot 2.5\ in + T_{2.3} \cdot 4.5\ in + T_{3.3} \cdot 14.5\ in + \mathbf{T_{4.3}} \cdot 51.5\ in}{T_{i3}} \right) - \frac{c_3}{3} = 55.73\ in$$

$$M_{ult3.3} := A_{ps} \cdot \varepsilon_{s1.3} \cdot E_{ps} \cdot \langle J_{d3} \rangle = 3208.63\ kip \cdot ft$$

$$\phi_{ult3.3} := \frac{\varepsilon_{c1.3}}{c_3} = 0.000042\ \frac{1}{in}$$

Theoretical Moment-Curvature Overview:

$M_{cr} = 998.05\ kip \cdot ft$ $M_{ult3.2} = 2939.76\ kip \cdot ft$

$\phi_{cr} = 0.000003272\ \frac{1}{in}$ $\phi_{ult3.2} = 0.00003\ \frac{1}{in}$

$M_{ult3.1} = 2400.72\ kip \cdot ft$ $M_{ult3.3} = 3208.63\ kip \cdot ft$

$\phi_{ult3.1} = 0.000007\ \frac{1}{in}$ $\phi_{ult3.3} = 0.000042\ \frac{1}{in}$

Ultimate Loads from Moment Calculations: (four-point bending tests)

Test 3.1:

$a_1 = 5.9\ ft$

$b_1 = 34.44\ ft$

$P_{ult1m} := 2 \cdot \frac{L_c \cdot M_{ult3.1}}{b_1 \cdot (a_1 + L_c - b_1)} = 391.42\ kip$ *ultimate load based on moment capacity*

Test 3.2:

$a_2 = 32.92\ ft$

$b_2 = 7.42\ ft$

$P_{ult2m} := 2 \cdot \frac{L_c \cdot M_{ult3.2}}{a_2 \cdot (b_2 + L_c - a_2)} = 420.46\ kip$ *ultimate load based on moment capacity*

Test 3.3:

$a_3 = 20.17\ ft$

$b_3 = 20.17\ ft$

$P_{ult3m} := 2 \cdot \frac{L_c \cdot M_{ult3.3}}{a_3 \cdot (b_3 + L_c - a_3)} = 318.21\ kip$ *ultimate load based on moment capacity*

Theoretical Strut and Tie Cracking Capacity: (1/) (AASHTO C5.8.2.2-1)

$d := 54\ in + 9.5\ in = 63.5\ in$

$b_w := 6\ in$

$V_{cr1} := \left(0.2 - 0.1\left(\frac{a_1}{d}\right)\right) \cdot \sqrt{\frac{f_c}{1000}} \cdot ksi \cdot b_w \cdot d = 128.94\ kip$

$V_{cr2} := \left(0.2 - 0.1\left(\frac{L_c - L_{spr} - a_2}{d}\right)\right) \cdot \sqrt{\frac{f_c}{1000}} \cdot ksi \cdot b_w \cdot d = 87.11\ kip$

$V_{cr3} := \max\left(\left(0.2 - 0.1\left(\frac{L_c - L_{spr} - a_3}{d}\right)\right), 0.0632\right) \cdot \sqrt{\frac{f_c}{1000}} \cdot ksi \cdot b_w \cdot d = 91.99\ kip$

Shear Capacity: (1/5)

Prestress Transfer/Development Lengths:

$d_b := 0.6\ in$ *diameter of prestressing strand*

$L_{tr} := min\left(50 \cdot d_b, \left(\frac{f_{pe}}{3000\ psi}\right) \cdot d_b\right) = 30\ in$ *transfer length*

$f_{ps} := \varepsilon_{s1.3} \cdot E_{ps} = 227.43\ ksi$

$L_f := \left(\frac{f_{ps} - f_{pe}}{1000\ psi}\right) \cdot d_b = 37.68\ in$

$L_d := L_{tr} + L_f = 5.64\ ft$ *development length*

V_c calculation:

Minimum V_{ci} calculation:

$d_p := \max\left(h + h_f + 1.5\ in - CGS, 0.8\ \left(h + h_f + 1.5\ in\right)\right) = 55.86\ in$ *distance from CGS to max compression fiber*

$f_{ce} := f_{pe} = 164.63\ ksi$ *effective prestress stress*

$b_w := 6\ in$ *web width*

$d := d_p = 55.86\ in$ *distance from CGS to max compression fiber*

$f_y := 60\ ksi$ *yield strength of non-prestressed reinforcement*

$A_s := 0.31\ in^2$ *area of non-prestressed longitudinal reinforcement*

$A_{ps} \cdot f_{pe} = 500.16\ kip > 0.4\ \left(A_{ps} \cdot f_{pu} + A_s \cdot f_y\right) = 335.54\ kip$ *ACI 318-19 [22.5.6.3.1]*

$V_{ci} := 2 \cdot \lambda \cdot \sqrt{f_c} \cdot psi \cdot b_w \cdot d = 80.98\ kip$ *flexure-shear strength ACI 318-19 [22.5.6.3.1c]*

V_{cw} calculation:

$f_{pc} := \frac{F_e}{A} = 808.31\ psi$ *compressive stress in concrete at centroid of composite section due to prestress*

$V_{cw} := \left(3.5\ \lambda \cdot \sqrt{f_c} \cdot psi + 0.3\ f_{pc}\right)\ b_w \cdot d_p = 223\ kip$ *web-shear strength*

Shear Capacity: (2/5)

$a_1 = 70.75\ in$
$b_1 = 413.25\ in$
$x_1 := x_1 - 7\ in = 87.75\ in$

V_{ci} calculation Test 1: (using max load from testing)

$P_{max1} = 431\ kip$

$V_{d1} := \text{abs}\left(\left(w + w_{deck}\right)\left(\frac{L_c}{2} - x_1\right)\right) = 20.08\ kip$ *shear due to DL (uniform SW beam and SW deck)*

$V_{u1} := \left(\frac{\left(\frac{P_{max1}}{2}\right)}{L_c} \cdot \left(L_c - a_1 + b_1\right)\right) = 354.24\ kip$ *shear due to ultimate load (from test)*

$V_{i1} := V_{u1} - V_{d1} = 334.15\ kip$

$M_{u1} := \frac{\left(\frac{P_{max1}}{2}\right)}{L} \cdot \left(L_c - b_1 + a_1\right) \cdot b_1 = 2575.7\ kip \cdot ft$ *moment due to ultimate load (from test)*

$M_{d1} := \frac{\left(w + w_{deck}\right) \cdot x_1}{2}\left(L_c - x_1\right) = 183.01\ kip \cdot ft$ *moment due to DL (uniform SW beam and SW deck)*

$M_{max1} := M_{u1} - M_{d1} = 2392.69\ kip \cdot ft$

$f_{d1} := \frac{M_{d1} \cdot C_b'}{I_c'} = 166.15\ psi$

$f_{pec} := \frac{F_e}{A_c'} - \frac{F_e \cdot e \cdot C_b'}{I_c'} = 1.29\ ksi$

$M_{cre1} := \left(\frac{I_c'}{C_b'}\right)\left(6\ \lambda \cdot \sqrt{f_c} \cdot psi + f_{pec} - f_{d1}\right) = 2036.17\ kip \cdot ft$

$V_{ci1} := 0.6\ \lambda \cdot \sqrt{f_c} \cdot psi \cdot b_w \cdot d_p + V_{d1} + \frac{V_{i1} \cdot M_{cre1}}{M_{max1}} = 328.74\ kip$

$V_{c1} := min\left(V_{cw}, V_{ci1}\right) = 223\ kip$ *nominal shear strength provided by concrete for Test 1*

Shear Capacity: (3/5)

$a_2 = 395\ in$
$b_2 = 89\ in$
$x_2 := x_2 - 7\ in = 412\ in$

V_{ci} calculation Test 2: (using max load from testing)

$P_{max2} = 410\ kip$

$V_{d2} := \text{abs}\left(\left(w + w_{deck}\right)\left(\frac{L_c}{2} - x_2\right)\right) = 16.45\ kip$ *shear due to DL (uniform SW beam and SW deck)*

$V_{u2} := \left(\frac{\left(\frac{P_{max2}}{2}\right)}{L_c} \cdot \left(L_c - b_2 + a_2\right)\right) = 322.91\ kip$ *shear due to ultimate load (from test)*

$V_{i2} := V_{u2} - V_{d2} = 306.46\ kip$

$M_{u2} := \frac{\left(\frac{P_{max2}}{2}\right)}{L} \cdot \left(L_c - a_2 + b_2\right) \cdot a_2 = 2793.09\ kip \cdot ft$ *moment due to ultimate load (from test)*

$M_{d2} := \frac{\left(w + w_{deck}\right) \cdot x_2}{2}\left(L_c - x_2\right) = 232.11\ kip \cdot ft$ *moment due to DL (uniform SW beam and SW deck)*

$M_{max2} := M_{u2} - M_{d2} = 2560.99\ kip \cdot ft$

$f_{d2} := \frac{M_{d2} \cdot C_b'}{I_c'} = 210.73\ psi$

$M_{cre2} := \left(\frac{I_c'}{C_b'}\right)\left(6\ \lambda \cdot \sqrt{f_c} \cdot psi + f_{pec} - f_{d2}\right) = 1987.08\ kip \cdot ft$

$V_{ci2} := 0.6\ \lambda \cdot \sqrt{f_c} \cdot psi \cdot b_w \cdot d_p + V_{d2} + \frac{V_{i2} \cdot M_{cre2}}{M_{max2}} = 278.53\ kip$

$V_{c2} := min\left(V_{cw}, V_{ci2}\right) = 223\ kip$ *nominal shear strength provided by concrete for Test 2*

Shear Capacity: (4/5)

$a_3 = 242\ in$
$b_3 = 242\ in$
$x_3 := x_3 - 7\ in = 259\ in$

V_{ci} calculation Test 3: (using max load from testing)

$P_{max3} = 330\ kip$

$V_{d3} := \text{abs}\left(\left(w + w_{deck}\right)\left(\frac{L_c}{2} - x_3\right)\right) = 0.79\ kip$ *shear due to DL (uniform SW beam and SW deck)*

$V_{u3} := \left(\frac{\left(\frac{P_{max3}}{2}\right)}{L_c} \cdot \left(L_c - b_3 + a_3\right)\right) = 165\ kip$ *shear due to ultimate load (from test)*

$V_{i3} := V_{u3} - V_{d3} = 164.21\ kip$

$M_{u3} := \frac{\left(\frac{P_{max3}}{2}\right)}{L} \cdot \left(L_c - a_3 + b_3\right) \cdot a_3 = 3242.18\ kip \cdot ft$ *moment due to ultimate load (from test)*

$M_{d3} := \frac{\left(w + w_{deck}\right) \cdot x_3}{2}\left(L_c - x_3\right) = 331.95\ kip \cdot ft$ *moment due to DL (uniform SW beam and SW deck)*

$M_{max3} := M_{u3} - M_{d3} = 2910.23\ kip \cdot ft$

$f_{d3} := \frac{M_{d3} \cdot C_b'}{I_c'} = 301.37\ psi$

$M_{cre3} := \left(\frac{I_c'}{C_b'}\right)\left(6\ \lambda \cdot \sqrt{f_c} \cdot psi + f_{pec} - f_{d3}\right) = 1887.24\ kip \cdot ft$

$V_{ci3} := 0.6\ \lambda \cdot \sqrt{f_c} \cdot psi \cdot b_w \cdot d_p + V_{d3} + \frac{V_{i3} \cdot M_{cre3}}{M_{max3}} = 131.57\ kip$

$V_{c3} := min\left(V_{cw}, V_{ci3}\right) = 131.57\ kip$ *nominal shear strength provided by concrete for Test 3*

Shear Capacity: (5/5)

V_{se} calculation: (for tests near ends 24-in < x < 144-in)

$s_e := 12\ in$ *spacing for #5 stirrups for 24-in < x < 144-in*

$A_v := 2 \cdot (A_s) = 0.62\ in^2$ *area of shear reinforcement (2#5 bars)*

$V_{se} := \frac{A_s \cdot f_y \cdot d}{s_e} = 86.58\ kip$ *nominal shear strength provided by shear reinforcement (for tests near end)*

V_{sm} calculation: (for tests near midspan 144-in < x < 402-in)

$s_m := 16\ in$ *spacing for #5 stirrups for 144-in < x < 402-in*

$A_v = 0.62\ in^2$ *area of shear reinforcement (2#5 bars)*

$V_{sm} := \frac{A_v \cdot f_y \cdot d}{s_m} = 129.87\ kip$ *nominal shear strength provided by shear reinforcement (for tests near midspan)*

V_n **nominal one-way shear capacity:**

$V_{n1} := V_{c1} + V_{se} = 309.58\ kip$ *nominal shear capacity for Test 1 North end*

$V_{n2} := V_{c2} + V_{se} = 309.58\ kip$ *nominal shear capacity for Test 2 South end*

$V_{n3} := V_{c3} + V_{sm} = 261.45\ kip$ *nominal shear capacity for Test 3 near midspan*

Ultimate Loads from Shear Calculations: (four-point bending tests)

Test 3.1:

$a_1 = 5.9\ ft$

$b_1 = 34.44\ ft$

$P_{ult1v} := 2 \cdot \frac{V_{n1} \cdot L_c}{\langle L_c - a_1 + b_1 \rangle} = 376.66\ kip$ *ultimate load based on shear capacity*

Test 3.2:

$a_2 = 32.92\ ft$

$b_2 = 7.42\ ft$

$P_{ult2v} := 2 \cdot \frac{V_{n2} \cdot L_c}{\langle L_c - b_2 + a_2 \rangle} = 393.07\ kip$ *ultimate load based on shear capacity*

Test 3.3:

$a_3 = 20.17\ ft$

$b_3 = 20.17\ ft$

$P_{ult3v} := 2 \cdot \frac{V_{n3} \cdot L_c}{\langle L_c - b_3 + a_3 \rangle} = 522.89\ kip$ *ultimate load based on shear capacity*

Failure Mode Based on Comparing Maximum Load to Maximum Theoretical Capacities:

	Test 1 (Shear):	Test 2 (Shear):	Test 3 (Flexure):
Experimental Maximum Load:	$P_{max1} = 431$ ***kip***	$P_{max2} = 410$ ***kip***	$P_{max3} = 330$ ***kip***
Theoretical Maximum Load (Flexure):	$P_{ult1m} = 391.42$ ***kip***	$P_{ult2m} = 420.46$ ***kip***	$P_{ult3m} = 318.21$ ***kip***
Theoretical Maximum Load (Shear):	$P_{ult1v} = 376.66$ ***kip***	$P_{ult2v} = 393.07$ ***kip***	$P_{ult3v} = 522.89$ ***kip***
	$x_1 = 87.75$ ***in***	$L_c - x_2 = 120$ ***in***	$x_3 = 259$ ***in***

APPENDIX J. GIRDER 4 CALCULATIONS

GDOT Girders: Conforming BT-54 Composite Capacity (Theoretical) Calculations

Variables: **Ana Contreras**

$f_c := 12619$ *girder concrete compressive strength (at time of test)*

$f_{ci} := 8070$ *girder concrete compressive strength (at time of strand release, per SCP)*

$A := 659\ in^2$ *girder cross-sectional area*

$I := 268077\ in^4$ *girder moment of inertia*

$E_c := 57 \cdot \sqrt{f_c} \cdot ksi = 6403.06\ ksi$ *girder modulus of elasticity*

$L := 45.5\ ft$ *girder length*

$h := 54\ in$ *girder height*

$C_b := -27.63\ in$ *girder lower neutral axis distance*

$C_t := h + C_b = 26.37\ in$ *girder upper neutral axis distance*

$S_b := \frac{I}{-C_b} = 9702.39\ in^3$ *girder bottom section modulus*

$S_t := \frac{I}{C_t} = 10165.98\ in^3$ *girder top section modulus*

$e := -19.99\ in$ *girder eccentricity (14 bottom strands, 4 top strands)*

$A_s := 0.217\ in^2$ *strand cross-sectional area (one strand)*

$\#strands := 14$ *number of strands (excluding top 4 strands)*

$A_{ps} := \#strands \cdot A_s = 3.04\ in^2$ *strand total area of steel*

$f_{pu} := 270\ ksi$ *strand ultimate prestressing stress*

$f_y := 0.9 \cdot f_{pu} = 243\ ksi$ *strand yielding prestressing stress (assumed)*

$E_{ps} := 28700\ ksi$ *strand modulus of elasticity*

$F_{se} := 0.75 \cdot f_{pu} \cdot A_s = 43.94\ kip$ *strand effective force (75%)*

Variables:

$f_{cdeck} := 6178$ *deck concrete compressive strength (at time of test)*

$h_f := 8\ in$ *deck thickness (not including extra 1.5 inch chamfer)*

$E_{cdeck} := 57 \cdot \sqrt{f_{cdeck}} \cdot ksi = 4480.21\ ksi$ *MOE of deck*

$E_{cbeam} := 57 \cdot \sqrt{f_c} \cdot ksi = 6403.06\ ksi$ *MOE of beam*

$\eta := \frac{E_{cdeck}}{E_{cbeam}} = 0.7$ *modular ratio*

$b_{e1} := \eta \cdot 6\ ft = 4.2\ ft$ *deck effective width 6-ft (transformed to match strength of beam)*

$A_{deck1} := b_{e1} \cdot h_f = 403.03\ in^2$ *deck cross-sectional area, 8-inch thick section (transformed)*

$b_{e2} := \eta \cdot 42\ in = 29.39\ in$ *deck effective width 42-inch (transformed to match strength of beam)*

$A_{deck2} := b_{e2} \cdot 1.5\ in = 44.08\ in^2$ *deck cross-sectional area, 1.5-inch thick section (transformed)*

$\lambda := 1$

$f_r := 7.5 \cdot \lambda \cdot \sqrt{f_c} \cdot psi = 0.84\ ksi$ *rupture stress*

$w := 150\ pcf \cdot A = 686.46\ \frac{lbf}{ft}$ *girder self-weight*

$M_w := \frac{w \cdot L^2}{8} = 177.64\ kip \cdot ft$ *girder self-weight moment*

$w_{deck} := 150\ pcf \cdot ((6\ ft \cdot 8\ in) + (42\ in \cdot 1.5\ in)) = 665.63\ \frac{lbf}{ft}$ *deck self-weight*

$M_{SD} := \frac{w_{deck} \cdot L^2}{8} = 172.25\ kip \cdot ft$ *deck self-weight moment*

Variables:

$L_c := L - 14\ in = 44.33\ ft$ *clear distance between end roller supports*

$L_{spr} := 48\ in$ *distance between two point loads (spreader beam roller supports clear distance)*

Test 4.1: $P_{max1} := 500\ kip$

$x_1 := 120\ in - 7\ in = 113\ in$ *distance from point load to end of beam*

$a_1 := x_1 - \frac{L_{spr}}{2} = 7.42\ ft$

$a_1 = 89\ in$ *clear distance from center of north bearing to first point load*

$b_1 := L_c - a_1 - L_{spr} = 32.92\ ft$

$b_1 = 395\ in$ *clear distance from center of south bearing to second point load*

Test 4.2: $P_{max2} := 500\ kip$

$x_2 := 45.5\ ft - 120\ in - 7\ in = 419\ in$ *distance from point load to end of beam*

$a_2 := x_2 - \frac{L_{spr}}{2} = 32.92\ ft$

$a_2 = 395\ in$ *clear distance from center of north bearing to first point load*

$b_2 := L_c - a_2 - L_{spr} = 7.42\ ft$

$b_2 = 89\ in$ *clear distance from center of south bearing to second point load*

Test 4.3: $P_{max3} := 331\ kip$

$x_3 := L - 231.5\ in - 7\ in = 307.5\ in$ *distance from point load to end of beam*

$a_3 := x_3 - \frac{L_{spr}}{2} = 23.63\ ft$

$a_3 = 283.5\ in$ *clear distance from center of north bearing to first point load*

$b_3 := L_c - a_3 - L_{spr} = 16.71\ ft$

$b_3 = 200.5\ in$ *clear distance from center of south bearing to second point load*

Composite Properties Calculations:

Bottom neutral axis distance of composite section

$$C_b' := \frac{\left(A_{deck1} \cdot \left(h + 1.5\ in + \frac{h_f}{2}\right)\right) + \left(A_{deck2} \cdot \left(h + \frac{1.5\ in}{2}\right)\right) + \left(A \cdot -C_b\right)}{A_{deck1} + A_{deck2} + A} = 40.32\ in$$

Top neutral axis distance of composite section

$$C_t' := h + h_f + 1.5\ in - C_b' = 23.18\ in$$

Moment of inertia of composite section

$$I_c' := I + A \cdot \left(C_b' + C_b\right)^2 + \frac{b_{e1} \cdot h_f^3}{12} + A_{deck1} \cdot \left(\left(h + 1.5\ in + \frac{h_f}{2}\right) - C_b'\right)^2 + \frac{b_{e2} \cdot (1.5\ in)^3}{12} + A_{deck2} \cdot \left(\left(h + \frac{1.5\ in}{2}\right) - C_b'\right)^2 = 533798.74\ in^4$$

Cross-sectional area of composite section

$$A_c' := A + \left(h_f \cdot b_{e1}\right) + \left(1.5\ in \cdot b_{e2}\right) = 1106.11\ in^2$$

Radius of gyration of composite section

$$r := \sqrt{\frac{I_c'}{A_c'}} = 21.97\ in \qquad r^2 = 482.59\ in^2$$

Top section modulus of composite section (top of precast member)

$$S_{tc} := \frac{I_c'}{C_t'} = 23031.5\ in^3$$

Bottom section modulus of composite section (bottom of precast member)

$$S_{bc} := \frac{I_c'}{C_b'} = 13238.04\ in^3$$

Top section modulus of composite section (top of slab)

$$S_{tcs} := \frac{I_c'}{C_t' + h_f} = 17121.61\ in^3$$

Bottom section modulus of composite section (bottom of slab)

$$S_{bcs} := \frac{I_c'}{C_t'} = 23031.5\ in^3$$

Losses Calculations BT-54 with Composite Deck (1/3)

Losses Before Release (10 May 2025)

$f_{pJ} := 0.75 \cdot f_{pu} = 202.5$ ***ksi***

$F_J := f_{pJ} \cdot \#strands \cdot A_s + 40$ ***kip*** $= 655.2$ ***kip*** total force in all 14 strands (plus 4 top strands @ 10 kips each) at time of tension

Relaxation in Strand, R1 (10 May 2024 to 15 May 2024)

$t1 := 1$ $t2 := 120$ $f_{pi}' := f_{pJ} = 202.5$ ***ksi***

$$\Delta f_p R1 := f_{pi}' \cdot \left(\frac{\log(t2) - \log(t1)}{45} \right) \cdot \left(\frac{f_{pi}'}{f_y} - 0.55 \right) = 2.65 \text{ ksi}$$

Losses Just After Release (15 May 2024)

$F_i := \left(f_{pJ} - \Delta f_p R1 \right) \cdot \#strands \cdot A_s = 607.14$ ***kip***

$F_j := 0.9 \cdot F_i = 546.43$ ***kip*** *assumed 0.9*

Elastic Shortening in Strand, ES (15 May 2025)

$E_{ps} = 28700$ ***ksi*** $f_{ci} = 8070$ $E_{ci} := 57000 \cdot \sqrt{f_{ci}} \cdot psi = 5120.49$ ***ksi***

$$\eta_i := \frac{E_{ps}}{E_{ci}} = 5.6$$

$$f_{cs} := \frac{-F_j}{A} - \frac{F_j \cdot e^2}{I} - \frac{M_w \cdot e}{I} = -1.48 \text{ ksi}$$

$\Delta f_p ES := -\eta_i \cdot f_{cs} = 8.32$ ***ksi***

Losses Calculations BT-54 with Composite Deck (2/3)

Losses After ~13 Months (20 June 2025) Note: deck casted on 14 February 2025

Creep, CR (15 May 2024 to 20 June 2025)

$K_{cr} := 2$ *for pretensioned members*

$f_{pj} := f_{pJ} - \Delta f_p R1 - \Delta f_p ES = 191.53$ ***ksi***

$P_j := f_{pj} \cdot \#strands \cdot A_s = 581.86$ ***kip***

$f_{cs} := \frac{-P_j}{A} - \frac{P_j \cdot e^2}{I} - \frac{M_w \cdot e}{I} = -1.59$ ***ksi***

$f_{csd} := \frac{-M_{SD} \cdot C_b'}{I_c'} = -0.16$ ***ksi***

$\Delta f_p CR := 0.80 \left(-K_{cr} \cdot \frac{E_{ps}}{E_c} \left(f_{cs} - f_{csd} \right) \right) = 10.29$ ***ksi*** Note: only 80% of total CR because of 405 day age

Shrinkage, SH (15 May 2024 to 20 June 2025)

$RH := 70$ *relative humidity in Atlanta, GA*

$K_{SH} := 1$ *for pretensioned members*

$V := A \cdot L = 359814$ ***in***^{3} *volume of girder*

$S := 2 \cdot A + 2 \cdot h \cdot L + 26$ ***in*** $\cdot L + 42$ ***in*** $\cdot L = 97414$ ***in***^{2} *approximate surface area of girder*

$\varepsilon_{SH} := 8.2 \cdot 10^{-6} \cdot K_{SH} \cdot \left(1 - \frac{0.06}{\textbf{in}} \cdot \frac{V}{S} \right) (100 - RH) = 0.0001915$

$\Delta f_p SH := \varepsilon_{SH} \cdot E_{ps} = 5.5$ ***ksi***

Relaxation in Strand, R2 (15 May 2024 to 28 April 2025)

$t2 = 120$ $t3 := 8352$ $f_{pi}' := f_{pj} = 191.53$ ***ksi***

$\Delta f_p R2 := f_{pi}' \cdot \left(\frac{\log(t3) - \log(t2)}{45} \right) \cdot \left(\frac{f_{pi}'}{f_y} - 0.55 \right) = 1.87$ ***ksi***

Losses Calculations BT-54 with Composite Deck (3/3)

Relaxation in Strand, R3 (28 April 2024 to 20 June 2025, Deck Casted)

$t3 = 8352$ $t4 := 9624$ $f_{pi}' := f_{pj} - \Delta f_pR2 + f_{csd} \cdot \frac{E_{ps}}{E_c} = 188.96$ ***ksi***

$\Delta f_pR3 := f_{pi}' \cdot \left(\frac{\log(t4) - \log(t3)}{45} \right) \cdot \left(\frac{f_{pi}'}{f_y} - 0.55 \right) = 0.06$ ***ksi***

Effective Force in Prestress (after losses) 20 June 2025 Test Day

$F_e := \left(f_{pJ} - \Delta f_pR1 - \Delta f_pR2 - \Delta f_pR3 - \Delta f_pES - \Delta f_pCR - \Delta f_pSH \right) \cdot \#strands \cdot A_s = 528.04$ ***kip***

$Losses := \left(1 - \frac{F_e}{F_J} \right) \cdot 100 = 19.41$ *loss percentage*

$F_{e1} := \left(f_{pJ} \cdot \left(1 - \frac{1}{Losses} \right) \right) \cdot A_s = 41.68$ ***kip*** *effective force in individual strand*

$f_{se} := f_{pJ} \cdot \left(1 - \frac{Losses}{100} \right) = 163.2$ ***ksi***

Initial Beam Curvature (1/4):

Curvature due to beam prestress: (negative)

$f_{pe} := f_{se} = 163.2\ \textit{ksi}$ *refined through previous losses calculations*

$CGS := -C_b + e = 7.64\ \textit{in}$ *finding CGS from bottom beam*

$\varepsilon_{bi} := \frac{-f_{pe}}{E_{ps}} = -0.0056865$ *strain at CGS due to prestress*

$\varepsilon_{ti} := \frac{\varepsilon_{bi} \cdot C_t}{-e + C_t} = -0.003235$ *strain at top of beam due to prestress*

$h_i := h - CGS = 46.36\ \textit{in}$ *distance between top of beam and CGS*

$\phi_i := \frac{\varepsilon_{bi} + \varepsilon_{ti}}{h} = -0.0001652\ \frac{1}{\textit{in}}$ *initial (negative) curvature in beam due to prestress*

Initial Beam Curvature (2/4):

Test 4.1:
Curvature due to beam SW: (negative)

$M_{w1} := \frac{w \cdot x_1}{2} \left(L_c - x_1\right) = 112.85$ **kip · ft** *moment due to beam SW at test location*

$f_{swb1} := \frac{-M_{w1} \cdot e}{I} = 100.98$ **psi** *stress at CGS due to beam SW*

$\varepsilon_{swb1} := \frac{f_{swb1}}{E_c} = 0.00001577$ *strain at CGS due to beam SW*

$f_{swt1} := \frac{M_{w1} \cdot C_t}{I} = 133.21$ **psi** *stress at top of beam due to beam SW*

$\varepsilon_{swt1} := \frac{f_{swt1}}{E_c} = 0.0000208$ *strain at top of beam due to beam SW*

$h_1 := h - CGS = 46.36$ **in** *distance between top of beam and CGS*

$\phi_{1b} := \frac{\varepsilon_{swb1} + \varepsilon_{swt1}}{h_1} = 0.0000008 \ \frac{1}{\text{in}}$ *initial (positive) curvature in beam due to beam SW*

Curvature due to deck SW: (positive)

$M_{SD1} := \frac{w_{deck} \cdot x_1}{2} \left(L_c - x_1\right) = 109.43$ **kip · ft** *moment due to deck SW at test location*

$f_{deckswb1} := \frac{-M_{SD1} \cdot e}{I} = 97.92$ **psi** *stress at CGS due to deck SW*

$\varepsilon_{deckswb1} := \frac{f_{deckswb1}}{E_c} = 0.00001529$ *strain at CGS due to deck SW*

$f_{deckswt1} := \frac{M_{SD1} \cdot C_t}{I} = 129.17$ **psi** *stress at top of beam due to deck SW*

$\varepsilon_{deckswt1} := \frac{f_{deckswt1}}{E_c} = 0.00002017$ *strain at top of beam due to deck SW*

$h_1 = 46.36$ **in** *distance between top of beam and CGS*

$\phi_{1d} := \frac{\varepsilon_{deckswb1} + \varepsilon_{deckswt1}}{h_1} = 0.000000765 \ \frac{1}{\text{in}}$ *initial (positive) curvature in beam due to deck SW*

$\phi_{initial1} := \phi_{1b} + \phi_{1d} + \phi_i = -0.00016365 \ \frac{1}{\text{in}}$ *total initial (negative) curvature in composite beam prior to Test 4.1*

Initial Beam Curvature (3/4):

Test 4.2:
Curvature due to beam SW: (negative)

$M_{w2} := \frac{w \cdot x_2}{2} \left(L_c - x_2\right) = 112.85$ ***kip·ft*** *moment due to beam SW at test location*

$f_{swb2} := \frac{-M_{w2} \cdot e}{I} = 100.98$ ***psi*** *stress at CGS due to beam SW*

$\varepsilon_{swb2} := \frac{f_{swb2}}{E_c} = 0.00001577$ *strain at CGS due to beam SW*

$f_{swt2} := \frac{M_{w2} \cdot C_t}{I} = 133.21$ ***psi*** *stress at top of beam due to beam SW*

$\varepsilon_{swt2} := \frac{f_{swt2}}{E_c} = 0.0000208$ *strain at top of beam due to beam SW*

$h_2 := h_1 = 46.36$ ***in*** *distance between top of beam and CGS*

$\phi_{2b} := \frac{\varepsilon_{swb2} + \varepsilon_{swt2}}{h_2} = 0.0000008 \frac{1}{in}$ *initial (positive) curvature in beam due to beam SW*

Curvature due to deck SW: (positive)

$M_{SD2} := \frac{w_{deck} \cdot x_2}{2} \left(L_c - x_2\right) = 109.43$ ***kip·ft*** *moment due to deck SW at test location*

$f_{deckswb2} := \frac{-M_{SD2} \cdot e}{I} = 97.92$ ***psi*** *stress at CGS due to deck SW*

$\varepsilon_{deckswb2} := \frac{f_{deckswb2}}{E_c} = 0.00001529$ *strain at CGS due to deck SW*

$f_{deckswt2} := \frac{M_{SD2} \cdot C_t}{I} = 129.17$ ***psi*** *stress at top of beam due to deck SW*

$\varepsilon_{deckswt2} := \frac{f_{deckswt2}}{E_c} = 0.00002017$ *strain at top of beam due to deck SW*

$h_2 = 46.36$ ***in*** *distance between top of beam and CGS*

$\phi_{2d} := \frac{\varepsilon_{deckswb2} + \varepsilon_{deckswt2}}{h_2} = 0.000000765 \frac{1}{in}$ *initial (positive) curvature in beam due to deck SW*

$\phi_{initial2} := \phi_{2b} + \phi_{2d} + \phi_i = -0.00016365 \frac{1}{in}$ *total initial (negative) curvature in composite beam prior to Test 4.2*

Initial Beam Curvature (4/4):

Test 4.3:
Curvature due to beam SW: (negative)

$M_{w3} := \frac{w \cdot x_1}{2} \left(L_c - x_1\right) = 112.85$ **kip·ft** *moment due to beam SW at test location*

$f_{swb3} := \frac{-M_{w1} \cdot e}{I} = 100.98$ **psi** *stress at CGS due to beam SW*

$\varepsilon_{swb3} := \frac{f_{swb1}}{E_c} = 0.00001577$ *strain at CGS due to beam SW*

$f_{swt3} := \frac{M_{w1} \cdot C_t}{I} = 133.21$ **psi** *stress at top of beam due to beam SW*

$\varepsilon_{swt3} := \frac{f_{swt1}}{E_c} = 0.0000208$ *strain at top of beam due to beam SW*

$h_3 := h_1 = 46.36$ **in** *distance between top of beam and CGS*

$\phi_{3b} := \frac{\varepsilon_{swb3} + \varepsilon_{swt3}}{h_3} = 0.0000008 \ \frac{1}{\text{in}}$ *initial (positive) curvature in beam due to beam SW*

Curvature due to deck SW: (positive)

$M_{SD3} := \frac{w_{deck} \cdot x_3}{2} \left(L_c - x_3\right) = 159.55$ **kip·ft** *moment due to deck SW at test location*

$f_{deckswb3} := \frac{-M_{SD3} \cdot e}{I} = 142.77$ **psi** *stress at CGS due to deck SW*

$\varepsilon_{deckswb3} := \frac{f_{deckswb3}}{E_c} = 0.0000223$ *strain at CGS due to deck SW*

$f_{deckswt3} := \frac{M_{SD3} \cdot C_t}{I} = 188.33$ **psi** *stress at top of beam due to deck SW*

$\varepsilon_{deckswt3} := \frac{f_{deckswt3}}{E_c} = 0.00002941$ *strain at top of beam due to deck SW*

$h_3 = 46.36$ **in** *distance between top of beam and CGS*

$\phi_{3d} := \frac{\varepsilon_{deckswb3} + \varepsilon_{deckswt3}}{h_3} = 0.0000011154 \ \frac{1}{\text{in}}$ *initial (positive) curvature in beam due to deck SW*

$\phi_{initial3} := \phi_{3b} + \phi_{3d} + \phi_i = -0.0001633 \ \frac{1}{\text{in}}$ *total initial (negative) curvature in composite beam prior to Test 4.3*

Cracking Moment:

$$M_{cr} := \frac{f_r \cdot I_c'}{C_b'} = 929.43 \ \textit{kip} \cdot \textit{ft}$$

$$\phi_{cr} := \frac{M_{cr}}{E_c \cdot I_c'} = 0.000003263 \ \frac{1}{\textit{in}}$$

$$M_{cr95} := 0.95 \cdot M_{cr} = 882.96 \ \textit{kip} \cdot \textit{ft}$$

$$\phi_{cr95} := 0.95 \cdot \phi_{cr} = 0.0000031 \ \frac{1}{\textit{in}}$$

Ultimate Moment (1/9):
Test 4.1:

$\varepsilon_{si1} := 0.002153$ *strain measured from test (input)*

$d_1 := h + h_f + 1.5\ \textit{in} - 2.5\ \textit{in} = 61\ \textit{in}$ *depth to centroid of strands from top of composite girder*

$c_1 := 9.0855\ \textit{in}$ *trial and error iterative c value (input until equilibrium)*

$\varepsilon_{s1.1} := -\varepsilon_{bi} + \varepsilon_{si1} = 0.007839$ *strain in lowest strand level at ultimate (test + effective prestress)*

$\varepsilon_{s2.1} := \frac{\varepsilon_{s1.1} \cdot (d_1 - 2\ \textit{in} - c_1)}{d_1 - c_1} = 0.00754$ *strain in 2nd strand level at ultimate*

$\varepsilon_{s3.1} := \frac{\varepsilon_{s1.1} \cdot (d_1 - 12\ \textit{in} - c_1)}{d_1 - c_1} = 0.00603$ *strain in 3rd strand level at ultimate*

$\varepsilon_{s4.1} := \frac{\varepsilon_{s1.1} \cdot (d_1 - 49.5\ \textit{in} - c_1)}{d_1 - c_1} = 0.0003646063$ *strain in top strand level at ultimate*

$\varepsilon_{c1.1} := \frac{\varepsilon_{si1} \cdot c_1}{d_1 - c_1} = 0.00038$ *strain at top of concrete deck at ultimate*

$\varepsilon_{c2.1} := \frac{\varepsilon_{si1} \cdot (c_1 - 8\ \textit{in})}{d_1 - c_1} = 0.0000450179$ *strain at top of 1.5-inch deck haunch at ultimate*

$\varepsilon_{c3.1} := \frac{\varepsilon_{si1} \cdot (c_1 - 9.5\ \textit{in})}{d_1 - c_1} = -0.0000171902$ *strain at top of top flange at ultimate*

$\varepsilon_{c4.1} := \frac{\varepsilon_{si1} \cdot (c_1 - 14\ \textit{in})}{d_1 - c_1} = -0.0002038143$ *strain at top of web at ultimate*

$T_{1.1} := 8 \cdot A_s \cdot \varepsilon_{s1.1} \cdot E_{ps} = 390.59\ \textit{kip}$ *tension force from lowest strand level*

$T_{2.1} := 4 \cdot A_s \cdot \varepsilon_{s2.1} \cdot E_{ps} = 187.77\ \textit{kip}$ *tension force from 2nd strand level*

$T_{3.1} := 2 \cdot A_s \cdot \varepsilon_{s3.1} \cdot E_{ps} = 75.08\ \textit{kip}$ *tension force from 3rd strand level*

$\mathbf{T_{4.1}} := \text{if}\left(c_1 > 12\ \textit{in}, 0\ \textit{kip}, \left(2 \cdot A_s \cdot \varepsilon_{s4.1} \cdot E_{ps}\right)\right) = 4.54\ \textit{kip}$ *tension force from top strand level*

$T_{tl} := T_{1.1} + T_{2.1} + T_{3.1} + \mathbf{T_{4.1}} = 657.97\ \textit{kip}$ *total tension force from prestress*

Ultimate Moment (2/9):
Test 4.1:

$$C_{1.1} := \begin{cases} \text{if } c_1 < 8\ \textit{in} \\ \quad \dfrac{(\varepsilon_{c1.1}) \cdot E_{cdeck}}{2} \cdot c_1 \cdot 72\ \textit{in} \\ \text{else} \\ \quad \dfrac{(\varepsilon_{c1.1} + \varepsilon_{c2.1}) \cdot E_{cdeck}}{2} \cdot c_1 \cdot 72\ \textit{in} \end{cases} = 618.11\ \textit{kip}$$

compression force from 8-inch concrete deck

$$C_{2.1} := \begin{cases} \text{if } c_1 \leq 8\ \textit{in} \\ \quad 0\ \textit{kip} \\ \text{else if } 8\ \textit{in} < c_1 \leq 9.5\ \textit{in} \\ \quad \dfrac{(\varepsilon_{c2.1}) \cdot E_{cdeck}}{2} \cdot c_1 \cdot 43.5\ \textit{in} \\ \text{else if } c_1 > 9.5\ \textit{in} \\ \quad \dfrac{(\varepsilon_{c2.1} + \varepsilon_{c3.1}) \cdot E_{cdeck}}{2} \cdot c_1 \cdot 43.5\ \textit{in} \end{cases} = 39.86\ \textit{kip}$$

compression force from 1.5-inch concrete deck haunch

$$C_{3.1} := \begin{cases} \text{if } c_1 \leq 9.5\ \textit{in} \\ \quad 0\ \textit{kip} \\ \text{else if } 9.5\ \textit{in} < c_1 \leq 14\ \textit{in} \\ \quad \dfrac{(\varepsilon_{c3.1}) \cdot E_c}{2} \cdot c_1 \cdot 42\ \textit{in} \\ \text{else if } c_1 > 14\ \textit{in} \\ \quad \dfrac{(\varepsilon_{c3.1} + \varepsilon_{c4.1}) \cdot E_c}{2} \cdot c_1 \cdot 42\ \textit{in} \end{cases} = 0\ \textit{kip}$$

compression force from 4.5-inch top flange

$$C_{4.1} := \begin{cases} \text{if } c_1 \leq 14\ \textit{in} \\ \quad 0\ \textit{kip} \\ \text{else} \\ \quad \dfrac{(\varepsilon_{c4.1}) \cdot E_c}{2} \cdot c_1 \cdot 6\ \textit{in} \end{cases} = 0\ \textit{kip}$$

compression force from web

$$C_{t1} := C_{1.1} + C_{2.1} + C_{3.1} + C_{4.1} = 657.97\ \textit{kip}$$

compression force from concrete

$$T_{t1} - C_{t1} = 0.002691\ \textit{kip}$$

equilibrium of forces must = 0 to find c

Ultimate Moment (3/9):

Test 4.1:

$$J_{d1} := 63.5\ in - \left(\frac{T_{1.1} \cdot 2.5\ in + T_{2.1} \cdot 4.5\ in + T_{3.1} \cdot 14.5\ in + \mathbf{T_{4.1}} \cdot 51.5\ in}{T_{t1}} \right) - \frac{c_1}{3} = 55.69\ in$$

$$M_{ult4.1} := A_{ps} \cdot \varepsilon_{s1.1} \cdot E_{ps} \cdot \left(J_{d1} \right) = 3172.32\ kip \cdot ft$$

$$\phi_{ult4.1} := \frac{\varepsilon_{c1.1}}{c_1} = 0.0000415\ \frac{1}{in}$$

Ultimate Moment (4/9):
Test 4.2:

$\varepsilon_{si2} := 0.002278$ *strain measured from test (input)*

$d_2 := h + h_f + 1.5\ \textit{in} - 2.5\ \textit{in} = 61\ \textit{in}$ *depth to centroid of strands from top of composite girder*

$c_2 := 8.97785\ \textit{in}$ *trial and error iterative c value (input until equilibrium)*

$\varepsilon_{s1.2} := -\varepsilon_{bi} + \varepsilon_{si2} = 0.007964$ *strain in lowest strand level at ultimate (test + effective prestress)*

$$\varepsilon_{s2.2} := \frac{\varepsilon_{s1.2} \cdot (d_2 - 2\ \textit{in} - c_2)}{d_2 - c_2} = 0.00766$$ *strain in 2nd strand level at ultimate*

$$\varepsilon_{s3.2} := \frac{\varepsilon_{s1.2} \cdot (d_2 - 12\ \textit{in} - c_2)}{d_2 - c_2} = 0.00613$$ *strain in 3rd strand level at ultimate*

$$\varepsilon_{s4.2} := \frac{\varepsilon_{s1.2} \cdot (d_2 - 49.5\ \textit{in} - c_2)}{d_2 - c_2} = 0.0003861344$$ *strain in top strand level at ultimate*

$$\varepsilon_{c1.2} := \frac{\varepsilon_{si2} \cdot c_2}{d_2 - c_2} = 0.00039$$ *strain at top of concrete deck at ultimate*

$$\varepsilon_{c2.2} := \frac{\varepsilon_{si2} \cdot (c_2 - 8\ \textit{in})}{d_2 - c_2} = 0.0000428191$$ *strain at top of 1.5-inch deck haunch at ultimate*

$$\varepsilon_{c3.2} := \frac{\varepsilon_{si2} \cdot (c_2 - 9.5\ \textit{in})}{d_2 - c_2} = -0.0000228644$$ *strain at top of top flange at ultimate*

$$\varepsilon_{c4.2} := \frac{\varepsilon_{si2} \cdot (c_2 - 14\ \textit{in})}{d_2 - c_2} = -0.0002199151$$ *strain at top of web at ultimate*

$T_{1.2} := 8 \cdot A_s \cdot \varepsilon_{s1.2} \cdot E_{ps} = 396.81\ \textit{kip}$ *tension force from lowest strand level*

$T_{2.2} := 4 \cdot A_s \cdot \varepsilon_{s2.2} \cdot E_{ps} = 190.78\ \textit{kip}$ *tension force from 2nd strand level*

$T_{3.2} := 2 \cdot A_s \cdot \varepsilon_{s3.2} \cdot E_{ps} = 76.32\ \textit{kip}$ *tension force from 3rd strand level*

$\mathbf{T_{4.2}} := \text{if}\left(c_2 > 12\ \textit{in}, 0\ \textit{kip}, \left(2 \cdot A_s \cdot \varepsilon_{s4.2} \cdot E_{ps}\right)\right) = 4.81\ \textit{kip}$ *tension force from top strand level*

$T_{t2} := T_{1.2} + T_{2.2} + T_{3.2} + \mathbf{T_{4.2}} = 668.72\ \textit{kip}$ *total tension force from prestress*

Ultimate Moment (5/9):
Test 4.2:

$$C_{1.2} := \text{if } c_2 < 8\ in \quad \left\| \frac{(\varepsilon_{c1.2}) \cdot E_{cdeck}}{2} \cdot c_2 \cdot 72\ in \right. \quad \text{else} \quad \left\| \frac{(\varepsilon_{c1.2} + \varepsilon_{c2.2}) \cdot E_{cdeck}}{2} \cdot c_2 \cdot 72\ in \right. = 631.26\ kip$$

compression force from 8-inch concrete deck

$$C_{2.2} := \text{if } c_2 \leq 8\ in \quad \| 0\ kip \quad \text{else if } 8\ in < c_2 \leq 9.5\ in \quad \left\| \frac{(\varepsilon_{c2.2}) \cdot E_{cdeck}}{2} \cdot c_2 \cdot 43.5\ in \right. \quad \text{else if } c_2 > 9.5\ in \quad \left\| \frac{(\varepsilon_{c2.2} + \varepsilon_{c3.2}) \cdot E_{cdeck}}{2} \cdot c_2 \cdot 43.5\ in \right. = 37.46\ kip$$

compression force from 1.5-inch concrete deck haunch

$$C_{3.2} := \text{if } c_2 \leq 9.5\ in \quad \| 0\ kip \quad \text{else if } 9.5\ in < c_2 \leq 14\ in \quad \left\| \frac{(\varepsilon_{c3.2}) \cdot E_c}{2} \cdot c_2 \cdot 42\ in \right. \quad \text{else if } c_2 > 14\ in \quad \left\| \frac{(\varepsilon_{c3.2} + \varepsilon_{c4.2}) \cdot E_c}{2} \cdot c_2 \cdot 42\ in \right. = 0\ kip$$

compression force from 4.5-inch top flange

$$C_{4.2} := \text{if } c_2 \leq 14\ in \quad \| 0\ kip \quad \text{else} \quad \left\| \frac{(\varepsilon_{c4.2}) \cdot E_c}{2} \cdot c_2 \cdot 6\ in \right. = 0\ kip$$

compression force from web

$$C_{t2} := C_{1.2} + C_{2.2} + C_{3.2} + C_{4.2} = 668.72\ kip$$

compression force from concrete

$$T_{t2} - C_{t2} = -0.000079\ kip$$

equilibrium of forces must = 0 to find c

Ultimate Moment (6/9):

Test 4.2:

$$J_{d2} := 63.5\ in - \left(\frac{T_{1.2} \cdot 2.5\ in + T_{2.2} \cdot 4.5\ in + T_{3.2} \cdot 14.5\ in + \mathbf{T_{4.2}} \cdot 51.5\ in}{T_{t2}} \right) - \frac{c_2}{3} = 55.71\ in$$

$$M_{ult4.2} := A_{ps} \cdot \varepsilon_{s1.2} \cdot E_{ps} \cdot \left(J_{d2} \right) = 3224.15\ kip \cdot ft$$

$$\phi_{ult4.2} := \frac{\varepsilon_{c1.2}}{c_2} = 0.0000438\ \frac{1}{in}$$

Ultimate Moment (7/9):
Test 4.3:

$\varepsilon_{si3} := 0.002826$ *strain measured from test (input)*

$d_3 := h + h_f + 1.5\ in - 2.5\ in = 61\ in$ *depth to centroid of strands from top of composite girder*

$c_3 := 8.60119\ in$ *trial and error iterative c value (input until equilibrium)*

$\varepsilon_{s1.3} := -\varepsilon_{bi} + \varepsilon_{si3} = 0.008512$ *strain in lowest strand level at ultimate (test + effective prestress)*

$\varepsilon_{s2.3} := \frac{\varepsilon_{s1.3} \cdot (d_3 - 2\ in - c_3)}{d_3 - c_3} = 0.00819$ *strain in 2nd strand level at ultimate*

$\varepsilon_{s3.3} := \frac{\varepsilon_{s1.3} \cdot (d_3 - 12\ in - c_3)}{d_3 - c_3} = 0.00656$ *strain in 3rd strand level at ultimate*

$\varepsilon_{s4.3} := \frac{\varepsilon_{s1.3} \cdot (d_3 - 49.5\ in - c_3)}{d_3 - c_3} = 0.0004709263$ *strain in top strand level at ultimate*

$\varepsilon_{c1.3} := \frac{\varepsilon_{si3} \cdot c_3}{d_3 - c_3} = 0.00046$ *strain at top of concrete deck at ultimate*

$\varepsilon_{c2.3} := \frac{\varepsilon_{si3} \cdot (c_3 - 8\ in)}{d_3 - c_3} = 0.0000324237$ *strain at top of 1.5-inch deck haunch at ultimate*

$\varepsilon_{c3.3} := \frac{\varepsilon_{si3} \cdot (c_3 - 9.5\ in)}{d_3 - c_3} = -0.0000484751$ *strain at top of top flange at ultimate*

$\varepsilon_{c4.3} := \frac{\varepsilon_{si3} \cdot (c_3 - 14\ in)}{d_3 - c_3} = -0.0002911714$ *strain at top of web at ultimate*

$T_{1.3} := 8 \cdot A_s \cdot \varepsilon_{s1.3} \cdot E_{ps} = 424.12\ kip$ *tension force from lowest strand level*

$T_{2.3} := 4 \cdot A_s \cdot \varepsilon_{s2.3} \cdot E_{ps} = 203.96\ kip$ *tension force from 2nd strand level*

$T_{3.3} := 2 \cdot A_s \cdot \varepsilon_{s3.3} \cdot E_{ps} = 81.75\ kip$ *tension force from 3rd strand level*

$\mathbf{T_{4.3}} := \text{if}\left(c_3 \geq 12\ in, 0\ kip, \left(2 \cdot A_s \cdot \varepsilon_{s4.3} \cdot E_{ps}\right)\right) = 5.87\ kip$ *tension force from top strand level*

$T_{t3} := T_{1.3} + T_{2.3} + T_{3.3} + \mathbf{T_{4.3}} = 715.7\ kip$ *total tension force from prestress*

Ultimate Moment (8/9):
Test 4.3:

$$C_{1.3} := \begin{cases} \text{if } c_3 < 8\ \textit{in} \\ \quad \dfrac{(\varepsilon_{c1.3}) \cdot E_{cdeck}}{2} \cdot c_3 \cdot 72\ \textit{in} \\ \text{else} \\ \quad \dfrac{(\varepsilon_{c1.3} + \varepsilon_{c2.3}) \cdot E_{cdeck}}{2} \cdot c_3 \cdot 72\ \textit{in} \end{cases} = 688.51\ \textit{kip}$$

compression force from 8-inch concrete deck

$$C_{2.3} := \begin{cases} \text{if } c_3 \le 8\ \textit{in} \\ \quad 0\ \textit{kip} \\ \text{else if } 8\ \textit{in} < c_3 \le 9.5\ \textit{in} \\ \quad \dfrac{(\varepsilon_{c2.3}) \cdot E_{cdeck}}{2} \cdot c_3 \cdot 43.5\ \textit{in} \\ \text{else if } c_3 > 9.5\ \textit{in} \\ \quad \dfrac{(\varepsilon_{c2.3} + \varepsilon_{c3.3}) \cdot E_{cdeck}}{2} \cdot c_3 \cdot 43.5\ \textit{in} \end{cases} = 27.18\ \textit{kip}$$

compression force from 1.5-inch concrete deck haunch

$$C_{3.3} := \begin{cases} \text{if } c_3 \le 9.5\ \textit{in} \\ \quad 0\ \textit{kip} \\ \text{else if } 9.5\ \textit{in} < c_3 \le 14\ \textit{in} \\ \quad \dfrac{(\varepsilon_{c3.3}) \cdot E_c}{2} \cdot c_3 \cdot 42\ \textit{in} \\ \text{else if } c_3 > 14\ \textit{in} \\ \quad \dfrac{(\varepsilon_{c3.3} + \varepsilon_{c4.3}) \cdot E_c}{2} \cdot c_3 \cdot 42\ \textit{in} \end{cases} = 0\ \textit{kip}$$

compression force from 4.5-inch top flange

$$C_{4.3} := \begin{cases} \text{if } c_3 \le 14\ \textit{in} \\ \quad 0\ \textit{kip} \\ \text{else} \\ \quad \dfrac{(\varepsilon_{c4.3}) \cdot E_c}{2} \cdot c_3 \cdot 6\ \textit{in} \end{cases} = 0\ \textit{kip}$$

compression force from web

$C_{t3} := C_{1.3} + C_{2.3} + C_{3.3} + C_{4.3} = 715.69\ \textit{kip}$ *compression force from concrete*

$T_{t3} - C_{t3} = 0.009027\ \textit{kip}$ *equilibrium of forces must = 0 to find c*

Ultimate Moment (9/9):

Test 4.3:

$$J_{d3} := 63.5\ in - \left(\frac{T_{1.3} \cdot 2.5\ in + T_{2.3} \cdot 4.5\ in + T_{3.3} \cdot 14.5\ in + \mathbf{T_{4.3}} \cdot 51.5\ in}{T_{t3}} \right) - \frac{c_3}{3} = 55.79\ in$$

$$M_{ult4.3} := A_{ps} \cdot \varepsilon_{s1.3} \cdot E_{ps} \cdot \left\langle J_{d3} \right\rangle = 3450.68\ kip \cdot ft$$

$$\phi_{ult4.3} := \frac{\varepsilon_{c1.3}}{c_3} = 0.0000539\ \frac{1}{in}$$

Theoretical Moment-Curvature Overview:

$M_{cr} = 929.43\ kip \cdot ft$ $M_{ult4.2} = 3224.15\ kip \cdot ft$

$\phi_{cr} = 0.000003263\ \frac{1}{in}$ $\phi_{ult4.2} = 0.000044\ \frac{1}{in}$

$M_{ult4.1} = 3172.32\ kip \cdot ft$ $M_{ult4.3} = 3450.68\ kip \cdot ft$

$\phi_{ult4.1} = 0.000041\ \frac{1}{in}$ $\phi_{ult4.3} = 0.000054\ \frac{1}{in}$

Ultimate Loads from Moment Calculations: (four-point bending tests)

Test 4.1:

$a_1 = 7.42\ ft$

$b_1 = 32.92\ ft$

$P_{ult1m} := 2 \cdot \frac{L_c \cdot M_{ult4.1}}{b_1 \cdot (a_1 + L_c - b_1)} = 453.73\ kip$ *ultimate load based on moment capacity*

Test 4.2:

$a_2 = 32.92\ ft$

$b_2 = 7.42\ ft$

$P_{ult2m} := 2 \cdot \frac{L_c \cdot M_{ult4.2}}{a_2 \cdot (b_2 + L_c - a_2)} = 461.14\ kip$ *ultimate load based on moment capacity*

Test 4.3:

$a_3 = 23.63\ ft$

$b_3 = 16.71\ ft$

$P_{ult3m} := 2 \cdot \frac{L_c \cdot M_{ult4.3}}{a_3 \cdot (b_3 + L_c - a_3)} = 346.12\ kip$ *ultimate load based on moment capacity*

Theoretical Strut and Tie Cracking Capacity: (1/) (AASHTO C5.8.2.2-1)

$d := 54\ in + 9.5\ in = 63.5\ in$

$b_w := 6\ in$

$V_{cr1} := \left(0.2 - 0.1\left(\frac{a_1}{d}\right)\right) \cdot \sqrt{\frac{f_c}{1000}} \cdot ksi \cdot b_w \cdot d = 80.99\ kip$

$V_{cr2} := \left(0.2 - 0.1\left(\frac{L_c - L_{spr} - a_2}{d}\right)\right) \cdot \sqrt{\frac{f_c}{1000}} \cdot ksi \cdot b_w \cdot d = 80.99\ kip$

$V_{cr3} := \max\left(\left(0.2 - 0.1\left(\frac{L_c - L_{spr} - a_3}{d}\right)\right), 0.0632\right) \cdot \sqrt{\frac{f_c}{1000}} \cdot ksi \cdot b_w \cdot d = 85.54\ kip$

Shear Capacity: (1/5)

Prestress Transfer/Development Lengths:

$d_b := 0.6\ in$ *diameter of prestressing strand*

$L_{tr} := min\left(50 \cdot d_b, \left(\frac{f_{pe}}{3000\ psi}\right) \cdot d_b\right) = 30\ in$ *transfer length*

$f_{ps} := \varepsilon_{s1.3} \cdot E_{ps} = 244.31\ ksi$

$L_f := \left(\frac{f_{ps} - f_{pe}}{1000\ psi}\right) \cdot d_b = 48.66\ in$

$L_d := L_{tr} + L_f = 6.56\ ft$ *development length*

V_c calculation:

Minimum V_{ci} calculation:

$d_p := \max\left(h + h_f + 1.5\ in - CGS, 0.8\ \left(h + h_f + 1.5\ in\right)\right) = 55.86\ in$ *distance from CGS to max compression fiber*

$f_{ce} := f_{pe} = 163.2\ ksi$ *effective prestress stress*

$b_w := 6\ in$ *web width*

$d := d_p = 55.86\ in$ *distance from CGS to max compression fiber*

$f_y := 60\ ksi$ *yield strength of non-prestressed reinforcement*

$A_s := 0.31\ in^2$ *area of non-prestressed longitudinal reinforcement*

$A_{ps} \cdot f_{pe} = 495.81\ kip > 0.4\ \left(A_{ps} \cdot f_{pu} + A_s \cdot f_y\right) = 335.54\ kip$ *ACI 318-19 [22.5.6.3.1]*

$V_{ci} := 2 \cdot \lambda \cdot \sqrt{f_c \cdot psi} \cdot b_w \cdot d = 75.3\ kip$ *flexure-shear strength ACI 318-19 [22.5.6.3.1c]*

V_{cw} calculation:

$f_{pc} := \frac{F_e}{A} = 801.28\ psi$ *compressive stress in concrete at centroid of composite section due to prestress*

$V_{cw} := \left(3.5\ \lambda \cdot \sqrt{f_c \cdot psi} + 0.3\ f_{pc}\right)\ b_w \cdot d_p = 212.34\ kip$ *web-shear strength*

Shear Capacity: (2/5)

$a_1 = 89\ in$
$b_1 = 395\ in$
$x_1 := x_1 - 7\ in = 106\ in$

V_{ci} calculation Test 1: (using max load from testing)

$P_{max1} = 500\ kip$

$V_{d1} := \text{abs}\left(\left(w + w_{deck}\right)\left(\frac{L_c}{2} - x_1\right)\right) = 18.03\ kip$ *shear due to DL (uniform SW beam and SW deck)*

$V_{u1} := \left(\frac{\left(\frac{P_{max1}}{2}\right)}{L_c} \cdot \left(L_c - a_1 + b_1\right)\right) = 393.8\ kip$ *shear due to ultimate load (from test)*

$V_{i1} := V_{u1} - V_{d1} = 375.77\ kip$

$M_{u1} := \frac{\left(\frac{P_{max1}}{2}\right)}{L} \cdot \left(L_c - b_1 + a_1\right) \cdot b_1 = 3406.21\ kip \cdot ft$ *moment due to ultimate load (from test)*

$M_{d1} := \frac{\left(w + w_{deck}\right) \cdot x_1}{2}\left(L_c - x_1\right) = 212\ kip \cdot ft$ *moment due to DL (uniform SW beam and SW deck)*

$M_{max1} := M_{u1} - M_{d1} = 3194.22\ kip \cdot ft$

$f_{d1} := \frac{M_{d1} \cdot C_b'}{I_c'} = 192.17\ psi$

$f_{pec} := \frac{F_e}{A_c'} - \frac{F_e \cdot e \cdot C_b'}{I_c'} = 1.27\ ksi$

$M_{cre1} := \left(\frac{I_c'}{C_b'}\right)\left(6\ \lambda \cdot \sqrt{f_c} \cdot psi + f_{pec} - f_{d1}\right) = 1937.82\ kip \cdot ft$

$V_{ci1} := 0.6\ \lambda \cdot \sqrt{f_c} \cdot psi \cdot b_w \cdot d_p + V_{d1} + \frac{V_{i1} \cdot M_{cre1}}{M_{max1}} = 268.58\ kip$

$V_{c1} := min\left(V_{cw}, V_{ci1}\right) = 212.34\ kip$ *nominal shear strength provided by concrete for Test 1*

Shear Capacity: (3/5)

$a_2 = 395\ in$
$b_2 = 89\ in$
$x_3 := x_2 - 7\ in = 412\ in$

V_{ci} calculation Test 2: (using max load from testing)

$P_{max2} = 500\ kip$

$V_{d2} := \text{abs}\left(\left(w + w_{deck}\right)\left(\frac{L_c}{2} - x_2\right)\right) = 16.45\ kip$ *shear due to DL (uniform SW beam and SW deck)*

$V_{u2} := \left(\frac{\left(\frac{P_{max2}}{2}\right)}{L_c} \cdot \left(L_c - b_2 + a_2\right)\right) = 393.8\ kip$ *shear due to ultimate load (from test)*

$V_{i2} := V_{u2} - V_{d2} = 377.35\ kip$

$M_{u2} := \frac{\left(\frac{P_{max2}}{2}\right)}{L} \cdot \left(L_c - a_2 + b_2\right) \cdot a_2 = 3406.21\ kip \cdot ft$ *moment due to ultimate load (from test)*

$M_{d2} := \frac{\left(w + w_{deck}\right) \cdot x_2}{2}\left(L_c - x_2\right) = 232.11\ kip \cdot ft$ *moment due to DL (uniform SW beam and SW deck)*

$M_{max2} := M_{u2} - M_{d2} = 3174.1\ kip \cdot ft$

$f_{d2} := \frac{M_{d2} \cdot C_b'}{I_c'} = 210.4\ psi$

$M_{cre2} := \left(\frac{I_c'}{C_b'}\right)\left(6\ \lambda \cdot \sqrt{f_c} \cdot psi + f_{pec} - f_{d2}\right) = 1917.71\ kip \cdot ft$

$V_{ci2} := 0.6\ \lambda \cdot \sqrt{f_c} \cdot psi \cdot b_w \cdot d_p + V_{d2} + \frac{V_{i2} \cdot M_{cre2}}{M_{max2}} = 267.02\ kip$

$V_{c2} := min\left(V_{cw}, V_{ci2}\right) = 212.34\ kip$ *nominal shear strength provided by concrete for Test 2*

Shear Capacity: (4/5)

V_{ci} calculation Test 3: (using max load from testing)

$a_3 = 283.5\ in$
$b_3 = 200.5\ in$
$x_3 := x_3 - 7\ in = 300.5\ in$

$P_{max3} = 331\ kip$

$V_{d3} := \text{abs}\left(\left(w + w_{deck}\right) \left(\frac{L_c}{2} - x_3\right)\right) = 3.89\ kip$ *shear due to DL (uniform SW beam and SW deck)*

$V_{u3} := \left(\frac{\left(\frac{P_{max3}}{2}\right)}{L_c} \cdot \left(L_c - b_3 + a_3\right)\right) = 191.32\ kip$ *shear due to ultimate load (from test)*

$V_{i3} := V_{u3} - V_{d3} = 187.43\ kip$

$M_{u3} := \frac{\left(\frac{P_{max3}}{2}\right)}{L} \cdot \left(L_c - a_3 + b_3\right) \cdot a_3 = 3215.31\ kip \cdot ft$ *moment due to ultimate load (from test)*

$M_{d3} := \frac{\left(w + w_{deck}\right) \cdot x_3}{2} \left(L_c - x_3\right) = 326.59\ kip \cdot ft$ *moment due to DL (uniform SW beam and SW deck)*

$M_{max3} := M_{u3} - M_{d3} = 2888.72\ kip \cdot ft$

$f_{d3} := \frac{M_{d3} \cdot C_b'}{I_c'} = 296.05\ psi$

$M_{cre3} := \left(\frac{I_c'}{C_b'}\right) \left(6\ \lambda \cdot \sqrt{f_c} \cdot psi + f_{pec} - f_{d3}\right) = 1823.22\ kip \cdot ft$

$V_{ci3} := 0.6\ \lambda \cdot \sqrt{f_c} \cdot psi \cdot b_w \cdot d_p + V_{d3} + \frac{V_{i3} \cdot M_{cre3}}{M_{max3}} = 144.78\ kip$

$V_{c3} := min\left(V_{cw}, V_{ci3}\right) = 144.78\ kip$ *nominal shear strength provided by concrete for Test 3*

Shear Capacity: (5/5)

V_{se} calculation: (for tests near ends 24-in < x < 144-in)

$s_e := 12\ \textbf{in}$ *spacing for #5 stirrups for 24-in < x < 144-in*

$A_v := 2 \cdot \langle A_s \rangle = 0.62\ \textbf{in}^2$ *area of shear reinforcement (2#5 bars)*

$V_{se} := \frac{A_s \cdot f_y \cdot d}{s_e} = 86.58\ \textbf{kip}$ *nominal shear strength provided by shear reinforcement (for tests near end)*

V_{sm} calculation: (for tests near midspan 144-in < x < 402-in)

$s_m := 16\ \textbf{in}$ *spacing for #5 stirrups for 144-in < x < 402-in*

$A_v = 0.62\ \textbf{in}^2$ *area of shear reinforcement (2#5 bars)*

$V_{sm} := \frac{A_v \cdot f_y \cdot d}{s_m} = 129.87\ \textbf{kip}$ *nominal shear strength provided by shear reinforcement (for tests near midspan)*

V_n **nominal one-way shear capacity:**

$V_{n1} := V_{c1} + V_{se} = 298.92\ \textbf{kip}$ *nominal shear capacity for Test 1 North end*

$V_{n2} := V_{c2} + V_{se} = 298.92\ \textbf{kip}$ *nominal shear capacity for Test 2 South end*

$V_{n3} := V_{c3} + V_{sm} = 274.65\ \textbf{kip}$ *nominal shear capacity for Test 3 near midspan*

Ultimate Loads from Shear Calculations: (four-point bending tests)

Test 4.1:

$a_1 = 7.42\ ft$

$b_1 = 32.92\ ft$

$P_{ult1v} := 2 \cdot \frac{V_{n1} \cdot L_c}{(L_c - a_1 + b_1)} = 379.54\ kip$ *ultimate load based on shear capacity*

Test 4.2:

$a_2 = 32.92\ ft$

$b_2 = 7.42\ ft$

$P_{ult2v} := 2 \cdot \frac{V_{n2} \cdot L_c}{(L_c - b_2 + a_2)} = 379.54\ kip$ *ultimate load based on shear capacity*

Test 4.3:

$a_3 = 23.63\ ft$

$b_3 = 16.71\ ft$

$P_{ult3v} := 2 \cdot \frac{V_{n3} \cdot L_c}{(L_c - b_3 + a_3)} = 475.17\ kip$ *ultimate load based on shear capacity*

Failure Mode Based on Comparing Maximum Load to Maximum Theoretical Capacities:

	Test 1 (Shear):	Test 2 (Shear):	Test 3 (Flexure):
Experimental Maximum Load:	$P_{max1} = 500$ ***kip***	$P_{max2} = 500$ ***kip***	$P_{max3} = 331$ ***kip***
Theoretical Maximum Load (Flexure):	$P_{ult1m} = 453.73$ ***kip***	$P_{ult2m} = 461.14$ ***kip***	$P_{ult3m} = 346.12$ ***kip***
Theoretical Maximum Load (Shear):	$P_{ult1v} = 379.54$ ***kip***	$P_{ult2v} = 379.54$ ***kip***	$P_{ult3v} = 475.17$ ***kip***
	$x_1 = 106$ ***in***	$L_c - x_2 = 120$ ***in***	$x_3 = 300.5$ ***in***

APPENDIX K. PROPOSED GUIDE FOR REPAIR OF PRESTRESSED CONCRETE GIRDERS

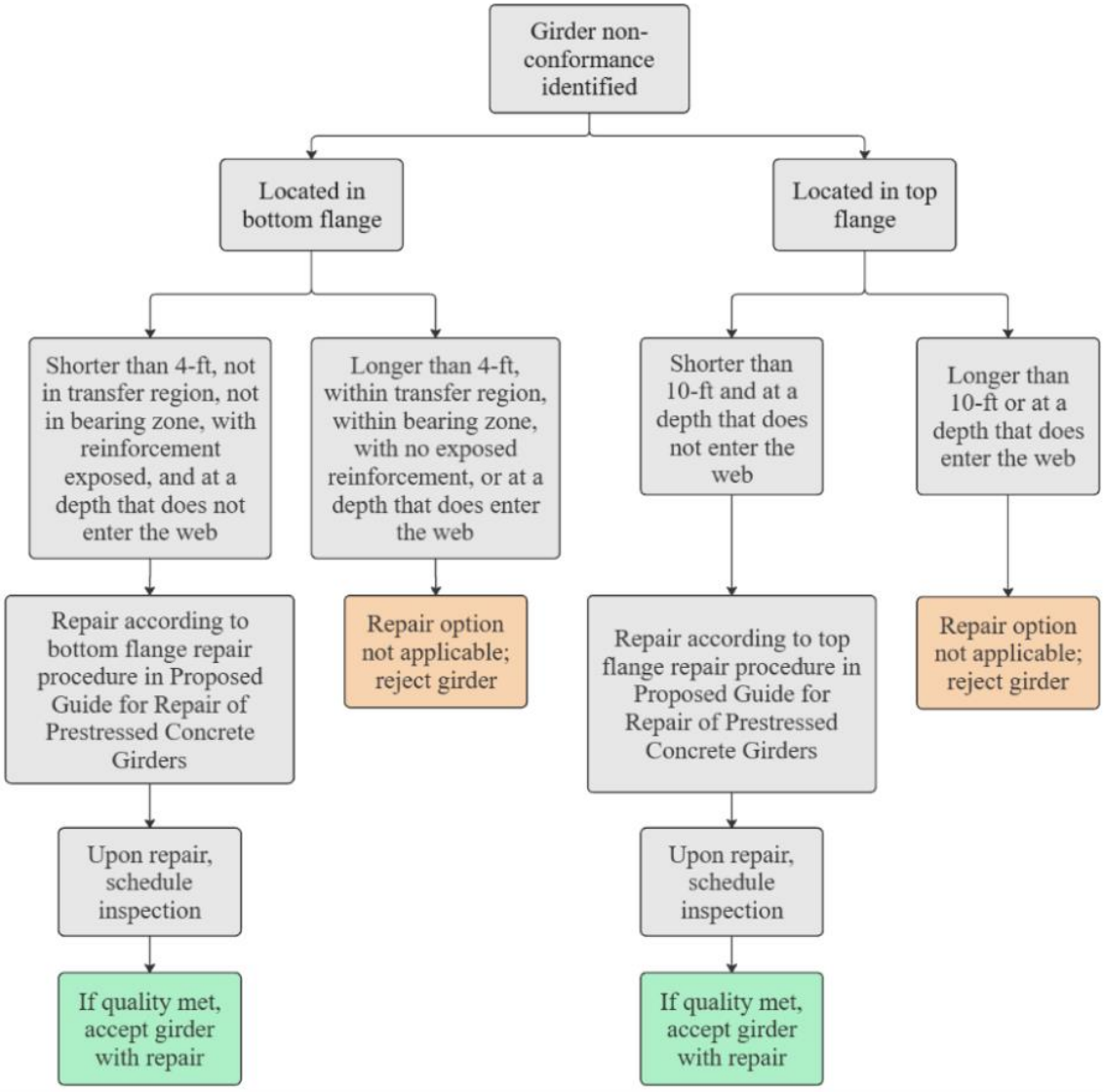

Figure 242. Flowchart. Proposed decision-making flowchart.

GEORGIA DEPARTMENT OF TRANSPORTATION
OFFICE OF MATERIALS AND TESTING

PROPOSED GUIDE FOR REPAIR OF PRESTRESSED CONCRETE GIRDERS

I. TOP FLANGE NONCONFORMITY (L < 10 FT)

Prestressed girders with top flange nonconformities <10 ft in length with a depth not extending into the girder web are accepted with repairs that follow the procedure in this guide.

1. Top flange nonconformities accepted with repairs:
   a. Top flange nonconformity not located at the end of the girder (Figure 1).

Figure 1. Top flange nonconformity not located at the end of the girder.

   b. Top flange nonconformity located at the end of the girder (Figure 2).

Figure 2. Top flange nonconformity located at the end of the girder.

2. Top flange repair procedure accepted:
    a. If a cracked concrete section is being retained by prestressed or non-prestressed steel reinforcement, carefully remove the loose segment of concrete to expose a sound concrete surface. If non-prestressed steel reinforcement is partially exposed, clear a 1-in. area around the reinforcement, if possible.
    b. Chip the sound concrete surface to a 0.25-in. amplitude (Figure 3).

Figure 3. Top flange 0.25-in. amplitude chipped surface.

    c. Drill holes (spaced approximately 6 in. on center; Figure 4) using a 0.25-in. diameter masonry drill bit with a hammer drill to a depth specified by an epoxy resin chosen from the GDOT Qualified Products List. Thoroughly clean all loose debris, dust, and laitance from the concrete surface to be repaired. Remove dust from the drilled holes using compressed air, ensuring the epoxy resin manufacturer specifications are met.

Figure 4. Drilled holes for c-bars.

d. Prefabricate segments of #3 reinforcing bars and bend into a c-bar to a length that allows full embedment in the drilled hole. Follow the dimensions shown in Figure 5,

where,

L_1 = Reinforcing bar depth distance required by the chosen epoxy resin manufacturer specifications.

L_2 = Distance from surface of nonconformity to end of radius bend, within the clear cover of the top flange.

L_3 = Distance from end of first radius bend to top of second radius bend, within the clear cover of the future composite concrete deck.

L_4 = Required straight extension distance for #3 reinforcing bar, 3-in.

R = Allowed radius bend for #3 reinforcing bar.

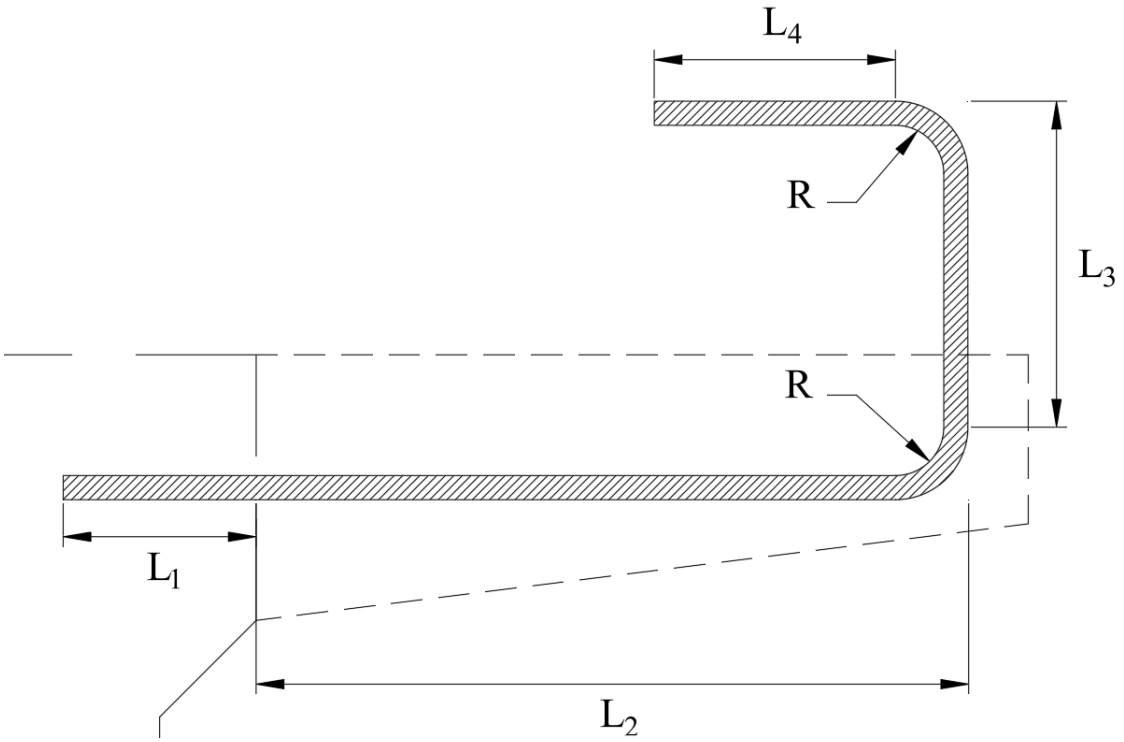

Figure 5. Top flange c-bar bend schematic.

e. Anchor the c-bars into the drilled holes with the chosen epoxy resin bonding agent and allow to cure, ensuring the manufacturer's specifications are met.

f. Use formwork that fits the existing, conforming top flange shape to produce a uniform, conforming prestressed girder section.

g. Using a concrete mixture proportion that meets or exceeds the existing concrete girder design strength, cast the repair, ensuring the concrete surrounding the repair surface is properly consolidated. After the repair concrete has achieved initial set, create an amplitude on the top of the top flange repair surface that matches the girder top surface.

h. Cure the repair concrete under moist curing conditions. Allow the repair to cure for 28 days before inducing any loads on the repair.

II. BOTTOM FLANGE NONCONFORMITY, NOT IN BEARING ZONE (L < 4 FT)

Prestressed girders with bottom flange nonconformities that are located outside the bearing zone and transfer length region ($60 \cdot d_b$) with exposed reinforcement and that are <4 ft in length with a depth not extending into the girder web are accepted with repairs that follow the procedure in this guide.

1. Bottom flange nonconformities accepted with repairs:
   a. Bottom flange nonconformity with prestressing strands and non-prestressed reinforcement exposed, with above access for concrete replacement (Figure 6).

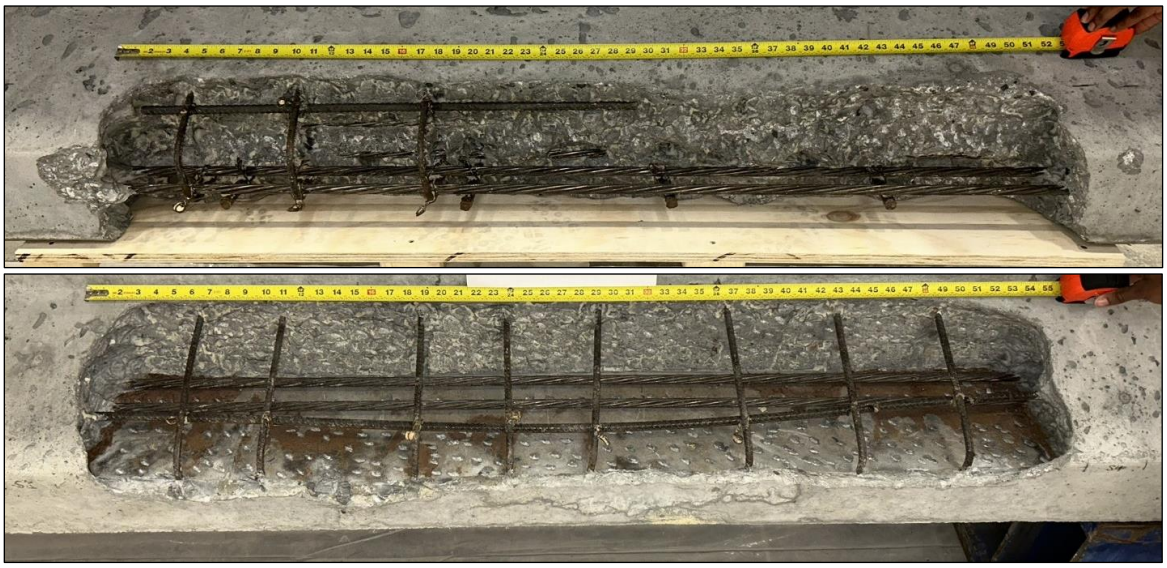

Figure 6. Bottom flange nonconformities with above access for concrete replacement.

   b. Bottom flange nonconformity with prestressing strands and non-prestressed reinforcement exposed, requiring a chimney formwork for concrete replacement (Figure 7).

Figure 7. Bottom flange nonconformity requiring a chimney formwork for concrete replacement.

2. Bottom flange repair procedure accepted:
   a. If the nonconformance is a honeycombed concrete section, carefully remove the unsound concrete to expose a sound concrete surface.

If the nonconformance is a cracked concrete section that is being retained by prestressed or non-prestressed steel reinforcement, carefully remove the loose segment of concrete to expose a sound concrete surface. If non-prestressed steel reinforcement is partially exposed, clear a 1-in. area around the reinforcement, if possible.

b. Chip the sound concrete surface to a 0.25-in. amplitude without damaging the prestressing strands. Thoroughly clean loose debris, dust, and any laitance on the concrete surface to be repaired.

   Use formwork that fits the existing, conforming bottom flange shape to produce a uniform, conforming prestressed girder section. If a chimney formwork is required for concrete replacement, size the chimney (dashed circle, Figure 8) to allow proper flow of self-consolidating concrete (SCC) into the formwork. Figure 8 shows an example of a chimney formwork with air vent holes (solid circle, Figure 8), as well as a clear polycarbonate sheet to allow inspection of proper flow of SCC.

Figure 8. Chimney formwork example.

Upon removing the formwork, an imperfection will remain at the base of the chimney opening (circle, Figure 9) that will require proper finishing to achieve a smooth surface that matches the girder surface.

Figure 9. Imperfection due to chimney opening.

c. Using an SCC mixture proportion that meets or exceeds the existing concrete girder design strength with a spread of 20 to 28 in., cast the repair. The aggregate should be the same mineral as the large aggregate in the girder so that thermal characteristics between the repair and substrate are similar. The maximum size aggregate should not be larger than 0.5 in. Ensure the concrete surrounding the repair surface is properly consolidated by tapping on the formwork exterior with a rubber mallet. Continue to fill the chimney and tap the formwork until excess concrete flows out of the air vent holes, ensuring the repair void is properly filled.
d. Cure the repair concrete under moist curing conditions. Allow the repair to cure for 28 days before inducing any loads on the repair.

III. NONCONFORMITIES NOT SUITABLE FOR REPAIR

Prestressed girders with the following nonconformities are not accepted for repair and shall be rejected.

1. Bottom flange nonconformities not accepted for repair:
   a. End nonconformity with loss of prestressing force, located within the transfer region of $60 \cdot d_b$ (Figure 10).

Figure 10. Bottom flange nonconformity within transfer length.

   b. End nonconformity with loss of prestressing force, located in the bearing zone (Figure 11).
   c. Shallow nonconformity with no steel reinforcement exposed, located at the bottom of the girder (Figure 12).

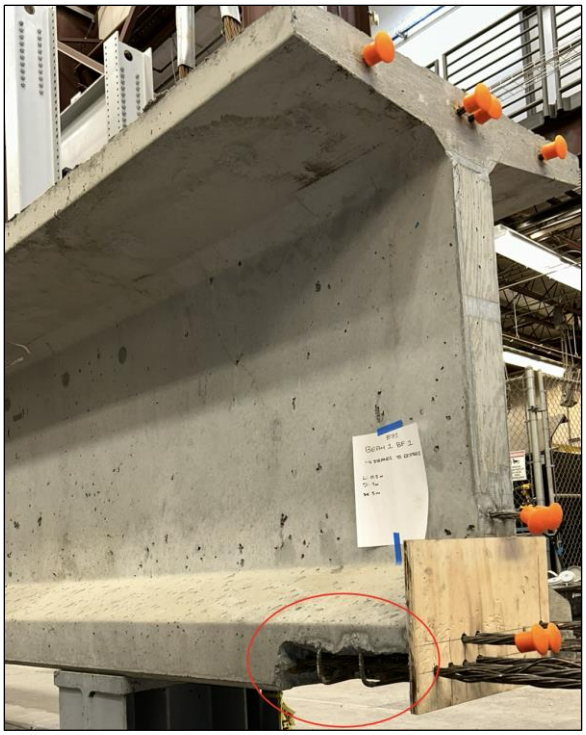

Figure 11. Bottom flange nonconformity within bearing zone.

Figure 12. Bottom flange nonconformity with no exposed reinforcement.

ACKNOWLEDGMENTS

The authors would like to thank Standard Concrete Products, especially Mr. Richard Potts, and Mr. Richard Potts, Mr. Brett Martin, Mr. Fletcher Smith, and Mr. Jake Sanders for providing the design assistance and construction for the four girders that were used in this project.

We are also grateful to our sponsors at the Georgia Department of Transportation who provided valuable insights and recommendations: Mr. Donn Digamon, Mr. Peter Wu, Mr. Steve Gaston, Mr. Nathan Wilson, Mr. John Smith, Mr. William Bilsback, Mr. Jason Waters, Ms. Amanda Sheldon, Mr. Rabindra Koirala, and Mr. Brennan Roney.

We would like to acknowledge the Precast/Prestressed Concrete Institute (PCI) for conference and meeting support, and we specifically thank Ms. Marti Harrell (Executive Director of Georgia/Carolinas PCI), Dr. William Nickas (Managing Director, Transportation Systems, PCI), and Mr. Ed Wasserman (Tennessee DOT, retired) for sharing their knowledge.

The testing portion of this project truly required a team effort. The authors acknowledge Mr. Theodore M. Lemire and Mr. Joshua D. Gargan for their exceptional effort on the project. Additionally, we thank Ms. Georgia Nevin, Ms. Mary “Molly” Denton, Ms. Alexis Tri, Ms. Juliet Swinea, Ms. Shirin Raschid Farrokhi, Mr. Matthew Mann, Dr. Jessica Thangjitham, Mr. Griffin Fish, Mr. Vijay Rathore, Mr. Dylan Balkaran, Mr. Benjamin “Bo” Rider, Mr. Alexander Rice, Mr. William Harding, Mr. Andrew Stamper, Ms. Priscilla Pierre, Mr. Abel Tharakan, and Mr. Caleb Kinneer for help with the deck construction and

testing. We would also like to express our gratitude to Mr. Jeremy Mitchell and Mr. Jeremy Stephens for their dedication to the laboratory.

Finally, the authors would like to express our gratitude to Ms. LaShone Simmons and Ms. Grace Kang for providing administrative and business support to the project.

REFERENCES

1. Precast/Prestressed Concrete Institute (PCI). (2006). *Manual for the Evaluation and Repair of Precast, Prestressed Concrete Bridge Products*. Publication MNL-137-06. PCI, Chicago, IL.

2. Illinois Department of Transportation (IDOT). (2015). *Manual for Fabrication of Precast Prestressed Concrete Products*. IDOT, Bureau of Materials and Physical Research, Springfield, IL.

3. New York State Department of Transportation (NYSDOT). (2017). *Prestressed Concrete Construction Manual* (3rd edition). NYSDOT, Office of Structures, Albany, NY.

4. Michigan Department of Transportation (MDOT). (2018). *Structural Precast Concrete QUI Manual*.

5. Tadros, M.K., Badie, S.S., and Tuan, C.Y. (2010). *Evaluation and Repair Procedures for Precast/Prestressed Concrete Girders with Longitudinal Cracking in the Web*. National Cooperative Highway Research Program (NCHRP) Report 645, Transportation Research Board, Washington, D.C.

6. Georgia Department of Transportation (GDOT). (2014). *Standard Operating Procedure 3 (SOP-3): Quality Control and Quality Assurance of Precast/Prestressed Concrete Members and Structural Precast Concrete Members*. Office of Materials and Testing, Atlanta, GA. Available online: https://www.dot.ga.gov/PartnerSmart/Business/Source/sop/sop03.pdf.

7. Precast/Prestressed Concrete Institute Northeast (PCINE). (2018). *Guidelines for Resolution of Non-Conformances in Precast Concrete Bridge Elements*. Report No: PCINE-18-RNPCBE, PCINE, Chicago, IL. Available online: https://www.pci.org/PCI_Docs/PCI_Northeast/Technical_Resources/Bridge/PCINE_Guidelines_for_Resolution_of_Non-Conformances_in_Precast_Concrete__Bridge_Elements_.pdf.

8. Arson, C. and Li, K. (2020). *Mechanical Integrity and Sustainability of Pre-Stressed Concrete Bridge Girders Repaired by Epoxy Injection – Phase II*. Draft Report, Research Project 17-08, Georgia Department of Transportation (GDOT), Atlanta, GA. Available online: https://dlg.galileo.usg.edu/data/dlg/ggpd/pdfs/dlg_ggpd_s-ga-bt700-pr4-bm1-b2017-be6-bpt-p-b2-belec-p-btext.pdf.

9. Stewart, L.K., Kurtis, K.E., and Emmenegger, L.P. (2020). Quantifying the Impact of Cover Deficiencies on Bridge Deck Service Life: Recommendations for Contracting. Draft Report, Research Project 17-05, Georgia Department of Transportation (GDOT), Atlanta, GA. Available online: https://g92018.eos-intl.net/eLibSQL14_G92018_Documents/17-05.pdf.

10. Lee, S.-C., Cho, J.-Y., and Oh, B.H. (2010). "Shear Behavior of Large-scale Post-tensioned Girders with Small Shear Span-depth Ratio." *ACI Structural Journal*, *107*(2), pp. 137–145.

11. Oh, B.H. and Kim, K.S. (2004). "Shear Behavior of Full-scale Post-tensioned Prestressed Concrete Bridge Girders." *ACI Structural Journal*, *101*(2), pp. 176–182.

12. Shahawy, M. and Batchelor, B. (1996). "Shear Behavior of Full-scale Prestressed Concrete Girders – Comparison between AASHTO Specifications and LRFD Code." *PCI Journal*, *41*(3), pp. 48–62. Available online: https://www.pci.org/PCI_Docs/Publications/PCI%20Journal/1996/May-June/Shear%20Behavior%20of%20Full-Scale%20Prestressed%20Concrete%20Girders%20-%20Comparison%20Between%20AASHTO%20Specifications%20and%20LRFD%20Code.pdf.

13. Grace, N., Enomoto, T., and Abdel-Sayed, G. (2003). "Experimental Study and Analysis of a Full-scale CFRP/CFCC Double-Tee Bridge Beam." *PCI Journal*, *48*(4), pp. 120–139.

14. Georgia Department of Transportation (GDOT). (2021). Section 500, "Concrete Structures." *Standard Specifications Construction of Transportation Systems*. Available online: https://www.dot.ga.gov/PartnerSmart/Business/Source/specs/2021StandardSpecifications.pdf.

15. Georgia Department of Transportation (GDOT). (2024). Section 500, "Concrete Structures." *Supplemental Specifications Modifying the 2021 Standard Specifications Construction of Transportation Systems.* Available online: https://www.dot.ga.gov/PartnerSmart/Business/Source/special_provisions/2021%20Supplemental%20Specifications/2021Supplemental%20Specifications%202024%20Edition.pdf.

16. ASTM C39/C39M-21. (2021). Standard Test Method for Compressive Strength of Cylindrical Concrete Specimens. ASTM International, West Conshohocken, PA. Available online: https://www.astm.org.

17. ASTM C143/C143M-15a (2015). Standard Test Method for Slump of Hydraulic-Cement Concrete. ASTM International, West Conshohocken, PA, 2015, Available online: https://www.astm.org.

18. ASTM C1611/C1611M-18. (2018). Standard Test Method for Slump Flow of Self-Consolidating Concrete (SCC), ASTM International, West Conshohocken, PA. Available online: https://www.astm.org.

19. Horta, A. (2005). *Evaluation of Self-consolidating Concrete for Bridge Structure Applications*. Master's thesis, Georgia Institute of Technology, Atlanta, GA.

20. ASTM C882/C882M-20. (xxxx). Standard Test Method for Bond Strength of Epoxy-Resin Systems Used With Concrete By Slant Shear. ASTM International, West Conshohocken, PA. Available online: https:/www.astm.org.

21. Mathey, R.G., Clifton, J.R., Anderson, E.D., and Beeghly, H.F. (1973). *Performance of Coated Steel Reinforcement in Concrete. Part 1. Investigation of Bond in Pullout Specimens.* NBSIR 73-401, National Bureau of Standards, U.S. Department of Commerce, Washington, DC. Available online: https://www.govinfo.gov/content/pkg/GOVPUB-C13-755b5f47a2c525ee0349a4a74cc69c5d/pdf/GOVPUB-C13-755b5f47a2c525ee0349a4a74cc69c5d.pdf.

22. American Association of State Highway and Transportation Officials (AASHTO). (1993). *AASHTO Guide for Design of Pavement Structures*. AASHTO, Washington, DC. Available online: https://habib00ugm.wordpress.com/wp-content/uploads/2010/05/aashto1993.pdf.

23. American Association of State Highway and Transportation Officials (AASHTO). (2017). Section 5.6.3, "Strut-and-Tie Method." *AASHTO LRFD Bridge Design Specifications* (8th ed.). AASHTO, Washington, DC.